HYDROGEN BONDING IN ISOSTRUCTURALITY, POLYMORPHISM, AND COCRYSTAL DESIGN

A Thesis
Submitted for the Degree of
Doctor of Philosophy

By
N. JAGADEESH BABU

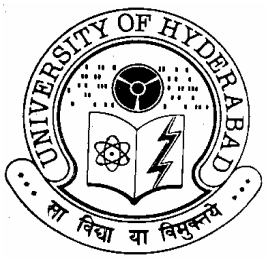

School of Chemistry
University of Hyderabad
Hyderabad 500 046
India

July 2008

Dedicated at

The Lotus Feet of Bhagawan Sri Sathya Sai Baba

STATEMENT

I hereby declare that the matter embodied in this thesis entitled **"Hydrogen Bonding in Isostructurality, Polymorphism, and Cocrystal Design"** is the result of investigations carried out by me in the School of Chemistry, University of Hyderabad under the supervision of Prof. Ashwini Nangia.

In keeping with the general practice of reporting scientific observations due acknowledgements have been made wherever the work described is based on the findings of other investigators.

Hyderabad
July 2008

N. Jagadeesh Babu

CERTIFICATE

Certified that the work **"Hydrogen Bonding in Isostructurality, Polymorphism, and Cocrystal Design"** has been carried out by N. Jagadeesh Babu under my supervision and that the same has not been submitted elsewhere for a degree.

Dean
School of Chemistry

Prof. Ashwini Nangia
Thesis Supervisor

ACKNOWLEDGEMENT

I express my deep sense of gratitude and profound thanks to **Prof. Ashwini Nangia** for his inspiring guidance and constant encouragement throughout the course of this research work. I have been able to learn a great deal in this fascinating field of research through his inspiring lectures and thought provoking discussions, and I consider my association with him a rewarding experience.

I thank Prof. D. Basavaiah, Dean, School of Chemistry, former Deans Prof. M. Periasamy, Prof. E. D. Jemmis, and faculty for their co-operation in providing facilities in the School. I thank Prof. Gautam R. Desiraju for his motivating lectures during group discussions.

I would like to thank Prof. J. A. K. Howard, University of Durham, UK for helpful discussions and suggestions. I thank Dr. R. Modal for his help in collecting single crystal data for few compounds studied in this thesis.

I am thankful to Dr. Chelli. Janardhana, Dr. K. Anil Kumar, Dr. A. Solomon, Dr. G. Nageshwara Rao, Dr. Jagadeeshwara Rao, Prof. M. Anil Kumar, Dr. Sundareshan, and all other teachers and lecturers who taught me throughout my career. My sincere thanks to my Zoology madam of Sarada Jr. College and my school teachers Chittamma and Lalithamba for their constant encouragement.

I am grateful to UGC and DST, New Delhi, for providing fellowship support. I thank DST for providing single crystal X-ray diffractometer facility and UPE programme of UGC for infrastructure facilities.

I thank each and every non-teaching staff of the School of Chemistry, CIL, COSIST building and the Computer Centre for their assistance on various occasions. Much of the research displayed in this thesis comes from single crystal X-ray diffraction, IR and PXRD techniques. I take this opportunity to thank Dr. P. Raghavaiah, Smt. Ayesa Parwez, Mr. Nageshwara Rao for their kind help in acquiring the data with great deal of expertise and care. Dr. P. Raghavaiah is also good friend to me. I thank Mr. Sathyanarayana, Mr. Bhaskar Rao, Smt. Vijayalakshmi for their help in recording NMR spectra. I thank Mr. Shetty, Mr. Vijay Bhaskar, Mr. Dilip, Mr. Sai, Mr. Sharma, Mr. Jayaram, Mr. Desbandu, Mr. Durgesh, Mr. Shetty, Mr. Joseph for their cooperation.

I wish to thank my friendly and cooperative lab mates Venu anna, Vishweshwar, Sumod, Basavoju, Srinivasulu, Sreenivas Reddy, Bala Krishna Reddy, Malla Reddy,

Binoy, Saikat, Sreekanth, Bipul, Ranjit, Naba, Palash, Suryanarayan, Rajesh and Narendar for creating a cheerful working atmosphere in the lab. I also thank Aparna, Sairam, Sunil, Tejendar, Prashant, Dinabandu, Archan, Rahul, Yasir, Pati, Sanjeev and Sandeep for their help on various occasions.

My stay on this campus has been pleasant with the association of many students, Pavan anna, Vamsee anna, Gupta anna, Suresh, Narsi reddy, Mahipal, Phani Murali, Ravikanth, Shyam Raj, Prabhakar, Reddaiah, Devender, Raju, K.V. Rao, Ramesh Reddy, Aravind, Veerender, Shekar Reddy, Satpal, Satish, Nagraj, Mallesh, Sanjeev, Guru, Selva, Manab, Balraman, Bhuvan, Phani, Ramsuresh, Venu, Anji, Ramesh, Narahari, Rajeshwar, Ramesh, Rajesh, Abhijith, Molay, Ravi, Srinivas, G.D.P, Rambabu, Armugan, Tanmoy, Bharath, D.K, Ramu, Satish, Chaitanya, Vikram, Biju, Bhargavi, Shiva, Venkatesh, Kishore, Ram Kumar, Narayana, Shekhar, Haneesh, Satish, Anji, Murali, Anshuman, Tapan, Lucky, Venkat, Sreenivas reddy, Sashi, Anil, Jyothi, Anil & Sunil, and all others whose names are not mentioned due to lack of space.

It would like to thank my SSIHL friends, T. Satish, Preeti, Sampy, Mahidar, Rajesh, Manoj, Munni, Sowmya, Sujana, Suresha, Kishore, Prasadam, Reddy, Curly Murli, Grandhi, Sasa, Prathap, Bhakta, Chaitanya, Harsha, Bodi Br., Ravi, for their ever willing support and encouragement. My heartfelt thanks to ‘behind-the-scenes’ people Santu, Shalu, Srilu, Ananta, Bharathi, Neeraja, Anil and Manogna for believing and encouraging me when ever things seemed impossible and finally for their wonderful friendship. I also thank Murli, Srinu, Dilli and Suresh annayyas for their wishes.

The unconditional love of my Amma & Nanna and their blessings made me what I am today and I owe everything to them. I would like to thank all my family members, Pedda akka, Pedda Baavagaaru, Chinna akka, Chinna Baavagaaru, Annayya and Vadina for their love, support and guidance throughout my life. I thank Sai Paapa, Dumbu Gaadu and Chitti Paapa for their smiles and wishes. My special thanks to our relatives, friends and all others who have made a contribution to my life.

I would like to express my love and gratitude to Bhagawan Sri Sathya Sai Baba, who is my source of Inspiration, and who taught me the basic principles of life. I thank him for giving me patience and perseverance to endure challenges in my life. I dedicate this thesis at his lotus feet.

N. Jagadeesh Babu

SYNOPSIS

This thesis entitled "**HYDROGEN BONDING IN ISOSTRUCTURALITY, POLYMORPHISM, AND COCRYSTAL DESIGN"** consists of seven chapters.

CHAPTER ONE

INTRODUCTION TO CRYSTAL ENGINEERING

Crystal engineering or the design of organic solids is one of the mainline areas in chemical research today. It relies on molecular building blocks that are assembled into organized structures with desired properties and functions. Among all intermolecular interactions, hydrogen bonds are the most reliable and directional interactions, and play a pivotal role in organizing the molecules. In the same way that synthetic chemists refer to "yield" to quantify a desired product, crystal engineers typically determine the successful formation of a supramolecular product according to the frequency or occurrence of preferred intermolecular interactions between molecules as synthon predictability. Identification of such synthons is a key step and greatly facilitates the synthetic aspects of crystal and cocrystal engineering.

CHAPTER TWO

STRONG HYDROGEN BONDING IN NEUTRAL POLYCARBOXYLIC ACIDS

2,3,5,6-pyrazinetetracarboxylic acid, 2356PYZTA, and 2,3,5-pyrazinetricarboxylic acid, 235PYZTA, dihydrate crystal structures, without any charged species or highly activated donor/acceptors are shown to have a very short intermolecular O_{acid}–H···O_{water} neutral hydrogen bond (O···O = 2.2-2.5 Å). Unusual shortening in these structures is ascribed to synergistic π- and σ- cooperativity in the finite, neutral array, named as Synthon Assisted Hydrogen Bond. Pyrazine, pyridine and benzene tetracarboxylic acid (2356PYZTA, PYR2356TA, and BZN1245TA respectively) are three dimensionally isostructural and contain similar multi-center array of synthon assisted hydrogen bonds. Interestingly isostructurality is retained in these crystal structures due to the higher strength of SAHB bond and flexibility of water. Two dimensional isostructural pyridine-2,4,6-tricarboxylic acid dihydrate, PYR246TA, and benzene-1,3,5-tricarboxylic acid hydrate, BZN135TA, crystal structures are centered around hydrogen bonding of water. 5-methylpyrazine-2,3-dicarboxylic acid (5MPYZ23DA) is anhydrate, an exception to this family of hydrate

crystal structures. It is an achiral molecule that crystallized in the chiral $P6_5$ space group which contains the rare carboxylic acid–pyridine trimer motif in hexagonal 2D Kagomé lattice and a C–H···O helix in the third dimension.

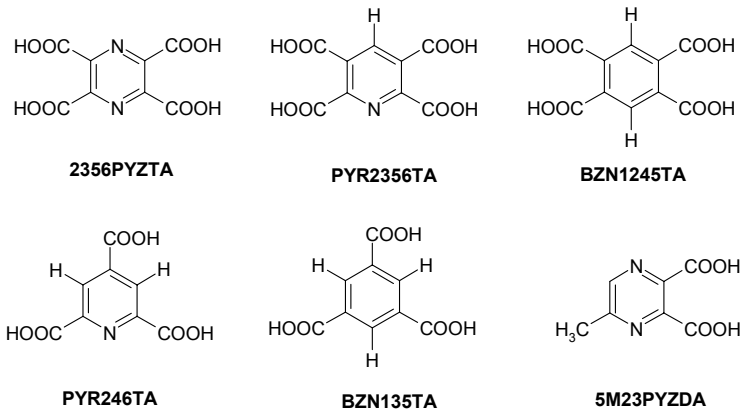

Scheme 1. Polycarboxylic acids discussed in chapter 2.

CHAPTER THREE

HIGH *Z′* POLYMORPH–SHORTER HYDROGEN BONDS

The presence of multiple molecules in the asymmetric unit or high *Z′* structures continue to interest crystallographers even though it is still not properly understood why some categories of structures show high frequency of *Z′* >1. A polymorphic system with variable *Z′* can reveal a great deal of information, as the high *Z′* form can easily be compared with its lower *Z′* form (*Z′* ≤ 1). Pyrazine-*N,N′*-dioxide, PYZNO has dimorphs containing similar trimers of C–H···O interactions but sustained by two and one symmetry-independent molecules in form 1 (Orthorhombic, *Pbca, Z′* = 2, form 1, **5a**) and 2 (Monoclinic, $P2_1/c$, *Z′* = 1, form 2, **5b**) respectively. Upon noting that C–H···O interactions are shorter (stronger) in high *Z′* form 1 of PYZNO, and also the same situation in a different polymorphic system 4,4-diphenyl-2,5-cylcohexadienone (*Z′* = 1, 2, 4, 12) from our group, we examined the generality of our observation in polymorph clusters in the CSD. Out of 38 polymorphic systems that can only form C–H···O interactions, the higher *Z′* crystal structure has shorter C–H···O interaction in 26 cases (68% probability), and the lower *Z′* form has shorter interaction in 12 cases. The accepted notion that high *Z′* in alcohol/ phenol crystal structures is due to H bond stabilization was evaluated statistically in 32 polymorphic systems with variable *Z′*. We believe that shorter (stronger) hydrogen bonds in high *Z′* crystal structures provide enthalpic advantage in bringing together multiple molecules during crystal nucleation.

CHAPTER FOUR

POLYMORPHISM IN TEMOZOLOMIDE AND FUROSEMIDE APIS

The phenomenon of polymorphism has attracted the interest of pharmaceutical industry, because polymorphs can exhibit different pharmaceutically relevant properties like dissolution rate, oral absorption, bioavailability and stability. For this reason it is crucial to screen for all possible polymorphs of a drug molecule and chose the right one with desirable characteristics in product formulation, preferably the most stable polymorph to avoid later phase transitions. Polymorphs of antitumour drug Temozolomide and loop diuretic Furosemide are chosen to study the influence of conformer changes on hydrogen bonding and crystal packing (Scheme 2). The main advantage with single crystal X-ray diffraction study is that detailed information about conformer changes, hydrogen bonding and molecular packing is accurately known.

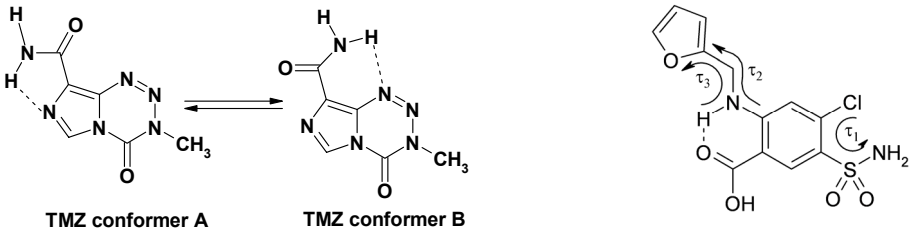

(a) (b)

Scheme 2. (a) Conformers of Temozolomide via rotation about the C_{amide}–$C_{imidazole}$ bond. (b) Furosemide molecule with accessible sulfonamide and furan ring torsions.

Temozolomide (TMZ, **6**) can undergo rotation about the C_{amide}–$C_{imidazole}$ bond to give two conformers, *A* and *B*. Conformer *B* is 1.44 kcal mol^{-1} higher in energy than conformer A. The stable conformer *A* is present in TMZ polymorphs 1 (**6a**) and 2 (**6b**) whereas both conformers crystallized in TMZ polymorph 3 (**6c**). Solid-state phase transitions, lattice energy calculations showed that the polymorph 1 is the most stable polymorph followed by form 2 and 3. The metastable nature of TMZ polymorphs 2 and 3 is due to the presence of unused hydrogen bond donors/ acceptors and strained conformer *B* respectively. Three polymorphs of Furosemide (FMD, 7) were characterized. There are four conformers present in three polymorphs: FMD form I (**7a**) has two molecules in the asymmetric unit whereas form II and III (**7b & 7c**) contain one molecule each. High energy metastable conformers (4.44 and 4.55 kcal/mol) are stabilized in crystal lattice of

stable FMD form I, while a stable conformer is present in the metastable FMD form III crystal lattice. This intra and intermolecular compensation in crystal structures or systematic effects are shown to increase the propensity of polymorphism especially in conformationally flexible molecules. Polymorphism in both these systems is based on differences in molecular conformations and hydrogen bond synthons.

CHAPTER FIVE

CARBOXAMIDE–PYRIDINE *N*-OXIDE SYNTHON IN COCRYSTAL DESIGN

Unlike the robust acid–pyridine heterosynthon, carboxamide and pyridine groups generally do not aggregate via amide–pyridine heterosynthon because N–H···N interaction is considerably weaker than N–H···O hydrogen bond of the amide dimer. The pyridine-*N*-oxide was selected as a complementary group for carboxamide to exploit the better acceptor strength of the anionic oxygen to form carboxamide–pyridine-*N*-oxide heterosynthon (Scheme 3).

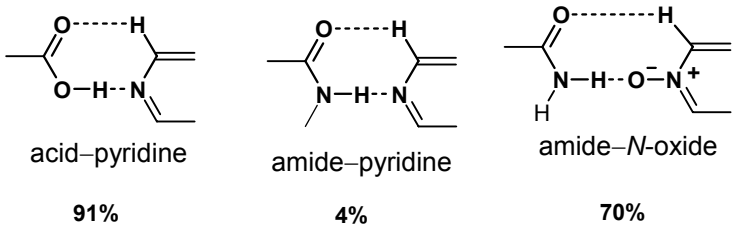

Scheme 3. Heterosynthons with their occurrence probability indicated.

In order to establish synthon robustness, 20 crystal structures were analyzed (13 cocrystals from this chapter as shown in scheme 4, and 7 structures from a previous thesis in our group) that contain amide and pyridine-*N*-oxide functional groups. Amide–pyridine-*N*-oxide heterosynthon competes with amide dimer homosynthon. 14 structures have amide–pyridine-*N*-oxide, 5 structures with amide–amide dimer and one structure contains neither of the expected synthons. Amide dimer is favoured for three reasons: presence of an intramolecular N–H···O hydrogen bond as in picolinamide-*N*-oxide, competition from another strong hydroxyl or water (–OH) group in cocrystal **14** and **15** and steric factors imposed by dibenzazepine group of CBZ in cocrystals **16** and **17** as confirmed from Crystal Structure Prediction on CBZ•QUINO (1:1) cocrystal in Cerius[2]. Absence of these commonly observed synthons in cocrystal **18TB** (triclinic) prompted us

to carry out more experiments which resulted in polymorphic cocrystal **18M** (monoclinic) with strong amide–*N*-oxide heterosynthon. Apart from generating diverse supramolecular structures, cocrystals offer the potential to modify physical and chemical properties of substances, e.g. hydration. 4-picoline-*N*-oxide deliquesces within a day; while its 2:1 cocrystal of picoline-*N*-oxide and barbital (**13)** held by amide–*N*-oxide heterosynthon does not absorb moisture at 50% relative humidity (RH) levels up to four weeks. Cocrystal **13** has better resistance to hydration as the hydrogen bonding in crystal structure is completely different from that of individual components.

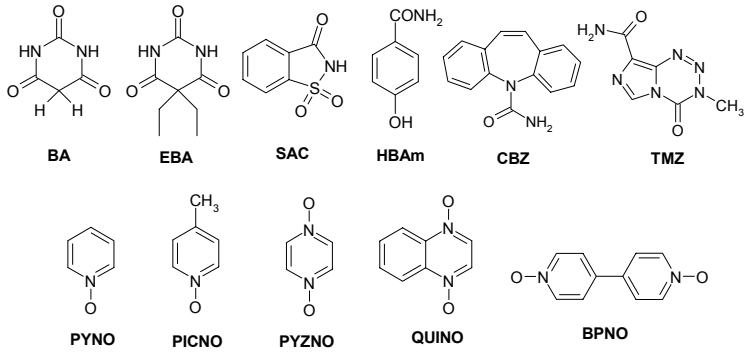

No	Cocrystal	No	Cocrystal
8	BA•QUINO (1:1)	**14**	HBAm•BPNO (1:0.5)
9	BA•PICNO (1:2)	**15**	HBAm•PYZNO•H_2O (1:0.5:1)
10	BA•PYZNO (1:0.5)	**16**	CBZ•QUINO (1:1)
11	SAC•BPNO (1:0.5)	**17**	CBZ•PYZNO (1:0.5)
12	EBA•PYNO (1:1)	**18T**	TMZ•BPNO (1:0.5)
13	EBA•PICNO (1:2)	**18M**	TMZ•BPNO (2:1)
		19	TMZ•BPNO (1:1)

Scheme 4. Cocrystals discussed in chapter 5.

CHAPTER SIX

PHARMACEUTICAL COCRYSTALS OF TEMOZOLOMIDE

Pharmaceutical cocrystals are a subclass of cocrystals that are formed between an API and a Generally Regarded As Safe chemical (GRAS) designed to improve the properties of drug molecules like solubility, stability and hydration control, etc. Chemical stability is a main concern for anti-tumour drug temozolomide. Two major problems that are encountered during crystallization are the hydrolytic cleavage of TMZ tetrazinone ring by nucleophilic attack by water, methanol or ethanol (**20, 21** & **22**) and undesired

formation of solvates (**23**, **24** & **25)**. The active species diazomethane required to bring about the antitumour activity is actually knocked off during this hydrolytic cleavage of tetrazinone ring. Therefore improving the stability of TMZ is crucial. With the knowledge that TMZ is stable at acidic pH <5 but labile at pH >7, it was co-crystallized with some GRAS organic acid *p*H adjusters to improve its stability during crystallization (Table 1).

Table 1. Crystal structures of TMZ prepared and discussed in chapter 6.

S.No	Crystal structure	Stoichiometry	Predominant Synthon	Conformer
		Hydrolyzed TMZ		
20	Hydrolyzed TMZ · H_2O	1:1	Amide–water	*A*
21	TMZ · Methanolyzed TMZ	1:1	Amide–tetrazinone Amide catemer	*A*
22	Ethanolyzed TMZ		Amide–imidazole	-
		TMZ solvates		
23	TMZ · H_2O	1:1	Amide–tetrazinone	*A*
24	TMZ · $MeNO_2$	1:1	Amide–amide	*A*
25	TMZ · DMSO	1:0.5	Amide–amide	*A*
		TMZ cocrystals with COOH partners		
26	TMZ · Formic acid · H_2O	2:1:1	Amide–acid Amide–amide	*A* + *B*
27	TMZ · Acetic acid	1:1	Amide–acid	*A*
28	TMZ · Oxalic acid	1:0.5	Amide–acid	*A*
29	TMZ · Succinic acid	1:0.5	Amide–acid	*A*
30	TMZ · DL Malic acid	1:0.5	Amide–acid	*A*
31	TMZ · *p*-Aminobenzoic acid · H_2O	3:1:1	Amide–acid Amide–amide	*A*
32	TMZ · Fumaric acid · H_2O	1:0.5:1	Amide–amide Amide–tetrazinone	*A*
33	TMZ · Salicylic acid	1:1	Amide–acid	*B*
34	TMZ · Hydrolyzed TMZ · Cinnamic acid · H_2O	3:1:1:1	Amide–amide Acid–imidazole	*A* + *B*
		TMZ cocrystals with $CONH_2$ partners		
35	TMZ · Isonicotinamide	2:1	Amide–amide	*A* + *B*
36	TMZ · Nicotinamide	2:1	Amide–amide	*A* + *B*
37	TMZ · Pyrazinamide	1:1	Amide–pyrazine Amide–imadazole	*A*
38	TMZ · 4-hydroxybenzamide	2:1	Amide–amide	*A*
39	TMZ · Saccharin	1:0.5	Amide–amide	*B*

The donor/acceptor imbalance of TMZ molecule is matched by the cocrystal former. The presence of carboxamide and several N-heterocycle functional groups of TMZ were exploited for facile cocrystal preparation with different acid and amide partners. Cocrystals of TMZ with COOH partners are more useful than $CONH_2$ partners as they

bring down solution *p*H levels below <5 during crystallization thus circumventing hydrolytic cleavage of TMZ molecules, and thereby improving the hydrolytic stability. In addition to stability aspects in cocrystals, recurrence of stronger synthons is evaluated systematically when multiple functional groups like amide, acid, imidazole, tetrazine, pyridine and pyrazine are present during co-crystallization experiments. Conformer flexibility of temozolomide is noted in cocrystals similar to its polymorphs.

CHAPTER SEVEN

CONCLUSIONS

The role of strong hydrogen bonded synthons and their importance in the design of crystal structures and cocrystals is discussed in this thesis. Occurrence of unusually short hydrogen bonds and isostructural behaviour in a family of neutral polycarboxylic acid hydrate crystal structures is explained in chapter 2, invoking the synergistic π- and σ-cooperativity in the finite array named as Synthon Assisted Hydrogen Bond (SAHB). The ability of water molecule to orient its hydrogen bond donor/ acceptor groups is central to isostructurality leading to the successful pyrazinyl $\rightarrow$ pyridyl $\rightarrow$ phenyl replacement because of N $\Leftrightarrow$ C–H exchange. Reasons for the presence of multiple molecules (high Z') in pyrazine-2,3-dicarboxylic acid anhydrate is due to the presence of acid–pyridine trimer synthon.

The connection between short hydrogen bonds and the occurrence of multiple molecules in the asymmetric unit of C−H···O hydrogen bonded polymorphic systems with variable Z' is analyzed statistically in the Cambridge Structural Database (chapter 3). The higher Z' crystal structure has shorter C–H···O interaction in 26 cases (68% probability) indicating the enthalpic advantage in bringing together multiple molecules during crystal nucleation. Similar study is also extended to well known O−H···O hydrogen bond polymorphic clusters. Cluster of molecules formed may directly carry over from solution to the solid state without final stages of reorganization and symmetry evolution to the lower Z' form thus providing a chemical and thermodynamic basis for multiple Z' crystal structures sustained by short-strong C–H···O / O–H···O interactions.

The effect of molecular conformations on hydrogen bonding and crystal packing is discussed in three single component (PYZNO, TMZ, FMD) and one cocrystal polymorphic systems (TMZ–BPNO). The metastable nature of polymorphs is due to the presence of unused hydrogen bonds which are utilized in the stable form. The likelihood of polymorphism is shown to increase in conformationally flexible organic molecules due to the presence of several conformers and intra- and intermolecular energy compensation or systematic effects.

Utilization of strong hydrogen bonds or robust synthons in the preparation of several cocrystals and their use in modifying the existing physical and chemical properties of molecules and drugs are dealt in chapter 5 and 6. A novel amide–pyridine-*N*-oxide heterosynthon is designed and its robustness is established. 4-picoline-*N*-oxide deliquesces within a day but its cocrystal with diethyl barbital was shown to be resistant to hydration at 50% RH for up to four weeks indicating that cocrystals have the potential to modify existing physical and chemical properties of solids.

Several pharmaceutical cocrystals of antitumour drug Temozolomide with GRAS chemicals are shown to improve the hydrolytic stability of TMZ, which is found to undergo hydrolysis in polar solvents like water, methanol and ethanol. The greater enthalpic advantage of amide–acid synthon over amide dimer in various cocrystals is statistically quantified. Cocrystals with COOH partners showed no signs of hydrolysis when crystallized from polar solvents like water and methanol.

Salient crystallographic details of the crystal structures discussed in this thesis have been given in the appendix to this thesis. A full list of atomic coordinates has been deposited with the University of Hyderabad and is available upon request from Prof. Ashwini Nangia (ashwini.nangia@gmail.com).

CONTENTS

CHAPTER 1

INTRODUCTION TO CRYSTAL ENGINEERING

1.1 Supramolecular Chemistry

Molecular chemistry has, over many years, developed a wide range of very powerful procedures for constructing ever more sophisticated molecules from atoms linked by covalent bonds. Beyond molecular chemistry lies supramolecular chemistry which aims at setting up highly complex chemical systems from components interacting via non-covalent intermolecular forces. The concept and the term supramolecular chemistry was introduced by Lehn (1978)[1] in the words: *"Just as there is a field of molecular chemistry based on the covalent bond, there is a field of supramolecular chemistry, the chemistry of molecular assemblies and of the intermolecular bond."* In simple terms, supramolecular chemistry may be defined as *chemistry beyond the molecule*. This idea represents a departure from classical chemical thought in that it discards the notion that the molecular structure of an organic substance embodies all of its chemical and physical properties. Further, the properties of supermolecules are not just additive but also cooperative, i.e. the whole is more than the sum of its parts. This field has grown into two distinct branches – the study of supramolecular assembly in solution (molecular recognition) and in the solid-state (crystal engineering). The concepts, principles of recognition and the nature of interactions that mediate supramolecular constructions are nearly same in solution and solid-state. Studies of supramolecular aggregates in solution were dedicated to understand/ or mimic the events of mutual molecular recognition that take place in biological systems, for example, enzyme–substrate interactions. Inspired by the accidental discovery of crown ethers by Pedersen in 1967, the research groups of Lehn and Cram started to explore the chemistry of synthetic receptors for small charged and neutral molecules. Noting the importance of molecular recognition, three pioneering scientists − Charles J. Pederson, Donald J. Cram and Jean-Marie Lehn − were awarded the Nobel Prize in 1987 for their excellent contribution in this area. Other scientists Atwood, Vögtle, Gokel among others subsequently extended this work to synthetic receptors involving hydrogen bonding and other non-covalent interactions. Several reviews and books have been published on this fascinating field of supramolecular chemistry.[2]

1.2 Crystal Engineering

Today "Crystal Engineering"[3] is viewed as supramolecular chemistry in the solid state *i.e.* the construction of crystalline materials from molecules or ions using non-covalent interactions. It is developed by structural chemists and crystallographers to understand non-covalent interactions for the design of novel materials and solid-state reactions. The word "Crystal Engineering" was first introduced by a physicist named Pepinsky[4] at the meeting of American Physical Society held in Mexico City in August 1955 in an abstract entitled "*Crystal Engineering: a new concept in crystallography*". This idea was elaborated by Schmidt[5] during the period 1950 to 1970 in the context of engineering crystal structures having intermolecular contact geometry appropriate for photodimerization of cinnamic acids in the solid state. He noted that the introduction of a dichlorophenyl group in unsaturated molecules steers crystallization into a unit cell with a shortest axis of ca. 4 Å, a distance optimal for photodimerization of alkenes. Desiraju[6] generalized the definition of crystal engineering as "*the understanding of intermolecular interactions in the context of crystal packing and the utilization of such understanding in the design of new solids with desired physical and chemical properties"*. The subject started with the study of organic solids.[6] Crystal engineering today[7] is one of the mainline interdisciplinary research activity today, dealing with the self-assembly of molecular crystals, metal–organic architectures, nanostructures, and coordination polymers using hydrogen bonding, electrostatic, and van der Waals interactions, and metal coordination bonding.

According to Dunitz, a crystal is an ideal paradigm of a supermolecule, a *supermolecule par excellence*.[8] It is an assembly of literally millions of molecules self-crafted by mutual recognition at an amazing level of precision. The high degree of order in crystal structure is the result of complementary dispositions of shape features and functional groups in the interacting near-neighbour molecules. The close packing principle of Kitaigorodskii[9] postulates that molecules in a crystal pack such that the projections of one molecule dovetail into the hollows of its neighbour, i.e. bumps fit into hollows just like lock and key, so that the maximum numbers of intermolecular contacts are achieved. These intermolecular interactions or non-covalent interactions in organic compounds are of two types: isotropic medium range forces (C···C, C···H, H···H interactions) which define the

shape, size and close packing; and anisotropic long-range forces which are electrostatic and include hydrogen bonds and hetero-atom interactions (O–H···O, N–H···O, C–H···O, C–H···N, O–H···π, halogen···halogen, nitrogen···halogen and so on). The observed three-dimensional architecture in a crystal is the free energy minimum that results from the interplay of demands of isotropic van der Waals forces whose magnitude is proportional to the size of molecules, and anisotropic hydrogen bond interactions whose strengths are related to donor atom acidities and acceptor basicities. Therefore a proper understanding of the strength and directional preferences of hydrogen bonds and intermolecular interactions lies at the heart of controlling the target crystal structure.

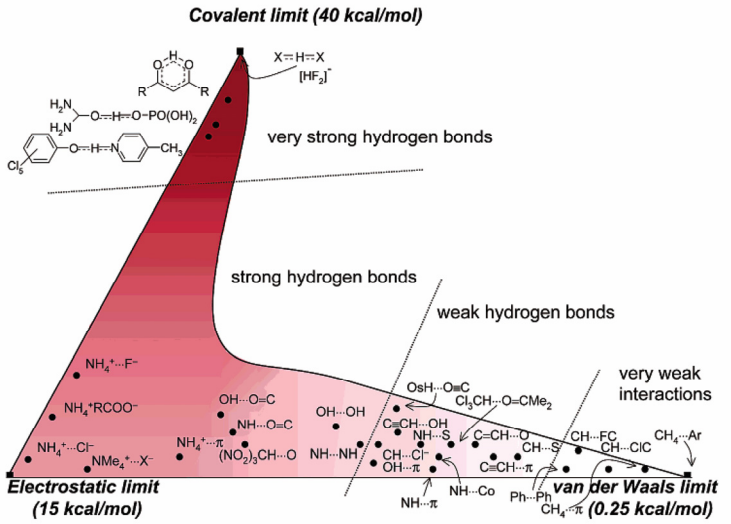

Figure 1. The hydrogen bridge, depicting various types of hydrogen bonds widely differing in energies which are indicated by the extent of colouring provides visual scales of energies. Figure taken from G. R. Desiraju, *Acc. Chem. Res.* **2002**, *35*, 565.

The strength and directionality of the hydrogen bond,[10] as compared to other non covalent intermolecular forces like van der Walls, π-π stacking, account for its significance due to which it is considered to be the most important interaction in directing the formation of molecular crystals. Hydrogen bond, X–H···A is an electrostatic interaction between a covalently bonded hydrogen atom or hydrogen bond donor and a strongly electronegative atom with lone pair of electrons or hydrogen bond acceptor. Based on the strength and directionality, hydrogen bonds may be classified into different categories:[11] very strong (15-40 kcal/mol, O–H···O^- and O^+–H···O), strong (4−15 kcal/mol, O–H···O and N–H···O) and weak (0.2−4 kcal/mol, C–H···O) as shown in figure 1. The very weakest of hydrogen bonds (C–H···O/N)[11,12] are barely distinguishable from

van der Waals interactions while the very strongest ones (O–H···O$^-$ and F–H···F$^-$)[13] are almost close to weak covalent bonds. Strong hydrogen bonds like O–H···O, O–H···N and N–H···O have enthalpic energies 5–10 kcal/mol. Intricate differences between strong and weak hydrogen bonds are discussed in chapter 2. Although single non-covalent interactions are very weak in terms of energy when compared to conventional covalent bonds, many such interactions collectively add up and play an important role in chemical and biological systems.[10a] Further they can be made and broken easily, facilitating rapid molecular recognition and chemical reaction. Hydrogen bonding is therefore a master key for supramolecular construction and its significance in crystal engineering must not be underestimated.

1.2.1 Supramolecular synthons and Retrosynthesis

The synthesis of complex natural products and aesthetically pleasing molecules has been practiced by organic chemists for decades.[14] It was in 1967 that Corey[14a] introduced a formalism in organic synthesis to organize the sequence of steps, and consequently to focus in the chemical thought process, from starting material to the target substance. Corey defined synthons as "*structural units within which molecules can be formed and/or assembled by known or conceivable synthetic operations*"[14a] and the term has been used since its inception to represent key structural units in the target molecules. A synthon is usually smaller and less complex than the target molecule and yet contains most of the vital bond connectivity and stereochemical information required to synthesize the goal substance. The analysis of a complex target molecule into simpler synthons is performed then through a series of rational bond disconnections, this exercise being termed as retrosynthesis. Recognizing that crystal engineering is the solid-state supramolecular equivalent of organic synthesis, Desiraju defined supramolecular synthons[15] are "*structural units within supermolecules which can be formed and/or assembled by known or conceivable intermolecular interactions*." Just as in traditional organic synthesis, where the retrosynthetic bond disconnection must be carried out in accordance with the reactivity of functional groups and their stereochemical preferences, so is the case in supramolecular synthesis wherein the complex interplay of close packing, hydrogen bonding and other intermolecular interactions during crystallization must be analyzed and exploited. Supramolecular synthons are therefore spatial

arrangements of intermolecular interactions between complementary functional groups and constitute the core of the retrosynthetic strategy for supramolecular structures. The synthon approach is advantageous in that it offers a considerable simplification in the understanding of crystal structures. The relationship between a molecule, a functional group and a supramolecular synthon and its utility in building up of the entire crystal structure is illustrated in scheme 1. In order to understand and predict correctly what type of intermolecular hydrogen bonds will form based on the molecular structure, one should be aware of specific synthon robustness, in other words the likelihood that it will be formed in many crystal structures. For example, the carboxylic acid dimer is same for both benzoic acid and terephthalic acid crystal structures. As individual hydrogen bonds or intermolecular interactions are by themselves weak, the identification of robust multi-point recognition motifs or supramolecular synthons is often more profitable in crystal design. It is, in a sense, like finding a high yield supramolecular reaction.[16] Designing a crystal structure effectively becomes synthon design,[7b,15] and this in turn, is only possible from a proper knowledge of the pertinent intermolecular interactions from various crystal structures.

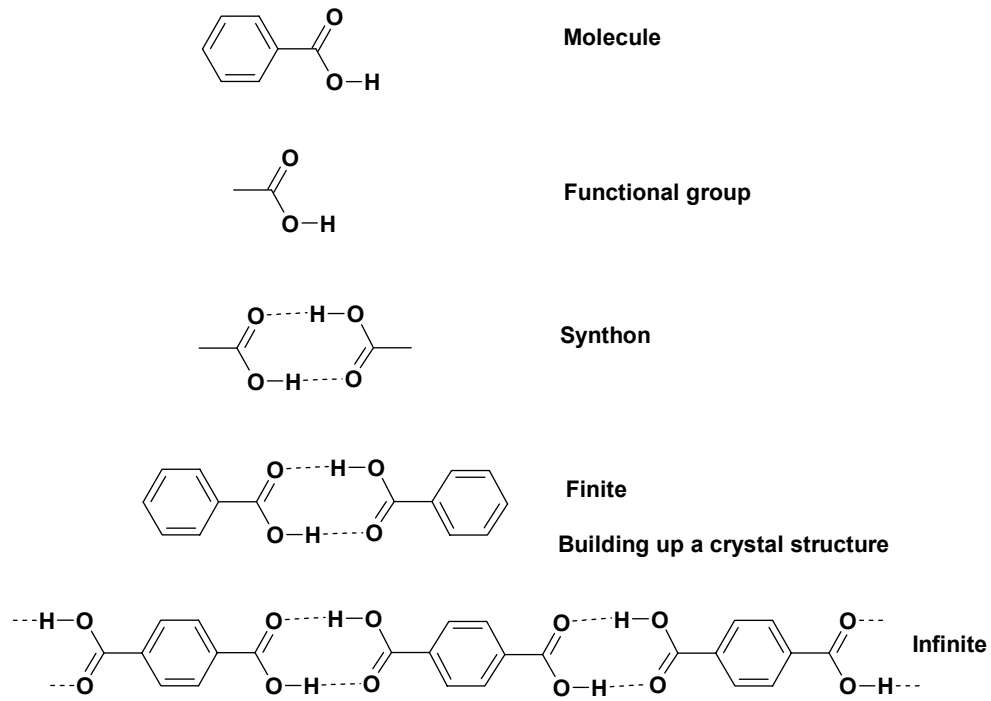

Scheme 1. Self assembly from molecule to crystal via supramolecular synthons.

1.2.2 Cambridge Structural Database (CSD) and Synthon Probabilities

The Cambridge Structural Database[17] is a storehouse of X-ray crystallographic data on organic and organometallic molecules. Starting from less than 2000 entries in 1965, the CSD today contains 4,36,000 accurate X-ray crystal structures. Direct use of the accumulated data is valuable in establishing standard molecular dimensions, determining conformational preferences and in the study of intermolecular interactions, all of which are crucial in structural chemistry and rational crystal design.[17b-e] In general it is difficult to predict whether or not a hydrogen bond between a potential donor X–H and a potential acceptor A in a given system will actually be formed. However, one can certainly define the probability of formation, i.e. the fraction of X–H···A hydrogen bonds among the number of such hydrogen bonds that could be formed in various crystal structures available from CSD. These probabilities can be determined for single hydrogen bonds, as well as for hydrogen bond arrays. Only if a hydrogen bond (or an array of hydrogen bonds) has a reasonably high probability of formation, it can be used in rational crystal design, i.e. crystal engineering.

Robustness of any particular synthon is assessed by its ability to withstand changes in molecular shape, substituent groups, competition from other intermolecular interactions and solvents. A hierarchy of supramolecular synthons was established by Allen et.al.[18] by calculating the probability of occurrence of 75 common non-covalent ring motifs constructed from O–H···O, O–H···N, N–H···O and N–H···N hydrogen bonds. It may be noted that recognition between unlike functional groups (e.g. acid–pyridine and melamine–barbital,) has far greater probability of formation than synthons between identical functional groups (e.g. acid dimer, amide dimer). Steiner[19] studied the formation of hydrogen bonds by carboxylic acid and other functional groups and found that only 33% of all carboxylic acid groups in crystals form acid dimer and 2.8% form catemer. The remaining 64% form hydrogen bonds with a variety of acceptors such as COO^-, P=O, pyridyl N, and water. For example, when pyridyl N atom is present as a competitor, it is much more likely that a carboxylic acid–pyridine heterosynthon is formed (91%) than a carboxylic acid dimer or catemer. Therefore acid–pyridine is considered to be highly robust than the acid dimer and this information may be utilized for crystal design. However in the absence of any other competing functional moieties,

the probability of acid dimer goes up to 90%. Similarly, another CSD study of supramolecular synthons of primary amides by Zaworotko and coworkers[20] has shown that 84% form amide dimers and 14% form catemers in the absence of competing hydrogen bond donors/acceptors. When there are competing groups such as carboxylic acid, secondary amide, aminopyridine, pyridine, water, alcohol, amines and etc. the formation of amide dimer and catemer is 35% and 18% respectively. Generally, one makes the observation that the probability of formation of synthon increases with the number of hydrogen bonds constituting a motif. Whereas two-point recognition normally operates only moderately well, three-point recognition is clearly better, and four-point recognition is highly successful. Zaworotko[21] sub-classified synthons as homosynthons and heterosynthons based on the interacting functional groups. If supramolecular synthon is formed between the same functional group it is a homosynthon, and between two different functional groups it is called as heterosynthon. Heterosynthons like acid–pyridine,[22] phenol–pyridine,[23] phenol–amine,[24] acid–amide,[25] aminopyridine–acid[26] and amide–pyridine-*N*-oxide[27] are well exploited in crystal engineering because of their strength and probability of formation (scheme 2).

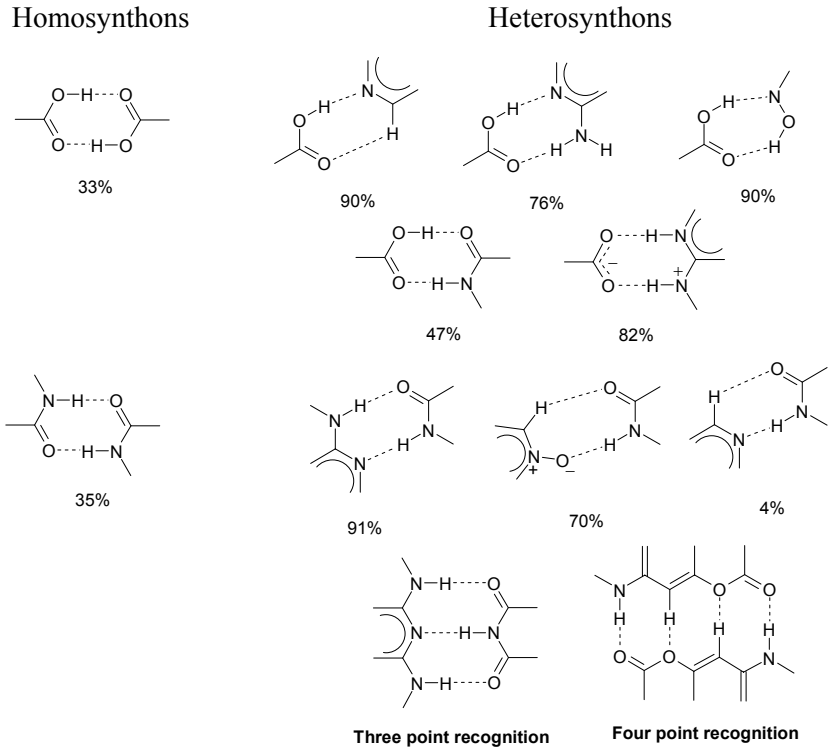

Scheme 2. Some examples of supramolecular synthons with their probabilities calculated from CSD statistical study.

1.3 Crystallization and various types of crystalline phases

Crystallization[28] is the process of formation of solid crystals from a homogenous solution or melt. It is one of the important techniques used for purification of compounds. It is based on the principles of solubility. The crystallization process consists of two major events, nucleation and crystal growth. In the nucleation step, the solute molecules dispersed in the solvent start to gather into clusters, on the nanometer scale (elevating solute concentration in a small region), that become stable under the current operating conditions. These stable clusters constitute the nuclei. However when the clusters are not stable, they re-dissolve. Therefore, the clusters need to reach a critical size and strength in order to become stable nuclei. Such critical size is dictated by the operating conditions (temperature, supersaturation, pressure, etc.). It is at the stage of nucleation that the molecules arrange in a defined and periodic manner that defines the crystal structure. The crystal growth is the subsequent growth of the nuclei that succeed in achieving the critical cluster size. Nucleation and growth continue to occur simultaneously while the supersaturation exists. Supersaturation is the driving force of the crystallization. Once supersaturation is completed, the solid-liquid system reaches equilibrium and the crystallization is complete. Single crystal X-ray diffraction and powder X-ray diffraction are the two important techniques to determine the crystal structure and its constituents. Once the crystal structure is available, the various forces responsible for holding the organic crystalline solids can be understood and exploited.

Many compounds often have the ability to crystallize in different crystal structures, a phenomenon known as polymorphism.[29] The subtle differences in the interplay of hydrogen bonds and other non-covalent interactions are responsible for polymorphism. The concept polymorphism and its importance in pharmaceutical industry will be discussed in the subsequent sections. According to Ostwald's rule,[30] the system moves to equilibrium from an initial high-energy state through minimal changes in free energy. Therefore the structure that crystallizes first is one which has the lowest energy barrier (highest energy, kinetically metastable). This form would then transform to the next lower energy polymorph and so on until a thermodynamically stable state is achieved. As the nature of crystallization process is governed by thermodynamic and kinetic factors, crystallization is highly variable and difficult to control. Apart from polymorphism,

crystallization is further complicated by including the solvent in the crystal lattice of the compound of interest. These are called as pseudopolymorphs or solvates.[31] Because the numbers of crystal structure with water are more, they have been separately categorized under hydrate crystal structures.[32] Based on the number of components in the crystal lattice, they are broadly classified as single molecular entities or multi-component species. Polymorphs represent single component crystals while multi-component crystals include salts, hydrates, solvates and cocrystals of the molecule with a second component ion, water, solvent or a cocrystal former respectively.[29b-d] When there is no periodic arrangement of molecules, i.e. randomly arranged with short range of contacts, they are defined as amorphous substances. All these phases are illustrated in scheme 3.

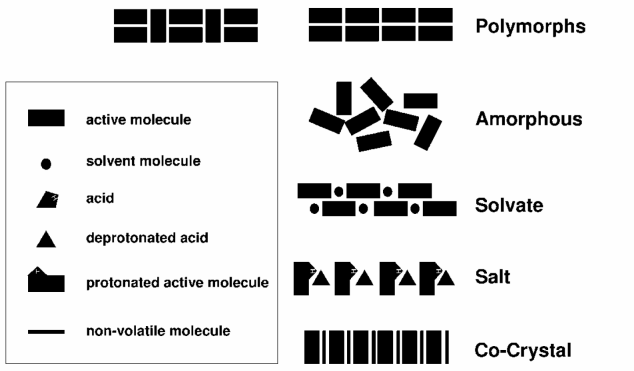

Scheme 3. Different types of solid phases for organic molecules.

1.4 Polymorphism

McCrone[33] defined polymorph as "*a solid crystalline phase of a given compound resulting from the possibility of at least two crystalline arrangements of the molecules of that compound in the solid state*". Allotropes and polymorphs are closely related. Polymorphism is used in general to refer to structural diversity of molecular compounds whereas allotropy is the structural diversity of elements. For example, carbon has three allotropes diamond, graphite and fullerene. The carbon atom is the same in three crystal structures; however the arrangement of atoms is different in different crystal structures, which consequently lead to the differences in their properties like hardness and conductivity. Similarly organic molecules in crystals exhibit polymorphism mainly by two mechanisms – packing polymorphism and conformational polymorphism.[29] Packing polymorphism is a mechanism by which molecules that are conformationally rigid can

be packed into different three-dimensional structures. The form 1 of anti-bacterial Nitrofurantoin contains amide dimer N–H···O hydrogen bonds, whereas form 2 arises from different packing arrangements of molecules connected by infinite chain of N–H···O hydrogen bonds or an amide catemer (Figure 2).[34a] Conformational polymorphism on the other hand arises from different conformers that can pack into different crystal structures as illustrated by ritanovir polymorphs (Figure 3).[34b] Configurational polymorphism is the term given for molecules exhibiting different tautomers in different crystal structures (*E* and *Z*). Nitroethanediamine *E/Z* tautomers present in the polymorphs of anti-ulcer drug Ranitidine HCl (Figure 4, Scheme 4)[34c] is an example of both conformational and configurational polymorph.

Polymorphism in organic solids is of fundamental importance because of its ability to alter physical and chemical properties in different crystal structures, such as melting point, density, dipole moment, hardness, compressibility, solubility, dissolution rates and bioavailability.[29] These differences impact on drug formulation and processing of the drug, due to which it has received particular attention in pharmaceutical industry.[29b,c] Stability presents a special concern while dealing with polymorphs. Because their energy differences are relatively small, form inter-conversion is common. For example, about two years after FDA approval, the HIV protease inhibitor Ritonavir appeared as a previously unknown, thermodynamically more stable polymorph II with a different conformer and stronger hydrogen bonds than the metastable form I.[34b] The new form was five times less soluble than form I, which caused the existing capsule product to fail its regulatory specifications, thus forcing removal of the capsule from the market until the product could be reformulated to meet the necessary performance criteria. The appearance of new form II was presumably due to the increase in the carbamate impurity levels. The estimated loss incurred due to the accidental appearance of new polymorph and its post effects is nearly 250 $ million dollars to the Abbott laboratories. Therefore risks of marketing a drug product without awareness and recognition of the thermodynamically most stable form are very high. Getting the right polymorph is not only important for drugs and pharmaceuticals but also for speciality chemicals like explosives, dyes, pigments, flavours and confectionery products. For example, oxotitanium phthalocyanine exists in four polymorphic forms. Among the four forms, one form is used as photosensitive charge generation material while other forms are

inactive.[35a] Different polymorphs of quinacridone and 2,9-dichloroquinacridone pigments have been characterized and only polymorphs that show extreme resistance to light, weather, temperature and with least solubility are selected amongst all forms.[35]

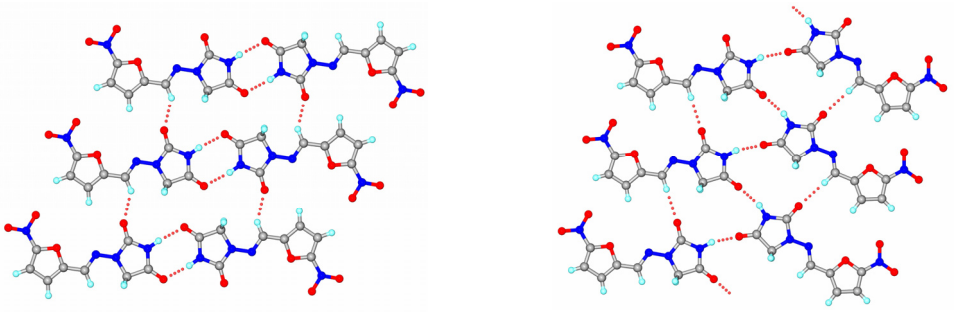

(a) (b)

Figure 2. Polymorphs of Nitrofurantoin drug. (a) Form 1. (b) Form 2. The amide molecule forms amide dimer in form 1 whereas it forms catemer motif. Polymorphism arises due to different modes of amide packing arrangements.

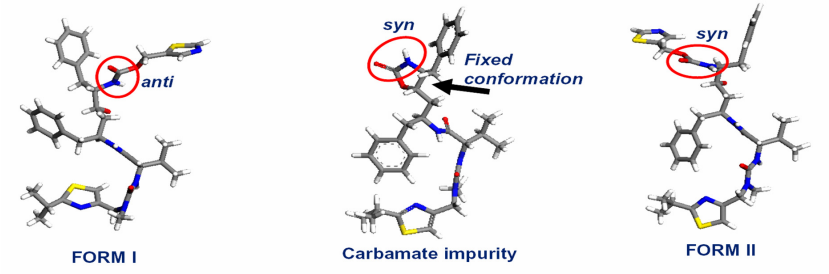

Figure 3. The *syn* and *anti* amide conformers of Ritonavir in form I and II. The accidental discovery of form II with *syn* amide conformer is presumed to be obtained due to the increase in the levels of carbmate impurity which has *syn* amide conformer.

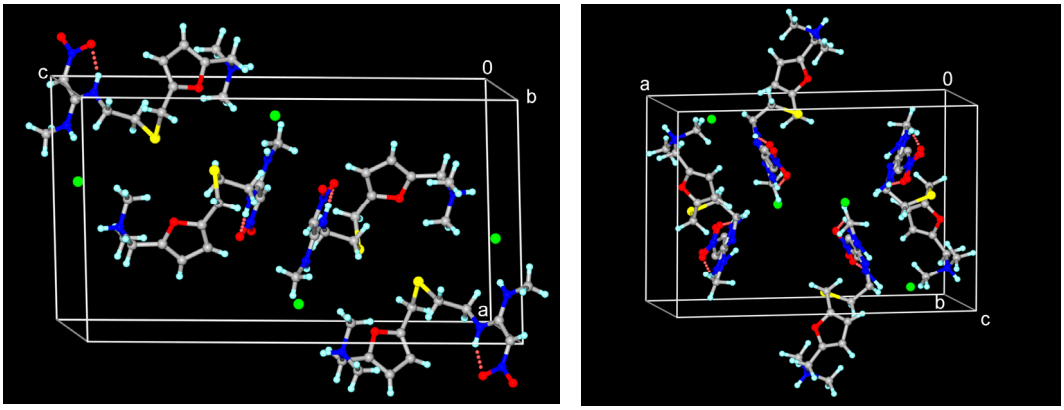

(a) (b)

Figure 4. Polymorphs of anti-ulcer drug Ranitidine HCl. (a) Form I. (b) Form II. Polymorphism arises due to different conformers /or tautomers of the molecules and consequently different modes of packing of molecules.

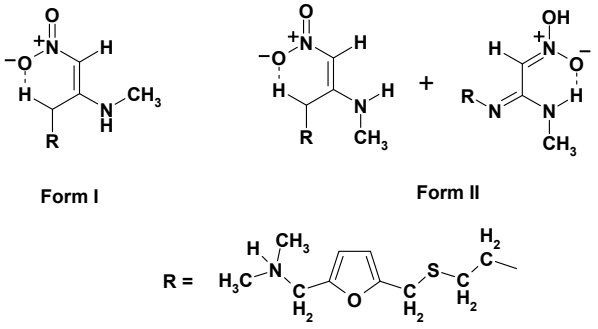

Scheme 4. Nitroethanediamine *E/Z* tautomers present in the polymorphs of Ranitidine HCl. Form I has exclusively one tautomer, whereas form II has both tautomers in 1:1 stoichiometry.

As different polymorphs have different physical and chemical properties, characterization of all polymorphs (thorough polymorph screening), identification of the stable form and controlled preparation of a particular metastable form has become one of the major challenges in modern crystal engineering and solid-state chemistry.[36] In addition, studies on polymorphism can afford fundamental information on molecular recognition, crystal nucleation,[37] and structure–property relationships.[38] Current approaches for discovery and selection of polymorphic forms include methods, such as varying solvent of crystallization, temperature, and extent of supersaturation. Recently few more novel techniques such as, crystallization with structurally related additives,[39] epitaxial growth,[40] laser induced nucleation,[41] crystallization in capillaries,[42] confinement within porous materials,[43] using polymers as heteronuclei,[44] mechanical grinding,[45] using supercritical liquids,[46a] using self assembled monolayer with different functional moieties,[46b] and potentiometric cycling.[47] High-throughput crystallization screens have been developed using a combinatorial approach to capture crystal form diversity.[48] Various methods of generating polymorphs were recently reviewed.[49]

Another important issue with respect to polymorphism is that different crystal forms can be considered as a patentable invention.[29b] Polymorphs patents have become the battleground in the ongoing struggle between Innovator and Generic drug manufacturers. As such, Generic pharmaceutical companies are increasingly devoting their time and effort in searching for novel crystal forms in order to allow them to gain an early access into the market place, while the Innovator companies are equally trying their best to patent on all the polymorphs of a particular drug so as to extend their monopoly in

pharmaceutical industry and to protect their product from generic competitors attack.[50] A well-known example of the use of the polymorph patent to hinder generic competition is Glaxo's Zantac®.[51] Glaxo obtained a patent on two forms (I followed by II) of the active ingredient Ranitidine hydrochloride. The differences between form I and II are shown in figure 4. In the mid 1990s, as the patent on the drug (form I) was approaching expiration, other companies began gearing up to market cheaper, generic versions of form I. Several attempts by generic manufactures to crystallize form I always produced a mixture of form I and II. They had to really figure out how to crystallize form I without any contamination from the form II, because form II was still protected by Galxo. This kept the generic companies products off the market for several years. During that period Glaxo was making $10 million in sales each day on its ulcer treatment, so every day it retained control over its drug was significant. Ultimately Novopharm could find a method to prepare exactly form I with non-detectable amounts of form II, and won the battle and since then generic entry was made into the market. There are several examples of patent litigation involving polymorph patents such as Neurontin® and Zoloft®, Paxil® and Cefadroxil®.

1.5 Isostructurality

Isostructurality[52] refers to identical or a nearly identical packing arrangement of chemically distinct/ or related compounds in a crystal and is inversely related to the phenomenon of polymorphism, which, instead refers to the ability of a single compound to crystallize in different packing arrangements. Both polymorphism and isostructurality are important in crystal engineering, materials science and pharmaceutical chemistry. One may want to know all possible crystal forms of a drug or to replace one molecule with another without disturbing the crystalline order. Two terms are commonly used in the literature: Isostructurality and Isomorphism. Two crystals are said to be *isomorphous*[53] if (*a*) they have the same space group and unit-cell dimensions and (*b*) the types and the positions of atoms in both are same except for a replacement of one or more atoms in one structure with different types of atoms in the other (*isomorphous replacement*), such as heavy atoms, or the presence of one or more additional atoms in one of them (*isomorphous addition*). Ideally, the substances are so closely similar that they can generally form a continuous series of solid solutions. On the other hand, two

crystals are said to be *isostructural*[54] if they have the same structure, but not necessarily the same cell dimensions nor the same chemical composition, and with a comparable variability in the atomic coordinates to that of the cell dimensions and chemical composition. For instance, calcite $CaCO_3$, sodium nitrate $NaNO_3$ and iron borate $FeBO_3$ are isostructural. Although there are slight differences in the definition, the term isomorphism is often used synonymously with isostructurality. The phenomenon of isomorphism is known for more than two centuries with the growth of potassium alum crystals from a saturated solution of ammonium alum. Kitaigorodskii was the first to review isostructurality behaviour in organic compounds.[52] Kàlmàn[55] has suggested two parameters, which quantify the extent of isostructurality between two crystal structures. They are the unit cell similarity index (Π) and isostructurality index ($I_i(n)$).

$$\Pi = \left| \frac{a+b+c}{a'+b'+c'} \right| - 1 \cong 0$$

where *a, b, c* and *a′, b′, c′* are orthogonalized lattice parameters of the related structures. For a pair of completely isostructural crystals Π should be close to zero.

$$I_i(n) = \left[1 - \left(\frac{\sum_i \Delta R_i^2}{n} \right)^{1/2} \right] \times 100$$

The isostructurality index, ($I_i(n)$) is a measure of the degree of internal isostructurality where n is the number of distance differences (ΔR_i) between the absolute coordinates of identical non-hydrogen atoms within the same section of asymmetric units of related structures. $I_i(n)$ should be close to 100% for isomorphous crystals.

Isostructurality is traditionally interpreted in three dimensions, i.e. isostructurality involves whole structures, which are infinite in three dimensions by means of three crystallographic translations. However, it is possible to extend the interpretation of the phenomenon to one- and two dimensional isostructurality.[56] If two crystal structures contain similar infinite two-dimensional molecular arrangements (layers) then they are termed as two-dimensionally isostructural. Accordingly, structures with similar rows of molecules are one-dimensionally isostructural. Isostructurality in steroids has been studied previously for compounds that are related by an exchange of functional groups (gamabufotalin/arenobufagin) or by epimerization (5α- and 5β-androstane-3 α,17β-

diol).[57] A C–H···O interaction in the crystal structure of 2-oxa-4-androstene-3,17-dione was replaced by a C–O–H···O hydrogen bond in its isostructural 6α-hydroxy analogue, is an example of 1D isostructurality from our group (Figure 5).[58] The fact that these two compounds form solid solution validates the isomorphous replacement of C–H atom by C–OH group.

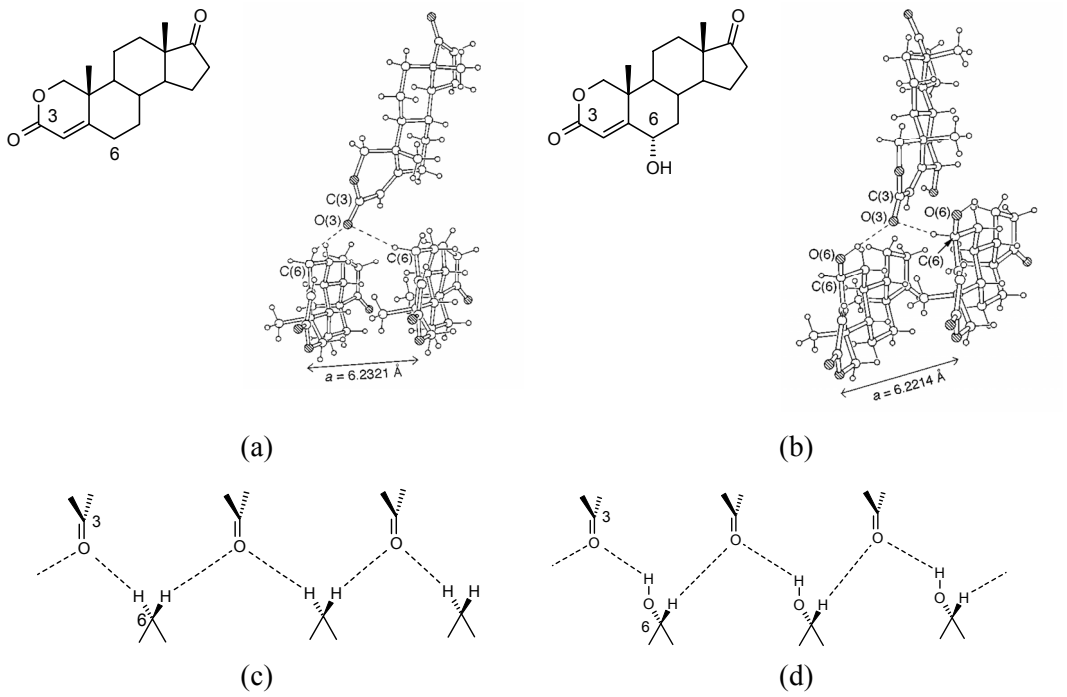

Figure 5. (a) 2-oxa-4-androstene-3-17-dione and its crystal structure. (b) 6α-Hydroxy-2-oxa-4-androstene-3,17-dione and its crystal structure. Note the identity of *a*-axis and the similarity in hydrogen bonding and arrangement of molecule in both these structures. Isostructurality is due to replacement of C–H···O synthon in (c) via C–O–H···O synthon in (d) without disturbing the overall arrangement of molecules.

Recently our group showed a rare case of examples which are both polymorphic and isostructural.[59] Triiodoresorcinol and triiodophloroglucinol crystallized as orthorhombic ($P2_12_12_1$) and monoclinic ($P2_1/n$) polymorphs mediated via inter-halogen I···I interactions. The orthorhombic polymorphs of both compounds are isostructural and correspondingly monoclinic polymorphs are also identical (Scheme 5a). The two oxygen atoms of triiodoresorcinol is shown to have disorder over three sites and form only weak tandem hydrogen bonds similar to triiodophloroglucinol. The above two examples illustrate isostructurality via C–H ⇔ C–OH replacements, i.e. weaker CH donor replaced by stronger OH donor. Another example which shows both polymorphism and

isostructurality is 2-amino-4-chloro-6-morpholinepyrimidine and 2-amino-4-chloro-6-piperidinopyrimidine.[60] The morpholine derivative yields two polymorphs, both with space group $P2_1/c$, having two and one molecules in the asymmetric unit respectively ($Z' = 2$ and 1, scheme 5b). Its piperidine derivative (O acceptor is replaced by CH_2), has only one crystal structure with two molecules in the asymmetric unit of $P2_1/c$ space group ($Z' = 2$, figure 5b). Interestingly it is found to be isomorphous with one of the polymorph of morpholine which also has $Z' = 2$. A second form with $Z' = 1$ is not observed for piperidine derivative. Normally consequences of such O ⇔ C–H replacements are severe on hydrogen bonding and overall crystal packing, because a strong oxygen acceptor is replaced by a weak phenyl C–H donor, is discussed in detail in chapter 2.

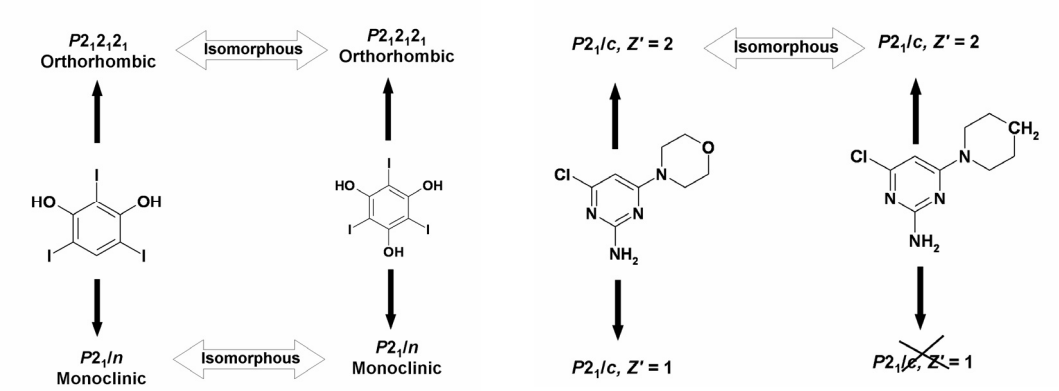

(a) (b)

Scheme 5. (a) Triiodoresorcinol and triiodophloroglucinol are dimorphic compounds exhibits isomorphous C–H ⇔ C–OH replacement. Orthorhombic and monoclinic forms are identical. (b) Piperidine derivative is a dimorphic substance with $Z' = 2$ and 1 in $P2_1/c$ space group, while the morpholine derivative has only one crystal structure with $Z' = 2$. It is isomorphous with piperidine $Z' = 2$ polymorph showing O ⇔ C–H replacement.

Isostructural crystals often lead to similar properties. The molecular DPP pigment and its cocrystal between two constituent DPP molecules are found to be isomorphous and exhibit similar colouristic properties.[35b, 61] A series of isostructural inclusion compounds or host-guest complexes present a unique opportunity to investigate structure and property relationships, because the host arrangement is effectively constant.[62a] As the solvates contain volatile solvents in the crystal structures, they are prone to undergo desolvation. In principle, two members of a series of isostructural inclusion compounds are expected to yield the same polymorph; however different polymorphs can be obtained some times or may even lead to amorphous form upon desolvation.[62, 29b]

1.6 Cocrystals and Pharmaceutical Cocrystals

Co-crystallization is an attempt at bringing together different molecular species within one periodic crystalline lattice without making or breaking covalent bonds. During co-crystallization, two things can happen: interacting molecules may fall apart yielding individual solids or crystallize together as a cocrystal. The goal of the recrystallization is to get a homomeric product or same phase (purification), whereas the co-crystallization strives for a heteromeric product or a binary phase as shown in figure 6. The term "co-crystal" and cocrystal are widely used in the literature. The most common method of obtaining cocrystals is to dissolve the components in a suitable solvent system and allowing for crystallization to take place. Gentle warming is necessary to dissolve the solids and sometimes an anti-solvent is added or the solution is subjected to sonication to accelerate crystallization. This empirical, trial-and-error method is referred as solution crystallization. Jones[63] suggested that by adding few drops of solvent during grinding/ kneading, referred to as solvent-drop or solvent-assisted grinding, one can accelerate the adduct formation due to lubrication.

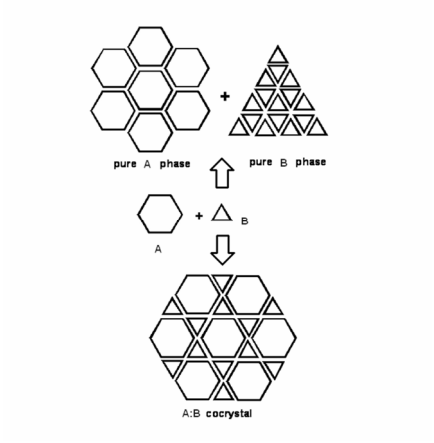

(a)

Accelerate co-crystallization
Manual or Ball mill grinding
Solvent drop grinding
Ultra-sonication

(b)

Figure 6. (a) Events that take place during co-crystallization. Two components may fall apart yielding individual phases or obtain as a cocrystal. (b) Various methods used for preparing cocrystals

There is currently an ongoing debate on the exact definition of cocrystal or co-crystal.[64] Zaworotko[65] proposed that a cocrystal is a multi-component crystal in which two or more molecules that are solid under ambient condition coexist through hydrogen bonds. Aakeröy[22a] further extended the definition to neutral compounds that are solids at

ambient temperature. The primary difference between solvates and co-crystals is the physical state of the isolated pure components. If one component is a liquid at room temperature, the crystals are designated as solvates; if both components are solids at room temperature, the crystals are designated as cocrystals. Nangia[25b,27b] recently suggested that the definition of cocrystal be made flexible to accommodate solvent (liquid) or gas as the second (third) component and the supramolecular interaction be not limited to hydrogen bonds[10] but include other intermolecular interactions, e.g. halogen bonds,[66] π–π stacking[67,25b] or any other non-covalent interactions. The advantage with cocrystals is that they can be used as probe to understand the structural preferences and balance of interaction between the molecules, and finally they impart new properties that are not present in individual solids.

The functional group plays a crucial role in organic synthesis as the reactivity of any molecule is related to the functional group(s) present in it. For example, carboxylic acids react with alcohols and amines to give esters and amides. However, in supramolecular chemistry the behaviour of a given functional group is not easily derived from the functional group present. Carboxylic acids not only form the expected dimer but also give hydrogen-bonded catemer and hydrated motifs. A detailed understanding of the supramolecular chemistry of the functional groups present in a given molecule is a therefore a prerequisite for designing a cocrystal. As the recognition mechanisms of molecules are extraordinarily selective during the crystallization, consequently, each crystal structure contains important information about the way in which intermolecular forces compete and collaborate and eventually create an energetically balanced system. Thus the identification of predictable intermolecular interactions or robust synthons formed by molecular functionalities is a crucial step in cocrystal design, which is available from the statistical analysis of CSD synthon probabilities as discussed earlier and from computational studies. The knowledge gained from the design principles can be utilized in the synthesis of new structures with optimized properties. In the case of reasonably strong hydrogen-bonded systems, in which there is a single interaction that dominates the crystal packing of regularly shaped small molecules, it is possible to make some predictions about the resulting crystal structures. However the design becomes more difficult in multi-functional molecules because of competition between similar strength donor/acceptor groups. In such cases, hydrogen bond rules serve as a guide.

1.6.1 Hydrogen bond rules: Etter[68] stated hydrogen bond rules in the 1990s that (1) *all acidic hydrogens available in a molecule will be used in hydrogen bonding in the crystal structure of that compound.* (2) *All good proton acceptors will be used in hydrogen bonding when there are available hydrogen-bond donors.* (3) *The best hydrogen-bond donor and the best hydrogen acceptor will preferentially form hydrogen bonds to one another.* If there is a possibility of forming six-member intramolecular hydrogen bond ring, it will usually form in preference to intermolecular hydrogen bonds. The 1:1 cocrystal of cyanuric acid and melamine[70] illustrates how all the potential hydrogen bond donor and acceptors are utilized to form an extensive two-dimensional network of hydrogen bonds (Scheme 6).

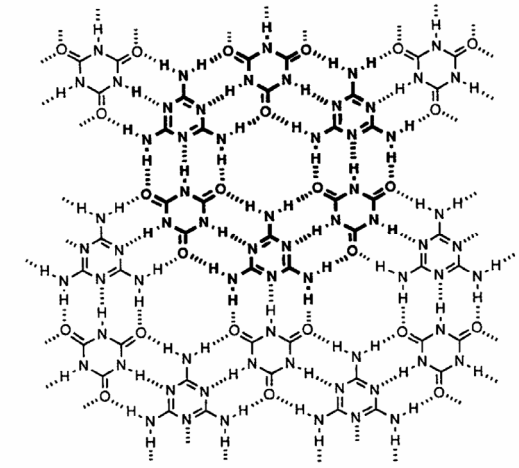

Scheme 6. Two dimensional architecture of 1:1 cyanuric and melamine cocrystal with saturated hydrogen bonds.

The third rule mainly deals with ranking H-bond donors and acceptors based on strength: the strongest donor interacts with the strongest acceptor, the second best donor bonds to the second best acceptor, and so on. Lauher and Fowler[71] reported a series of crystal structures designed using the hierarchic H-bond rule containing urea, pyridyl and acid functional groups. The strongest donor, COOH, bonds to the strongest acceptor, pyridine, and the left over urea group assembles as a 1D tape (Scheme 7a). Aakeröy further extended Etter's hydrogen bond hierarchy rule by the directed supramolecular construction of ternary cocrystals via acid–pyridine and amide–amide hydrogen bond synthons (Scheme 7b).[22g] Several research groups[22-27] have addressed the hierarchy of the supramolecular synthons that can occur for a range of common functional groups and observed that certain functional groups such as carboxylic acids, amides, and alcohols

are particularly amenable to the formation of supramolecular heterosynthons (i.e. non-covalent bonds between different but complementary functional groups). It is becoming evident that such interactions are the key to implement a design strategy in which a target molecule forms cocrystals with a series of cocrystal formers that are carefully selected for their ability to form supramolecular heterosynthons. However, there are some organic crystals where hierarchic H-bond rule is strictly not observed as discussed by Nangia.[23a] Cocrystal of *m*-hydroxybenzoic acid and isonicotinamide has hierarchic acid–pyridine and amide dimer hydrogen bonds, but the isomeric *p*-hydroxybenzoic acid and isonicotinamide cocrystal showed completely different phenol–pyridine and acid–amide synthons (Scheme 8).[16, 23a]

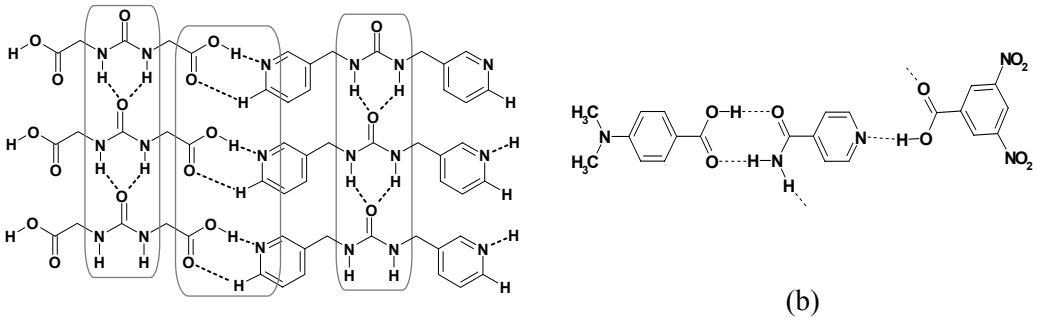

(a) (b)

Scheme 7. Hierarchic hydrogen bonding between acid, pyridine and amide groups in cocrystals. (a) Acid–pyridine heterosynthon and urea tape synthon in binary cocrystal of *meta*-pyridylmethylurea and dicarboxylic acid methylurea. (b) 3,5-dinitrobenzoic acid is stronger acid donor than N,N′-dimethyl-*p*-aminobenzoic acid and hence forms H-bond with better acceptor pyridine. i.e acid–pyridine. Subsequently dimethyl benzoic acid forms acid–amide heterosynthon in a ternary cocrystal.

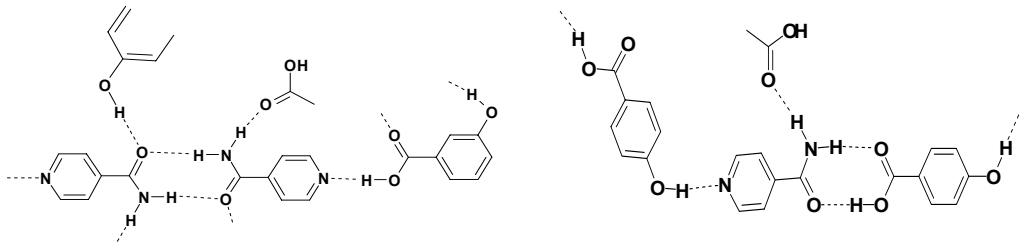

(a) (b)

Scheme 8. Very different hydrogen bond synthons in isomeric cocrystals containing COOH, pyridine, $CONH_2$, and OH functional groups. (a) Hierarchic H-bonding (acid–pyridine, amide–amide, carbonyl–hydroxyl) in *m*-hydroxy benzoic acid and isonicotinamide. (b) Non-hierarchic H-bonding (acid–amide, hydroxyl–pyridine) in *p*-hydroxybenzoic acid and isonicotinamide.

Schmidt[5,72] carried out topochemical reactions on the three polymorphs of *trans*-cinnamic acids (Scheme 9). The geometry of the molecules and the distance limit between the reactants is crucial for these reactions to take place. The α and β forms react in a [2 + 2] fashion to give rise to cyclobutane dimers when irradiated in the solid state as the double bonds in the monomer crystal are closer than *ca.* 4.2. Å. However γ form is photostable because the double bond separations are around 4.9 Å. Inspired by Schmidt's excellent work, MacGillivray[73] designed a series of cocrystal which reliably aligns olefins in the solid state to undergo photochemical reactions. This method involves a linear template (resorcinol), which enforces the topochemical alignment of olefins in the solid state, by way of hydrogen bonds, such that they undergo regio and stereo controlled [2 + 2] photochemical reactions in cocrystal as shown in scheme 10.

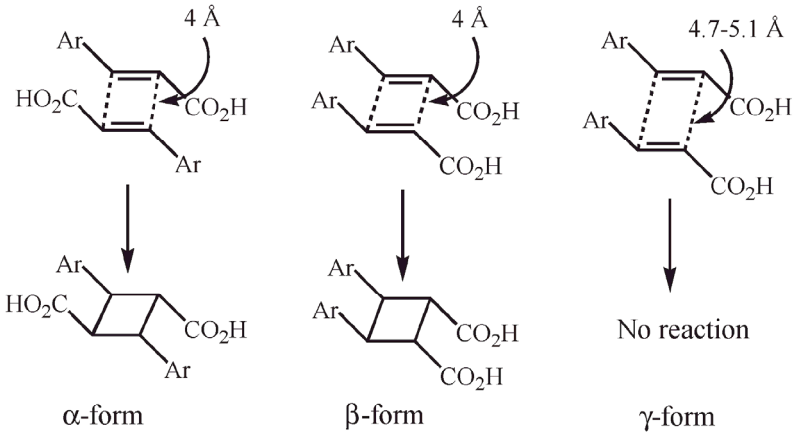

Scheme 9. Topochemical reactions of trans cinnamic acid polymorphic forms. The α and β forms undergo [2+2] addition reaction when exposed to light, while γ form is stable. The geometrical distance criteria required for reaction to take place should be 4Å between alkenes which is present in α and β forms only.

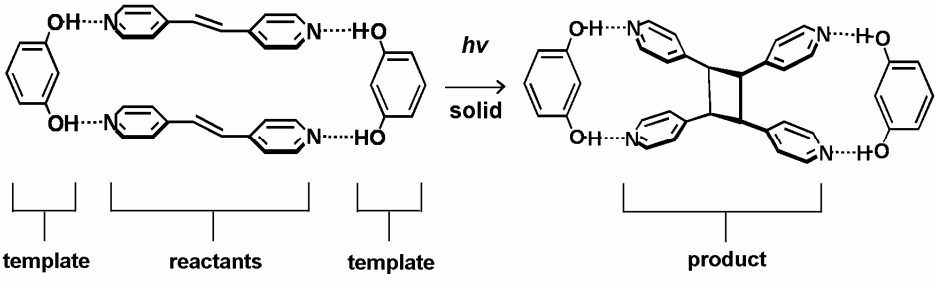

Scheme 10. Topochemical reaction of bipyridyl ethylene in cocrystal of resorcinol and bipyridyl ethylene. Resorcinol acts as a linear template to hold reacting alkene moieties by O–H···N hydrogen bonds at a particular distance such that they allow photochemical reactions to take place. Product is a cylcobutane derivative.

An advantage of cocrystals is that, existing properties of solids can be optimized by altering hydrogen bonding motifs and introducing hydrophilic/hydrophobic groups in the second component.[65] Indeed, such an approach, for which the term *non-covalent derivatization* was coined, has already been used in the context of modifying the stability of Polaroid film.[74] The incorporation of an auxiliary complexing reagent (*bis*-(*N,N*diethyl) terephthalamide) within the crystalline lattice of a hydroquinone developer has provided improved diffusion control and redox stabilization which render photographic films with better superior immediate images as well as stability during the storage conditions (Scheme 11). The process of forming such non-covalent derivatives or cocrystals can be often used as environmentally benign alternative to conventional covalent derivatization which bypasses several solvent-requiring synthetic transformations.

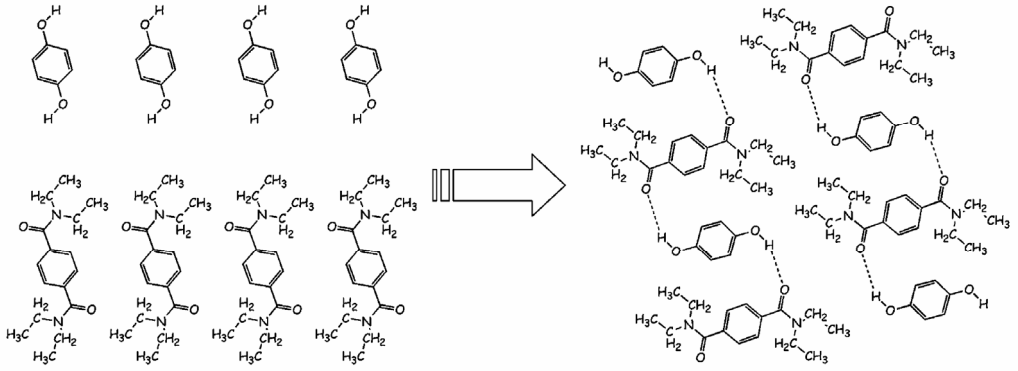

Scheme 11. Cocrystal of hydroquinone and bis-(*N,N*-diethyl)terephthalamide (1:1). The physical properties of hydroquinone are now modified with non-covalent terephthalamide derivative through hydrogen bonds.

1.6.2 Pharmaceutical cocrystals

These are a subclass of cocrystals that are formed between an Active Pharmaceutical Ingredient (API) and a non-toxic chemical to the human body.[65,75] Generally Regarded As Safe (GRAS) chemicals approved by Food and Drug Administration (FDA)[76] may be selected as the second component. These are more attractive in the pharmaceutical industry as several problems encountered with APIs, in terms of their solubility, dissolution rates, and stability can be surmounted without the need to make or break covalent bonds of the drug molecule. Itraconazole, an antifungal agent, is extremely water insoluble and administered both orally and intravenously. In order to achieve the

required oral bioavailability, the oral formulation of itraconazole is the amorphous form (Sporanox beeds). It was observed that itraconazole cocrystals,[77] especially itraconazole–succinic acid cocrystal (Figure 7), exhibits a similar dissolution profile to that of the sporanox beeds, is an alternative to the existing amorphous formulation. Cocrystal of carbamazepine and saccharin (CBZ–SAC)[78] appears to be superior to existing crystal forms of CBZ with respect to stability, favourable dissolution, suspension stability, and favourable oral absorption profile. Hydration behaviour of caffeine and theophylline was controlled by their 1:1 cocrystals with oxalic acid.[79] More examples are recently reviewed by Zaworotko.[80] Pharmaceutical cocrystals of anti-tumour drug Temozolomide are discussed in chapter 6.

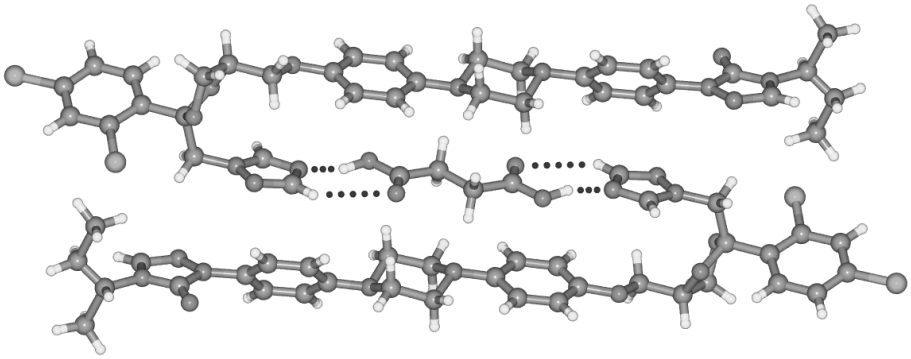

Figure 7. Structure of *cis*-itraconazole and succinic acid cocrystal. Succinic acid molecule is comfortably fitting between the two itraconazole molecules *via* O–H···N hydrogen bonding. Solubility of this cocrystal is similar to the amorphous formulation.

A case study of melamine–cyanuric acid cocrystal is the first example showing how cocrystals can significantly alter the relevant physical properties in a negative manner.[70,80] Melamine is intentionally added to increase the protein content in the food of pets. Nearly 4000 deaths of pets occurred due to the renal failure which forced "pet food recall". Investigations concluded the presence of cyanuric acid as another co-contaminant along with melamine. The presence of melamine and cynuric acid has not been conclusively linked to the deaths of animals, as both the chemicals were previously thought to be non-toxic. Further studies on the combination of melamine and cyanuric acid revealed the intratubular precipitation of cocrystal leading to the kidney failure and consequently death of animals. From the crystal engineering viewpoint, melamine and cyanuric acid (1:1 molar ratio) form an extensive two-dimensional networks in the solid-state based on the robust three-point molecular recognition (Scheme 6) and it was

observed that the resulting melamine–cyanuric acid cocrystal is highly insoluble in water seems a plausible answer for the deaths of animals.

1.6.3 Cocrystal vs Salt

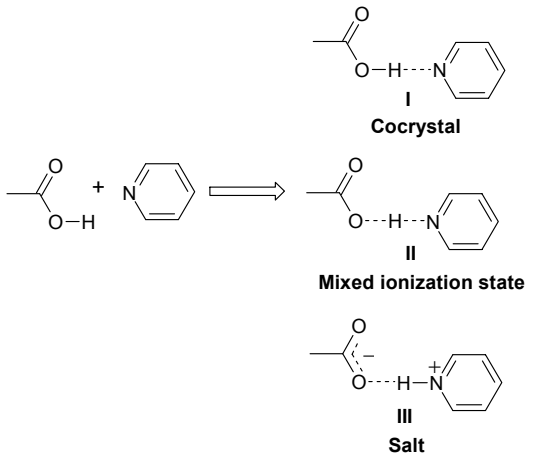

$\Delta pK_a = pK_a\,(pyrNH^+) - pK_a\,(COOH)$

$\Delta pK_a < 0$, neutral synthon (I), O–H···N

$0 < \Delta pK_a < 3.75$, mixed ionization state, O···H···N (II) or I/III, O–H···N/ N^+–H···O^-

$\Delta pK_a > 3.75$, ionic N^+–H···O^-

Scheme 12. The p*K*a rule to predict the H-bonding motifs in multi-component crystal.

Salts and cocrystals belong to multi-component crystals which can be distinguished by the location of the proton between an acid and a base.[22a,81,82] At the salt end of the spectrum proton transfer is complete, and on the opposite end proton transfer is absent in cocrystals (neutral complexes) as shown in scheme 12. It is generally accepted that reaction of an acid with a base will be expected to form a salt if the ΔpK_a (ΔpK_a = pK_a(base) – pK_a(acid)) is greater than 3.75, which is an essential criteria while selecting the appropriate counter ions to preparation of salts of API in order to improve its solubility. However, for acid-base complexes with similar pK_a values, the extent of proton transfer in the solid state is not predictable and a continuum exists between the two extremes. For these systems, both the ΔpK_a value (pK_a of base – pK_a of acid) and the crystalline environment determine the extent of proton transfer. Nangia and coworkers[22a] based on the analysis of several cocrystals and salts, concluded that the carboxylic acid–pyridine O–H···N interaction will be neutral when $\Delta pK_a < 0$ and it will have an intermediate H bond character, O–H···N and/or N^+–H···O^-, when the transition range $0 < \Delta pK_a < 3.75$. The interaction will be ionic N^+–H···O^- when $\Delta pK_a > 3.75$. Similar observation was noted by Childs and Stahly[82] in their analysis of 20 complexes of theophylline with COOH partners, which resulted in 16 salts, 2 cocrystals and 2 mixed

ionizations states with transition range $0 < \Delta pK_a < 2.5$. The pK_{HB} scale, proposed by Laurence,[83] measures the free energy of hydrogen bonded complex ($1.364\ pK_{HB} = -\Delta G_{HB}$ in kcal mol^{-1}) could be a better guide in predicting H-bond pairing compared to pK_a values as it deals with sharing of H atom between two electronegative atoms, while the pK_a scale considers only the ability of the proton to be transferred from acid to base. The pK_{HB} values are quite sensitive to factors that modify H-bonding ability, *e.g.* inductive/resonance effects, steric hindrance, lone-pair repulsion, and intramolecular H-bonding.

In pharmaceutical industry, both single-component crystals (polymorphs) and multi-component crystals (salts, solvates, hydrates and cocrystals) are equally important to modify the physical and chemical properties of the drugs. Salts and cocrystals have the potential to be much more useful in pharmaceutical products than solvates or hydrates because the number of pharmaceutically acceptable solvents is very small, and moreover solvents tend to undergo dehydration/desolvation in the solid dosage forms. Solvent loss some times leads to amorphous compounds, which are chemically less stable and can crystallize into less soluble forms.[29c] In contrast, the number of acceptable counter ions and cocrystal formers are more, and unlike solvates they are stable as complexes. However hydrate of salts or cocrystals is still possible as water often found to be included in most of the crystalline forms. The need for the amorphous or polymorph or pseudopolymoprh (solvate/hydrate) or salt or a cocrystal is API specific. A thorough screening[48] for all the possible forms of API is considered to be an indispensable step in pharmaceutical industry which further allows to choose the best form with all the desirable properties for further drug formulation and processing. Single crystal X-ray diffraction, powder XRD diffraction, IR/Raman Spectroscopy, DSC/TGA and other thermal methods, Microscopy and Solid-state NMR spectroscopy techniques are currently used to characterize these various crystalline phases.[29d] Solving the crystal structures from powder XRD data is one of the current challenges of crystal engineering.[84]

1.7 Crystal structure prediction

The possibility to reliably calculate crystal structure from only molecular information is known as *ab initio* crystal structure prediction (CSP),[85] which is considered to be the

ultimate challenge in crystal engineering. Polymorphism and crystal structure prediction are related aspects of crystal engineering as both of them deal with the occurrence of alternative structures in a narrow energy range.[86] Most methods of CSP are based on a search for the crystal structure that corresponds to the global minimum in the lattice energy. CSP involve three general steps: 1) Building a molecular structure from the chemical bonding diagram 2) Searching for plausible packing arrangements of the molecule 3) Ranking the generated structures by some criteria, usually lowest lattice energy. Recognizing the importance of CSP, blind tests were conducted by the Cambridge Crystallographic Data Centre (CCDC) in 1999, 2001, 2004 and 2007 to test how well currently available methods of crystal structure prediction perform.[87] The progress during the last two decades has been substantial, bringing the possibility of successful structure predictions within reach and establishing it as a tool in combination with experimental methods to gain profound expertise on crystalline materials. Predicting conformationally flexible molecules, cocrystals, and $Z' > 1$ structures is a current challenge in CSP.[88] There is renewed interest in why some compounds crystallize with more than one molecule in the asymmetric unit ($Z' > 1$)[89,90,91] which is expected to shed light on the future directions of crystal structure prediction.

To summarize, modern crystal engineering has emerged as a rich discipline whose success requires an iterative process of synthesis, crystallography, crystal structure analysis, and computational methods. By focusing on the molecular recognition events during nucleation and growth, crystal engineering has uncovered new ways of controlling the internal structure and symmetry of crystals and of producing materials with useful chemical and physical properties. Recent advances in crystal engineering are proved to be successful in several exciting new areas of research, such as catalysis, electronic materials, magnetic sensors, non-linear optics, nanotechnology, protein-receptor binding, microporous materials, supramolecular devices, molecular modelling and drug design.[7]

1.8 References

1. J.-M. Lehn, *Pure Appl. Chem*., **1978**, *50*, 871.
2. (a) J.-M. Lehn, *Supramolecular Chemistry: Concepts and Perspectives*, VCH: Weinheim, **1995**. (b) J. L. Atwood, J. W. Steed, *Encyclopedia of Supramolecular Chemistry*, Marcel Dekker, New York**, 2004.** (c) J. W. Steed, D. R. Turner, K. J. Wallace, *Core Concepts of Supramolecular Chemistry and Nanochemistry*, John Wiley & Sons, Wiley, **2007**. (d) E. Weber, *Supramolecular chemistry II-Host Design and Molecular Recogniton*, Springer-Verlag, Berlin, **1995**.
3. (a) R. Bishop, F. Toda, D. D. MacNicol, *Solid-State Supramolecular Chemistry*: *Crystal Engineering* Vol.6, in *Comprehensive Supramolecular Chemistry*, Pergamon, Chichester (UK), **1996**. (b) G. R. Desiraju, *Curr. Sci*. **2001**, *81*, 1023. (c) D. Braga, G. R. Desiraju, J. S. Miller, A.. G. Orpen, S. L. Price, *CrystEngComm* **2002**, *4*, 500. (d) A. Nangia, G. R. Desiraju, *Acta Cryst*. **1998**, *A54*, 934. (e) C. B. Aakeroy, *Acta Cryst*. **1997**, *B53*, 569. (f) D. Braga, *Chem. Commun*. **2003**, 2751. (g) G. R. Desiraju, *Nature 412*, **2001**, 397.
4. R. Pepinsky, *Phys. Rev*. **1955**, *100*, 52.
5. G. M. J. Schmidt, *Pure Appl. Chem*. **1971**, *27*, 647.
6. G.R. Desiraju, *Crystal Engineering: The Design of Organic Solids*, Elsevier, Amsterdam, **1989**.
7. (a) E. R. T. Tiekink, J. J. Vittal (Eds.), *Frontiers in Crystal Engineering*, Wiley, **2006**. (b) G. R. Desiraju (Ed.), *Crystal Design: Structure and Function, Perspectives in Supramolecular Chemistry*, Vol 7. Wiley & Sons, **2003**. (c) E. Weber (Ed.), *Design of Organic Solids*, Springer-Verlag, Berlin, **1998**. (d) G. R. Desiraju, *J. Mol. Struct*. **2003**, *656*, 5. (e) K. Biradha, *CrystEngComm* **2003**, *5*, 374. (f) C. V. K. Sharma, *Cryst. Growth Des.* **2002**, *2*, 465. (g) M. D. Hollingsworth, *Science* **2002**, *295*, 2410. (h) L. Brammer, *Chem. Soc. Rev.* **2004**, *33*, 476. (i) D. Braga, L. Brammer, N. R. Champness, *CrystEngComm* **2005**, *7*, 1. (j) P. Erk, H. Hengelsberg, M. F. Haddow, R. van Gelder, *CrystEngComm* **2004**, *6*, 474. (k) B. Moulton, M. J. Zaworotko, *Chem. Rev*. **2001**, *101*, 1629. (l) D. Philip, J. F. Stoddart, *Angew. Chem. Int. Ed.* **1996**, *35*, 1154. (m) G. R. Desiraju, *Angew. Chem. Int. Ed.* **2007**, *46*, 8342.

8. (a) J. D. Dunitz, *Pure Appl. Chem*. **1991**, *63*, 177. (b) J. D. Dunitz, in *Perspectives in Supramolecular Chemistry*; (Ed.) G.R. Desiraju, Wiley, NewYork, **1996**, *2*, 1.
9. A. I. Kitaigorodskii, *Molecular Crystals and Molecules*, Academic Press, New York, **1973**.
10. (a) G. A. Jeffrey, W. Saenger, *Hydrogen Bonding in Biological Structures*, Springer-Verlag, Berlin, **1991**. (b) G. A. Jeffrey, *An Introduction to Hydrogen bonding*, Oxford University Press, Oxford, **1997**. (c) T. Steiner, *Angew. Chem. Int. Ed.* **2002**, *41*, 48. (d) G. A. Jeffrey, *Crystallogr. Rev.* **2003**, *9*, 135.
11. G. R. Desiraju, T. Steiner, *The Weak Hydrogen Bond in Structural Chemistry and Biology*, Oxford University Press, Oxford, **1999**.
12. (a) G. R. Desiraju, *Acc. Chem. Res.* **1996**, *29*, 441. (b) G. R. Desiraju, *Acc. Chem. Res.* **2002**, *35*, 565. (c) G. R. Desiraju, *Chem. Commun.* **2005**, 2995.
13. (a) G. Gilli, P. Gilli, *J. Mol. Struct.* **2000**, *552*, 1. (b) J. Emsley, *J. Chem. Soc. Rev.* **1980**, *9*, 91. (c) C. L. Perrin, J. B. Nielson, *Annual. Rev. Phys. Chem.* **1997**, *48*, 511.
14. (a) E.J. Corey, *Pure Appl. Chem*. **1967**, *14*, 19. (b) E. J. Corey and X.-M. Cheng, *The Logic of Chemical Synthesis*, **1989**, Wiley, New York. (c) K. C. Nicolaou and E. J. Sorensen, *Classics in Total Synthesis*, **1995**, VCH, Weinheim.
15. (a) G. R. Desiraju, *Angew. Chem. Int. Ed. Engl.* **1995**, *34*, 2311. (b) A. Nangia, G. R. Desiraju, *Top. Curr. Chem.* **1998**, *198*, 57.
16. C. B. Aakeröy, A. M. Beatty, B. A. Helfrich, *J. Am. Chem. Soc.* **2002**, *124*, 14425.
17. (a) Cambridge Structural Database, CSD, version 5.29, ConQuest 1.10, November 2007 release, January update. (b) F. H. Allen, *Acta Crystallogr*. **2002**, *B58*, 380. (c) A. Nangia, *CrystEngComm* **2002**, *4*, 93. (d) F. H. Allen, R. Taylor, *Chem. Soc. Rev.* **2004**, *33*, 463. (e) F. H. Allen, W. D. S. Motherwell, *Acta. Crystallogr.* **2002**, *B58*, 407.
18. F. H. Allen, W. D. S. Motherwell, P. R. Raithby, G. P. Shields, R. Taylor, *New. J. Chem*. **1999**, 25.
19. T. Steiner, *Acta Crystallogr.* **2001**, B*57*, 103.
20. J. A. McMahon, J. A. Bis, P. Vishweshwar, T. R. Shattock, O. L. McLaughlin, M. J. Zaworotko, *Z. Kristallogr.* **2005**, *220*, 340.

21. R. D. B. Walsh, M. W. Bradner, S. Fleishman, L. A. Morales, B. Moulton, N. Rodríguez-Hornedo, M. J. Zaworotko, *Chem. Commun.* **2003**, 186.
22. (a) C. B. Aakeröy, D. J. Salmon, *CrystEngComm* **2005**, *7*, 439. (b) B. R. Bhogala, S. Basavoju, A. Nangia, *CrystEngComm* **2005**, *7*, 551. (c) B. R. Bhogala, S. Basavoju, A. Nangia, *Cryst. Growth Des*. **2005**, *5*, 1683. (d) A. V. Trask, W. D. S. Motherwell, W. Jones, *Cryst. Growth Des.* **2005**, *5*, 1013. (e) X. Gao, T. T. Friščić, L. R. MacGillivray, *Angew. Chem. Int. Ed.* **2004**, *43*, 232. (f) B. R. Bhogala, A. Nangia, *Cryst. Growth Des.* **2003**, *3*, 547. (g) C. B. Aakeröy, A. M. Beatty, B. A. Helfrich, *Angew. Chem. Int. Ed.* **2001**, *40*, 3240. (h) B. R. Bhogala, A. Nangia, *New. J. Chem.* **2008**, *32*, 800. (i) P. Vishweshwar, A. Nangia, V. M. Lynch, *J. Org. Chem.* **2002**, *67*, 556.
23. (a) P. Vishweshwar, A. Nangia, V. M. Lynch, *CrystEngComm* **2003**, *5*, 164. (b) K. Biradha, M. J. Zaworotko, *J. Am. Chem. Soc.* **1998**, *120*, 6431. (c) J. A. Bis, O. L. McLaughlin, P. Vishweshwar, M. J. Zaworotko, *Cryst. Growth Des.* **2006**, *6*, 2648.
24. (a) V. R. Vangala, R. Mondal, C. K. Broder, J. A. K. Howard, G. R. Desiraju, *Cryst. Growth Des.* **2005**, *5*, 99.
25. (a) P. Vishweshwar, A. Nangia, V. M. Lynch, *Cryst. Growth Des*. **2003**, *3*, 783. (b) L. S. Reddy, P. M. Bhatt, R. Banerjee, A. Nangia, G. J. Kruger, *Chem. Asian J.* **2007**, *2*, 505.
26. J. A. Bis, M. J. Zaworotko, *Cryst. Growth Des.* **2005**, *5*, 1169.
27. (a) L. S. Reddy, N. J. Babu, A. Nangia, *Chem. Commun.* **2006**, 1369. (b) N. J. Babu, L. S. Reddy, A. Nangia, *Mol. Pharma.* **2007**, *4*, 417.
28. http://en.wikipedia.org/wiki/Crystallization
29. (a) J. Bernstein, *Polymorphism in Molecular Crystals*, Clarendon, Oxford, **2002**. (b) R. Hilfiker, *Polymorphism in the Pharmaceutical Industry*, Wiley–VCH, Weinheim, Weinheim, **2006**. (c) H. G. Brittan, *Polymorphism in Pharmaceutical Solids*, Marcel Dekker, New York, **1999**. (d) S. R. Byrn, R. R. Pfeiffer and J. G. Stowell, *Solid-State Chemistry of Drugs*; West Lafayette, IN, **1999**. (e) T. L. Threlfall, *Analyst* **1995**, *120*, 2435. (f) B. Rodríguez-Spong, C. P. Price, A. Jayashankar, A. J. Matzger, N. Rodríguez-Hornedo, *Adv. Drug. Del. Rev.* **2004**, *56*, 241. (g) J. Bernstein, R. J. Davey, J. -O. Henck, *Angew. Chem. Int. Ed.* **1999**, *38*, 3440.

30. W. F. Ostwald, *Z. Phys. Chem.* **1897**, *22*, 289.
31. (a) A. Nangia, G. R. Desiraju, *Chem. Commun.* **1998**, 605. (b) A. L. Bingham, D. S. Hughes, M. B. Hursthouse, R. W. Lancaster, S. Tavener, T. L. Threlfall, *Chem. Commun.* **2001**, 603. (c) A. Nangia, *Cryst. Growth Des.* **2006**, *6*, 2.
32. (a) L. Infantes, J. Chisholm, S. Motherwell, *CrystEngComm* **2003**, *5*, 480. (b) A. Gillon, N. Feeder, R. J. Davey, R. Storey, *Cryst. Growth Des.* **2003**, *3*, 663. (c) G. R. Desiraju, *J. Chem. Soc.* **1991**, *6*, 426.
33. W. C. McCrone, *Polymorphism in Physics and Chemistry of the Organic Solid-State*, Vol 2 ed. D. Fox, M. M. Labes, A. Weisemberg, Interscience, New York, **1965**, pp725-767.
34. (a) E. W. Pienaar, M. R. Caira, A. P. Lotter, *J. Cryst. Spectro. Res.* **1993**, *23*, 785. (b) S. R. Chemburkar, J. Bauer, K. Deming, H. Spiwek, K. Patel, J. Morris, R. Henry, S. Spanton, W. Dziki, W. Porter, J. Quick, P. Bauer, J. Donaubauer, B. A. Narayanan, M. Soldani, D. Riley, K. McFarland, *Org. Process Res. Dev.* **2000**, *4*, 413. (c) M. Mirmehrabi, S. Rohani, K. S. K. Murthy, B. Radatus, *J. Cryst. Growth* **2004**, *260*, 517.
35. (a) O. Okada, M. L. Klein, *J. Chem. Soc. Faraday Trans.* **1996**, *92*, 2463. (b) Z. Hao, A. Iqbal, *Chem. Soc. Rev.* **1997**, *26*, 203. (c) N. Panina, F. J. J. Leusen, F. F. B. J. Jassen, P. Verwer, H. Meekes, E. Vleig, G. Deroover, *J. Appl. Cryst.* **2007**, *40*, 105.
36. (a) N. Blagden, R. J. Davey, *Cryst. Growth Des.* **2003**, *3*, 873. (b) R. Davey, *Chem. Commun.* 2003, 1463. (c) J. Dunitz, J. Bernstein, *Acc. Chem. Res.*, **1995**, *28*, 193.
37. (a) R. J. Davey, K. Allen, N. Blagden, W. I. Cross, H. F. Lieberman, M. J. Quayle, S. Righini, L. Seton, G.J.T.Tiddy, *CrystEngComm* **2002**, *4*, 257. (b) D. Das, R. Banerjee, R. Mondal, J. A. K. Howard, R. Boese, G. R. Desiraju, *Chem. Commun.* **2006**, 555. (c) G. R. Desiraju, *Nat. Mater.* **2002**, *1*, 77.
38. (a) C. M. Reddy, K. A. Padmanabhan, G. R. Desiraju, *Cryst. Growth Des.* **2006**, *6*, 2720. (b) C. M. Reddy, S. Basavoju, G. R. Desiraju, *Chem. Commun.* **2005**, *19*, 2439. (c) J. Bernstein, *Nat. Mater.* **2005**, *4*, 427.
39. (a) P. K. Thallapally, R. K. R. Jetti, A. K. Katz, H. L. Carrell, K. Singh, K. Lahiri, S. Kotha, R. Boese, G. R. Desiraju, *Angew. Chem. Int. Ed.*, **2004**, *43*,

1149. (b) C. –H. Gu, K. Chatterjee, V. Young Jr, D. J. W. Grant, *J. Cryst. Growth* **2002**, *235*, 471.

40. (a) C. A. Mitchell, L. Yu, M. D. Ward, *J. Am. Chem. Soc.* **2001**, *123*, 10830.
41. X. Sun, B. A. Garetz, A. S. Myerson, *Cryst. Growth Des.* **2006**, *6*, 684.
42. J. L. Hilden, C. E. Reyes, M. J. Kelm, J. S. Tan, J. G. Stowell, K. R. Morris, *Cryst. Growth Des.* **2003**, *3*, 921.
43. G. Di Profio, S. Tucci, E. Curcio, E. Drioli, *Cryst. Growth Des.* **2007**, *7*, 526.
44. (a) M. D. Lang, A. L. Grzesiak, A. J. Matzger, *J. Am. Chem. Soc.* **2002**, *124*, 14834. (b) C. P. Price, A. L. Grzesiak, A. J. Matzger, *J. Am. Chem. Soc.* **2005**, *127*, 5512.
45. A. V. Trask, N. Shan, W. D. S. Motherwell, W. Jones, S. Feng, R. B. H. Tan, K. J. Carpenter, *Chem. Commun.* **2005**, 880.
46. (a) A. Bouchard, N. Jovanović, G. W. Hofland, E. Mendes, D. J. A. Crommelin, W. Jiskoot, G. Witkamp, *Cryst. Growth Des.* **2007**, *7*, 1432. (b) R. Hiremath, J.A. Basile, S.W. Varney, J. A. Swift, *J. Am. Chem. Soc.* **2005**, *127*, 18321.
47. A. Llinás, K. J. Box, J. C. Burley, R. C. Glen, J. M. Goodman, *J. Appl. Crystallogra.* **2007**, *40*, 379.
48. S. L. Morissette, Ö. Almarsson, M. L. Peterson, J. F. Remenar, M. J. Read, A. V. Lemmo, S. Ellis, M. J. Cima, C. R. Gardner, *Adv. Drug. Del. Rev.* **2004**, *56*, 275.
49. A. Linás, J. M. Goodman, *Drug. Disc. Today* **2008**, *13*, 198.
50. http://www.fda.gov/cder/ondc/Presentations/WilsonDeCamp.doc
51. http://findarticles.com/p/articles/mi_m1200/is_8_166/ai_n7069007/pg_1
52. A. I. Kitaigorodskii, *Organic Chemical Crystallography*, Consultants Bureau, **1961**, pp 222-240.
53. http://reference.iucr.org/dictionary/Isomorphous_crystals
54. http://reference.iucr.org/dictionary/Isostructural_crystals
55. (a) A. Kálmán, L. Párkáanyi, L. Fábián, *Acta Crystallogr.* **1993**, *B49*, 1039. (b) L. Fábián, A. Kálmán, *Acta Crystallogr.* **1999**, *B55*, 1099.
56. L. Fábián, A. Kálmán, *Acta Crystallogr.* **2004**, *B60*, 547.
57. (a) G. Argay, A. Kálmán, B. Ribár, S. Vladimirov, D. Zivanov-Stackic, *Acta. Crystallogr.* **1987**, *C43*, 922. (b) A. Kálmán, G. Argay, D. Zivanov-Stackic, S. Vladimirov, B. Ribár, *Acta. Crystallogr.* **1992**, *C48*, 812.

58. (a) A. Anthony, M. Jaskólski, A. Nangia, G. R. Desiraju, *Chem. Commun.* **1998**, 2537. (b) A. Anthony, M. Jaskólski, A. Nangia, *Acta Crystallogr.* **2000**, *B56*, 512.
59. N. K. Nath, B. K. Saha, A. Nangia, *New. J. Chem.* **2008**, ASAP, DOI: 10.1039/b804905j.
60. K. F. Bowes, C. Glidewell, J. N. Low, M. Melguizo, A. Quesada, *Acta. Crystallogr.* **2003**, *C59*, o4.
61. H. Karfunkel, H. Wilts, Z. Hao, A. Iqbal, J. Mizuguchi, Z. Wu, *Acta. Crystallogr.* **1999**, *B55*, 1075.
62. (a) M. Caira, in *Encyclopedia of Supramolecular Chemistry*, Eds J. L Atwood, J. Steed, Marcel Dekker, New York, **2004**, pp 767-775. (b) G. P. Bettinetti, M. R. Caira, M. Sorrenti, L. Catenacci, M. Ghirardi, L. Fábián, *J. Therm. Anal. Cal.* **2004**, *77*, 695.
63. (a) A.V. Trask, W. Jones, *Top. Curr. Chem.* **2005**, *254*, 41. (b) T. Friščić, L. Fábián, J. C. Burley, W. Jones, W. D. S. Motherwell, *Chem. Commun.* **2006**, 5009. (c) A. Jayasankar, A. Somwangthanaroj, Z. J. Shao, N. Rodríguez-Hornedo, *Phama. Res.* **2006**, *23*, 2381.
64. (a) G. R. Desiraju, *CrystEngComm* **2003**, *5*, 466. (b) J. D. Dunitz, *CrystEngComm* **2003**, *5*, 506. (b) F. Lara-ochaoa, G. Espinosa-peréz, *Supramol. Chem.* **2007**, *19*, 553.
65. Ö. Almarsson, M. J. Zaworotko, *Chem. Commun.* **2004**, 1889.
66. P. Metrangolo, H. Neukirch, T. Pilati, G. Resnati, *Acc. Chem. Res.* **2005**, *38*, 386.
67. (a) G. W. Coates, A. R. Dunn, L. M. Henling, D. A. Dougherty, R. H. Grubbs, *Angew. Chem. Int. Ed. Engl.* **1997**, *36*, 248. (b) V. R. Vangala, A. Nangia, V. M. Lynch, *Chem. Commun.* **2002**, 1304.
68. (a) M. C. Etter, *Acc. Chem. Res.* **1990**, *23*, 120. (b) M. C. Etter, *J. Phys. Chem.* **1991**, *95*, 4601.
69. (a) M. C. Etter, *Acc. Chem. Res.* **1990**, *23*, 120. (b) M. C. Etter, *J. Phys. Chem.* **1991**, *95*, 4601.
70. C. T. Seto, G. M. Whitesides, *J. Am. Chem. Soc.* **1990**, *112*, 6409.

71. (a) Y.-L. Chang, A.-N. West, F. W. Fowler, J. W. Lauher, *J. Am. Chem. Soc.* **1993**, *115*, 5991. (b) J. J. Kane, R. F. Liao, J. W. Lauher, F. W. Fowler, *J. Am. Chem. Soc*. **1995**, *117*, 12003.
72. (a) M. D. Cohen, G. M. J. Schmidt, F. I. Sonntag, *J. Chem. Soc.* **1964**, 2000. (b) G. M. J. Schmidt, *J. Chem. Soc.* **1964**, 2014.
73. L.R. MacGillivray, J. L. Reid, J. A. Ripmeester, *J. Am. Chem. Soc.* **2000**, *122*, 7817.
74. (a) A. S. Canon, J. C. Warner, *Cryst. Growth Des.* **2002**, *2*, 255. (b) B. M. Foxman, D. J. Guarrera, L. D. Taylor, D. vanEngen, J. C. Warner, *Crystal Engineering* **1998**, *1*, 109.
75. (a) N. Rodríguez-Hornedo, Guest Editor, Special Section on Pharmaceutical Cocrystals, *Mol. Pharma.* **2007**, *4*, 299–434. (b) P. Vishweshwar, J. A. McMahon, J. A. Bis, M. J. Zaworotko, *J. Pharma. Sci*. **2006**, *95*, 499. (c) W. Jones, W. D. S. Motherwell, A. V. Trask, *Mat. Res. Soc.* **2006**, *31*, 875.
76. GRAS chemicals list is available at http://www.cfsan.fda.gov/~dms/eafus.html.
77. J. F. Remenar, S. L. Morissette, M. L. Peterson, B. Moulton, J. M. MacPhee, H. R. Guzmán, Ö. Almarsson, *J. Am. Chem. Soc.* **2003**, *125*, 8456.
78. M. B. Hickey, M. L. Peterson, L. A. Scoppettuolo, S. L. Morrisette, A. Vetter, H. Guzmán, J. F. Remenar, Z. Zhang, M. D. Tawa, S. Haley, M. J. Zaworotko, Ö. Almarsson, *Eur. J. Pharm. Biopharm.* **2007**, *67*, 112.
79. (a) A. V. Trask, W. D. S. Motherwell, W. Jones, *Cryst. Growth Des.* **2005**, *5*, 1013. (b) A. Trask, W. D. S. Motherwell, W. Jones, *Int. J. Pharm*. **2006**, *320*, 114.
80. N. Shan, M. J. Zaworotko, *Drug. Disc. Today* **2008**, *13*, 440.
81. C. B. Aakeröy, M. E. Fasulo, J. Desper, *Mol. Pharma.* **2007**, *4*, 317.
82. S. L. Childs, G. P. Stahly, A. Park, *Mol. Pharma.* **2007**, *4*, 323.
83. C. Laurence, H. Berthelot, *Perspect. Drug. Discovery Des.* **2000**, *18*, 39.
84. K. D. M. Harris, E. Y. Cheung, *Chem. Soc. Rev.* **2004**, *33*, 526.
85. S. L. Price, *Encyclopedia of Supramolecular Chemistry*, Eds J. L Atwood, J. Steed, Marcel Dekker, New York, **2004**, pp 371-379.
86. G. R. Desiraju, *Science* **1997**, *278*, 404.
87. (a) J. P. M. Lommerse, W. D. S. Motherwell, H. L. Ammon, J. D. Dunitz, A. Gavezzotti, D. W. M. Hofmann, F. J. J. Leusen, W. T. M. Mooij, S. L. Price, B.

Schweizer, M. U. Schmidt, B. P. van Eijck, P. Verwer, D. E. Williams, *Acta Crystallogr.* **2000**, *B56*, 697. (b) W. D. S. Motherwell, H. L. Ammon, J. D. Dunitz, A. Dzyabchenko, P. Erk, A. Gavezzotti, D. W. M. Hofmann, F. J. J. Leusen, J. P. M. Lommerse, W. T. M. Mooij, S. L. Price, H. Scheraga, B. Schweizer, M.U. Schmidt, B. P. van Eijck, P. Verwer, D. E. Williams, *Acta Crystallogr.* **2002**, *B58*, 647. (c) G. M. Day, W. D. S. Motherwell, H. L. Ammon, S. X. M. Boerrigter, R. G. Della Valle, E. Venuti, A. Dzyabchenko, J. D. Dunitz, B. Schweizer, B. P. van Eijck, P. Erk, J. C. Facelli, V. E. Bazterra, M. B. Ferraro, D. W. M. Hofmann, F. J. J. Leusen, C. Liang, C. C. Pantelides, P. G. Karamertzanis, S. L. Price, T. C. Lewis, H. Nowell, A. Torrisi, H. A. Scheraga, Y. A. Arnautova, M. U. Schmidt, P. Verwer, *Acta Crystallogr.* **2005**, *B61*, 511.

88. (a) T. Beyer, T. Lewis, S. L. Price, *CrystEngComm* **2001**, *44*, 1. (b) J. D. Dunitz, *Chem. Commun.* **2003**, *9*, 545.
89. J. W. Steed, *CrystEngComm* **2003**, *5*, 169.
90. (a) G. R. Desiraju, *CrystEngComm* **2007**, *9*, 91. (b) K. M. Anderson, J. W. Steed, *CrystEngComm* **2007**, *9*, 328.
91. S. Roy, R. Banerjee, A. Nangia, G. J. Kruger, *Chem. Eur. J* **2006**, *12*, 3777. (b) A. Nangia, *Acc. Chem. Res.* **2008**, *41*, 595.

CHAPTER 2

STRONG HYDROGEN BONDING IN NEUTRAL POLYCARBOXYLIC ACIDS

2.1 Introduction

The hydrogen bond was discovered almost 100 years ago, but still it is a topic of vital scientific research. The reason for this continued interest lies in the eminent importance of hydrogen bonding in the structure, function, and dynamics of a vast number of chemical and biological systems.[1] The hydrogen bond, X–H···A is an electrostatic attractive interaction between a covalently bonded hydrogen atom or hydrogen bond donor and a strongly electronegative atom with lone pair of electrons or hydrogen bond acceptor. Hydrogen bonds cover a wide and continuous energy scale from −0.5 to nearly −40 kcal mol^{-1}. The very weakest of hydrogen bonds (C–H···O/N with 0.5–2.0 kcal mol^{-1}) are barely distinguishable from van der Waals interactions while the very strongest ones (O–H···O^- and F–H···F^- have bond energies between 20–40 kcal mol^{-1}) are almost close to weak covalent bonds. Strong hydrogen bonds like O–H···O, O–H···N and N–H···O have enthalpic energies of 5–10 kcal mol^{-1}. Although non-covalent interactions are very weak in terms of energy when compared to conventional covalent bonds, many such interactions collectively add up and play an important role in chemical and biological systems. Further they can be made and broken easily, facilitating rapid molecular recognition and chemical reaction.

2.2 Classification of hydrogen bonds

Based on their strength and directionality, Desiraju and Steiner classified hydrogen bonds into three categories:[2] weak, strong and very strong hydrogen bonds. Some of the examples and properties of all these hydrogen bond types are listed in table 1. These hydrogen bonds can be explained pictorially by considering the potential energy curves[3] (Figure 1). It can be represented as an unsymmetrical double-well potential for weak and strong hydrogen bonds, C−H···O and O−H···O, where hydrogen atoms are firmly confined to one of the atom with high energy barrier from the zero point energy level. But for very strong hydrogen bonds, two minima become more equal and form a shallow, symmetrical double-well potential such that the proton has sufficient vibrational

energy to tunnel through the small activation barrier, O−H···O ↔ O···H−O. When the barrier completely disappears, it becomes a single-well potential, where position of the hydrogen atom is centered between the two heavy atoms, i.e. O···H···O. These are called as low-barrier hydrogen bonds or short-strong hydrogen bonds.[4]

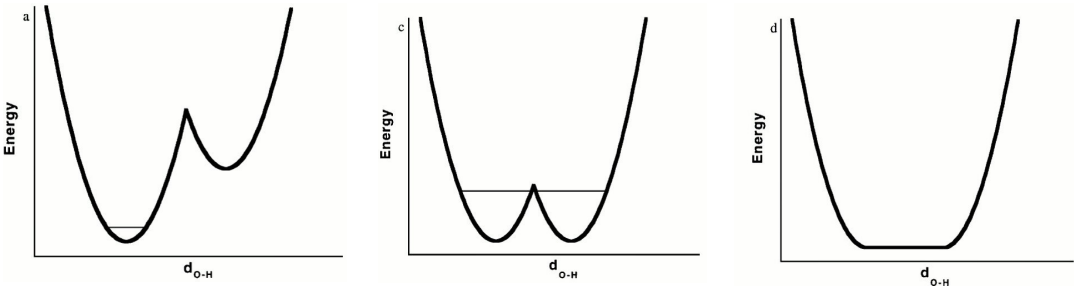

(a) (b) (c)

Figure 1. (a) Unsymmetrical double-well potential for weak and strong hydrogen bonds. (b) Symmetrical double-well potential for very strong or low-barrier hydrogen bonds. (c) Single well potential with hydrogen atom located exactly at the centre of hydrogen bond.

Table 1. Some properties of very strong, strong and weak hydrogen bonds.[2]

	Very Strong	**Strong**	**Weak**
Bond energy, (kcal mol^{-1})	15–40	4–15	< 4
Examples	$[F\cdots H\cdots F]^-$ $[N\cdots H\cdots N]^+$ P−OH···O=P	O−H···O=C N−H···O=C O−H···O−H	C−H···O/N O/N−H···π
Bond lengths	H–A ≈ X–H	H···A > X–H	H···A >>X–H
Lengthening of X–H (Å)	0.05–0.2	0.01–0.05	≤ 0.01
d (H···A) range (Å)	1.2–1.5	1.5–2.2	2.0–3.0
D (X···A) range (Å)	2.2–2.5	2.5–3.2	3.0–4.0
θ (X–H···A) range (°)	175–180	130–180	90–180
IR ν, relative shift	> 25%	5–25%	< 5%
^{1}H-chemical shift downfield (ppm)	14–22	< 14	–
Bonds shorter than vdW	100%	Almost 100%	30–80%
Effect on crystal packing	Strong	Distinctive	Variable
Covalency	Pronounced	Weak	Vanishing
Electrostatics	Dominant	Significant	Moderate

Low Barrier Hydrogen Bonds, LBHB, (O···O distance < 2.5Å) have drawn special attention in recent years as they are invoked to explain enzyme catalyzed reactions. Their presence in the transition state or in an enzyme-intermediate complex suggests that they play an important role in stabilizing the transition states of enzymatic reactions.[4] The formation of such LBHB can supply 10 to 20 kcal mol^{-1} and thus facilitate difficult enzymatic reactions. Short hydrogen bonds with Gly 193, Ser 195 and His 57 in the transition state of hydrolysis reaction of peptide Chymotrypsin[4a] is shown in figure 2.

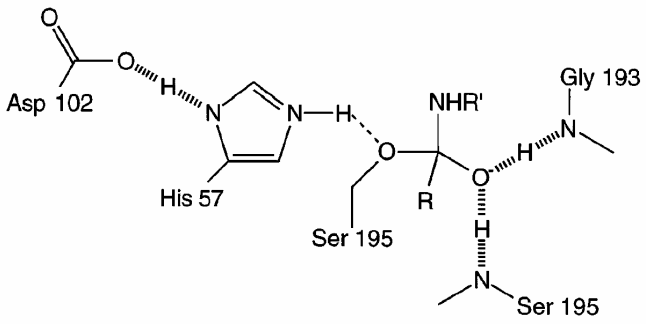

Figure 2. Low-barrier hydrogen bonds with Gly 193, Ser 195 and Asp 102 are proposed to stabilize transition state of hydrolysis reaction of peptide Chymotripsin.

In general most of the weak and strong neutral hydrogen bonds in molecular crystals that are purely electrostatic in nature fall under Isolated Hydrogen Bond category (IHB, C−H···O, C−H···N, O−H···O and N−H···O) but few of them also form Polarization Assisted Hydrogen Bonds via σ-cooperativity (PAHB, ···O−H···O−H···O−H···O−H···).[1c] On the other hand very strong hydrogen bonds with significant covalent or quasi-covalent character are formed with unusually activated donor and acceptors, as between an acid and its conjugate base or in the hydrates of strong acids. The very strong hydrogen bonds may be further classified into three categories:[5] (i) (±) CAHB: Charge Assisted Hydrogen Bonds[6] which are again divided into negative or positive charge assisted hydrogen bonds (O–H···O^- and O^+–H···O) depending on the accumulated charge on the heavy atom (ii) RAHB: Resonance Assisted Hydrogen Bonds[7] or π-cooperative hydrogen bonds, where the two oxygen atoms are connected by a π-conjugated system of single and double bonds (–O–H···O=C–C=C–O–H···). (iii) SAHB: Synthon Assisted Hydrogen Bonds, as a result of finite synergy from combination of σ and π-cooperative hydrogen bonds is elaborated in this thesis. Classification of hydrogen bonds in molecular crystals is summarized in scheme 1.

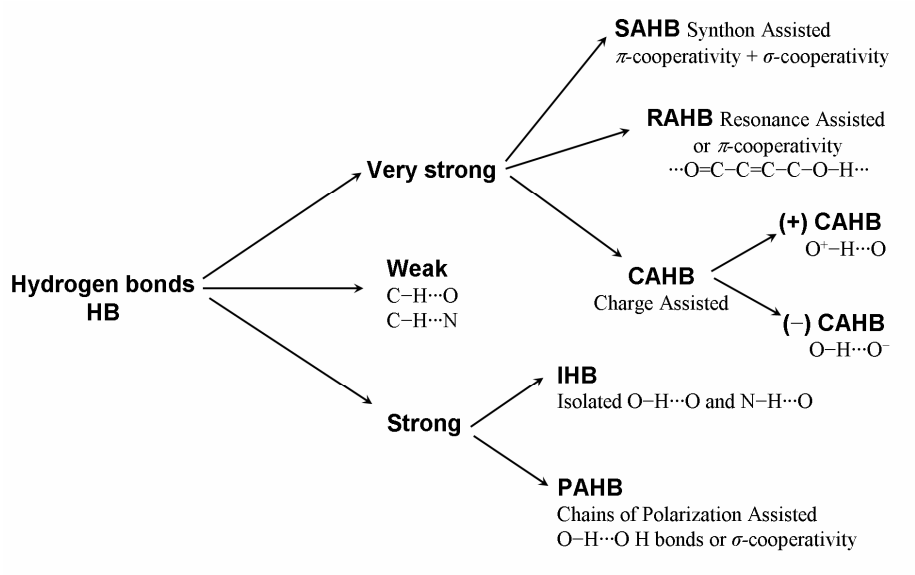

Scheme 1. Classification of Hydrogen bonds in molecular crystals.

2.3 Cooperativity

Hydrogen bonds possess the important property of cooperativity. Accordingly energy of an array of *n* interconnected hydrogen bonds is greater than the sum of those of *n* isolated bonds [$(O{-}H{\cdots}O{-}H{\cdots}O{-}H{\cdots})_n > n$ x (O−H···O)]. In other words, the whole is greater than the sum of its parts. Two principal mechanisms are responsible for this cooperativity or non-additivity, and both operate by mutual polarization of the involved groups.

2.3.1 *σ*-bond cooperativity

If an $X^{\delta-}{-}H^{\delta+}$ group forms a hydrogen bond $X^{\delta-}{-}H^{\delta+}{\cdots}A^{\delta-}$, it becomes more polar. The same is true if it accepts a hydrogen bond, $Y^{\delta-}{-}H^{\delta+}{\cdots}X^{\delta-}{-}H^{\delta+}$. Thus in a chain of two hydrogen bonds, both donor and acceptor become stronger leading to better hydrogen bonding. This effect is often called as *σ*-bond cooperativity, since the charge flow is through X−H *σ* bonds, but the terms polarization enhanced hydrogen bonding or polarization assisted hydrogen bonding have also been proposed.[8] The most typical examples are phenols and alcohols, which form infinite chains of O–H···O hydrogen bonds,[9] have remarkably short O···O distances (2.664 Å for phenol, figure 3a). Recent quantum-mechanical calculations indicate that *σ*-cooperativity can provide strength of

hydrogen bond enhancement up to 66% in long water chains with respect to water dimers.[9a] The σ-cooperativity usually tapers off around six to seven O–H···O hydrogen bonds. The polarization of a water molecule as an enhanced acceptor group has been illustrated in an exceptionally short C−H···O_{water} H-bond (d = 1.96 Å, D = 3.02 Å, θ = 169.3°; $\Delta\nu_{CH}$ = 202 cm^{-1}) in the complex (1,4-diethynylbenzene)· $(water)_2$· $(triphenylphosphine\ oxide)_4$.[10] The donation of water hydrogens to P=O groups (1.85 Å, 161°; 1.77 Å, 168°) creates a more negative electrostatic potential around the oxygen atom which results in a very short C−H···O hydrogen bond (figure 3b).

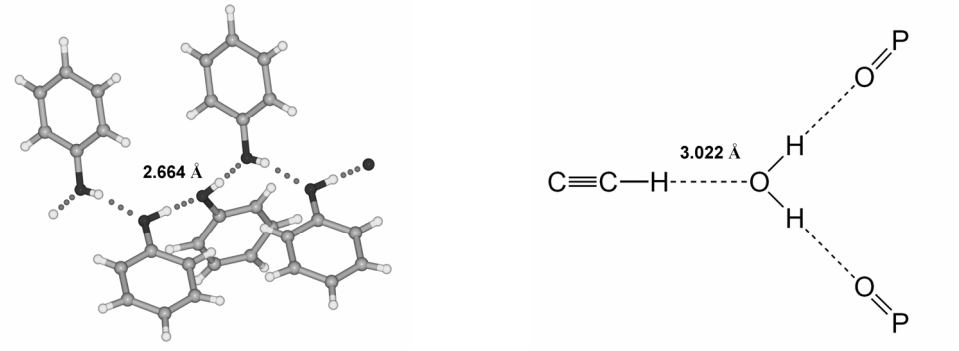

(a) (b)

Figure 3. (a) Infinite O–H···O hydrogen bonds in phenol crystal structure. (b) Very short C–H···O distance of 3.022 Å between 1,4-diethylnylbenzene and a water molecule is due to polarization assistance of O–H···O interactions with P=O oxygen atoms.

2.3.2 π-bond cooperativity

X−H groups may also be polarized by charge flow through π-bonds.[1] For example an amide N−H group becomes stronger donor if the amide O atom accepts a hydrogen bond, X−H···O=C−N−H. This results because the zwitterionic resonance form is stabilized in the amide dimer or catemer (figure 4a). The C=O bond length in formamide is increased by 0.018 Å and the C−N peptide bond length is decreased by 0.023 Å. Gilli et al. described this phenomenon as Resonance Assisted Hydrogen Bonding (RAHB) in the context of β-diketone enol system (figure 4b).[7a] Several neutral entities like carboxylic acids, ···O=C−O−H···; inorganic oxo acids, ···O=S(O)(O−H)···OH··· or ···O=$P(O−H)_2$−OH···; β-diketone enols, ···O=C−C=C−O−H···; δ-diketone enols, ···O=C−C=C−C=C−O−H··· contain very short O−H···O hydrogen bonds, all of them could be accounted by π-bond cooperativity.[7]

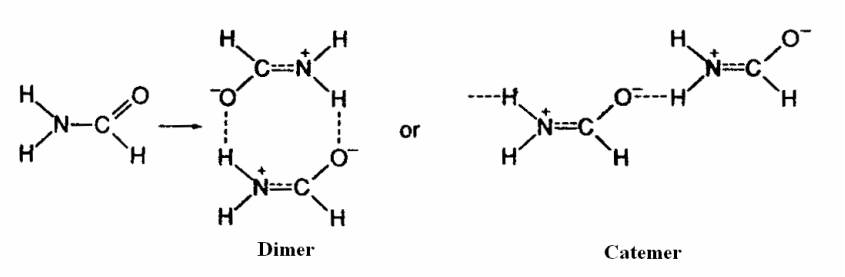

(a)

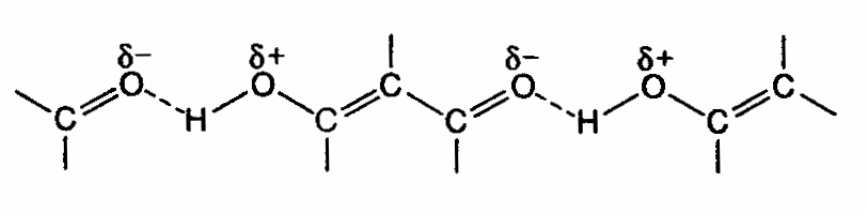

(b)

Figure 4. π-bond cooperativity in (a) formamide dimer and catemer. (b) β-diketone enols system.

2.4 Synthon Assisted Hydrogen Bonding, SAHB

Vishweshwar et al.[11] reported the low-temperature (123K) X-ray crystal structure of 2,3,5,6-pyrazinetetracarboxylic acid dihydrate, 2356PYZTA, with a very short intermolecular O_{acid}–H···O_{water} hydrogen bond (O···O = 2.4791(13) Å, H···O = 1.53 Å, θ = 171(2)º, Figure 5). It is interesting to note that a neutral pyrazine tetra acid with out activated donors/acceptors is able to form very short hydrogen bond which is comparable to charge and resonance assisted hydrogen bonds. This shortening of the O_{acid}–H···O_{water} hydrogen bond was ascribed to synergistic π- and σ-cooperativity (O–H···O=C–O–H_{acid}··· and O_{water}–H···O/N), in the finite, neutral array I (Figure 5b), named as a synthon assisted hydrogen bond,[12] adds a new category to the current classification of very short hydrogen bonds. The COOH donor is activated because it accepts a H-bond from another COOH group (labeled #, π-cooperative assistance) and the acceptor ability of oxygen is enhanced because the water donates H-bonds to COOH and pyrazine N groups (polarization assistance, σ-cooperative). All the hydrogen bonds of the multicenter SAHB motif I, O_{acid}–H···O_{acid}, O_{water}–H···O_{acid}, and O_{water}–H···N_{pyr}/O_{acid}, contribute to the shortening of the O_{acid}–H···O_{water} bond. Thus, hydrogen bond shortening results from the extended synthon and not from a single interaction like CAHB category.

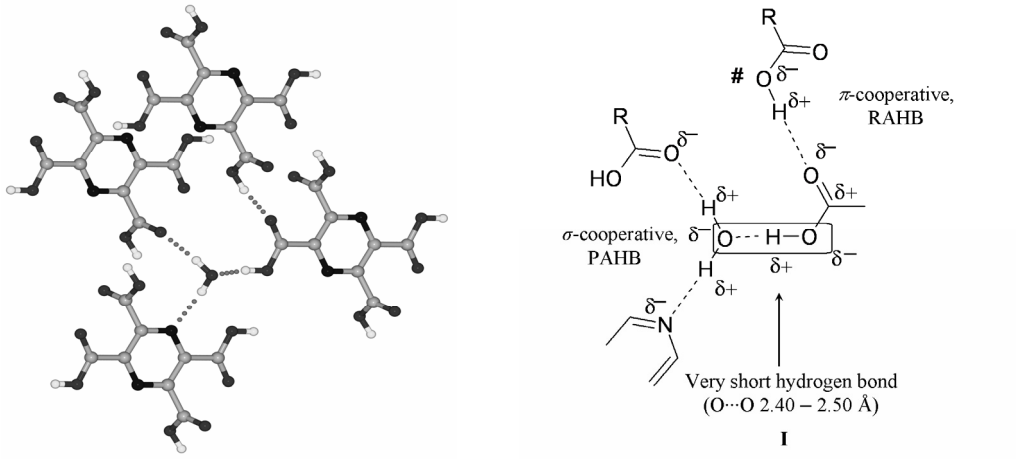

Figure 5. (a) Crystal structure of 2356PYZTA with short O_{acid}–H···O_{water} hydrogen bond. (b) Schematic representation of cooperative synthon **I** in pyrazine tetra acid. The acid group marked with # is replaced with H_2O in pyrazine dicarboxylic acids.

The short intermolecular O_{acid}–H···O_{water} hydrogen bond in 2356PYZTA is further characterized by variable temperature neutron diffraction[12] (O···O = 2.4751(11), 2.4765(10), 2.4807(12), and 2.4906(16) Å at 20, 100, 200, and 293K) so as to locate the proton accurately and to identify if there is any proton transfer or phase transition on varying the temperature. The hydrogen atom is covalently bonded to the COOH group and there is no proton migration to H_2O at all the temperatures studied. Furthermore, the C=O and C−O bond distances in the COOH group and the C−N=C angle in the pyrazine ring are in agreement with these H-bonding groups being present in a neutral form rather than as ionic/resonant species. Accordingly, potential energy well in 2356PYZTA may be treated as unsymmetrical (like in figure 1a) with an energy barrier for proton transfer because of large difference in pK_a values (COOH, ~2; H_2O, ~15). The absence of proton transfer in 2356PYZTA is crucial to the proposed π- and σ-cooperative H-bond shortening. If there is proton transfer to ionic or a delocalized hybrid structure, then H-bond shortening could well be a result of ionic donor/acceptor groups and/or resonance assistance, that is, CAHB/RAHB. However, the behaviour of the short O_{acid}–H···O_{water} hydrogen bond in 2356PYZTA is similar to short-strong CAHB/RAHB systems: (1) O···O distance < 2.50 Å, (2) quasi-covalent character of 0.27−0.30 valence units, (3) red shift in the O−H stretching frequency to 1200−1400 cm^{-1}, and (4) hydrogen bond energy of ~16 kcal mol^{-1}.

2.4.1 Fewer number of COOH groups on pyrazine ring

Several pyrazine tri and di carboxylic acids (2,3,5-pyrazinetricarboxylic acid, 235PYZTA,[12] 2,3-pyrazinedicarboxylic acid, 23PYZDA,[11] 5,6-dimethyl-2,3-pyrazinedicarboxylic acid dihydrate, 56DM23PYZDA,[11] 2,5-pyrazinedicarboxylic acid, 25PYZDA,[13a] 2,6-pyrazinedicarboxylic acid, 26PYZDA,[13b] and 5-methyl-2,3-pyrazinedicarboxylic acid, 5M23PYZDA[13c], scheme 2) with fewer number of COOH groups are systematically analyzed to study the effect on shortening of synthon assisted H-bond in multi-center array I (Figure 5b). Except 5MPYZDA,[14] all other pyrazine polycarboxylic acids crystallize as dihydrates similar to pyrazine tetra acid.

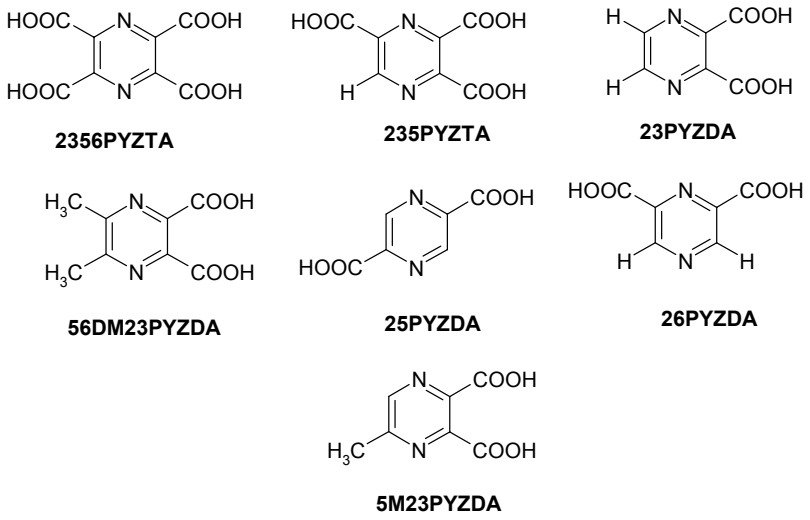

Scheme 2. Pyrazine polycarboxylic acids discussed in chapter 2.

Pyrazine di acids contain similar neutral O−H···O hydrogen bond motifs except that a water molecule replaces the COOH donor that initiates the hydrogen bond array (#COOH in **I** is replaced by water, shown as arrows in figure 6a & 6b, figure 5b). The water oxygen is polarized through hydrogen bonds with the COOH and pyrazine groups as before. The short O_{acid}−H···O_{water} H-bond is longer in all these di acids compared to pyrazine tetra acid (Table 2) for two reasons: firstly because the carboxylic acid is a stronger H-bond donor to water in tetra acid than in di acids due to more electron-withdrawing groups on the pyrazine ring. Secondly π-bond cooperativity is enhanced due to greater strength of hydrogen bond donor capacity of COOH over H_2O in di acids as shown in figure 6a and 6b.

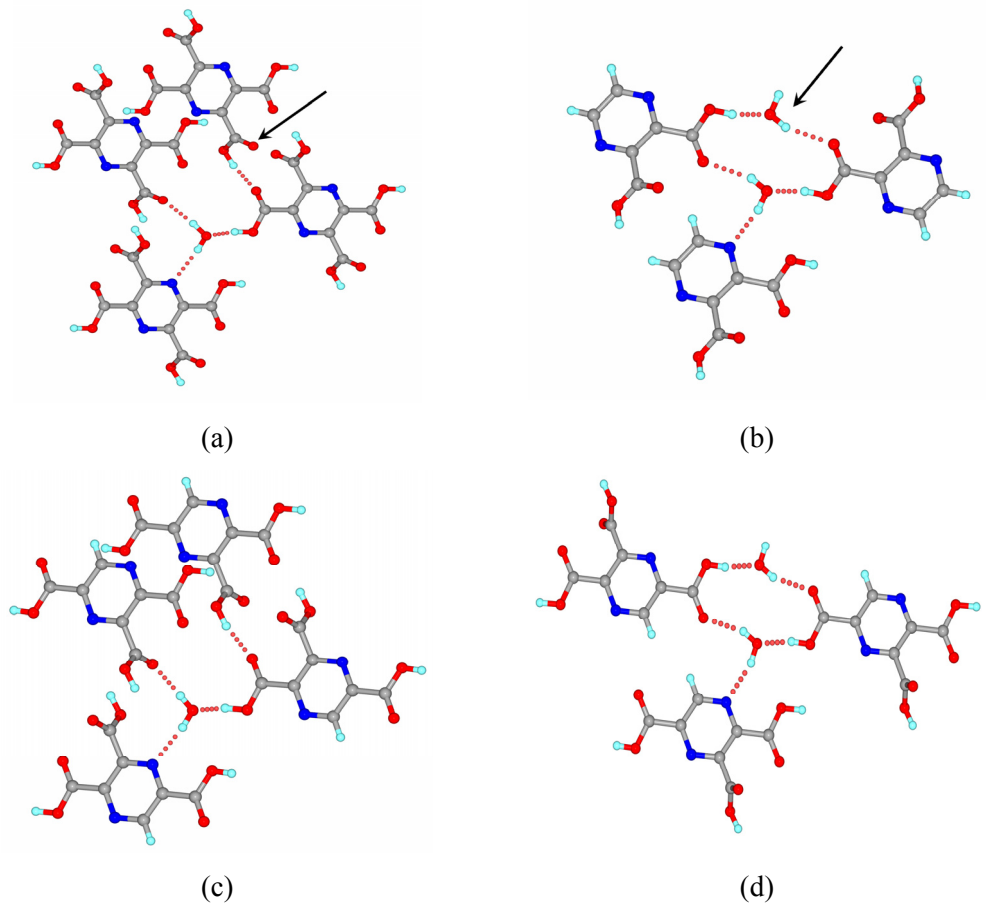

Figure 6. (a) SAHB motif in pyrazine tetra acid. (b) 23PYZDA as a representative crystal structure for SAHB motif in dicarboxylic acids. It has a similar neutral O−H···O motif as in tetra acid except that a water molecule replaces the COOH donor that initiates the H-bond array (highlighted with arrows). (c & d) The SAHB motif in tri acid has components that are similar to tetra acid (a) and di acids (b), giving an intermediate case of H-bond of motifs.

2,3,5-Pyrazinetricarboxylic acid, 235PYZTA, crystallized in the triclinic space group $P\bar{1}$ with one acid molecule and two water molecules in the asymmetric unit. The two COOH groups are roughly coplanar with the pyrazine ring, and the third COOH group is out of the plane (N1−C3−C6−O5 = 10.45 º, N2−C2−C5−O4 = 4.29 º, and N1−C1−C4−O1 = 81.02 º). The in-plane COOH group participates in the very short hydrogen bond, VSHB, similar to the crystal structure of pyrazine tetra acid. The O_{acid}−H···O_{water} H-bond (O4···O8 = 2.4726(12) Å) in pyrazine tri acid is stabilized by the synergy from π-cooperative hydrogen bond with second carboxylic acid and polarization assisted hydrogen bonds as in figure 6c. The third carboxylic acid forms a strong O_{acid}−H···O_{water} hydrogen bond motif with the second water molecule (O5···O7 = 2.5137(13) Å) similar

to that of all the pyrazine di acids as shown in figure 6d. Hence the crystal structure of pyrazine tri acid is analyzed as a combination of H-bond motifs in pyrazine tetra acid and di acids, containing hydrogen bonds of increasing distance from very short and short O_{acid}–H···O_{water} H-bonds to short and moderate O_{acid}–H···O_{acid}, O_{water}–H···O_{acid}, and O_{water}–H···N interactions. All the protons in pyrazine polycarboxylic acids are located in difference electron density maps and the neutral form of the COOH group is concluded from C=O and C−O bond distances and N−C=N angles.

Table 2. Geometrical parameters of hydrogen bonds in pyrazine polycarboxylic acids.

Compound	**T/K**	**H···A/ Å**	**D···A/ Å**	**∠D–H···A/ º**
Short O_{acid}–H···O_{water} H-bond				
2356PYZTA	123K	1.53	2.4791(13)	171.0
235PYZTA	123K	1.50	2.4726(12)	170.0
25PYZDA	153K	1.57	2.5148(13)	171.0
56DM23PYZDA	123K	1.57	2.5269(12)	167.4
23PYZDA	123K	1.61	2.5513(11)	168.0
26PYZDA	298K	1.88	2.624(2)	172.0
π–cooperative O_{acid}–H···O=C_{acid} H-bond				
2356PYZTA		1.90	2.7811(12)	172.0
235PYZTA		1.92	2.7461(12)	172.0
σ–cooperative O_{water}–H···$N_{pyrazine}$ H-bond				
2356PYZTA		2.14	2.9393(16)	157.6
235PYZTA		2.06	2.8947(13)	160.6
π–cooperative O_{acid}–H···O=C_{acid} H-bond				
2356PYZTA		1.81	2.7010(12)	163.3
235PYZTA		1.92	2.7461(12)	172.0

The more important reason for hydrogen bond shortening in array **I** is the polarization of the water, which is evident from the crystal structure of pyrazine tri acid. Even though the COOH donor in tetra acid with extra carboxylic acid group is marginally stronger than tri acid, H-bond is slightly shorter in tri acid (O···O = 2.4726(12) Å at 120 K) when compared to tetra acid (2.4791(13) Å at 123K, Table 2). This shortening of O_{acid}–H···O_{water} is due to an increase in the acceptor strength of water oxygen by polarization assisted hydrogen bonding. These σ-cooperative O_{water}–H···O_{acid} and

O_w–H···N hydrogen bonds which polarize the water oxygen are shorter in pyrazine tri acid (235PYZTA) compared to tetra acid (2356PYZTA) as shown in table 2. This shows that *the polarization of the water oxygen acceptor through σ-cooperative hydrogen bonding makes a significant contribution to H-bond shortening in neutral array* ***I***, with auxiliary support coming from π-cooperative hydrogen bonds.

2.4.2 Replacing pyrazine ring by pyridine and phenyl rings

In addition to changing the number of COOH on the pyrazine ring, the study was extended by replacing pyrazine ring with pyridine and phenyl with the same number of COOH groups as shown in scheme 3. Crystal structures of pyrazine-2,3,5,6-tetracarboxylic acid dihydrate, 2356PYZTA, pyridine-2,3,5,6-tetracarboxylic acid dihydrate,[14] PYR2356TA, and benzene-1,2,4,5-tetracarboxylic acid dihydrate,[15] BZN1245TA, are analyzed to study the effect of progressive pyrazinyl → pyridyl → Phenyl C–H ⇔ N replacement on the multi-center synthon assisted short hydrogen bond and overall crystal packing.

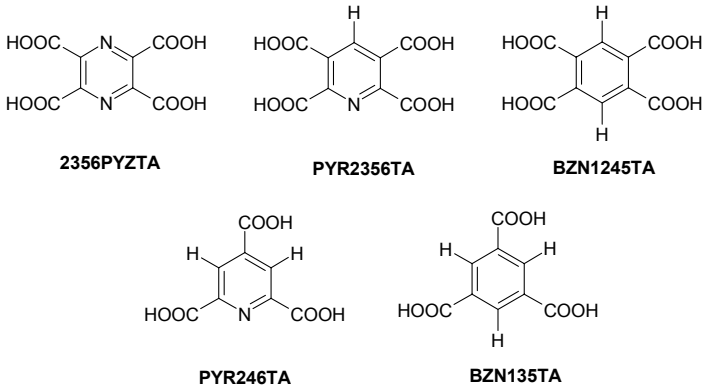

Scheme 3. Polycarboxylic acids with progressive C–H ⇔ N replacements.

Normally consequences of such C–H ⇔ N replacements are severe on hydrogen bonding and overall crystal packing, because a strong pyrazine or pyridine N acceptor is replaced by a weak phenyl C–H donor, as illustrated by examples culled from the Cambridge Structural Database:[15] *N*,*N*′-bis(3-pyridyl)urea, refcode GASNEU, *N*-phenyl-*N*-3-pyridylurea, MEPXEK and *N*,*N*′-diphenylurea, DPUREA. The sheet like structure in DPUREA is mediated by the usual urea α-network of N–H···O hydrogen bonds. When weak C–H donor is replaced with strong pyridyl N acceptor, it is able to disrupt the urea

α-network and forms N–H···N hydrogen bonds in GASNEU and MEPXEK (Figure 7).[16] Similarly Benzoic acid forms acid–acid homosynthon while nicotinic and pyrazinic acid contain acid–pyridine heterosynthon in their crystal structures (Figure 8). Nevertheless, aromatic CH ⇔ pyridyl N exchange in the lattice inclusion hosts (Figure 9)[17] and solid solution crystals[18] did not affect much on the overall crystal packing and yielded isostructural structures, as these crystal structures are mainly driven by size, shape and volume.[18a]

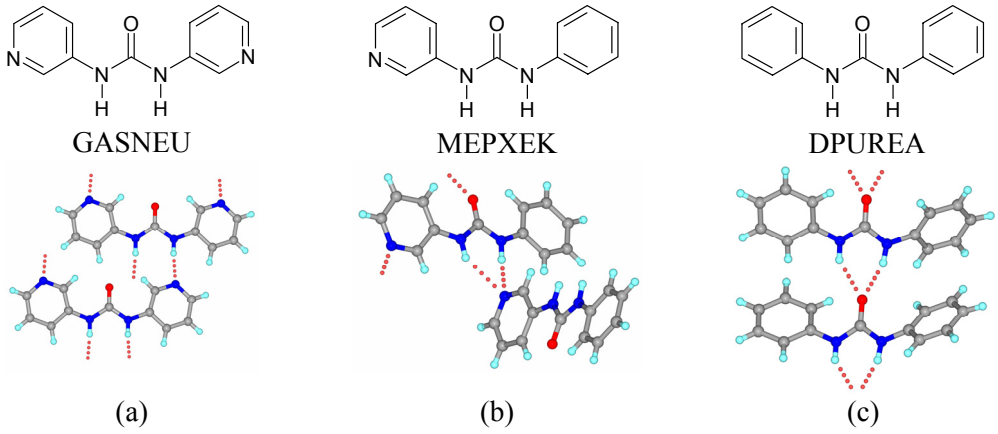

Figure 7. Usual α-network of N–H···O hydrogen bonds in DPUREA (c) is disrupted by pyridyl N acceptor in GASNEU (a) and MEPXEK (b) on C–H ⇔ N replacement.

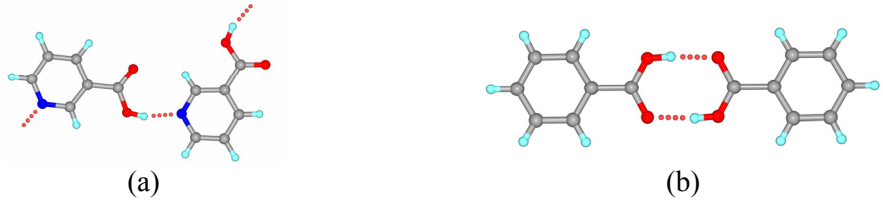

Figure 8. (a) Pyridine moiety preferably interacts with COOH in nicotinic acid. (b) While in its absence, COOH forms benzoic acid dimer homosynthon.

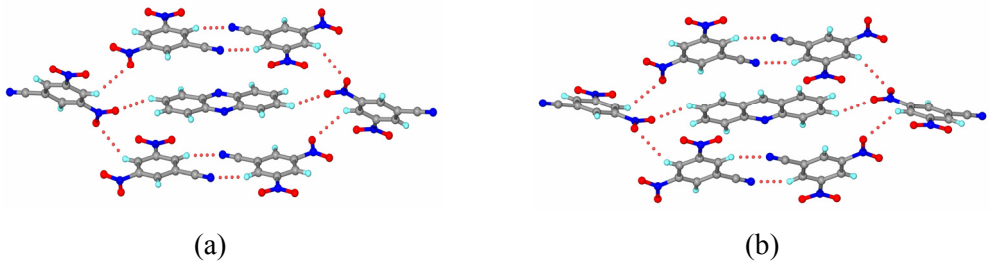

Figure 9. Representation of channels observed in three dimensional arrangement of host molecule 3,5-dinitrobenzonitrile. C–H ⇔ N replacement of phenazine by acridine yielded isostructural crystals in (a) and (b).

C–H ⇔ N replacement is a frequent modification in ligand optimization and 3D-QSAR to alter the hydrophobic/ hydrophilic balance and/or minimize side effects,[19] but its structural and functional consequences can be difficult to predict. A decrease in activity was rationalized by the O_{water}–H···N_{ligand} H-bond with quinazolinyl moiety being replaced by phenyl C–H overlap with a conserved water in the active site of scytalone dehydratase enzyme[20a] and epidermal growth factor inhibitor.[20b] Substitution of any of the C–H groups by N on the quinazoline ligand (marked * in Scheme 4) does not appreciably change the biological activity and gives comparable K_i or pIC_{50} values.

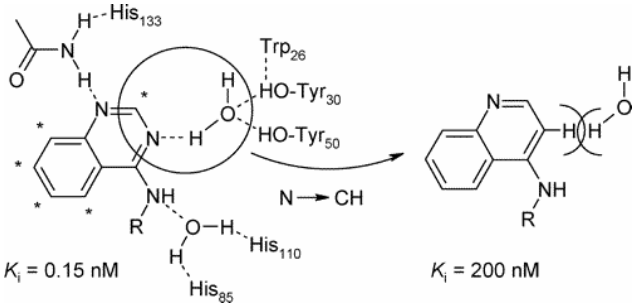

Scheme 4. Replacement of the H-bonded quinazolinyl N by CH resulted in reduced binding of the ligand to scytalone dehydratase enzyme by 3 orders of magnitude (right); replacing any of the * CH sites by N does not appreciably change the biological activity.

2.4.3 Isostructural C–H ⇔ N replacements in polycarboxylic acids

Isostructurality[21] is a connection between the three dimensional arrays of molecule and their somewhat "modified" derivative(s). These modifications can be either substitution or replacement(s) of atom(s) by others without any substantial change of the molecular isometry. The governing factors to permit or hinder the formation of similar molecular arrangements in the solid state are mainly the size of the molecules and substituents, chemical character of the substituent and site of the substitution.[18a] Isostructural pairs of molecules with functional group replacements are reported for O–H ⇔ C–H,[22] N–H ⇔ C–H,[23] halogen exchange,[24] P=O ⇔ P(l.p.),[25] H ⇔ *t*-Bu,[26] etc (⇔ indicates functional group exchange). There are several examples wherein a strong O–H···O or N–H···O hydrogen bond is replaced by a weak C–H···O interaction without disturbing the overall molecular arrangement.[23] In the literature there are no reports on C–H ⇔ N replacement especially in the presence of strong functional groups like COOH that can interfere with N acceptors. Interestingly pyrazine, pyridine and benzene tetracarboxylic acid are three dimensionally isomorphous and contain similar SAHB array of H-bonds (Table 3).

Table 3. Crystal data of polycarboxylic acid hydrate X-ray structures.

Crystal data	2356PYZTA	PYR2356TA	BZN1245TA
Space group	$P\bar{1}$	$P\bar{1}$	$P\bar{1}$
a / Å	5.4409(3)	5.5311(6)	5.4651 (6)
b / Å	6.4041(3)	6.2566(7)	6.4044 (7)
c / Å	8.6995(3)	9.0041(10)	9.1145 (11)
α / °	98.572(3)	70.187(2)	71.941 (3)
β / °	107.374(3)	76.251(2)	88.612 (3)
γ / °	105.519(3)	72.714(2)	72.933 (3)
V / Å^3	269.97(2)	276.64(5)	289.16 (6)
T / K	123	100	160
Refcode	HUCLEW[a]	YEPXUN	PYMELL11[b]

[a]Π of HUCLEW and YEPXUN is 0.009; [b]Π of YEPXUN and PYMELL11 is 0.013.

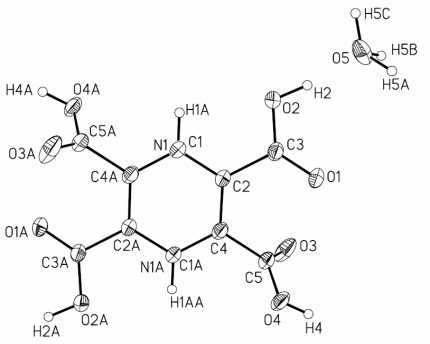

Figure 10. Asymmetric unit contains a half molecule of pyridine tetra acid and one water molecule. Half molecule of pyridine tetra acid is grown for clarity. Site occupancy for C1/N1 = 0.50. Two H atoms of water molecule are disordered over three sites on oxygen with s.o.f. H5a/5b = 0.75, H5c = 0.50. Thermal ellipsoids are drawn at 50% probability.

Pyridine-2,3,5,6-tetracarboxylic acid dihydrate, PYR2356TA, with one C–H donor and one pyridyl N acceptor is found to be an intermediate crystal structure between pyrazine tetracid with two N acceptors and benzene tetra acid with two C–H donors. The asymmetric unit of pyridine tetra acid has half molecule which is orientationally disordered such that N1 and C1 occupy the same site with 0.50 occupancy each (Figure 10). Two hydrogen atoms of water molecule are disordered over three sites on oxygen. H5a and H5b have refined site occupancy of 0.75 each and H5c is 0.50. The partial site occupancies of water molecule hydrogen atoms were derived from difference electron density maps in the 100K data set. This model of water refinement gives the best *R*-factor and is consistent with hydrogen bonding of water.

Multi-center synthon array of O_{acid}–H···O_{water}, O_{acid}–H···O_{acid}, O_{water}–H···O_{acid}, and O_{water}–H···$N_{pyridyl}$ hydrogen bonds in one of the orientation of pyridine tetra acid is similar to pyrazine tetra acid and distances are also comparable (Figure 11a1 and b1, table 4). The unit cell similarity index, Π,[21] of the two triclinic cells is 0.009 indicating good identity (Table 3). When C1 occupies the same site in the alternate orientation of pyridine tetra acid with 50% site occupancy factor, a $C_{pyridyl}$–H···O_{water} interaction replaces the O_{water}–H···$N_{pyridyl}$ hydrogen bond and forms a SAHB motif via O_{acid}–H···O_{water}, O_{acid}–H···O_{acid}, O_{water}–H···O_{acid}, and $C_{pyridyl}$–H···O_{water} array of hydrogen bonds. This orientation with $C_{pyridyl}$–H···O_{water} interaction in pyridine tetra acid is reminiscent of tetra-coordinated water in benzene tetracarboxylic acid dihydrate, B1245TA with similar packing in the crystal structure (Π = 0.013, CSD refcode PYMELL11, figure 11b1 and c1). A persistent square network of O–H···O hydrogen bonds mediated by the water molecule is present in all tetra acids as shown in figures 11a2, b2 and c2. Geometrical parameters of synthon assisted hydrogen bonds in all tetra acids are compared in table 4.

Table 4. Hydrogen bonds comparison in pyrazine, pyridine and benzene tetra acids.

Compound	H···A /Å	D···A /Å	D–H···A /º	H···A /Å	D···A /Å	D–H···A /º
Short O_{acid}–H···O_{water}				σ–cooperative O_{water}–H···$N_{pyrazine}$		
2356PYZTA	1.53	2.479(1)	171(2)	2.14	2.939(1)	157.6(1)
PYR2356TA	1.58	2.509(1)	172(3)	2.15	3.089(2)	161(4)
BZN1245TA	1.73	2.565(1)	175.0	------	------	------
π–cooperative O_{acid}–H···O=C_{acid}				σ–cooperative O_{water}–H···O=C_{acid}		
2356PYZTA	1.81	2.701(1)	163.3(1)	------	------	------
PYR2356TA	1.83	2.682(1)	168(3)	2.02	2.816(1)	158(3)
BZN1245TA	1.85	2.672(1)	165.3	2.11	2.858(1)	152(2)
π–cooperative O_{acid}–H···O=C_{acid}				C–H ···O_{water}		
2356PYZTA	1.90	2.781(1)	172(2)	------	------	------
PYR2356TA	1.93	2.896(1)	169(4)	2.15	3.089(2)	170(2)
BZN1245TA	1.92	2.766(1)	171(2)	2.33	3.276(2)	169.1

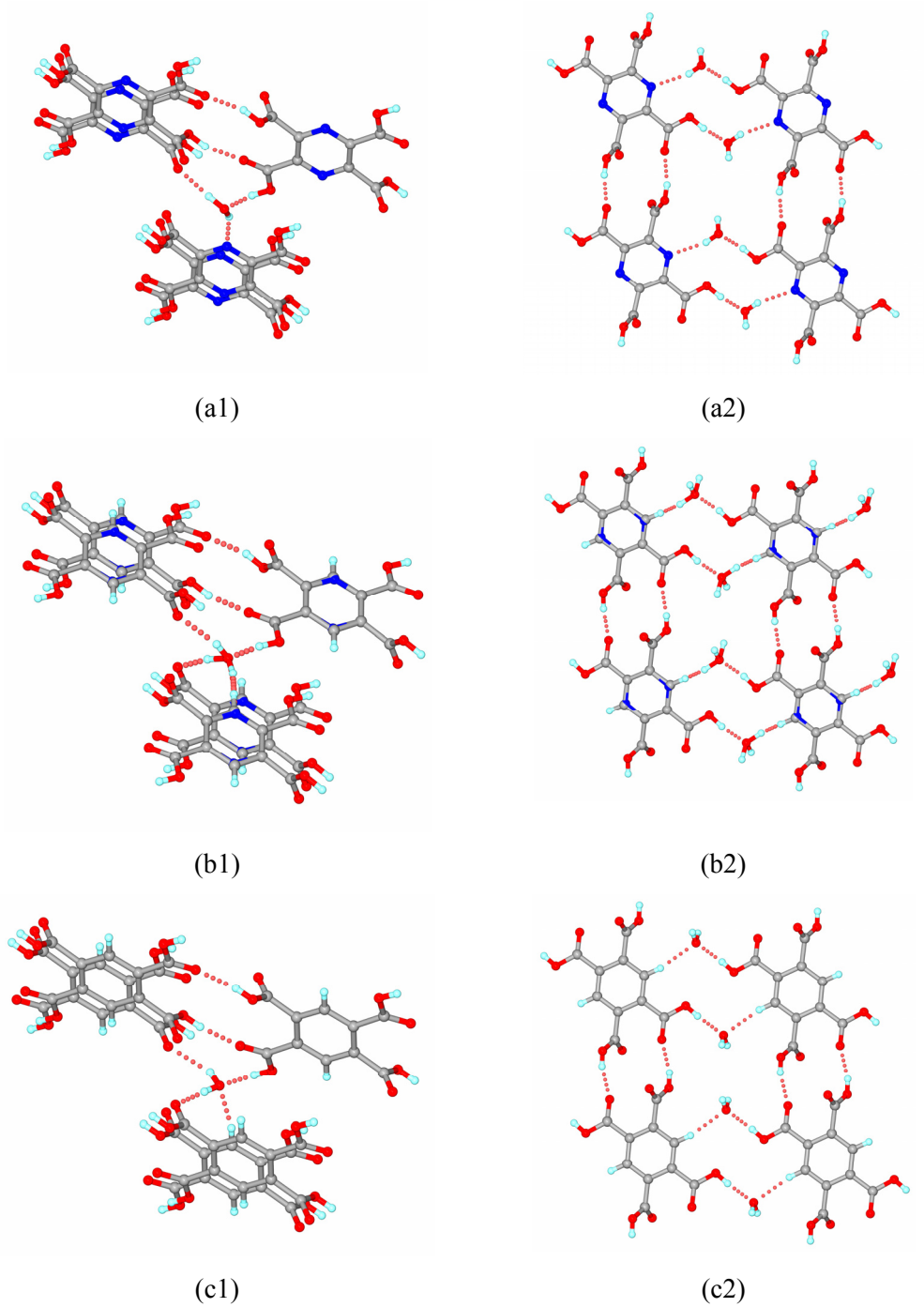

Figure 11. The multi-center synthon around strong O_{acid}–H···O_{water} hydrogen bond accommodates successive C–H ⇔ N replacement in similar supramolecular environments of (a1) pyrazine (b1) pyridine and (c1) benzene tetra acids. Heavy atom positions are identical but water H atoms reorganize depending on pyrazine, pyridine or benzene ring. Similar square network is observed in the respective crystal structures as shown in a2, b2 and c2. The water molecule accepts C–H···O interaction or donates to O–H···N hydrogen bond with disordered C1/N1 atom in pyridine tetra acid.

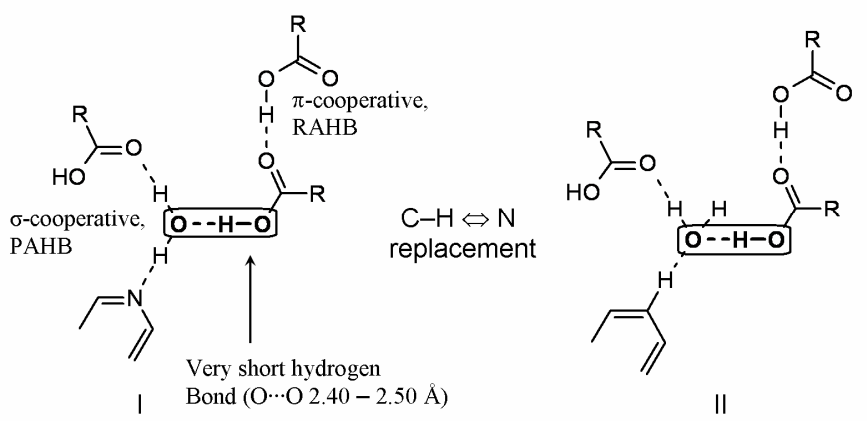

Scheme 5. The short O_{acid}–H···O_{water} hydrogen bond of synthon assisted hydrogen bond (SAHB) array is shown in lasso. A strong hydrogen bond pyrazine N acceptor (left) is isostructurally replaced by a weak phenyl C–H donor (right).

The multi-center synthon sustained by strong O–H···O H-bonds is similar and the water molecule serves as a template in assembling four tetra acid molecules around it. The variable coordination modes of water[27] in crystalline hydrates and the flexibility of H_2O in orienting their hydrogen bond donor/ acceptor groups is central to isostructurality. Water is able to serve as a H-bond donor to N acceptor in pyrazine and pyridine tetra acids and C–H···O acceptor in pyridine and benzene tetra acids by a slight reorganization of its donor hydrogen atoms so that the four acid molecules bonded to it occupy similar positions in the respective crystal structures (Scheme 5, figure 11). The driving force for the five-component assembly is the synthon assisted short O_{acid}–H···O_{water} hydrogen bond. The shortness of the strong H-bond, 2356PYZTA (1.53 Å) < PYR2356TA (1.58 Å) < BZN1245TA (1.73 Å) is due to higher COOH donor strength and better water acceptor capability is consistent with the SAHB model. *Thus a neutral, multi-center array of short/strong cooperative hydrogen bonds is a sufficient condition for aromatic CH ⇔ N isostructurality*.

Examples of phenyl CH ⇔ N replacement with fewer number of COOH groups were analyzed among hydrates in the Cambridge Structural Database.[15] Hydrogen bonding between trimesic acid, BZN135TA, and water in its 5/6 hydrate, complex with picric acid/water, and MeOH/water solvate (refcodes TRIMES10, TMAPIC10, XAVQEQ) has a similar layer arrangement as that of pyridine-2,4,6-tricarboxylic acid (PYR246TA) even though the overall crystal compositions are different. Similarity in tri acids is at the

2D layer motif but the detailed 3D packing is quite different because the second component(s) is not the same. A 2D section extracted from trimesic acid hydrate crystal structure and pyridine tricarboxylic acid hydrate is shown in figure 12. A similar C–H···O to O–H···N reorganization as in tetra acids takes place in the layer motif of benzene and pyridine tri acids but with concomitant interchange of C=O and C–OH positions along with reorganization of water hydrogen atoms.

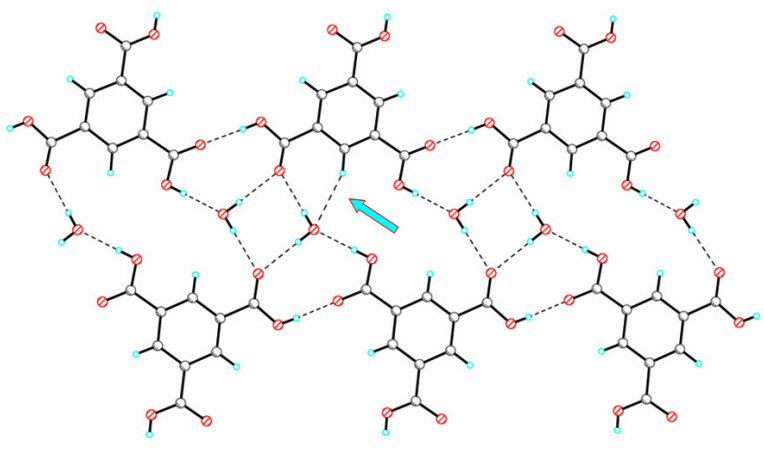

(a)

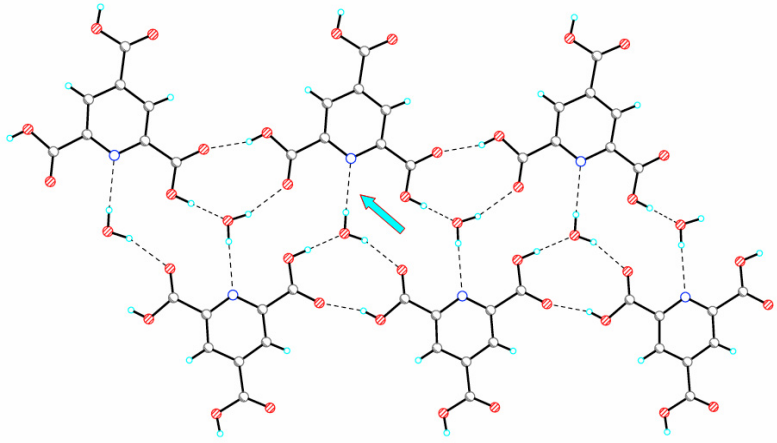

(b)

Figure 12. Hydrogen bonding of water with trimesic acid (a) and pyridine tricarboxylic acid (b) in a layer section of the structure. A slight shift of the tri acid molecule replaces C–H···O_{water} interaction of 2.72 Å by O_{water}–H···N hydrogen bond of 2.18 Å (see arrow). The COOH group and water protons reorganize in the above hydrogen bond networks even as the heavy atom positions are largely invariant.

Synthon assisted short hydrogen bond and flexibility of water molecule and COOH are important structural features for O_{water}–H···N ⇔ C–H···O_{water} mimicry in these 3D and 2D isostructural crystals (Scheme 5). It can be concluded that the larger the SAHB multi-center synthon, and the stronger the short O_{acid}–H···O_{water} bond, the more faithful is the phenyl to pyridyl exchange isostructurality. The O_{acid}–H···O_{water} hydrogen bond is comparable in tetracarboxylic acid series (H···O: 1.53, 1.58 and 1.73 Å in pyrazine, pyridine and benzene tetra acids) and hence they are all isostructural. Whereas the O_{acid}–H···O_{water} bond in benzene tricarboxylic acid dihydrate,[15] FONHEW, is longer (2.06 Å) than pyridine tricarboxylic acid dihydrate (1.70 Å) and, not surprisingly its hydrogen bonding is totally different from pyridine tri acid crystal structure.

2.5 5-Methylpyrazine-2,3-dicarboxylic acid: An unusual structure

5-Methylpyrazine-2,3-dicarboxylic acid, 5M23PYZDA, was crystallized from water with the intent of obtaining single crystals of commonly observed dihydrate in this family of pyrazine polycarboxylic acids. Surprisingly it crystallized as anhydrate. Two different morphologies, hexagonal and diamond shape crystals were obtained from water. Single crystal data on both morphologies of this molecule are solved and refined in chiral $P6_5$ space group. There are three symmetry-independent molecules in the asymmetric unit ($Z' = 3$). One of the carboxylic acids is nearly coplanar with the pyrazine ring and the other COOH is roughly orthogonal. It contains the well-known carboxylic acid–pyridine synthon[28] but as the rare trimer motif. The in-plane COOH groups (ip hereafter) of three symmetry-independent molecules form the acid–pyridine synthon trimer using one of the N atoms of the pyrazine ring. Similarly, the out-of-plane COOH groups (oop hereafter) bond to the second N atom (Figure 13). An alternation of ip and oop trimer motifs results in a hexagonal 2D lattice of Kagomé topology (Figure 14a).[29] Whereas there are several examples of metal–organic crystals exhibiting the Kagomé decoration, there is only one organic example.[29c] The 2D Kagomé hexagonal lattice in 5M23PYZDA is a polar *ab*-sheet because molecular dipoles do not cancel within a layer. Normally adjacent layers would be inversion related resulting in the dominant centrosymmetric packing (80% crystal structures). However in the present case methyl C–H donors hydrogen bond with oop C=O acceptors of adjacent layers and form a helical assembly of trimers along the *c*-axis via C–H···O interaction (2.23 Å, 166°, figure

14b, table 5). There is no significant inter-layer π–π stacking. The presence of multiple molecules[30] (Z' >1) and weak C–H···O interactions[31] are responsible for crystallization of achiral molecule 5M23PYZDA in the chiral space group $P6_5$. The absolute configuration of the enantiomorphous crystal could not be assigned because there is no heavy atom in the molecule and reflections were collected with Mo-Kα radiation only. Several examples of achiral molecules crystallizing in the enantiomorphous space groups are known in the literature.[32]

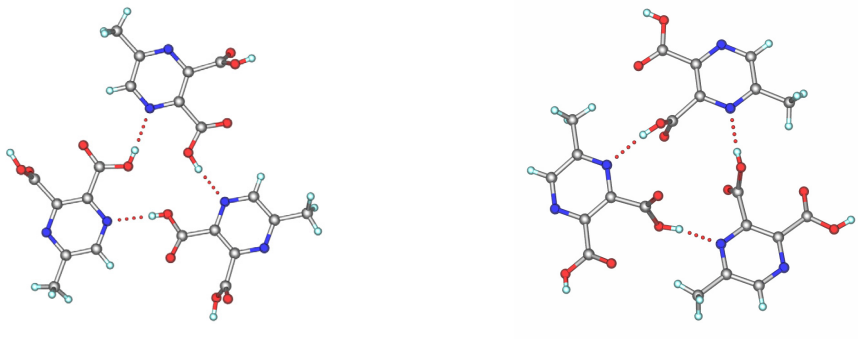

(a) (b)

Figure 13. (a) In-plane acid–pyridine trimer (torsion angles N1–C4–C5–O2 = –13°, N3–C11–C12–O6 = 0° and N5–C18–C19–O9 = 21°) (b) Out-of-plane trimer motif (N2–C6–C7–O3 = –78°, N4–C13–C14–O8 = 87° and N6–C20–C21–O11= 66°) between three symmetry-independent molecules of 5MPYZ23DA.

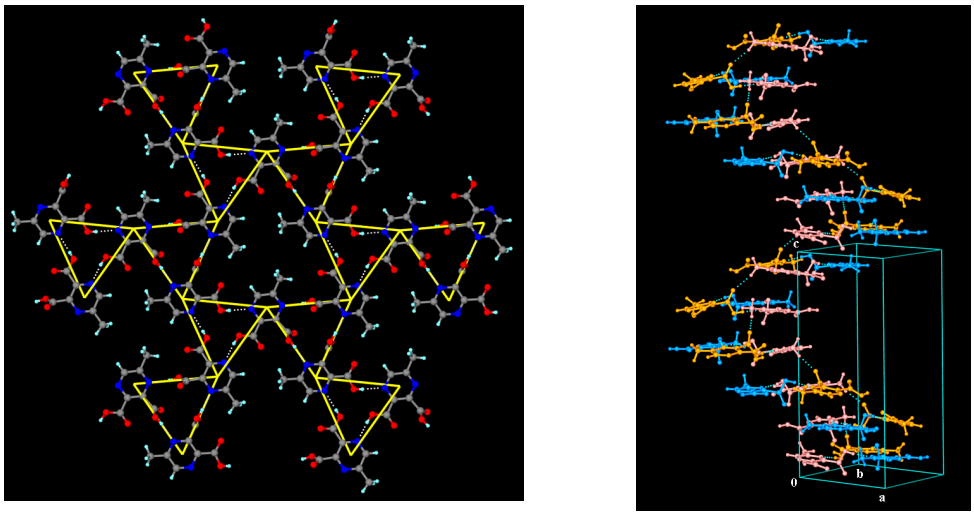

(a) (b)

Figure 14. (a) 2D organization of 5M23PYZDA molecules in the *ab*-layer mediated via acid–pyridine trimer synthons (in-plane and out-of-plane) in the Kagomé topology. (b) Acid–pyridine trimers are connected via a (Me)C–H···O=C(oop) interaction of 2.23 Å to form a helix along the *c*-axis.

Table 5. Hydrogen bonding parameters of 5M23PYZDA

Interaction	H···A/ Å	D···A/ Å	∠D–H···A/ º
In-plane acid–pyridine synthon trimer			
O2–H2···N5	1.75	2.723(4)	167
C17–H17···O1	2.79	3.541(5)	126
O9–H9···N3	1.76	2.746(4)	172
C10–H10···O10	2.77	3.441(5)	120
O6–H6···N1	1.77	2.748(3)	172
C3–H3···O5	2.64	3.384(4)	125
Out-of-plane acid–pyridine synthon trimer			
O4–H4···N4	1.74	2.712(4)	165
O8–H8···N6	1.79	2.769(4)	171
O12–H12···N2	1.71	2.690(3)	169
C–H···O interactions in helix			
C1–H1B···O11	2.23	3.293(5)	166
C8–H8B···O11	2.35	3.427(5)	169
C15–H15B···O7	2.47	3.524(5)	164
C1–H1A···O7	2.49	3.443(5)	145

2.5.1 Rationale for multiple molecules in the acid–pyridine trimer synthon

Pyrazine-2,3-dicarboxylic acid (refcode IYAWAG, space group $P2_1/c$, $Z' = 2$)[33a] and 5(ethoxycarbonyl)pyridine-2-carboxylic acid (ULUVUS, $P\bar{1}$, $Z' = 3$)[33b] are two other structures containing similar acid–pyridine trimer motif (Figure 15). The presence of multiple molecules in all these crystal structures with acid–pyridine trimer suggested that there could be a connection between $Z' > 1$ and the occurrence of trimer motif.

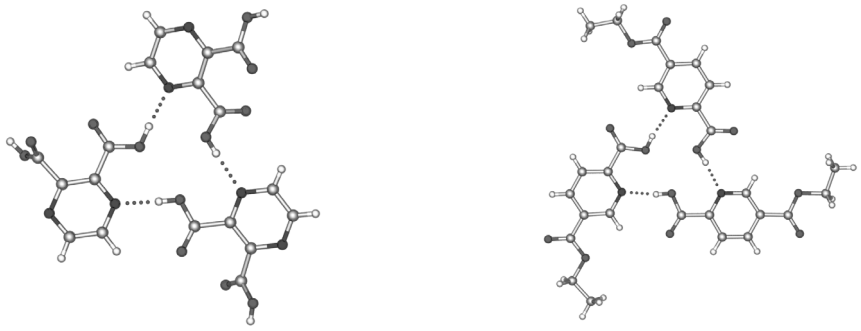

(a) (b)

Figure 15. Acid–pyridine trimer motif. (a) pyrazine-2,3-dicarboxylic acid (space group, $P2_1/c$, $Z' = 2$). (b) 5-(ethoxycarbonyl)pyridine-2-carboxylic acid ($P\bar{1}$, $Z' = 3$).

In general a trimer motif is possible in high symmetry hexagonal/ rhombohedral space groups with fractional Z' if the crystallographic three-fold axis passes through the center of the triangular void. This is possible only when the molecule has C_3 (or C_6) symmetry. Match of trigonal molecular and synthon symmetry occurs only in special cases. [17b] Since the above molecule is devoid of C_3 axis, the only way to arrange a trimer motif in a periodic lattice would be to have two or more symmetry-independent molecules. For example, in structure IYAWAG (Z' = 2), one can form infinite chain of acid–pyridine synthons through glide related molecules (Figure 16); a 2_1 screw-axis would result in similar chain of molecules. In order to assemble the trimer motif, a second molecule must be placed between glide-related molecules such that it simultaneously donates and accepts O–H···N hydrogen bonds. The only way to achieve the trimer arrangement in low symmetry crystal systems (e.g. monoclinic, triclinic) is by placing a symmetry-independent molecule within hydrogen bonding distance.

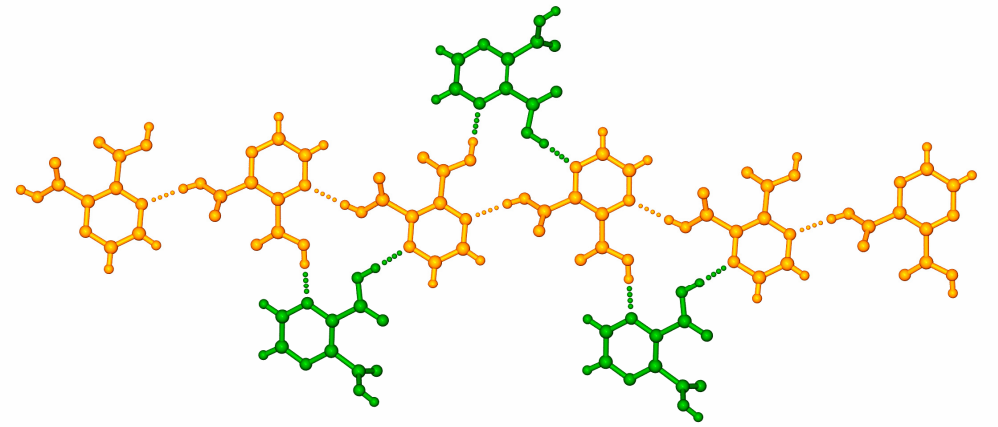

Figure 16. Crystal structure of pyrazine-2,3-dicarboxylic acid (refcode IYAWAG). Glide-related molecules readily form a tape but the trimer motif results only when a second molecule is added. Symmetry-independent molecules are colored differently.

Several dissymmetric molecules i.e. those devoid of C_3 or higher rotation axis form a helical or cyclic trimer with one crystallographic independent molecule in rhombohedral/ hexagonal symmetry, e.g. as in CSD refcodes WAJJOG01, YUYHIJ01 (helix) and HESKOF, REWWAR (cyclic). All these examples have hydrophobic pendent groups extending from the O–H···O trimer which can close pack efficiently around the synthon. Since 5MPYZ23DA is small and rigid dissymmetric molecule with no pendant groups to fill the voids, $Z' > 1$ is a requirement for the cyclic acid–pyridine trimer synthon.

2.6 Conclusions

The very short synthon assited O_{acid}–H···O_{water} hydrogen bond, SAHB, in polycarboxylic acid crystal structures is (i) intermolecular, (ii) not of the charge assisted type, iii) not of the acid–conjugate base type and (iv) does not contain highly activated donor/acceptor groups. The reason for H-bond shortening in a neutral array may be generalized as follows. *If an activated carboxylic acid donor* (pK_a 1-3) *hydrogen bonds to a water molecule that is in turn H-bonded to O/N acceptors, then the* O_{acid}–H···O_{water} *H-bond can be very short because the H-bond donor is strengthened by π-cooperativity, or resonance assistance, and the water oxygen acceptor strength is enhanced by σ-cooperativity, or polarization assistance*. The shortness of strong hydrogen bond depends on the higher COOH donor strength and better water acceptor capability by polarization assistance.

Surprisingly pyrazine, pyridine and benzene tetracarboxylic acid are three dimensionally isomorphous and the multi-center synthon sustained by strong O–H···O H-bonds is almost similar in all crystal structures. Generally consequences of C–H ⇔ N replacements are severe on hydrogen bonding and overall crystal packing, because a strong pyrazine or pyridine hydrogen bond N acceptor is replaced by a weak phenyl C–H donor. The water molecule serves as a template in assembling four tetra-acid molecules and its flexibility in orienting their H-bond donor/ acceptor groups is central to isostructurality. A 2D layer extracted from pyridine-2,4,6-tricarboxylic acid and trimesic acid hydrate and complexes with picric acid structures also highlight the importance of flexibility of water and COOH resulting a similar C–H···O to O–H···N reorganization.

5-Methylpyrazine-2,3-dicarboxylic acid crystallizes as anhydrate. It is an achiral molecule crystallized in the chiral $P6_5$ space group with three molecules in the asymmetric unit. It contains the rare acid–pyridine trimer motif in the hexagonal 2D Kagomé lattice. We showed that multiple number of molecules are required ($Z' > 1$) in order to construct novel acid–pyridine trimer motif. A helix mediated by weak C–H···O interactions and multiple Z' are responsible for chiral crystallization.

2.7 Experimental Section

1) Synthesis of Pyrazine-2,3,5-tricarboxylic acid[34]

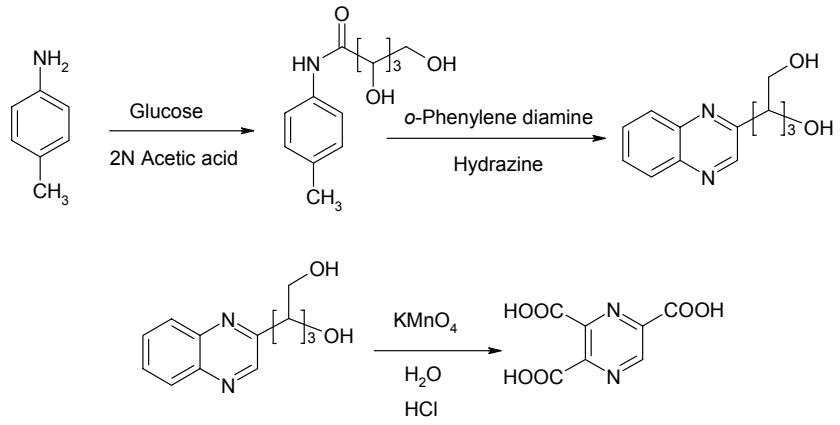

i) 2-(D-Arabo)-tetroxybutyl quinoxaline : 1.0 g (5.5 mmol) of D-glucose, 800 mg (7.3 mmol) of *p*-toluidine, 250 μL of water and 60 μL of 2N acetic acid were taken in a conical flask and the mixture was heated in a water bath for 30 min. The syrup formed during the reaction was allowed to cool for 2 h. Later, 500 μL (500 mg, 10.0 mmol) of hydrazine hydrate, 1.16 g (10.7 mmol) of *o*-phenylenediamine, and 8.3 mL of 2N acetic acid were added to the cooled syrup and again the mixture was heated for 20-30 min. The solution was left undisturbed overnight. The product formed was washed with alcohol-ether mixture and dried. Yield: 500 mg. M.P. 185-187 °C. ^{1}H-NMR (DMSO-d_6): δ 9.0 (s, 1H), 8.0-8.2 (m, 2H), 7.7-7.9 (m, 2H), 5.6 (d, 6 Hz, 1H), 5.1 (d, 6 Hz, 2H), 4.6 (dd, 7,6 Hz, 2H), 4.4 (dd, 6,6 Hz, 1H), 3.6-3.8 (m, 5H). IR (KBr): 3337, 3242, 1471, 1338, 1107, 1043, 979, 875, 758, 636 cm^{-1}.

ii) Pyrazine-2,3,5-tricarboxylic acid : 500 mg (2.0 mmol) of 2-(D-Arabo)-tetroxybutyl quinoxaline was dissolved in 10 mL hot water in a round bottom flask, which was immersed in an oil bath maintained at 90-98 ºC. To the yellow solution, which was stirred mechanically, KOH (250 mg, 4.5 mmol) was added. The color changed from yellow to red. Potassium permanganate (3.7 g, 23.0 mmol), dissolved in a minimum amount of hot water, was added drop wise to the reaction mixture over about 45-60 min. The reaction was allowed to proceed for 3 h. After adding a few drops of ethanol to destroy the excess $KMnO_4$ the mixture was filtered and the solid MnO_2 cake was washed with two 3 ml portions of water. The filtrate was evaporated in vacuum to 2 mL, cooled and acidified drop wise with conc. HCl. The crude white precipitate of required

compound, formed after 15-20 min. was filtered, dried and recrystallized from 20 % HCl. Yield: 200 mg. M.P.184 °C. ^{1}H-NMR (DMSO-d_6): δ 9.2 (s, 1H). IR (KBr): 3196, 2505, 1738, 1452, 1402, 1307, 1174, 1101, 935, 823, 792, 594 cm^{-1}

2) Synthesis of pyridine-2,3,5,6-tetracarboxylic acid[35]

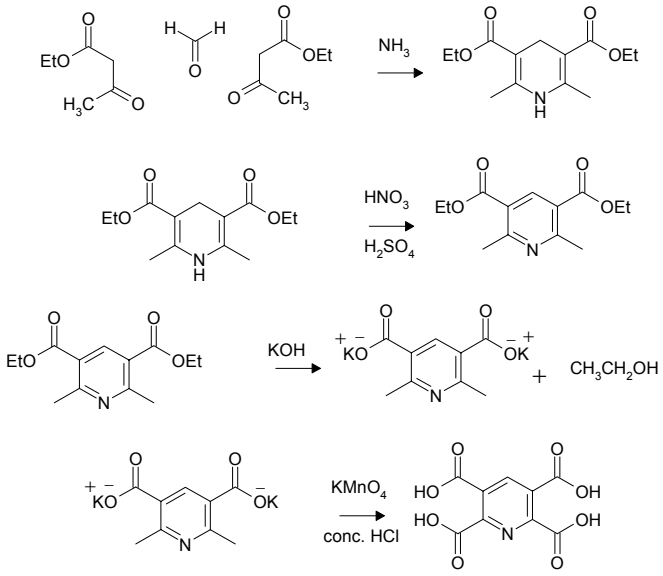

i) Diethyl 1,4-dihydro-2,6-dimethylpyridine-3,5-dicarboxylate : Ethyl acetoacetate (52 g, 51 mL, 0.4 mol) was taken in 250 ml RB flask and cooled to 0ºC. Aq. formaldehyde of 37-41% conc. (15 mL, 0.2 mol) was added followed by 9 drops of Et_2NH as catalyst during the course of the reaction. The solution was stirred for 6 h at 0 ºC and then 40 h at RT. The lower organic layer was separated from the aqueous phase in a separatory funnel and dried over 10 g of anhyd. Na_2SO_4. As the solution was highly viscous, 50 mL of ethanol was added and filtered into a RB flask and cooled to 0 ºC. A steady stream of NH_3 gas was passed through the solution at 0 ºC for 1.5 h. Then the RB flask was tightly sealed and stirred for 40 h at RT and later the seal was removed and stirred for 1 h to expel any unreacted NH_3 gas. The precipitated yellow solid was filtered and washed with EtOH, dried and recrystallized from hot EtOH. Yield: 34 g. ^{1}H-NMR ($CDCl_3$): δ 5.3 (s, 1H), 4.18 (q, 6.8 Hz, 4H), 3.27 (s, 2H), 2.2 (s, 6H), 1.29 (t, 6.8 Hz, 6H). IR (KBr): 3350, 3111, 2980, 1948, 1683, 1651, 1508, 1367, 1302, 1211, 1116, 1057, 754, 650, 588, 466 cm^{-1}.

ii) Diethyl 2,6-dimethylpyridine-3,5-dicarboxylate : A solution of 4.5 mL HNO_3 (0.135 mol), 3.7 mL H_2SO_4 (0.0536 mol) and 25 mL H_2O was prepared in a reagent bottle and kept in the refrigerator for 1 h. The above dihydropyridine derivative, 17.7 g (0.069 mol) was taken in 150 mL RB flask and to this was carefully added the above prepared cooled solution and the bottle was rinsed with 2 mL H_2O and added to the solution with constant stirring. This highly saturated solution was then shifted to an oil-bath maintained at 75-85 ºC with stirring. The reaction should be heated carefully with vigorous stirring. After 10 min, excess frothing set in and then gradually subsided indicating the process of oxidation. Then the reaction mixture was maintained at 90 ºC for about 20 min and the solution turned to deep red colour. The reaction mixture was cooled to RT and poured into a round bottom flask containing 25 mL of H_2O and approx. 50 g of chopped ice. The solution was then neutralized with aqueous NH_3 until the solution becomes alkaline. The precipitate was filtered, dried and weighed. Yield: 6.7 g. ^{1}H-NMR ($CDCl_3$): δ 8.68 (s, 1H), 4.41 (q, 6.8 Hz, 4H), 2.85 (s, 6H), 1.44 (t, 6.8 Hz, 6H). IR (KBr): 3423, 2980, 2932, 1718, 1591, 1556, 1473, 1444, 1367, 1298, 1253, 1222, 1122, 1043, 958, 856, 771, 696, 580, 567, 466 cm^{-1}.

iii) Dipotassium salt of 2,6-dimethylpyridine-3,5-dicarboxylate : Diethyl-2,6-dimethylpyridine-3,5-dicarboxylate (4.0 g, 0.0159 mol) was taken in a 100 mL RB flask and dissolved in 12.5 mL of abs. EtOH. A solution of KOH (2.20 g, 0.044 mol) in 12.5 mL of abs. EtOH was added drop wise over a period of 20 min and refluxed at 75 ºC for 1 h followed by stirring at RT. for 0.5 h. The precipitated compound was filtered, washed with ethanol and dried. Yield: 3.8 g. ^{1}H-NMR (D_2O): δ 7.62 (s, 1H), 2.44 (s, 6H). IR (KBr): 3339, 2197, 1604, 1564, 1421, 1369, 1151, 1035, 800, 667 cm^{-1}.

iv) Pyridine-2,3,5,6-tetracarboxylic acid : The dipotassium salt of 2,6- dimethyl pyridine-3,5-dicarboxylate (3.8 g, 0.0153 mol) was taken in 150 mL RB flask and dissolved in 15 mL water. A hot solution of 16 g $KMnO_4$ (0.101 mol) dissolved in 50 mL water was added drop wise over a period of 15-20 min and the reaction mixture was allowed to stir at RT for 24 h, and then heated to 75 ºC for 3 h followed by stirring at room temperature for 18 h. 3mL of ethanol was added to destroy excess $KMnO_4$. The reduced MnO_2 was filtered and washed with 10 mL of hot water. The filtrate was evaporated down to 5-8 mL on a hot plate and the highly saturated solution was

transferred to 100 mL RB flask and neutralized with 5.8 mL of conc. HCl. A white compound precipitated at the end of the neutralization. The solution was further stirred for 2 h and the precipitate was filtered, dried and weighed. Diffraction quality single crystals were obtained by crystallizing the product from 20 % aq. HCl. Yield: 1.5 g. ^{1}H-NMR (D_2O): δ 8.54 (s, 1H). IR (KBr): 3418, 3099, 2444, 1666, 1554, 1433, 1373, 1323, 854, 771, 617, 495 cm^{-1}.

3) Synthesis of pyridine-2,4,6-tricarboxylic acid[36]

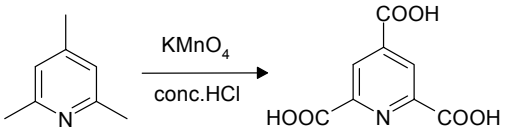

2,4,6-Trimethyl collidine (1.92 gm, 2.1 mL, 0.016 mol) was added to 30 mL of water in a 150 mL RB flask and stirred mechanically. A hot solution of $KMnO_4$ (20 gm, 0.126 mol) in 55 mL of water was added drop wise over a period of 20 min. The solution was stirred at rt for 15 h followed by stirring at 75 ºC for 3 h. The solution was further stirred for 15 h at rt. A few drops of EtOH were added to destroy excess $KMnO_4$. The reduced MnO_2 formed during the reaction was filtered and washed with 10 mL of hot water. The filtrate was extracted with 50 mL of EtOAc to ensure that any trace amount of unreacted collidine is removed. The filtrate was evaporated down to 15-20 mL on a hot plate and the solution was shifted to 50 mL flask and cooled by placing it in ice-chest. It was neutralized with 5.5 mL of conc. HCl with constant stirring. The precipitate formed at the end of the reaction was filtered, dried and weighed. Diffraction quality single crystals were obtained by crystallizing the product from 5 % aq. HCl. Yield: 0.7 g. ^{1}H-NMR (DMSO-d_6): δ 8.46 (s, 1H). IR (KBr): 3547, 3423, 2517, 1923, 1720, 1595, 1548, 1431, 1400, 1280, 1195, 814, 771, 758, 684, 509, 459 cm^{-1}.

4) Synthesis of 5-methy pyrazine 2,3-dicarboxylic acid[34a]

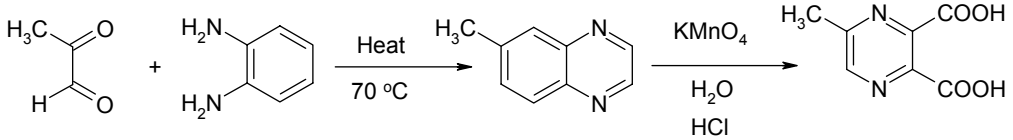

i) 2-Methyl Quinoxaline : 5.5 g (51 mmol) of o-phenylene diamine was dissolved in 90 mL of water, and the solution was heated to 70 °C. With stirring, a solution of 8.6 mL of 40 % methyl glyoxal (50 mmol) in 65 mL of hot water was added to the *o*-phenylene

diamine solution. The mixture was allowed to stand for 15 minutes and then was cooled to room temperature. 21 g of sodium carbonate monohydrate was added to the mixture. Methyl quinoxaline was extracted with three 50 mL portions of hexane solvent. The combined extracts were dried over anhydrous $MgSO_4$, filtered, and concentrated. The residual liquid, consisting of almost pure methyl quinoxaline was collected. Yield: 5.4 g (74 %). ^{1}H-NMR ($CDCl_3$): δ 8.7 (s, 1H), 8.00-7.95 (m, 2H), 7.70-7.64 (m, 2H), 2.77 (s, 3H). IR (neat): 3435, 3063, 3016, 1637, 1560, 1493, 1437, 1410, 1369 cm^{-1}.

ii) 5-Methylpyrazine-2,3-dicarboxylic acid : To 2 g (14 mmol) of methyl quinoxaline, 50 mL of water was added and heated to 80 °C. With rapid stirring a saturated aqueous solution of 12.8 g (81 mmol) of $KMnO_4$ was added, stirred for 30 minutes and filtered the reaction mixture to remove MnO_2. The filtrate (about 150 mL) was evaporated under reduced pressure to about 50 mL. The solution was stirred gently while 7 mL of conc. HCl was cautiously added. Evaporation under reduced pressure was then continued until a moist cake of solid KCl and the product remained in the flask. Some water and 25 mL of acetone was added to the solid material and the mixture was boiled under reflux for 15 minutes, then cooled to room temperature and filtered. The acetone filtrate was distilled to obtain 5-methylpyrazine-2,3-dicarboxylic acid. Compound was crystallized from water. Yield: 1.5 g (60%), M.P. 160 °C. ^{1}H-NMR (DMSO-d_6): δ 8.72 (s, 1H), 2.59 (s, 3H). IR (KBr): 3450, 2920, 1747, 1712, 1577, 1419, 1269, 1234, 1195, 1095, 794 cm^{-1}.

X-ray Diffraction

Low-temperature X-ray diffraction data reflections of 235PYZTA, PYR2356TA and PYR135TA were collected on Bruker SMART APEX CCD area detector with a Mo-Kα radiation (λ = 0.71073 Å). SMART was used for collecting frames, indexing reflections, and determining lattice parameters. SAINT was used for integration of reflections intensity and scaling. Absorption correction was done in SADABS and SHELX-TL was used for space group determination, structure solution, and least-squares refinements on F^2. Structures were solved by direct methods and non-hydrogen hydrogen atoms were refined anisotropically. O–H protons were refined from difference Fourier map. Orientationally disordered C1 and N1 atoms for PYR2356TA were modelled using

FVAR and PART and EADP in SHELXTL. Both atoms share the same site with equal occupancy. X-Seed was used to prepare figures.

2.8 References

1. (a) G. A. Jeffrey, W. Saenger, *Hydrogen Bonding in Biological Structures*, Springer-Verlag, Berlin, **1991**. (b) T. Steiner, *Angew. Chem., Int. Ed.* **2002**, *41*, 48. (c) G. A. Jeffrey, *Crystallogr. Rev.* **2003**, *9*, 135.
2. G. R. Desiraju, T. Steiner, *The Weak Hydrogen Bond in Structural Chemistry and Biology*, Oxford University Press, Oxford, **1999**.
3. (a) G. A. Jeffrey, *An Introduction to Hydrogen bonding*, Oxford University Press, Oxford, **1997**. (b)) P. Gilli, V. Bertolasi, L. Pretto, V. Ferretti, G. Gilli, *J. Am. Chem. Soc.* **2004**, *126*, 3845. (c) C. L. Perrin, J. B. Nielson, *Annual. Rev. Phys. Chem.* **1997**, *48*, 511.
4. (a) W. W. Cleland, M. M. Krevoy, *Science* **1994**, *264*, 1887. (b) W. W. Cleland, *Biochemistry* **1992**, *31*, 317. (c) P. A. Frey, *Magn. Reson. Chem.* **2001**, *39*, S190.
5. G. Gilli, P. Gilli, *J. Mol. Struct.* **2000**, *552*, 1.
6. (a) A. L. Macdonald, J. C. Speakman, D. Hadzi, *J. Chem. Soc. Perkin Trans. 2* **1972**, 825. (b) A. McAdam, M. Curie, J. C. Speakman, *J. Chem. Soc*. **1971**, 1994. (g) J. Emsley, *J. Chem. Soc. Rev.* **1980**, *9*, 91.
7. (a) G. Gilli, F. Bellucci, V. Ferretti, V. Bertolasi, *J. Am. Chem. Soc.* **1989**, *111*, 1023. (b) V. Bertolasi, P. Gilli, V. Ferretti, G. Gilli, *Chem. Eur. J.* **1996**, *2*, 925. (c) P. Gilli, V. Bertolasi, V. Ferretti, G. Gilli, *J. Am. Chem. Soc.* **2000**, *122*, 10405.
8. J. Del Bene, J. A. Pople, *J. Chem. Phys.* **1970**, *52*, 4858.
9. (a) T. Kar, S. Scheiner, *J. Phys. Chem. A* **2004**, *108*, 9161. (b) P. K. Thallapally, A. K. Katz, H. L. Carrell, G. R. Desiraju, *Chem.Commun.* **2002**, 344.
10. B. M. Kariuki, K. D. M. Harris, D. Philip and J. M. A. Robinson, *J. Am. Chem. Soc.* **1997**, *119*, 12679.
11. P. Vishweshwar, A. Nangia, V. M. Lynch, *Chem. Commun.* **2001**, 179.
12. P. Vishweshwar, N. J. Babu, A. Nangia, S. A. Mason, H. Puschmann, R. Mondal, J. A. K. Howard, *J. Phys. Chem. A* **2004**, *108*, 9406.

13. (a) P. Vishweshwar, A. Nangia, V. M. Lynch, *J. Org. Chem.* **2002**, *67*, 556. (b) H. Ptasiewicz-BĄK, L. Leiciejewicz, *J. Coord. Chem.* **2003**, *56*, 173. (c) N. J. Babu, A. Nangia, *Cryst. Growth Des.* **2006**, *6*, 1995.
14. N. J. Babu, A. Nangia, *Cryst. Growth Des*. **2006**, *6*, 1753.
15. Cambridge Structural Database, CSD, version 5.29, ConQuest 1.10, November **2007** release, January update. Crystal structures are visualized in Mercury 1.4.2. The CSD refcodes are given for some compounds.
16. L. S. Reddy, S. Basavoju, V. R. Vangala, A. Nangia, *Cryst. Growth Des.* **2006**, *6*, 161.
17. (a) K. K. Arora, V. R. Pedireddi, *Tetrahedron* **2004**, *60*, 919. (b) B. K. Saha, R. K. R. Jetti, L. S. Reddy, S. Aitipamula, A. Nangia, *Cryst. Growth Des.* **2005**, *5*, 887.
18. (a) A. I. Kitaigorodskii, *Organic Chemical Crystallography*, Consultants Bureau, **1961**, pp 222-240. (b) T. Smolka, R. Boese, R. Sustmann, *Struct. Chem.* **1999**, *10*, 429.
19. (a) B. Masereel, L. Pochet, D. Laeckmann, *Eur. J. Med. Chem.* **2003**, *38*, 547. (b) H. Aseefa, S. Kamath, J. K. Buolamwini, *J. Comput.-Aided Mol. Des.* **2003**, *17*, 475. (c) H. Kubinyi, *Pharmacokinetic Optimization in Drug Research. Biological, Physicochemical and Computational Strategies*; H. Kubinyi, B. Testa, H. van de Waterbeemd, G. Folkers, R. Guy, Eds. Wiley-VCH, **2001**, pp. 513-524.
20. (a) J. M. Chen, S. L. Xu, Z. Wawrzak, G. S Basarab, D. B. Jordan, *Biochemistry* **1998**, *37*, 17735. (b) V. Aparna, G. Rambabu, S. K. Panigrahi, J. A. R. P. Sarma, G. R. Desiraju, *J. Chem. Inf. Modeling* **2005**, *45*, 725.
21. (a) A. Kálmán, L. Párkáanyi, L. Fábián, *Acta Crystallogr.* **1993**, *B49*, 1039. (b) L. Fábián, A. Kálmán, *Acta Crystallogr.* **1999**, *B55*, 1099.
22. (a) A. Anthony, M. Jaskólski, A. Nangia, G. R. Desiraju, *Chem. Commun.* **1998**, 2537. (b) A. Anthony, M. Jaskólski, A. Nangia, *Acta Crystallogr.* **2000**, *B56*, 512. (c) L. Fábián, G. Argay, A. Kálmán, M. Báthori, *Acta Crystallogr.* **2002**, *B58*, 710.
23. (a) S. George, A. Nangia, M. Muthuraman, M. Bagieu-Beucher, R. Masse, J.-F. Nicoud, *New J. Chem.* **2001**, *25*, 1520. (b) C. Schmuck, J. Lex, *Eur. J. Org. Chem.* **2001**, 1519. (c) P. G. Jones, F. Vancea, *CrystEngComm* **2003**, *5*, 303.

24. (a) A. Dey, G. R. Desiraju, *CrystEngComm* **2004**, *6*, 642. (b) F. C. Pigge, V. R. Vangala, D. C. Swenson, *Chem. Commun.* **2006**, 2123.
25. M. Chakravarty, P. Kommana, K. C. K. Swamy, *Chem. Commun.* **2005**, 5396.
26. A. Kálmán, L. Fábián, G. Argay, *Chem Commun.* **2000**, 2255.
27. (a) L. Infantes, J. Chisholm, S. Motherwell, *CrystEngComm* **2003**, *5*, 480. (b) A. Gillon, N. Feeder, R. J. Davey, R. Storey, *Cryst. Growth Des.* **2003**, *3*, 663.
28. (a) B. R. Bhogala, A. Nangia, *Cryst. Growth Des.* **2003**, *3*, 547. (b) C. B. Aakeröy, D. J. Salmon, *CrystEngComm* **2005**, *7*, 439. (c) T. R. Shattock, P. Vishweshwar, Z. Wang, M. J. Zaworotko, *Cryst. Growth Des.* **2005**, *5*, 2046.
29. (a) J. J. Perry, G. J. Mcmanus, M. J. Zaworotko, *Chem. Commun.* **2004,** 2534. (b) B. Moulton, J. Lu, R. Hajndl, S. Hariharan, M. J. Zaworotko, *Angew. Chem., Int. Ed.* **2002**, *41*, 2821. (c) T. Nyui, T. Nogami, T. Ishida, *CrystEngComm* **2005**, *7*, 612.
30. (a) J. W. Steed, *CrystEngComm* **2003**, *5*, 169. (b) G. R. Desiraju, *CrystEngComm* **2007**, *9*, 91. (c) S. Roy, R. Banerjee, A. Nangia, G. J. Kruger, *Chem. Eur. J.* **2006**, *12*, 3777.
31. (a) G. R. Desiraju, *Acc. Chem. Res.* **1996**, *29*, 441. (b) G. R. Desiraju, *Acc. Chem. Res.* **2002**, *35*, 565.
32. (a) I. Azumaya, D. Uchida, T. Kato, A. Yokoyama, A. Tanatani, H. Takayanagi, T. Yokozawa, *Angew. Chem., Int. Ed.* **2004**, *43*, 1360. (b) E. Pidcock, *Chem. Commun.* **2005,** 3457. (b) T. Matsuura, H. Koshima, *J. Photochem. Photobiol. C: Photochem. Rev.* **2005**, *6*, 7.
33. T. Premkumar, S. Govindarajan, W. Starosta, J. Leciejewicz, *Acta Crystallogr.* **2004**, *E60*, o1305 (IYAWAG); (b) J. Gätjens, B. Meier, T. Kiss, E. M. Nagy, P. Buglyó, H. Sakurai, K. Kawabe, D. Rehder, *Chem. Eur. J.* **2003**, *9*, 4924 (ULUVUS).
34. Synthesis of pyrazine acids: (a) R. J. Light, C. R. Hauser, *J. Org. Chem.* **2002**, 67, 556. (b) H. I. X. Mager, W. Berends, *Recueil* **1958**, *77*, 827.
35. B. S. Furniss, A. J. Hannaford, P. W. G. Smith, A. R. Tatchell, *Vogel's Textbook of Practical Organic Chemistry*, ELBS, **1991**, pp. 1168-1169.
36. L. Syper, K. Kloc, J. Młochowski, *Tetrahedron* **1980**, *36*, 123.

CHAPTER 3

HIGH *Z′* POLYMORPHS–SHORTER HYDROGEN BONDS

3.1 Introduction

Conventionally the parameter *Z′* is used to denote the number of molecules in the crystallographic asymmetric unit. It is defined as the number of formula units in the unit cell divided by the number of independent general positions for that space group. Though the presence of multiple molecules in the asymmetric unit has been noted from the earliest days of crystallography, but little had been done at that time to correlate and compare data on such compounds. It was only routine crystal structure analysis that prompted researchers to solve and refine the data on compounds of interest. Some times such an occurrence might have even prevented structure solution and refinement because of the crystallographic difficulties associated with data collection of large unit cells, weak scattering and reflections with very low intensity in the earlier days. The Cambridge Structural Database[1] was searched by Padmaja et al. (1990)[2a] and observed that there was a significant fraction (8.3%) of molecules containing more than one molecule in the asymmetric unit (*Z′* > 1). Further reports on the frequency of *Z′* values in crystal structures usually appeared in connection with the compilations of space group frequencies by Sona and Gautam (1992),[2b] Wilson (1993),[2c] Brock and Dunitz (1994),[2d] Zorky (1995)[2e] and Steiner (2000)[2f] and Kubicki (2005)[2g] and recently Steed (2006).[2h,2i] Steiner's article is devoted solely to the frequency of *Z′* values in organic and organometallic crystal structures. Interestingly the proportion of *Z′* > 1 structures relative to all general crystal structures has remained almost invariant over the decades (8.3 % in 1990 and 8.8% in 2007)[3] even though the database size increased from 1,03,000 to 4,36,000 crystal structures during this period.

Some general features of crystal structures with *Z′* >1 based on the CSD data analysis reported by various groups may be summarized as follows: (i) Structures with *Z′* > 1 are often observed in the low symmetry triclinic and monoclinic space groups $P\bar{1}$, $P2_1/c$ and *Pc* (Padmaja and Viswamitra),[2a] and it is even more in the space group P1 (Brock and Dunitz).[2d] (ii) Almost 95% of crystal structures in CSD have *Z′* values of 0.5, 1 and 2,

and generally structures with internal molecular symmetry have $Z' < 1$ (examples centrosymmetric porphyrins have 41.2% incidence in CSD, Steiner).[2f] Nevertheless there are examples of high Z' even though they have internal molecular symmetry (CBr_4, $Z' = 4$ and Selenourea, $Z' = 9$).[1] (iii) The chiral molecules with no inversion centers, mirror and glide planes have noticeably $Z' > 1$ structures than the corresponding centrosymmetric structures.[2a,2f] (iv) The statistical study by Sona and Gautam[2b] has demonstrated that geometric characteristics of the crystallographically independent molecules are usually similar. There are several crystal structures with high Z' values, where all or some of the independent molecules have significantly different conformations (Nangia, figure 1).[4] (v) Some of the $Z' > 1$ structures were suspected due to the assignment of incorrect space group and presence of pseudosymmetry elements. In such cases it is possible to establish approximate symmetry transformations. Cholesterol and its solvates with $Z' = 8$ in space group P1,[5a] the high temperature phase of cholesterol with $Z' = 16$,[5f] and hydrated benzene-1,3,5-tricarboxylic acid with $Z' = 12$[1] have been determined with great care and pseudosymmetry have been thoroughly analyzed. Craven,[5a] Desiraju,[5b] Zorky,[5c] Kuleshova[5d] have emphasized on the presence of pseudosymmetry in $Z' > 1$ structures. (vi) $Z' > 1$ are most frequently observed for certain class of compounds like nucleosides, nucleotides and steroids. In organic compounds, $Z' > 1$ occurs with a frequency of 8.8% on average, but for steroids it is strongly elevated to 18.8%, and for nucleosides and nucleotides it reaches 20.8%.[2f] This indicates a general packing problem of these awkwardly shaped molecules which often cannot crystallize out in simple packing modes with single molecule in the asymmetric unit.

Although there is a large volume of scattered literature on the statistics of Z', a comprehensive understanding of why and when these high Z' structures occur is still not clear to this date. Moreover with the rising interest in organic crystal structure prediction,[6] it is necessary to understand this phenomenon in terms of the principles of packing or even to ascertain if there is any relationship between its occurrence and attributes such as chemical functionality, molecular weight or crystal system. In pursuit of these governing principles of high Z' structures and their underlying reasons, few authors have made an attempt to study and understand this interesting problem. It has been suggested by Craven[5a] in the context of high Z' requirements in cholesterol crystal structures, that the molecules of an awkward shape or molecules for which there is a

conflict between close packing requirements and those of intermolecular interactions, tend to form structures where $Z' > 1$. Gavezzotti and Fillippini[7] suggested that the number of crystal structures with more than one molecule in the asymmetric unit is higher for hydrogen bonded crystals when compared to general organic crystals. Their explanation is that oligomers of alcohols formed in the liquid state by hydrogen bonds are so stable that they can be carried over to the solid without substantial disruption of the crystal close packing. Their CSD statistics on alcohols have 40% incidence when compared with other organic crystals. Similar observation was noted by Kuleshova[5e] in the context of hydroxyl containing molecules with high Z' and the role of molecular association prior to crystallization promoting pseudosymmetry in crystals. The presence of pseudosymmetry in these types of crystals arises because small displacements of the fragments with respect to one another occur in order to achieve good close packing.

Brock and Duncan[8a] in their excellent historical review provides logical reasons to the anomalous space group frequencies for mono alcohols (51%) when compared with other organic crystals. Hydroxyl groups are good hydrogen bond donors and acceptors, but seldom (if ever) form closed dimers. Rather, the dominant patterns are chains and rings in which each hydroxyl group interacts with two others. If fully H-bonded aggregates of O–H groups are to be formed, two O atoms must be brought within ca. 2.8Å. If the hydroxyl containing molecules are thin, they can be related by 2_1 screw axes or by glide planes, or if very thin, by pure translation. If the molecules are bulkier, three O atoms related by 2_1 screw axes or by glide planes cannot get close enough to form hydrogen bonds. Crystallization in high symmetry space groups (where 3- and 4-fold screw and rotation-inversion axes are possible) is one solution. Crystallization with $Z' > 1$ is another way of achieving close packing (Figure 1). Of the 37 structures with a complete set of O–H···O bonds, 12 (32 %) crystallize in high symmetry (tetragonal, trigonal, hexagonal, and cubic) space groups. An additional 19 (51%) of the C_nH_mOH molecules crystallize with $Z' > 1$. The comparison value for the CSD as a whole is 8.3%. Only six C_nH_mOH molecules (16 %) crystallize in ‘‘normal’’ space groups with $Z' = 1$. Therefore, the phenomenon of $Z' > 1$ could be expected when the directional requirements of the individual intermolecular interactions are incompatible with each other in a situation where there is only a single molecule in the asymmetric unit. Steed[2] in his seminal work has summarized all the results on high Z' structures, reviewed reasons for their

occurrence, and added valuable comments on several aspects of the phenomenon. Based on Steed's seminal review and Brock's studies on alcohols, Nangia[4] has summarized some of the reasons for multiple molecules. (1) The molecule has a packing problem because of its awkward shape, which is reconciled by having two or more molecules in the asymmetric unit. (2) A conflict or frustration between the demands of directional hydrogen bonding and isotropic filling is reconciled through $Z' > 1$. The molecules organize in the stable clusters prior to reaching the highest symmetry arrangement in strong O–H···O hydrogen bonded structures because of enthalpic advantage from σ-cooperative chains in alcohols and phenols. (3) There are several low-lying molecular conformations inter-converting in solution and more than one molecule may crystallize out separately because of kinetic factors.

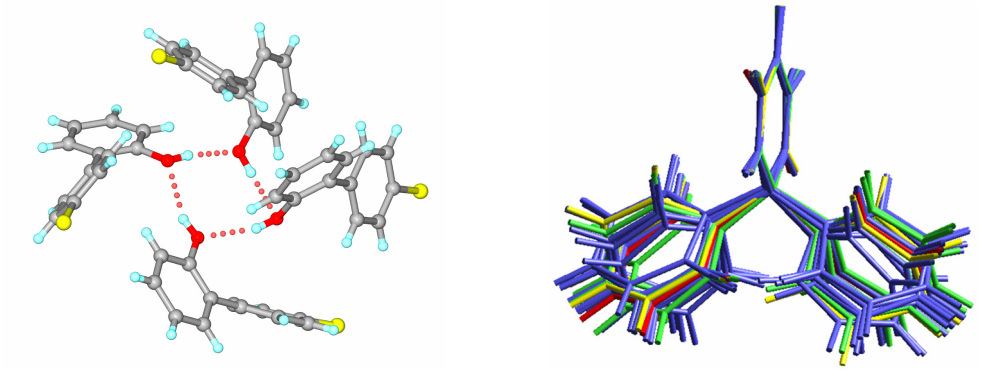

(a) (b)

Figure 1. (a) 4-chloro-2-hydroxybiphenyl forms a tetramer of O–H···O hydrogen bonds between four symmetry independent molecules ($Z' = 4$, refcode MEZNIO) in the $P2_1/c$ space group. (b) Overlay of nineteen crystallographic independent conformations of a tetramorphic 4,4-diphenyl-2,5-cyclohexadienone (Red, form A, $Z' = 1$; green, form B, $Z' = 4$; blue, form C, $Z' = 12$; yellow, form D, $Z' = 2$).

In general structures are formed if they are favoured energetically or kinetically, or for both reasons. High Z' crystal structures are considered to be a good source of information on the early events of crystallization (crystal nucleation and its growth), as it has been postulated that many high Z' structures are "fossil relic"[9] of the fastest growing crystal nucleus or "early snapshot or kinetic form"[10]. The proposed notion that the high Z' structures are kinetic forms is evident from the recent literature. Nangia[11a] showed that the crystals grown from melt or sublimation which represent kinetic conditions under which hydrogen bonded clusters are likely to crystallize without final stages of crystalline arrangement have significantly higher proportion of $Z' > 1$ structures.

Clegg[11b] showed that the early stages of crystal nuclei (poor quality crystals; too rapidly or incompletely crystallized samples) determined by synchrotron radiation have greater proportion of $Z' > 1$ structures (21%) followed by conventional X-ray determined structures, CSD value (12%) and slowly formed large crystals (for neutron diffraction) have the lowest incidence (5%) of multiple molecules.

Desiraju[3a,10] recently commented that the higher Z' structure is a crystal on the way. In a pair of polymorphs with variable Z', the higher Z' structure represents to a less stable, high energy minima in the crystallization pathway towards the final thermodynamic crystal with lower Z'. Steed[3b] in reply to Desiraju's article[3a] said that this generalization is oversimplification and misleading for three reasons: (1) Brocks elegant explanation on alcohol structures with high Z' is not based on crystallization kinetics. (2) There are many high Z' structures that do not exhibit polymorphism or exhibit polymorphism in that all have $Z' > 1$. Benzidine[12a] is a tetramorphic with variable Z' values (1.5, 3, 4, 4). 5-Methyl pyrazine-2,3-dicarboxylic acid[12b] always crystallized with $Z' = 3$ in space group $P6_5$ even after repeated crystallizations, contains rare acid–pyridine trimer synthon. The requisite criterion for making this acid–pyridine trimer synthon is the presence of minimum two molecules in the asymmetric unit as discussed chapter 2. In some cases frustration between chirality and the formation of centrosymmetric synthons led to the two-independent hydrogen bonding functionalities.[12c] (3) There are cases where high Z' polymorph is more stable than the lower Z' form.[10, 13] An up-to-date information on high Z' structures and relevant articles added to the current literature is posted on the website of Jonathan Steed.[9b]

Currently there is an ongoing debate on the occurrence of high Z' structures[3] and it is too early to draw any conclusions at this stage whether all $Z' > 1$ structures are kinetic or not. Secrets about the reasons of high Z' are best revealed in a polymorphic system, where the high Z' form can easily be compared with its low Z' (typically 1 or 0.5) polymorph.[10] The dimorphs of pyrazine-*N,N*′-dioxide (PYZNO), which contain similar trimers of C–H···O interactions but sustained by two and one symmetry-independent molecules in form 1 (**5a**) and 2 (**5b**), respectively is discussed in this chapter. The significance of C–H···O interactions in promoting multiple Z' crystal structures was evaluated in the Cambridge Structural Database.

3.2 Polymorphs of Pyrazine-*N,N'*-dioxide (PYZNO)

Two polymorphs of PYZNO, form 1 (**5a**) and form 2 (**5b**), were obtained in attempted co-crystallization experiments with Pyrazinamide and Carbamazepine. Attempted co-crystallization resulting in the discovery of novel polymorphs of one of the components is not surprising based on the recent literature reports.[14] Form 1 crystallizes in the orthorhombic *Pnma* space group and the asymmetric unit contains two symmetry independent half molecules of PYZNO. One molecule resides on the inversion centre and the other occupies the mirror plane (Figure 2a). Form 2 crystallizes in the monoclinic space group $P2_1/c$ and the asymmetric unit contains one half molecule of PYZNO which sits across the inversion centre (Figure 2b). Molecular tapes sustained by C–H···O hydrogen bonds are present in form 1 which extend into a 2D sheet structure as in figure 3a. Symmetry-independent layers of PYZNO are stacked in a sandwich arrangement in the orthorhombic polymorph 1 as shown in figure 3b. The monoclinic form 2 is not a completely layered structure like form 1; instead the molecules are arranged in helical motifs to give a 3D structure (Figure 3c and 3d). If three molecules of PYZNO are viewed as the smallest structural building unit, then the trimer is planar in form 1 but helical in form 2 (Figure 4a and 4b). The number of C–H···O interactions to/ from a given molecule is greater and shorter in form 1 compared to 2 (Table 1).

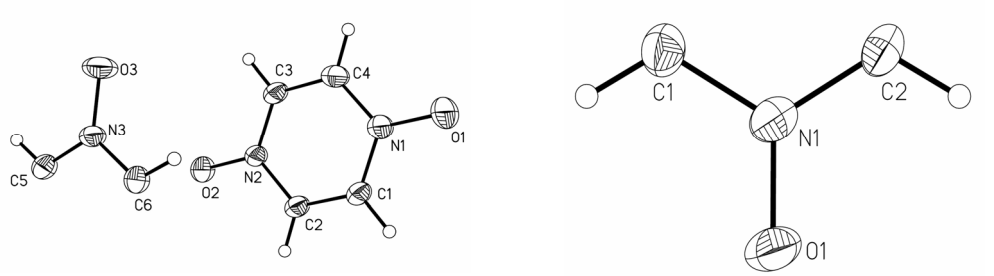

Figure 2. ORTEP drawn at 35% probability of non-hydrogen atoms. (a) PYZNO form 1. There are two half molecules in the asymmetric unit cell, one resides on the inversion center and another molecule on the mirror plane with 50% atom occupancy. (b) A half molecule of PYZNO resides on the inversion center in form 2.

These dimorphs were analyzed for their relative stability, variable *Z'*, and C–H···O interaction geometry. It is difficult to measure the melting point of form 1 and 2 (as indicator of form stability) because the compound decomposes upon heating. Form 1 has lower crystal lattice energy computed in Cerius[2] (Compass values: –18.87, –18.50 kcal mol^{-1}, per molecule of form 1 and 2 respectively).[15] Grinding[16] of pure form 2 in a

mechanical ball mill for 30 min showed 85% conversion to form 1 and the remaining solid is form 2 by powder X-ray diffraction. Conversion is complete to pure form 1 after 60 min (Figure 5a and 5b). When form 1 was ground for an additional 1 h, no phase transformation occurred but the material became amorphous (in part) because of very small particle size.

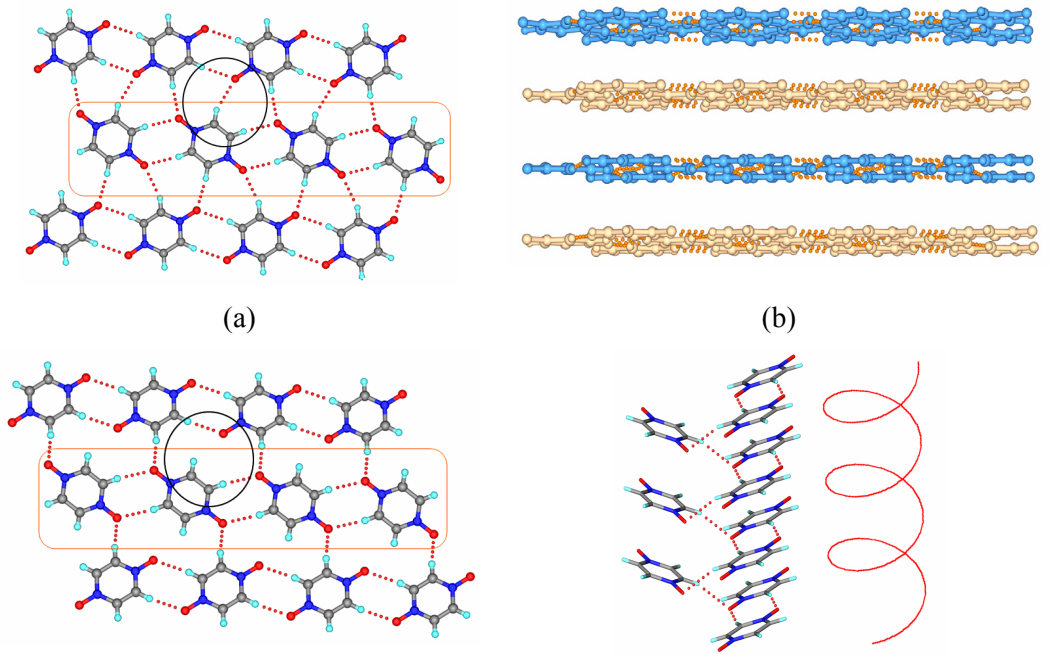

Figure 3. (a) Layered PYZNO form 1. (b) Stacking of symmetry independent layers in form 1 (colored differently) at 3.2 Å separation. No C–H···O bonds in between layers. (c) 2D section of helical form 2. (d) Right-handed helix viewed down the *a*-axis in monoclinic form 2. Circled C–H···O interaction in the layered form 1 makes a helical interaction in form 2 in the third dimension.

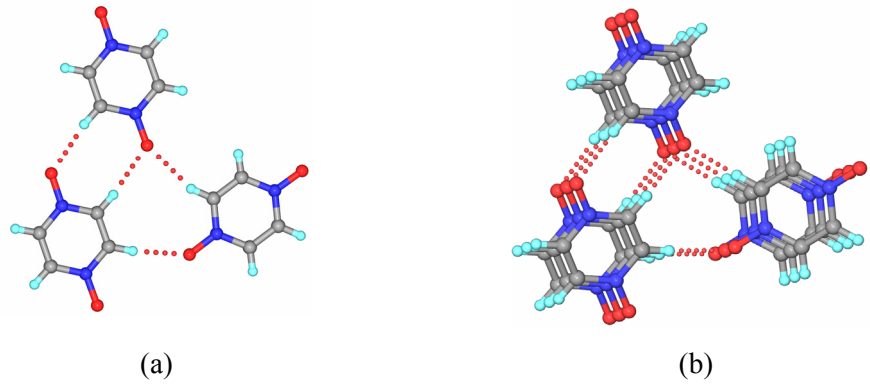

Figure 4. The structure-building unit. (a) Planar C–H···O trimer in form 1. (b) Helical trimer in form 2.

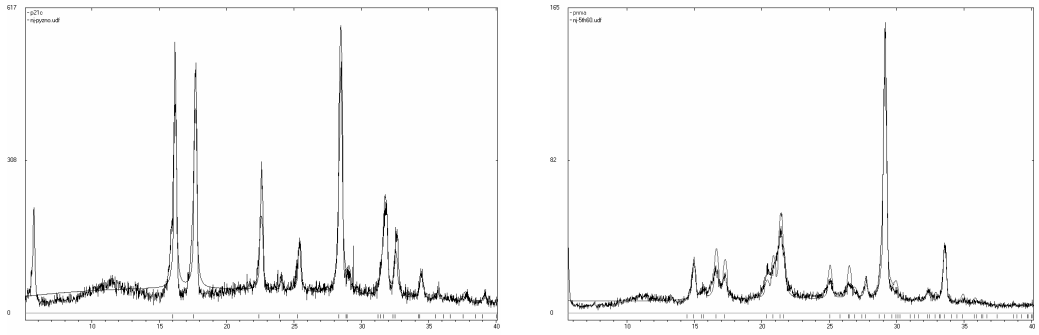

(a) (b)

Figure 5. (a) PXRD pattern of pure form 2 before grinding. (b) After 60 minutes of grinding, pattern matches with form 1. Continuing the grinding for another 1 h gave form 1 (no change). Black trace is the experimental powder pattern and gray lines are simulated PXRD from form 1 and form 2. The intense peak at ca. 5º is due to instrument artifact.

Table 1. C–H···O interactions in the crystal structures of PYZNO

Interaction	H···A/ Å	D···A/ Å	∠D–H···A/ º
	Form 1 (Z' = 0.5, 0.5)		
C1–H1···O2	2.01	3.090(4)	173
C2–H2···O1	2.16	3.232(4)	172
C3–H3···O1	2.24	3.264(4)	157
C4–H4···O2	2.13	3.200(4)	171
C5–H5···O3	2.12	3.162(3)	161
C6–H6···O3	2.15	3.226(3)	172
	Form 2 (Z' = 0.5)		
C1–H1···O1	2.12	3.164(3)	161
C2–H2···O1	2.15	3.210(3)	166

Thus, layered, orthorhombic form 1 of PYZNO is the thermodynamic polymorph and helical, monoclinic form 2 is a metastable polymorph, based on observed phase transition and computed crystal lattice energy. In general, crystal structures that have close-packed molecular layers are more stable than those with a 3-dimenisonal arrangement, e.g. graphite and diamond. The greater stability of a layered polymorph compared to its 3-D crystal packing form is noted in a recent example of trimorphic 2-hydroxy-1,4-naphthoquinone.[1] Two of its forms are layered while the third one is three dimensionally packed structure. In a pair of polymorphs with variable Z', the higher Z' structure could represent a less stable, high energy minima in the crystallization pathway towards the final thermodynamic crystal with lower Z'. The fact that stable *Pnma*

structure in the present case has two symmetry-independent half molecules compared to one half molecule in the kinetic $P2_1/c$ form runs contrary to the proposed notion that high Z' structures are kinetic forms.[3a,10] The structures having $Z' = 0.5 + 0.5$, in other words, two symmetry independent half molecules situated on distinct special positions are phenomenologically identical to $Z' = 2$ structures in which the molecules occupy general positions. We noted that C–H···O interactions are shorter (stronger) in high Z' form 1 of PYZNO when compared to low Z' form 2 (Figure 6a). Table 1 gives the shortest linear interaction 2.01 Å for high Z' form 1, whereas it is 2.12 Å for low Z' form 2. A similar correlation was also observed in a tetramorphic cluster 4,4-Diphenyl-2,5-cyclohexadienone from our research group.[4a] HEYHUO02 has shortest H···O distance of 2.30 Å and the highest Z' value 12, HEYHUO01 has H···O distance of 2.33 Å, $Z' = 4$, HEYHUO03 and HEYHUO have even longer H···O distances of 2.47 and 2.55 Å and smaller Z' values of 2 and 1, respectively (Figure 6b).

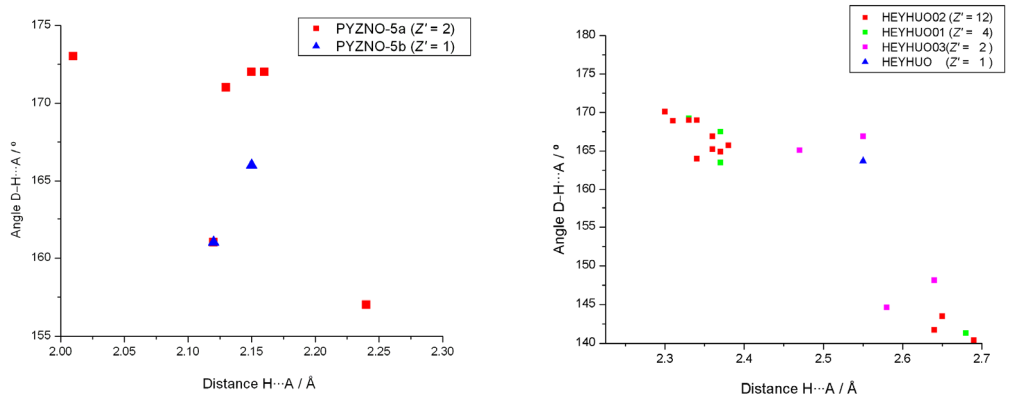

(a) (b)

Figure 6. Distance–angle C–H···O scatter plots to illustrate the high Z'–strong C–H···O correlation in polymorphs. (a) PYZNO (2 forms); (■) high Z' form 1 and (▲) low Z' form 2. (b) Diphenyl-2,5-cyclohexadienone (4 forms); (■) HEYHUO02 with $Z' = 12$, (■) HEYHUO01 with $Z' = 4$, (■) HEYHUO03 with $Z' = 2$ and (▲) HEYHUO with $Z' = 1$.

3.3 High *Z′*–shorter hydrogen bonds in CSD polymorphic clusters

Upon noting that C–H···O interactions are shorter (stronger) in high Z' forms of PYZNO and HEYHUO polymorphic systems, we examined the generality of our observation in polymorph clusters in the CSD.[1] Out of 38 polymorphic systems retrieved and analyzed, the higher Z' crystal structure has shorter C–H···O interaction in 26 cases, and the lower Z' form has shorter interaction in 12 cases. Details of these refcodes are listed in table 2.

When all the C–H···O interactions in 38 polymorphs sets are plotted (distance vs angle), it is observed that the significant short and linear interactions (<2.3 Å and >150°) are more frequent in high *Z′* polymorphs. There are 13/194 red dots (high *Z′*) compared with 3/77 blue dots (low *Z′*) in the upper left quadrant of the scatter plot (Figure 7a). That the high *Z′*-strong C–H···O correlation is followed in 26 out of 38 polymorph sets, or in 68% of cases, is quite good considering that C–H···O interactions are weak (1-3 kcal mol^{-1}), have moderate directionality (140-180º), when compared to O–H···O hydrogen bonds. The above C–H···O strength–high *Z′* relation is derived in the subset of molecules that can only form C–H···O interactions to the exclusion of O–H···O/ N–H···O hydrogen bonds. It is difficult to dissect and analyze the subtle effects of weak interactions in a strong H-bond environment. Nevertheless, there are at least two recent examples highlighting the significance of C–H···O interactions in high *Z′* crystal structures of ionic and strong H-bonded molecules.[17]

Table 2. CSD refcodes for C–H···O hydrogen bond polymorph clusters

26/38 clusters have shorter C–H···O in the higher *Z′* polymorph						
AFECUJ	AZADAG	HEYHUO	HIRPAZ	HIXHIF	NANQUO	NAXFUO
OHIBOW	OMIYEO	ZOGQAN	QAMNAT	QAPZEN	QEJZAH	QNGHSU
QOGNEF	RAKWIJ	RIGHUK	SEBTAU	TNBENZ	TOLKEK	WEDSEE
XESSUJ	XOCXUI	YABHEP	ZEXXOP	KESNEC		
12/38 polymorph clusters have shorter C–H···O in the lower *Z′* polymorph						
FEFPEM	FIMNAQ	GAGSIR	GOLLUO	NMBYAN	MELXEG	RAXRAK
XUDXID	EBIGUR	PEFTIE	XELLOP	MEQVAG		

The higher frequency of high *Z′* crystal structures in alcohols, phenols, nucleosides (e.g. cholesterol *Z′* = 8, 16, α-cembrene-1,3-diol *Z′* = 9) is explained due to the dominance of intermolecular O–H···O hydrogen bonds[7,8] together with the packing problem or frustration between these two requirements in the crystal structure. This accepted notion that high *Z′* in alcohol/ phenol crystal structures is due to H-bond stabilization was evaluated statistically. Out of 32 polymorph clusters O–H···O bonded polymorph crystal structures having variable *Z′,* 22 clusters follow the trend of strong O–H···O with high *Z′* (40/116 red interactions compared with 14/47 blue dots at <1.8 Å, > 160˚, figure 7b) and

7 cases have longer hydrogen bonds in higher *Z′* forms; 3 clusters were difficult to classify because the crystal structure with shorter H-bond was determined at lower temperature and the distance difference is not so large. Details of these refcodes are listed in table 3.

Table 3. CSD refcodes for O–H···O hydrogen bond polymorph clusters

22/32 clusters have shorter O–H···O in the higher *Z′* polymorph						
COLTAY	ENAZOI	ESALUF	LUXXAD	FUGJUM	IOBNZA	KACRUC
KARCOW	KETVEK	KIXLOS	NEMYIO	PINCOL	SALOXM	TEHNID
TELYAK	TEMBES	TEVFIK	UBEDUA	WANMUU	WETFAD	ZIGPAG
UCAYED						
7/32 clusters have shorter O–H···O in the lower *Z′* polymorph						
GLUCIT	HYQUIN	NOLFUP	QODQUV	UCAYED	YEJNAC	ZUHRID
No definite conclusion in 3 polymorph clusters after temperature correction						
EZAQEB	JAKKUB	ESTRON				

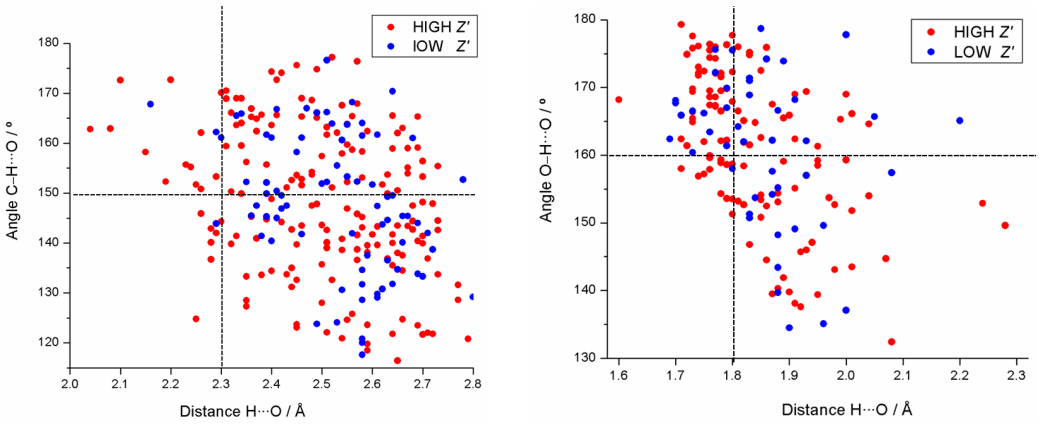

(a) (b)

Figure 7. (a) Hydrogen bond strength-high *Z′* correlation for C–H···O hydrogen bond polymorph clusters. There are 13/194 red dots (high *Z′*) compared with 3/77 blue dots (low *Z′*) in the upper left quadrant at 1.80 Å/ 160°. (b) Similar correlation for O–H···O hydrogen bond polymorph clusters. There are 40/116 red dots (high *Z′*) compared with 14/47 blue dots (low *Z′*) at <1.8 Å, > 160°.

The percentage of crystal structures that follow the H-bond strength–high *Z′* correlation in O–H···O bonds (69%) is incidentally comparable to that for C–H···O interactions (68%). This is quite surprising because statistical trends are usually better correlated for stronger

interactions because they generally have tightly clustered distance/ angle histogram and scatter plot. There are two plausible reasons for the lower incidence of crystal structures in which higher Z' goes together with stronger O–H···O hydrogen bonds. (1) O–H···O bonds are already quite strong and so further strengthening in a putative higher Z' form could be difficult to achieve. Weak, soft C–H···O interactions are adaptable to make slightly stronger bonds. (2) If σ-bond cooperativity, which is a frequent motif and major force in O–H···O strengthening,[18] is absent then hydrogen bonds will invariably be longer. Pentafluorophenol has three crystalline polymorphs: $P2_1/c$, $Z' = 1$, infinite chains; Cc, $Z' = 3$, discrete chain; $P2_12_12_1$, $Z' = 3$, helical pattern (Figure 9).[10,19] H-bonds in Cc form are longer than those in $P2_1/c$ structure because the motif is finite and interrupted at the third molecule and prevents corresponding O–H···O chains whereas H-bonds are shorter in $P2_12_12_1$ polymorph because it has infinite O–H···O hydrogen bonded helices (Figure 8).

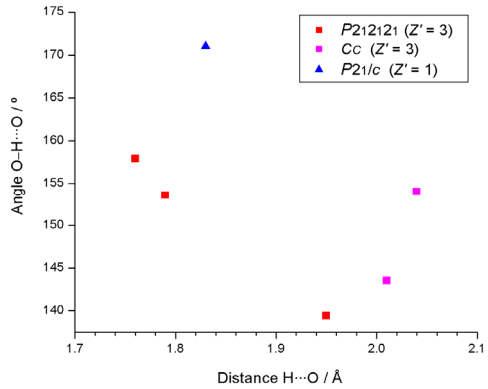

Figure 8. Pentafluorophenol trimorphs. (▲) $P2_1/c$ structure with $Z' = 1$ has infinite O–H···O chains. Among $Z' = 3$ dimorphs, (■) Cc form has discrete chains (longer H-bonds) and (■) $P2_12_12_1$ structure has helical motif (shorter H-bonds).

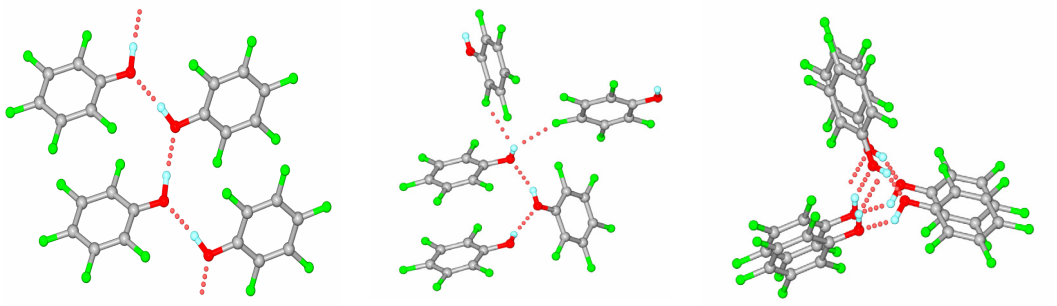

(a) (b) (c)

Figure 9. Pentafluorophenol trimorphs. (a) $P2_1/c$ structure with $Z' = 1$ has infinite O–H···O hydrogen bonded chains. Among $Z' = 3$ dimorphs, (b) Cc form has discrete chains (longer H-bonds) (b) $P2_12_12_1$ structure has helical motif (shorter H-bonds)

Analysis of the interaction geometry in polymorph sets suggests that enthalpy is important in bringing together multiple molecules during crystal nucleation because high *Z*′ crystal structures have shorter (stronger) hydrogen bonds than the low *Z*′ polymorphs. We postulate that clusters of molecules sustained by stronger interactions carry over from solution to the solid state without going through final stages of reorganization and symmetry evolution to the low(er) *Z*′ form, leading to multiple molecules and pseudosymmetry in the crystal lattice, that is, *Z*′ > 1. For example, the same structure-building C–H···O trimer is present in both form 1 and 2 of PYZNO, albeit with a minor difference that it is planar in form 1 but helical in form 2 (Figure 4). Whereas this has been noted in crystal structures sustained by O–H···O chains/helices and those crystallized from the melt, our database results generalize these arguments and extend them to exclusively C–H···O bonded molecular crystals. The structural consequences of short C–H···O interactions may be comparable to those of conventional O–H···O and N–H···O H-bonds.[20] Even though structural data retrieved from the CSD are perhaps at the lower limit of what is considered statistically significant, the trends are clearly indicative.

3.4 Conclusions

The presence of multiple molecules in the asymmetric unit or high *Z*′ structures continue to interest crystallographers even though it is still not properly understood why some categories of structures show high frequency of *Z*′ >1. Pyrazine-*N,N*′-dioxide is a dimorph containing similar trimers of C–H···O interactions but sustained by two and one symmetry-independent molecules in form 1 (*Z*′ = 2) and 2 (*Z*′ = 1) respectively. Upon noting that C–H···O interactions are shorter (stronger) in high *Z*′ in PYZNO form 1 and in a different polymorphic system 4,4-diphenyl-2,5-cylcohexadienone from our group, we examined the generality of our observation in polymorph clusters in the CSD. Out of 38 polymorphic systems that can only form C–H···O interactions, the higher *Z*′ crystal structure has shorter C–H···O interaction in 26 cases (68% probability), and the lower *Z*′ form has shorter interaction in 12 cases. Number of significant short and linear interactions (<2.3 Å and >150°) are more frequent in high *Z*′ polymorphs. Similar study was extended to O–H···O bonded polymorph clusters and found that higher *Z*′ structure has shorter O–H···O bond distances in 22/32 sets. Analysis of the interaction geometry in C–H···O /and O–H···O H-bonded polymorph sets indicate that there is a connection

between hydrogen bond strength and multiple molecules in the asymmetric unit. We believe that shorter (stronger) hydrogen bonds in high *Z′* crystal structures have enthalpic advantage in bringing together multiple molecules during the crystal nucleation. Cluster of molecules formed may directly carry over from solution to the solid state without final stages of reorganization and symmetry evolution to the lower *Z′* form thus providing a chemical and thermodynamic basis for multiple *Z′* crystal structures sustained by C–H···O / O–H···O interactions. As more crystal structures and polymorph clusters of variable *Z′* are deposited in the database, current hypotheses such as crystals on the way, H-bond strength promoting high *Z′*, and thermodynamic stability of lower *Z′* structures should get refined with time.

3.5 Experimental section

Synthesis of pyrazine-*N,N′*-dioxide

0.5 g (6.25 mmol) of pyrazine was dissolved in 10 mL EtOAc. To the stirred solution, 2.76 g (12.5 mmol) of 70-75% pure *m*-CPBA dissolved in 15 mL EtOAc was added, and the mixture was allowed to react for 24 h. The white to pale brown colored precipitate was filtered and washed with EtOAc, dried and weighed. Bulk material is PYZNO form 2. Yield: 0.37 g. M.P: 285 °C (dec). IR (KBr, cm^{-1}): 3107, 3024, 2096, 1915, 1714, 1483, 1446, 1261, 1032, 873, 804, 542, 410. ^{1}H–NMR (D_2O): δ 9.0 (s, 4H).

Crystallization of PYZNO form 1: The PYZNO form 1 was obtained during co-crystallization with pyrazinamide. Instead of the CBZ–PYZNO cocrystal, pure PYZNO single crystals of form 1 appeared. Pyrazinamide (48 mg, 0.392 mmol), pyrazine-*N,N′*-dioxide (20 mg, 0.196 mmol) were dissolved in 5 mL water in a 25 mL beaker and the solvent was allowed to evaporate slowly over 3-4 d to get form 1. Subsequently it is obtained by crystallization from water, DMF or MeOH + water by slow evaporation without pyrazinamide additive at room temperature.

Crystallization of PYZNO form 2: The PYZNO form 2 obtained when co-crystallization of PYZNO (19 mg, 0.169 mmol) and carbamazepine (CBZ, 80 mg, 0.339 mmol) was attempted by acetonitrile assisted grinding of the binary solids as slurry in mortar-pestle, and the microcrystalline powder was dissolved in 5 mL of DMF for single

crystal growth. Crystals of plate and needle morphology appeared after 1 day. Plate-shaped crystals belong to $P2_1/c$ form 2 and needle-shaped crystal is the *Pnma* form 1. Both forms were obtained concomitantly in this crystallization. If crystals of pure PYZNO were not picked after 1 day, the expected 1:0.5 CBZ–PYZNO cocrystal was obtained on 4-5 d. The presence of amide–*N*-oxide adduct appears to be important because crystals of PYZNO form 2 were not isolated when the components were mixed without grinding. Form 2 crystal was also obtained in attempted synthesis of a coordination polymer network as the free ligand.[21]

Phase Transitions

Bulk material of both the polymorphs was readily obtained in preparative quantities. 100% pure $P2_1/c$ form 2 was obtained as white precipitate from EtOAc at the end of the PYZNO preparation. The pure *Pnma* form 1 (100 %) was obtained either by solid-state ball mill grinding for 1 h of form 2 or slow crystallization from DMF. The sample was shaken in a Wig-L-Bug type mixer mill equipped with 5 mL stainless steel grinding jar and balls of 4 mm diameter. Grinding was performed at 20 Hz oscillation rate. Powder X-ray diffraction patterns were recorded at regular intervals on a PANalytical 1830 diffractometer using Cu-Kα X-radiation (λ = 1.54056 Å) at 35 kV and 25 mA, over 2θ range of 5-50° at scan rate of 1° min^{-1}. Powder_Cell program was used for least squares refinement and to generate calculated diffraction lines from the X-ray crystal structure.

Cambridge Structural Database Search

CSD version 5.29, ConQuest 1.10, November 2007 release, was searched to assess the correlation of C–H···O interaction strength with high Z' in polymorphic systems. Crystal structures with $Z' > 1$, polymorph, after 1994, no O–H, no N–H, 3D coordinates determined, *R*-factor < 0.1, no disorder, no errors, not polymeric, no powder structures and only organic compounds were searched. 38 polymorphic pairs are selected manually where different polymorphs contain different Z' in the asymmetric unit. C–H···O interactions were neutron-normalized and values were tabulated. Distance–angle scatter plot of C–H···O interactions was plotted in Origin 7.0. Similar search was extended to O–H···O bonded polymorph clusters. 40 polymorphic pairs are selected manually. 8 clusters of polymorphs (ASIXEF, CACBAK, FEFQUD, INOCET, REPFOH, VOSQUP,

WEFKEY and YAXDUW) were discarded as hydroxyl group either forms intramolecular or no hydrogen bonds. Finally 32 sets are considered for analysis.

3.6 References

1) (a) Cambridge Structural Database, CSD, version 5.29, ConQuest 1.10, November **2007** release, January update. (b) A. Nangia, *CrystEngComm* **2002**, *4*, 93. (c) J. Chisholm, E. Pidcock, J. V. De streek, L. Infantes, S. Motherwell, F. H. Allen, *CrystEngComm* **2006**, *8*, 11.
2) (a) N. Padmaja, S. Ramakumar, M. A. Viswamitra, *Acta Crystallogr.* **1990**, *A46*, 725. (b) V. Sona, N. Gautam, *Acta Crystallogr.* **1992**, *B48*, 111. (c) A. J. C. Wilson, *Acta Crystallogr.* **1993**, *A49*, 795. (d) C. P. Brock, J. D. Dunitz, *Chem. Mater.* **1994**, *6*, 118. (e) V. K. Belsky, O. N. Zorkaya, P. M. Zorky, *Acta Crystallogr.* **1995**, *A51*, 473. (f) T. Steiner, *Acta Crystallogr.* **2000**, *B56*, 673. (g) M. Kubecki, *J. Mol. Struct.* **2005**, *743*, 209. (h) K. M. Anderson, A. E. Goeta, K. S. B. Hancock, J. W. Steed, *ChemComm.* **2006**, 2138. (i) K. M. Anderson, K. Afarinkia, H Yu, A. E. Goeta, J. W. Steed, *Cryst. Growth Des.* **2006**, *6*, 2109.
3) (a) G. R. Desiraju, *CrystEngComm* **2007**, *9*, 91. (b) K. M. Anderson, J. W. Steed, *CrystEngComm* **2007**, *9*, 328.
4) (a) S. Roy, R. Banerjee, A. Nangia, G. J. Kruger, *Chem. Eur. J.* **2006**, *12*, 3777. (b) A. Nangia, *Acc. Chem. Res.* **2008**, *41*, 595.
5) (a) B. M. Craven, *Acta Crystallogr.* **1979**, *B35*, 1123. (b) G. R. Desiraju, J. C. Calabrese, R. L. Harlow, *Acta Crystallogr.* **1991**, *B47*, 77. (c) P. M. Zorky, *J. Mol. Struct.* **1996**, *374*, 9. (d) D. Britton, *Acta Crystallogr.* **2000**, *B56*, 828. (e) L. N. Kuleshova, M. Y. Antipin, I. V. Komkov, *J. Mol. Struct.* **2003**, *647*, 41. (f) L. Hsu, J. W. Kampf, C. E. Nordman, *Acta Crystallogr.* **2002**, *B58*, 260.
6) (a) S. L. Price, *Encyclopedia of Supramolecular Chemistry*, Eds J. L. Atwood, J. Steed, Marcel Dekker, New York, **2004**, pp 371-379. (b) J. D. Dunitz, *Chem. Commun.* **2003**, 545.
7) A. Gavezzotti, G. Fillippini, *J. Phys. Chem.* **1994**, *98*, 4831.
8) (a) C. P. Brock, L. L. Duncan, *Chem. Mater.* **1994**, *6*, 1307. (b) H.-J. Lehmler, L. W. Robertson, S. Parkin, C. P. Brock, *Acta Crystallogr.* **2002**, *B58*, 140. (b) C. P. Brock, *Acta Crystallogr.* **2002**, *B58*, 1025.

9) (a) J. W. Steed, *CrystEngComm* **2003**, *5*, 169. (b) http://www.dur.ac.uk/zprime

10) D. Das, R. Banerjee, R. Mondal, J. A. K. Howard, R. Boese, G. R. Desiraju, *Chem. Commun.* **2006**, 555.

11) (a) B. Sarma, S. Roy, A. Nangia, *Chem. Commun.* **2006**, 4918. (b) G. S. Nicol, W. Clegg, *CrystEngComm* **2007**, 9, 959.

12) (a) M. Rafilovich, J. Bernstein, *J. Am. Chem. Soc.* **2006**, 128, 12185. (b) N. J. Babu, A. Nangia, *Cryst. Growth Des.* **2006**, *6*, 1995. (c) A. M. Todd, K. M. Anderson, P. Byrne, A. E. Goeta, J. W. Steed, *Cryst. Growth Des.* **2006**, *6*, 1750. (c) X. Hao, J. Chen, A. Cammers, S. Parkin, C. P. Brock, *Acta Crystallogr.* **2005**, *B61*, 218.

13) (a) S. Roy, P. M. Bhatt, A. Nangia, G. J. Kruger, *Cryst. Growth Des.* **2007**, *7*, 476. (b) J. Bernstein, J. D. Dunitz, A. Gavezzotti, *Cryst. Growth Des.* **2008**, *8*, 2011.

14) (a) P. Vishweshwar, J. A. McMahon, M. Oliveira, M. L. Peterson, M. J. Zaworotko, *J. Am. Chem. Soc.* **2005**, *127*, 16802. (b) G. M. Day, A. V. Trask, W. D. S. Motherwell, W. Jones, *Chem. Commun.* **2006**, 54. (c) S. Ahn, F. Guo, B. M. Kariuki, K. D. M. Harris, *J. Am. Chem. Soc.* **2006**, *128*, 8441.

15) Crystal lattice energy program, www.accelrys.com.

16) (a) L. S. Reddy, P. M. Bhatt, R. Banerjee, A. Nangia, G. J. Kruger, *Chem. Asian J.* **2007**, *2*, 505. (b) A.V. Trask, W. Jones, *Top. Curr. Chem.* **2005**, *254*, 41. (c) A. V. Trask, N. Shan, W. D. S. Motherwell, W. Jones, S. Feng, R. B. H. Tan, K. J. Carpenter, *Chem. Commun.* **2005**, 880.

17) S. K. Chandran, A. Nangia, *CrystEngComm* **2006**, *8*, 581. (b) G. S. Nichol, W. Clegg, *Cryst. Growth Des.* **2006**, 6, 451.

18) G. A. Jeffrey, *An Introduction to Hydrogen Bonding*, Oxford University Press, New York, **1997**.

19) M. Gdaniec, *CrystEngComm* **2007**, *9*, 286.

20) B. M. Kariuki, K. D. M. Harris, D. Philip, J. M. A. Robinson, *J. Am. Chem. Soc.* **1997**, *119*, 12679.

21) C. Näther, P. Kowallik, I. Jeß, *Acta Crystallogr.* **2002**, *E58*, o1253.

CHAPTER 4

POLYMORPHISM IN TEMOZOLOMIDE AND FUROSEMIDE APIS

4.1 Introduction

Crystalline solids have regular arrangements of molecules that repeat in three dimensions, whereas amorphous solids lack the long-range order present in crystals. These differences in the long-range periodicity of the molecules result in substantially different physical and chemical properties of crystalline and amorphous solids in pharmaceutical substances.[1] Although amorphous solids often have desirable properties such as faster dissolution rates than their crystalline counterparts, they are not marketed as widely as crystalline forms because of their lower physico-chemical stability and their innate tendency to crystallize.[1] Most of the marketed pharmaceuticals are preferred in their crystalline stable forms. The arrangement of the molecules in a crystal determines its physical and chemical properties, i. e. physicochemical profile of the particular drug. At the supramolecular level, further variation in the crystalline forms of a solid compound is possible. They may either exist as single molecular entities or multi-component species. As single molecular entities, molecular solids can show polymorphism, which is defined as the ability of a substance to exist in two or more crystalline phases that have different arrangements and/or conformations of molecules in the crystal lattice without undergoing changes in its chemical composition.[2] Multi-component crystals include salts, hydrates, solvates and cocrystals of the drug molecule where a second component (counter-ion, water, solvent or a cocrystal former respectively) is incorporated into the crystal lattice. Sometimes multi-component crystals can also exhibit polymorphism as discussed in chapter 5.

A crystalline phase is created as a consequence of molecular aggregation processes in solution that lead to the formation of nuclei, which achieve a certain size during the nucleation phase to enable its growth into macroscopic crystals. The factors influencing the rate and mechanism by which crystals are formed are solubility, supersaturation, diffusivity, temperature, and reactivity of the surfaces towards nucleation. The various forces responsible for holding the organic crystalline solids together are mainly hydrogen bonds and other non-covalent interactions. The subtle differences in the interplay of

these interactions may lead to the formation of polymorphs. According to Ostwald's rule[3], the system moves to equilibrium from an initial high-energy state through minimal changes in free energy. Therefore the structure that crystallizes first is one which has the lowest energy barrier (highest energy, kinetic, metastable form). This form would then transform to the next lower energy polymorph and so on until a thermodynamically stable state is achieved. The kinetics under which this transformation occurs, however, are system specific. Therefore, the existence of a more stable polymorph does not necessarily imply that a metastable polymorph cannot be produced. This can be easily understood by considering the allotropes or polymorphs of elemental carbon i.e. graphite and diamond. The former is the thermodynamically preferred crystalline form, but kinetic factors in particular high energy activation barrier make the rate of transformation from diamond to graphite infinitely slow.[4] Furthermore, the structural analysis of various polymorphs at different stages would help us to understand the nature and the extent of self-assembly process that take place during crystallization.[5] In this context crystallization may be considered as a supramolecular reaction and like all chemical reactions it is controlled by kinetic and thermodynamic factors.[5d]

The structural differences between polymorphs originate through two mechanisms, namely, packing polymorphism and conformational polymorphism (Figure 1).[6,12b] Packing polymorphism is a mechanism by which molecules that are conformationally rigid can be packed into different three-dimensional structures. For example, the anti-bacterial Nitrofurantoin is a dimorphic substance.[7,8] The form 1 contains amide dimer N–H···O hydrogen bonds, whereas form 2 arises from different packing arrangements of molecules connected by infinite chain of N–H···O hydrogen bonds or an amide catemer. Two polymorphs of pyrazine-*N,N′*-dioxide discussed in the chapter 3 are packing polymorphs. Pyrazinamide, Carbamazepine, Paracetamol are other examples of packing polymorphism.[7] Conformational polymorphism (name coined by Corradini)[9] on the other hand arises from different conformers that can pack into different crystal structures. For example, Ritonavir[10] was previously known to exist in form I with *anti* amide conformation. After two years of the launch of the product, a second form II with *syn* amide conformer was accidentally crystallized. This is presumed to be obtained due to an increase in the level of carbamate impurity which has *syn* amide conformer (Figure 2a and 2b). ROY molecule,[11a,11b] 4,4-diphenyl-2,5-cyclohexadienone,[11c] Fuchsones,[11d]

Benzidine,[11e] Venlafaxine hydrochloride,[11f] Bis(*p*-tolyl) ketone *p*-Tosylhydrazone,[11g] Phenobarbital,[11h] and Barbital[7] are some examples of conformational polymorphs. Two recent reviews by Nangia[12] are exclusively dedicated to the subject of conformational polymorphism. In general, the differences in packing arrangements invariably affect the molecular geometry and, conversely, the differences in molecular geometry causes the molecules to pack differently. As a result, most examples of polymorphism in organic crystals have a mixed origin and exhibit differences in both the conformation and packing arrangement of the constituent molecules.

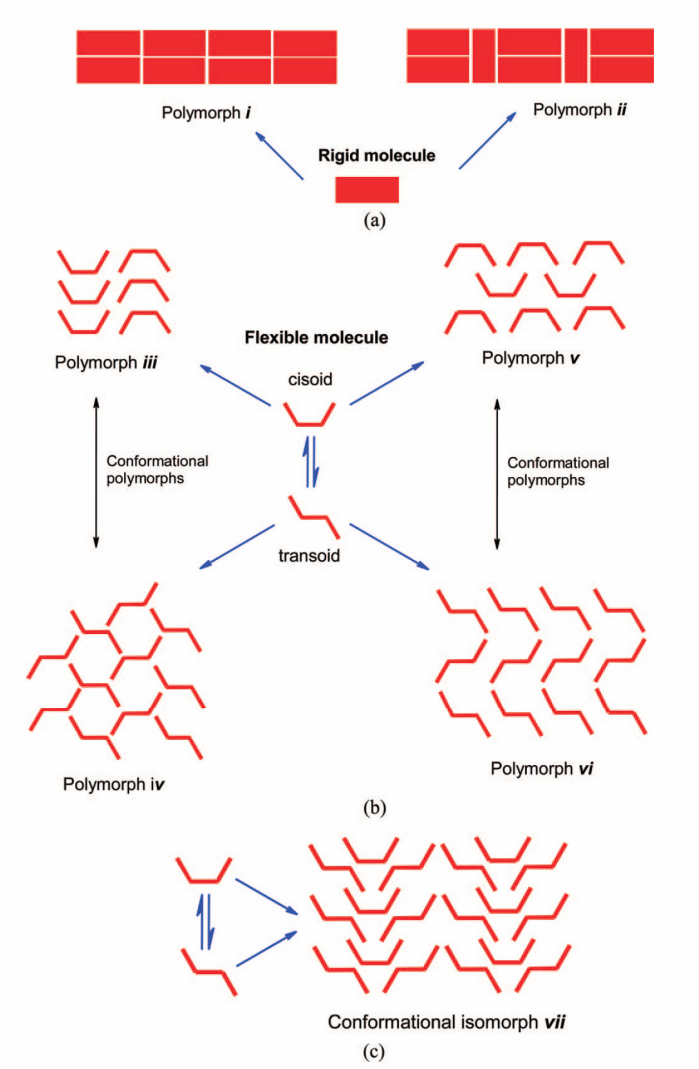

Figure 1. Schematic representation of polymorphs *i* and *ii* for a rigid molecule, (b) a conformationally flexible molecule has a greater number of packing arrangements, *iii*-*vi*, and (c) two symmetry independent molecules ($Z' > 1$) in conformational isomorph *vii*. Figure taken from A. Nangia, *Acc. Chem. Res.* **2008**, *41*, 595.

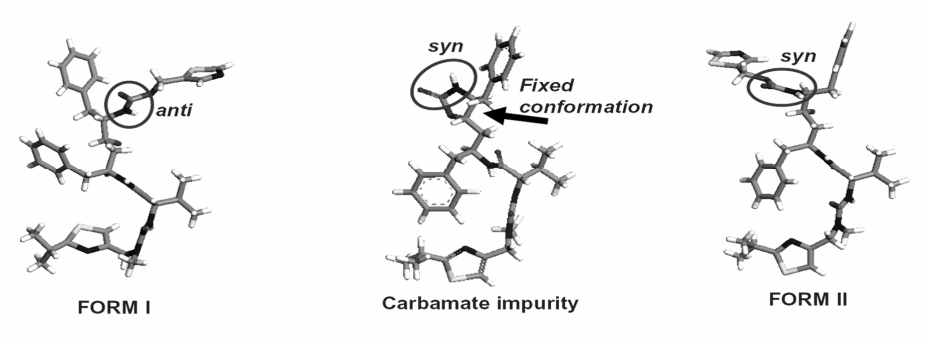

Figure 2a. The *syn* and *anti* amide conformers of ritonavir in form I and II. The accidental discovery of form II with *syn* amide conformer is presumed to be obtained due to an increase in the level of carbamate impurity which has fixed *syn* amide conformer.

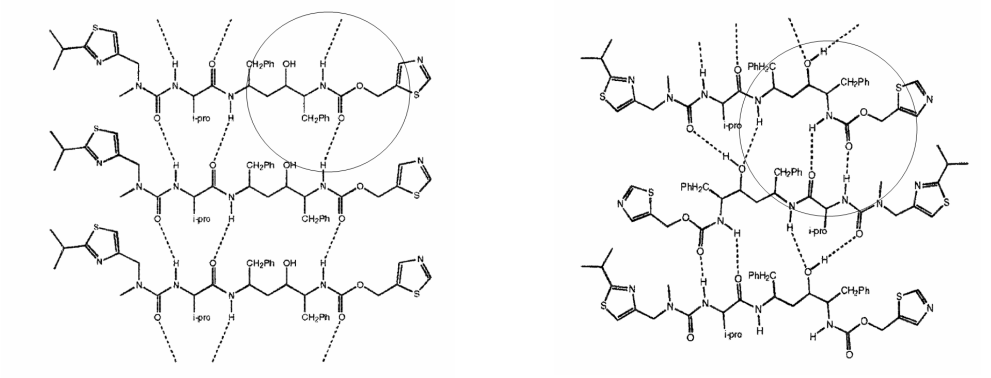

Form I Form II

Figure 2b. Ritonavir form I contains non-hierarchic hydrogen bonds (amide NH to carbonyl, alcohol OH to N of thiazole ring), whereas all the strong hydrogen bond donors and acceptors are matched in form II (alcohol OH to carbonyl and amide dimer).

Various analytical methods[1] are being currently used to characterize the crystalline form of a drug. The most valuable piece of information about the crystalline solid is the molecular structure, which is determined by single crystal X-ray diffraction. Powder X-ray diffraction provides a "fingerprint" of the solid phase which is used to differentiate between various crystalline phases and used for the determination of crystal structure at high resolution.[11h] Other spectral methods, such as Fourier Transform Infrared spectroscopy (FT-IR), Fourier Transform Raman scattering spectroscopy (FT-Raman), Solid-State Nuclear Magnetic Resonance spectroscopy (SSNMR) are used for further characterization. Of special significance are thermal methods[13] to establish the kinetic/thermodynamic stability relationships between the polymorphs. These are Differential Scanning Calorimetry (DSC), Thermo Gravimetric Analysis (TGA), and Hot Stage Microscopy (HSM).

There has been substantial research activity in the field of polymorphism driven by both fundamental scientific discovery and their importance across a wide range of industries like agrochemicals, dyes, foodstuffs and especially in the pharmaceutical industry. Recent books by Hilfiker,[14] Brittain,[15] Bernstein[6] and Byrn[1] highlight the importance of polymorphism in pharmaceuticals. There are numerous special issues of journals[16] dedicated to this particular topic and several annual reviews[17] and patents are published in the last decade. Despite its potential implications, the phenomenon of polymorphism is not always well understood, and even after many decades of research there is no consensus on what type of molecules exhibit polymorphism. Some molecules easily form polymorphs but some molecules like Benzoic acid[7] do not show signs of polymorphism even after extensive research. In 2006 a new crystal form of Maleic acid[18a] was discovered during attempted co-crystallization experiments with Caffeine, 124 years after the first crystal form was studied. Similarly a second polymorph of Aspirin[18b] was obtained in the presence of an additive Levetiracetam. These experiments show that additives can induce the appearance of polymorphic forms. It has been reported that changing the crystallization conditions such as solvents and temperature,[5b,19a] pseudoseeding,[19b] adding impurities, additives[19c,19d,19e] or polymer[19f] have yielded novel polymorphs in the literature. Of these methods, the induced nucleation or pseudoseeding[19b] with the adequate seed crystals of the form to be reproduced is the most straightforward and promising to get the desired polymorph by inhibiting the nucleation or the crystal growth of other undesired polymorphs. McCrone's statement[2] that 'the number of forms known for a given compound is proportional to the time and energy spent in research on that compound' appears to be prophetic today and validated by the discovery of many new polymorphs.[18,11e]

Since different inter and intramolecular interactions such hydrogen bonds, halogen interactions, π-stacking and van der Waals interactions are present in different crystal structures, different polymorphs will have different free energies and therefore exhibit different physical properties such as solubility, dissolution rate, density, heat capacity, crystal habit, melting point, thermal conductivity, optical activity, and particle morphology.[6] These differences impact on drug formulation and processing, dissolution rates and ultimately bioavailability of the drug.[14,15] Furthermore, stability presents a special concern. Because energy differences between polymorphs are usually small, form

inter-conversion is common. The phase transformations from a metastable to more stable form can affect the bioavailability and stability of the product drug.[14] For example, about two years after FDA approval, the HIV protease inhibitor Ritonavir[10] appeared as a previously unknown, thermodynamically more stable polymorph II with a different conformer and more number of stronger hydrogen bonds than the metastable form I (Figure 2b). The new polymorph caused the existing capsule product to fail its regulatory specifications, thus forcing removal of the capsule from the market until the product could be reformulated to meet the necessary performance criteria. The estimated loss incurred due to the accidental appearance of new polymorph and its post effects is nearly 250 $ million dollars to the Abbott laboratories.[10] Therefore risks of marketing a drug product without awareness and recognition of the thermodynamically most stable form are very high.

In the absence of solvents and humidity, the thermodynamically stable polymorph is the only one that is guaranteed not to convert into another polymorphic form and it is most often chosen for the drug development. The disadvantage of the thermodynamically stable form is that it is the least soluble polymorph and as a result has the least bioavailability. The differences in the solubility of various polymorphs are typically lower than a factor of two.[17c] Therefore, choosing the stable form with lower solubility is a small price to pay for the very large advantage gained with its absolute kinetic stability. In some cases a metastable crystalline phase may be purposely developed for the drug development when there is a significant increase in solubility and dissolution rate of metastable form (5 to 10 times) and thereby improving the absorption and/or bioavailability over the stable polymorph. Metastable form I is preferred than the stable form II of Ritonavir.[10]

Another important issue with respect to polymorphism is that different crystal forms can be considered as a patentable invention.[1,14,15] As such, Generic pharmaceutical companies are increasingly devoting their time and effort in searching for novel crystal forms in order to allow them to gain an early access into the market place, while the Innovator companies are equally giving their best to patent on all the polymorphs of a particular drug so as to extend their monopoly in pharmaceutical industry and to protect their product from generic competitors attack.[20] The Food and Drug Administration

(FDA) has strengthened regulation of the drug development process, requiring the identification and characterization of all possible polymorphs of a particular drug. Consequently polymorph screening,[21] characterizing all the possible crystalline forms of drug and identification of the stable form[22] has been regarded as an indispensable step in the early stages of drug development. Indeed such an exhaustive polymorph screening led to the discovery of the thermodynamically stable form of anti-depressant Venlafaxine hydrochloride[11f] in our laboratory by solid to solid phase transition at high temperature, which can not be obtained from usual solution crystallization techniques. Traditional methods to generate polymorphs include recrystallization from various solvents, changing the temperature and pressure, melt and sublimation crystallization, slurry conversion, and thermal microscopy. Recently, high-throughput (HT) polymorphism screening[23] has been developed with the aim of comprehensively addressing form diversity.

A recent review[24] of the Cambridge Structural Database (CSD) showed that only 5% of compounds are polymorphic. But its occurrence is more pronounced in drug molecules (30-50% in drug substances of <600 g mol^{-1} molecular weight)[1,14,17f] as they contain functional groups that are good hydrogen bond donors/acceptors and are also conformationally flexible molecules. This combination makes for a good drug but it also leads to polymorphism. Polymorphs of antitumour drug Temozolomide (TMZ) and loop diuretic Furosemide (FMD) are chosen to study the influence of conformer changes on hydrogen bonding and crystal packing. The single bond rotations of amide moiety in TMZ and sulphonamide and furan ring torsions in FMD render conformational flexibility to the chosen molecules. As polymorphism in TMZ[25b,c] and FMD[26b,c] is well established in the literature by PXRD patterns and other spectroscopy techniques, current study was undertaken to characterize them by single crystal XRD. The main advantage with single crystal X-ray diffraction study is that the detailed information about conformer changes, hydrogen bonding and molecular packing is accurately known. A thorough polymorphic screening[21] was carried out with the intent of obtaining novel polymorphs.

4.2 Polymorphs of Temozolomide

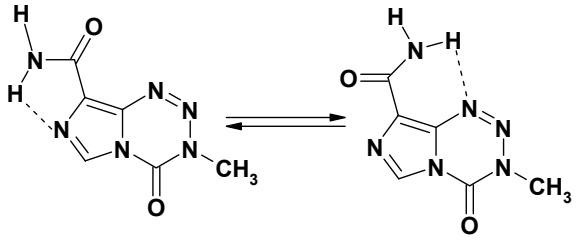

Scheme 1. Conformers of Temozolomide via rotation about the C_{amide}–$C_{imidazole}$ bond.

Temozolomide (8-carbamoyl-3-methylimidazo[5,1-*d*]-1,2,3,5-tetrazin-4(3*H*)-one, TMZ, **6**) is an antitumor prodrug, active against malignant melanoma, which acts by water-assisted tetrazinone ring opening and DNA alkylation of the incipient cytotoxic form.[25a] Only one crystal structure of TMZ is reported[25b] in the space group $P2_1/c$ with unit cell parameters a = 17.332(3), b = 7.351(2), c = 13.247(1) Å, β = 109.56(1)º. Nine unsolvated TMZ forms were disclosed in a recent US patent.[25c] However, the structural origins of polymorphism in TMZ are not known because the various polymorphic forms were characterized and differentiated by powder X-ray diffraction (PXRD) and IR spectroscopy. As mentioned earlier, the accurate information about hydrogen bonding and molecular packing in crystal structures is available from single crystal X-ray diffraction. The presence of carboxamide and N-heterocyclic functional groups (tetrazine, imidazole) in the same molecule are believed to be favourable structural features for polymorphism because of additional possibility for N–H···N hydrogen bonding in addition to the usual N–H···O bond of the amide group. For example, tetramorphs of pyrazinamide[27a] and dimorphs of isonicotinamide[27b] display differences in N–H···O and N–H···N hydrogen bond synthons. In comparison, temozolomide has a more complex molecular structure than pyrazinamide and isonicotinamide and expected to be polymorphic. TMZ can undergo rotation about the C_{amide}–$C_{imidazole}$ bond to give two conformers, *A* and *B*, both of which are stabilized by intramolecular N–H···N interaction with different N acceptor atom (Scheme 1).

4.2.1 Structural description and PXRD patterns of TMZ polymorphs

Polymorphs of temozolomide are named as polymorph 1, 2, 3, whereas they are designated as form I, II, III for furosemide polymorphs, in the order in which they are obtained. Crystallization of TMZ from common solvents such as EtOH, acetone and CH_3CN gave single crystals that matched with the unit cell of form 1 reported at room temperature (refcode DIPGIS10).[7] TMZ polymorphs 2 and 3 were obtained during attempted co-crystallization[11e,18] experiments with carbamazepine (CBZ) and pyridine-N-oxide partners.

TMZ polymorph 1, 6a: It crystallizes in the space group $P2_1/c$ with two symmetry-independent molecules ($Z' = 2$). Both molecules adopt conformation *A* that has an intramolecular N_{amide}–H···$N_{imidazole}$ bond of 5-member ring (Scheme 1). TMZ molecules hydrogen bond in the crystal structure via amide dimer synthon (N1–H1A···O3: 2.03 Å, 3.024(2) Å, 167.7º; N7–H7A···O1: 1.84 Å, 2.855(2) Å, 177.3º) between symmetry independent TMZ molecules and extend as helices down the [010] direction via N7–H7B···O4 (2.02 Å, 2.997(2) Å, 160.7º) and C6–H6B···O1 (2.28 Å, 3.279(2) Å, 151.5º) H bonds (Figure 3). Weak C–H···O, N–H···N and C–H···N interactions complete the crystal packing.

TMZ polymorph 2, 6b: Co-crystallization of TMZ with CBZ or 3-hydroxypyridine-N-oxide, with the intent of obtaining a 1:1 cocrystal, gave a second polymorph of TMZ in the space group $P2_1/n$. The crystal conformer is *A* ($Z' = 1$). The amide dimer between inversion related TMZ molecules (N1–H1A···O1: 1.84 Å, 2.848(1) Å, 170.1º) extends via C4–H4···O2 (2.14 Å, 3.208(1) Å, 165.0º) dimers as a one-dimensional tape parallel to the [120] direction (Figure 4). There are helices of C6–H6A···O1 (2.42 Å, 3.442(1) Å, 155.3º) and C6–H6B···N2 (2.61 Å, 3.276(1) Å, 118.8º) interactions. Surprisingly the amide a*nti* N–H is not involved in conventional intermolecular hydrogen bonding in this crystal structure.

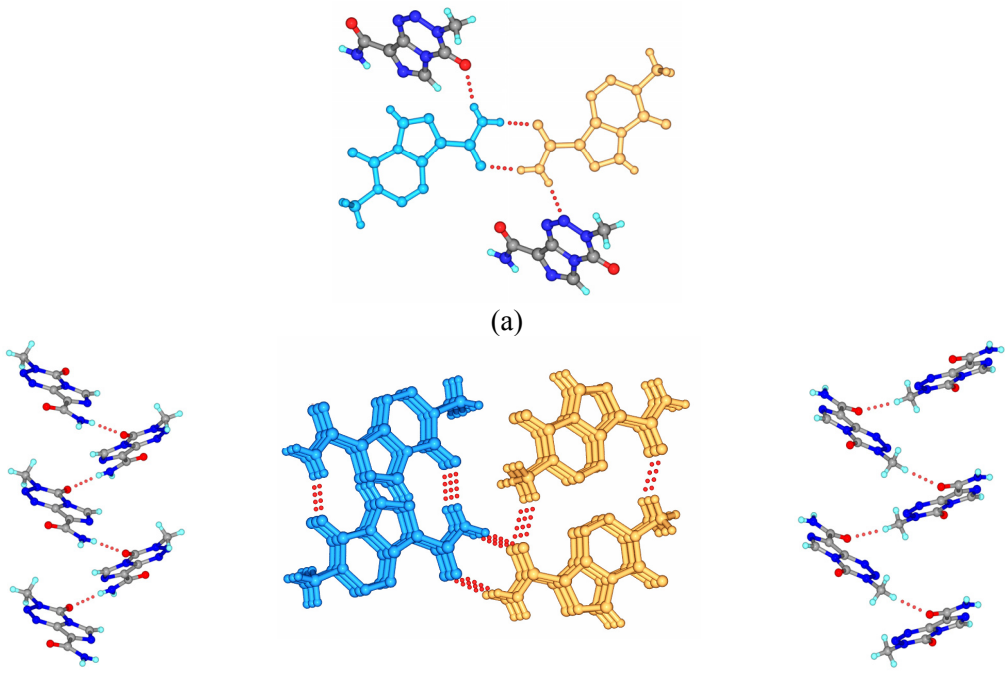

(a)

(b)

Figure 3. (a) The carboxamide dimer of crystallographic unique molecules (colored differently) in TMZ form 1. *Anti* N–Hs are involved in N7–H7B···O4 and N1–H1B···N11 bonds. (b) Helices mediated via N–H···O and C–H···O hydrogen bonds along the *b*-axis are connected by the amide dimer of symmetry-independent molecules.

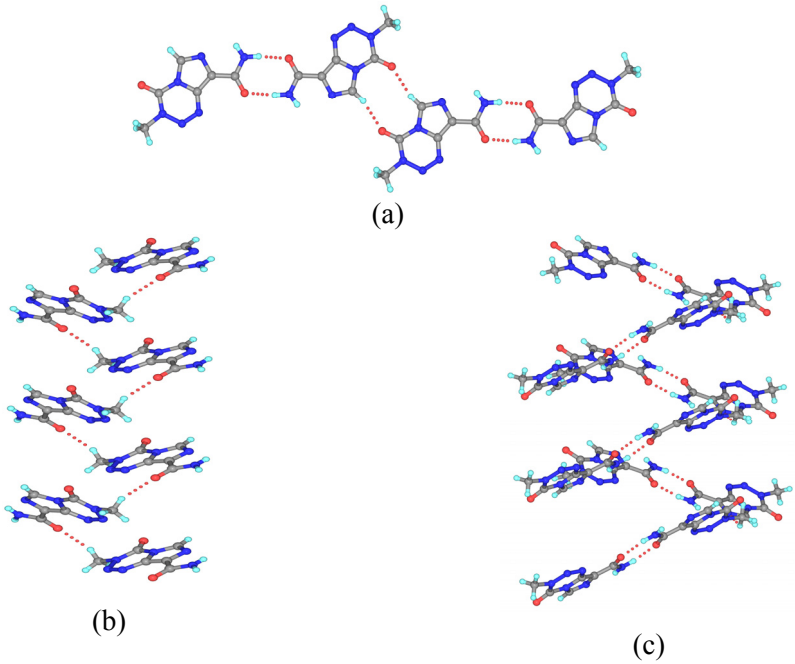

(a)

(b)

(c)

Figure 4. (a) N–H···O and C–H···O dimers assemble in a tape motif in form 2. The *anti* NH of $CONH_2$ makes only intramolecular hydrogen bond in this crystal structure. (b) Helical arrangement of TMZ via C6–H6A···O1 interaction along the *b*-axis. (c) A larger helix is present via N1–H1A···O1 and C6–H6B···N2 hydrogen bonds.

TMZ polymorph 3, 6c: Co-crystallization of TMZ and CBZ gave block-like crystals that matched with previously discussed two monoclinic crystal structures (same unit cell parameters) and a few irregular morphology crystals. This latter crystal was found to be a third polymorph of TMZ. Now there are two conformers *A* and *B* (Z' = 2, Scheme 1) in the space group $P\bar{1}$. The presence of different conformers of the same molecule in crystal structures, or conformational isomorphism due to $Z' > 1$ (Figure 1), is an interesting chemical occurrence that is as such not so common among polymorphic sets.[28] The amide group flips over to make an intramolecular N_{amide}–H···$N_{tetrazine}$ bond in conformer *B* (6-member ring). Although Z' = 2 in both polymorphs 1 and 3, the two crystallographic unique molecules have the same conformation in polymorph 1 (τ = –0.5, –3.5º) but different conformations in polymorph 3 (τ = 5.1, 178.3º). Figure 5 shows the amide dimer between conformers *A* and *B* (N1–H1A···O3: 2.11 Å, 3.114(4) Å, 169.3º; N7–H7A···O1: 1.86 Å, 2.863(5) Å, 171.7º) extends as 1D tapes via C6–H6A···O4 interaction (2.44 Å, 2.989(5) Å, 109.4º). Such parallel tapes are connected by N1–H1B···N8 (1.98 Å, 2.986(5) Å, 174.0º) and C4–H4···O2 dimer (2.27 Å, 3.327(5) Å, 164.6º) to form a 2D layer. Monoclinic polymorphs 1 and 2 are helical structures whereas triclinic polymorph 3 is layered. The serendipitous discovery of new polymorphs during attempted co-crystallization is known in the literature.[11e,18]

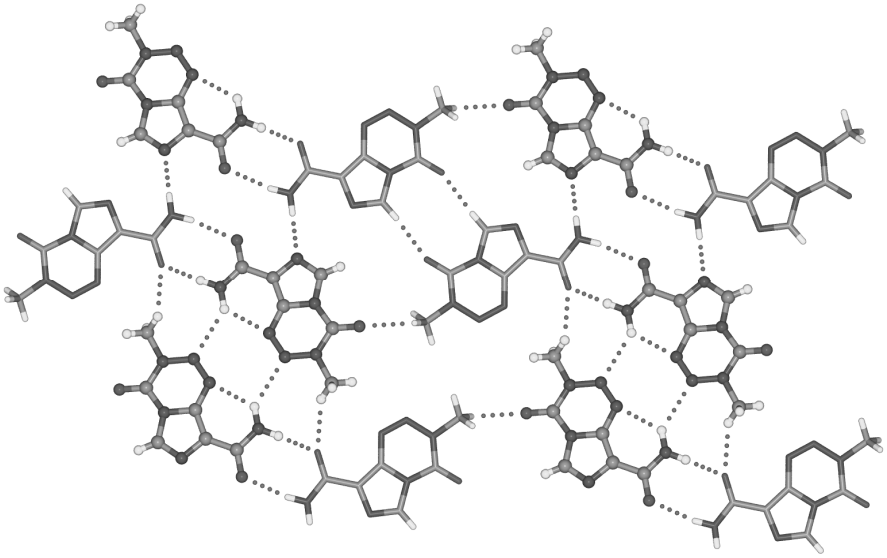

Figure 5. Amide N–H···O dimer of conformers *A* and *B* (capped-stick and ball-and-stick). N–H···O and C–H···O dimers extend the 1D tapes into 2D sheet in polymorph 3.

Powder X-ray diffraction (PXRD) patterns: The known polymorph 1 ($P2_1/c$)[25b] was found to be identical with patented form III.[25c] PXRD of polymorph 2 ($P2_1/n$) compares well with form IX of the same patent. Polymorph 3 however ($P\bar{1}$) is novel and does not match with any of the nine forms reported in the patent (Figure 6).

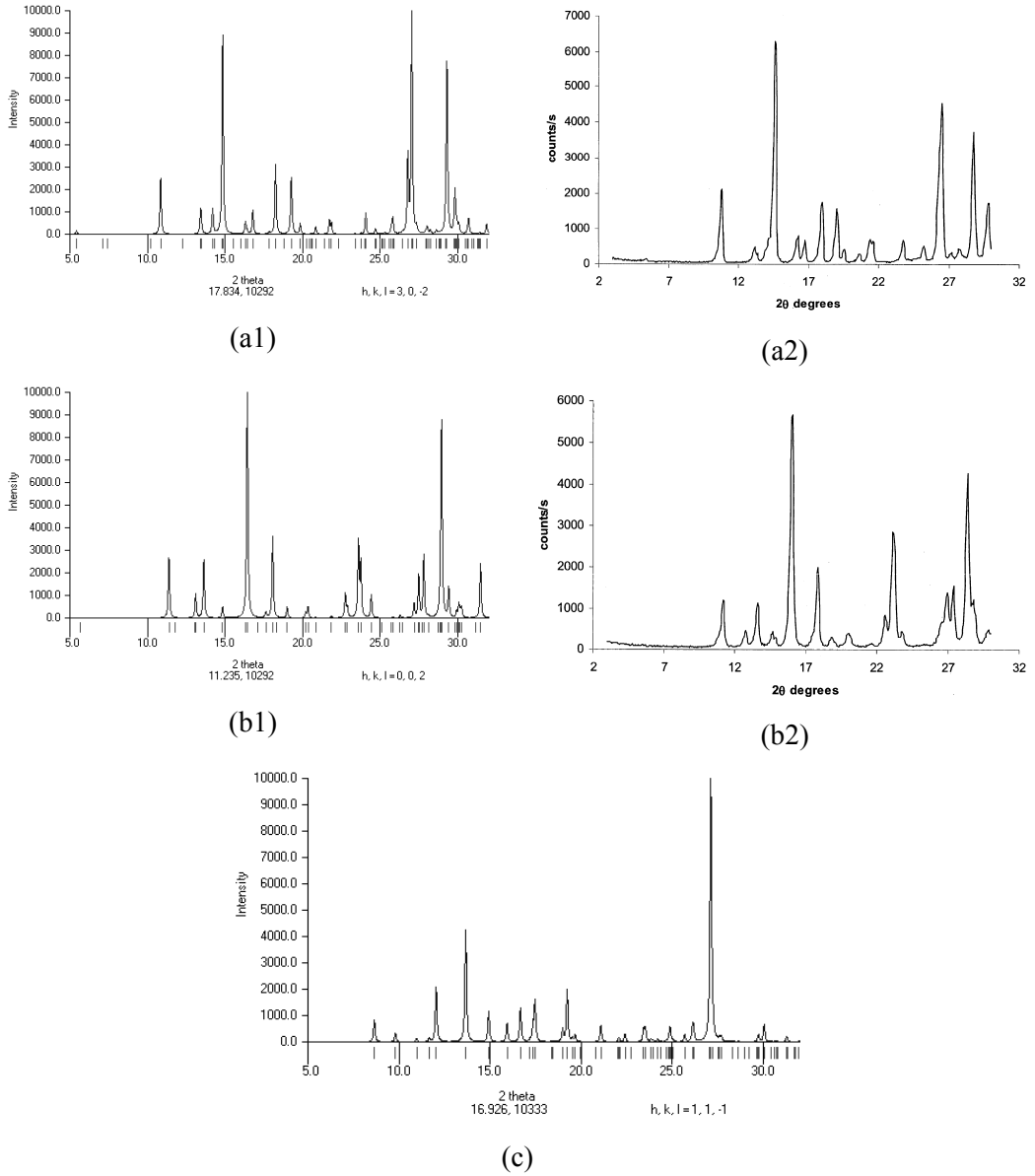

Figure 6. (a1) Simulated PXRD from TMZ polymorph 1 crystal structure. (a2) PXRD pattern of form III reported in US Patent 2005/0187206 A1. (b1) Simulated PXRD from TMZ polymorph 2 crystal structure. (b2) PXRD pattern of form IX reported in US Patent 2005/0187206 A1. The crystal structures of TMZ polymorphs 1 and 2 match with forms III and IX (of the patent). (c) Simulated PXRD from TMZ polymorph 3 crystal structure. This powder pattern does not match with any of the nine powder patterns reported in US Patent 2005/0187206 A1.

4.2.2 Grinding experiments and phase transitions of TMZ polymorphs

The grinding experiments,[29] solid-solid phase transitions[14,15,16c,16d] and slurry conversion studies or solvent mediated transformations[30] are very important in establishing the kinetic/thermodynamic stability of the polymorphs. As discussed earlier in chapter 3, metastable pyrazine-*N,N′*-dioxide form 2 converted to more stable form 1. Further grinding on PYZNO form 1 did not show any phase transition indicating that form 1 is thermodynamically stable polymorph. To carry out similar solid-state grinding experiments, sufficient quantities of the TMZ polymorphs are required. TMZ polymorph 1 is the mostly obtained form in almost all the crystallization batches, except in CH_3NO2, DMSO and supersaturated solution of CH_3CN which yielded solvated forms of temozolomide. TMZ polymorph 2 was obtained by co-crystallization experiments in small quantities of a few crystals. Therefore there is a need to stabilize this TMZ polymorph 2. We were successful in preparing bulk-material in a controlled way by desolvating the solvated forms of temozolomide. As these solvates are obtained easily, they were desolvated at the room temperature over a period of time to yield TMZ polymorph 2, which will be discussed in detail along with other structural characterization of cocrystals in chapter 6. Crystals of TMZ polymorph 3 obtained in an early experiment could not be reproduced in subsequent batches; hence further experiments could not be carried out on this sample. A reason for difficulties in crystallizing this particular form is due to the presence of the higher energy conformer B in the asymmetric unit of the crystal lattice will be discussed next.

Phase changes have been characterized by PXRD and IR patterns. There are substantial differences in the IR frequencies (range 3500-3000 cm^{-1}) indicating that hydrogen bonding of amide NH group is different for both the polymorphs of TMZ in the solid-state as shown figure 7. Ball mill grinding or manual grinding of pure TMZ polymorph 2 for 15 min in mortar/pestle did not show any changes in IR or PXRD pattern, indicating that there is no phase transformation. Addition of CH_3CN solvent during the grinding also did not have any affect. This could be due to the high activation energy required for phase transformation. Sometimes such a barrier can be easily surmounted with the seeds of the stable polymorph 1 or pseudoseeding.[19b] With this intention, a mixture of TMZ polymorphs (25 mg each of polymorph 1 and 2) was subjected to grinding for 15 min,

adding 1-2 mL of CH_3CN solvent. IR pattern on the resulting material matches nicely with the TMZ polymorph 1 (Figure 8), indicating that polymorph mixture has converted to the stable polymorph 1.

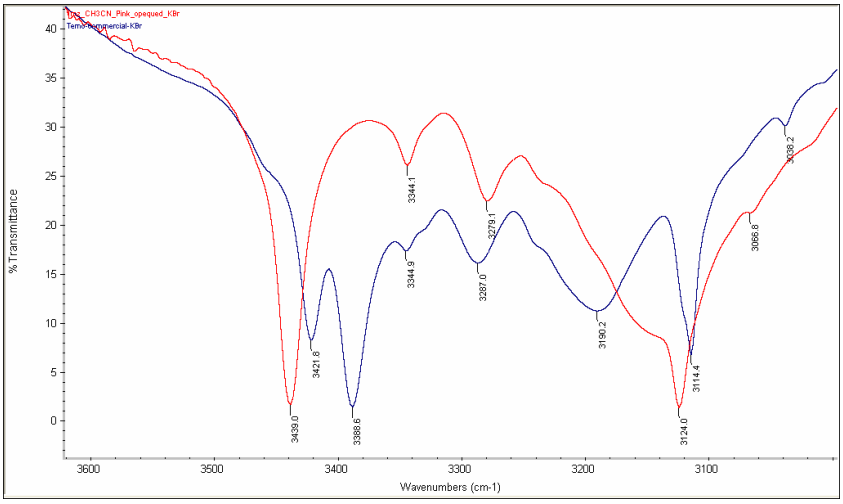

Polymorph 1

3421.8, 3388.5 3344.9, 3287.0 3190.2, 3114.4 cm^{-1}

Polymorph 2

3439.0, 3344.1 3279.1, 3124.0 cm^{-1}

Figure 7. IR spectra of TMZ polymorphs (KBr, cm^{-1}). Polymorph 1(blue) and polymorph 2 (red) are shown in different colours.

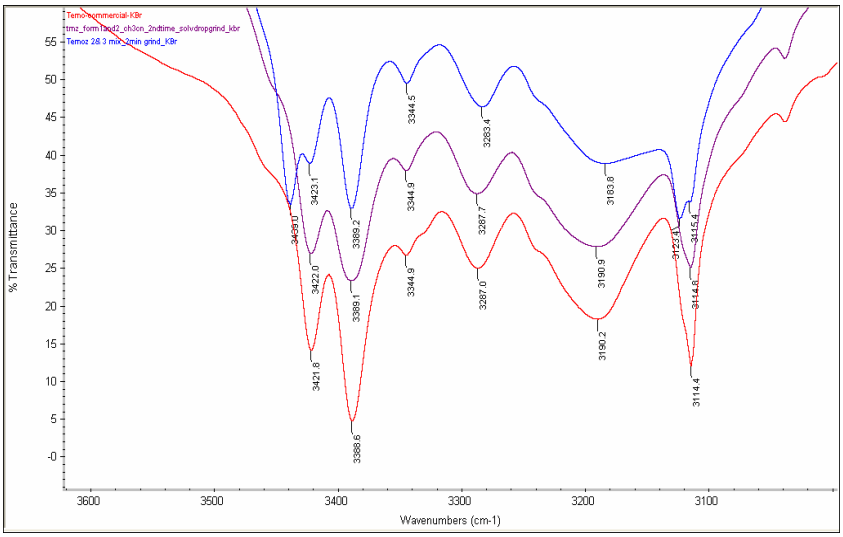

Polymorph 1 & 2 mixture
3439.0, 3423.1 3389.2, 3344.5 3283.4, 3183.6 3123.4, 3115.4 cm^{-1}

Mixture ground for 15 minutes
3422.0, 3389.1 3344.9, 3287.7 3190.9, 3114.8 cm^{-1}

Polymorph 1
3421.8, 3388.5 3344.9, 3287.0 3190.2, 3114.4 cm^{-1}

Figure 8. IR spectra of TMZ polymorphs mixture before grinding (Blue), after 15 min grinding (magenta). Resulting material (Magenta) nicely matches with the TMZ polymorph 1(red).

In order to confirm that TMZ polymorph 1 is the thermodynamically stable form, slurry grinding experiments are carried out. These slurry or aging experiments rely on the fact that a saturated solution of any metastable polymorph is supersaturated with respect to

the most stable polymorph. Given sufficient time, the most stable polymorph will crystallize in order to establish thermodynamic equilibrium and remove supersaturation.[30] 100 mg of TMZ polymorph 2 is added to 10 mL of CH_3CN and stirred for 2 days at RT. The IR and PXRD patterns confirmed that it has completely converted to TMZ polymorph 1. Further stirring for a week yielded polymorph 1, establishing that the polymorph 1 is the thermodynamically most stable form and polymorph 2 is a metastable polymorph.

The metastable nature of polymorph 2 is ascribed to hydrogen bonding differences in the two crystal structures. The amide *syn* NH makes N–H···O hydrogen bonds in both structures. The *anti* NH forms N–H···N bond in polymorph 1 whereas the donor is not intermolecularly hydrogen bonded in form 2 (Figure 3). Further C=O accepts hydrogen bonds from imiadazole CH and forms C–H···O dimer even though a better hydrogen bond amide anti NH donor is available, which is against the rule of hierarchy in hydrogen bond formation in crystals.[31] During the phase transition, molecular reorganization takes place and the unused *anti* N–H donor in polymorph 2 moves by half a molecular length translation to make intermolecular N–H···O bond in form 1 as shown in figure 9. The C=O acceptor now accepts hydrogen bonds from amide *anti* NH donor in accordance with hierarchic in hydrogen bonding. The helical architecture persists before and after reorganization. And the fact that both these polymorphs were obtained concomitantly[17b] during attempted co-crystallization experiments with CBZ point out that they have similar crystallization path way. In summary, the phase transition of TMZ polymorph 2 to 1 during grinding and slurry experiments may be understood by the stabilization from more number of hydrogen bonds in the product. All the unused hydrogen bonds in metastable polymorph 2 are utilized in the stable polymorph 1. Dimorphs of the pigment 2,9-dichloro-5,12-dihydroquino(2,3-b)acridine-7,14-dione[32] typify a similar situation. Two unused N–H donors and C=O acceptors in the black polymorph (–50.26 kcal mol^{-1}, Cerius^2) make N–H···O bonds in the red form (–59.93 kcal mol^{-1}).

The identification of unused hydrogen bond donors/ acceptors in crystal structures has attracted special mention.[33] Etter[31] proposed hydrogen bonding rules in molecular crystals. The first rule states that “all good proton donors and acceptors are used in

hydrogen bonding." Thus, molecules with strong donors, such as O─H, N─H, and C=O acceptor are expected to form conventional hydrogen bonds. Alloxan is the archetype amide with strong NH donors and C=O acceptors, but these groups hardly engage in any conventional hydrogen bonds.[33c,33d] When such strong hydrogen bonds are absent the acceptor may seek out C–H donors to form weak hydrogen bonds.[33a] Carbamazepine polymorphs are sustained by the persistent amide dimer but the *anti* NH donor is unused due to geometric constraint of the dibenzapine ring[33e] and the absence of other heteroatom acceptors in the molecule. The trimorph cluster of bis(*p*-tolyl) Ketone *p*-Tosylhydrazone[11g] is a rare example with SO_2NH functional group but do not utilize its strong hydrogen bond donors/acceptors in two of its polymorphs. However other polymorph contains conventional hydrogen bonds i.e. sulfonamide dimer. Interestingly thermodynamically stable form is the one without hydrogen bonds. The reason for the presence of hydrogen bonding or lack of it in these crystal forms is attributed to the molecular conformation.

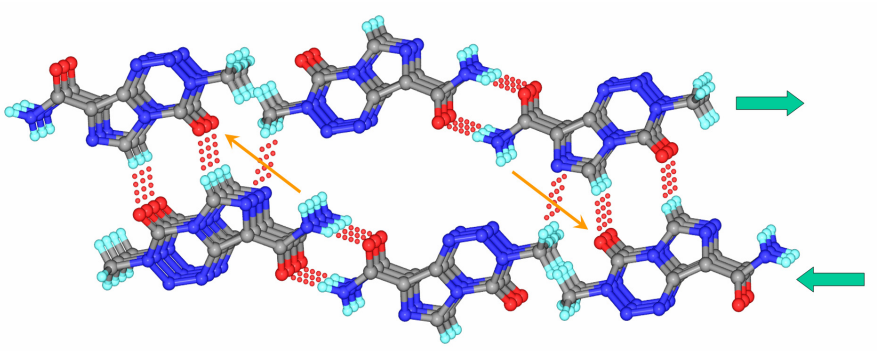

(a)

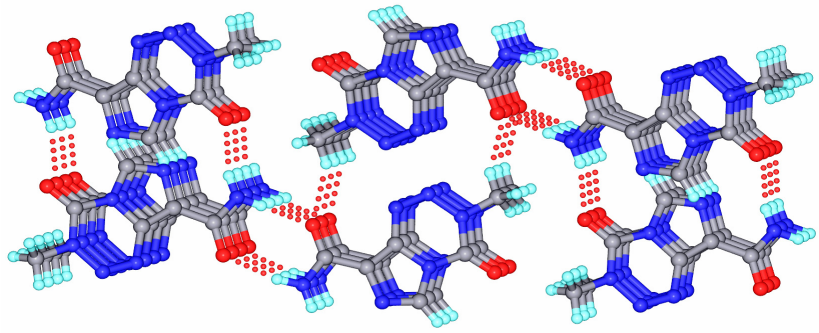

(b)

Figure 9. Hydrogen bond reorganization of TMZ polymorph 2 (a) to polymorph 1 (b). The unused amide *anti* N–H in form 2 (a, thin arrows) moves by half a molecular length translation to make intermolecular N–H···O bond in form 1 (b).

4.2.3 Conformer and lattice energy calculations

Conformer energies were calculated in Gaussian 03 (DFT, B3LYP/6-31G (d,p), Table 1) by fixing the main torsion angles to the experimental values but bond distances were allowed to relax at the nearest local minima. Conformer *B* is 1.44 kcal mol^{-1} higher in energy than conformer *A*. The difference in the energy of *A* and *B* conformers is due to electrostatics. Electron density at the imidazole and tetrazine N atoms (N2 and N6) flanking the amide group is quite different. ESP charges at the electronegative N atoms were computed in a putative perpendicular amide conformation *C* (Scheme 2, Figure 10) because intramolecular hydrogen bonding lowers the negative potential at the acceptor N atoms by about 20 kcal mol^{-1} (ESP charge at the same N atom in conformer *A* and *B* vs. *C* is compared in Table 1). The electrostatic potential at the imidazole N2 is greater than tetrazine N6 in conformer *C* (–40.41 vs. –32.46 kcal mol^{-1}, figure 10 for ESP maps). Hence, intramolecular N–H···$N_{imidazole}$ interaction (in 5-member ring) of conformer *A* should be stronger than N–H···$N_{tetrazine}$ interaction (in 6-member ring) of conformer *B*. Secondly, amide O–imidazole N repulsion in conformer *B* (N8···O3 2.82 Å) would be marginally more severe than amide O–tetrazine N repulsion in conformer *A* (N6···O1 2.96 Å). The marginally higher repulsion in conformer *B* could also be due to better overlap of lone pair lobes of heterocycle N and amide O atoms.

Table 1. Conformer energy computed in Gaussian 03 (DFT, B3LYP/6-31G (d,p)). ESP charges at imidazole N2 and tetrazine N6 were calculated in Spartan 04 (RHF/6-31G**).

Conformer	E_{conf} [kcal mol^{-1}]	N2–C2–C1–N1 τ [º]	ESP charge N2 (imidazole) [kcal mol^{-1}]	ESP charge N6 (tetrazine) [kcal mol^{-1}]
A	0.00	3.3	–22.83	----[a]
B	1.44	–178.3	----[a]	–10.01
C	7.38	–90.8	–40.41	–32.46

[a] Overlap with the electron density of amide O that lies adjacent to the ring N gives unrealistic high value of –65.16 (N2) and –59.14 (N6) kcal mol^{-1}.

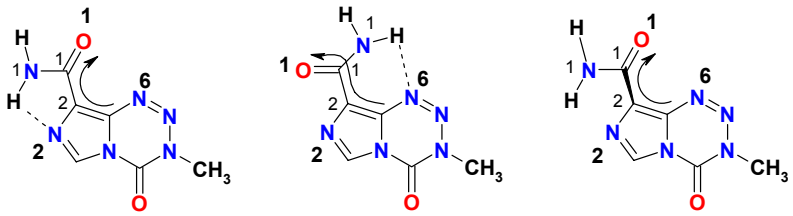

Scheme 2. Conformers *A*, *B* and *C* of TMZ. Conformer *A* (N–H···$N_{imidazole}$ bond) was taken from the X-ray structure of polymorph 1 and conformer *B* (N–H···$N_{tetrazine}$) was extracted from polymorph 3. The putative conformer *C* (perpendicular amide group) was generated computationally. Conformer energies are listed in Table 1.

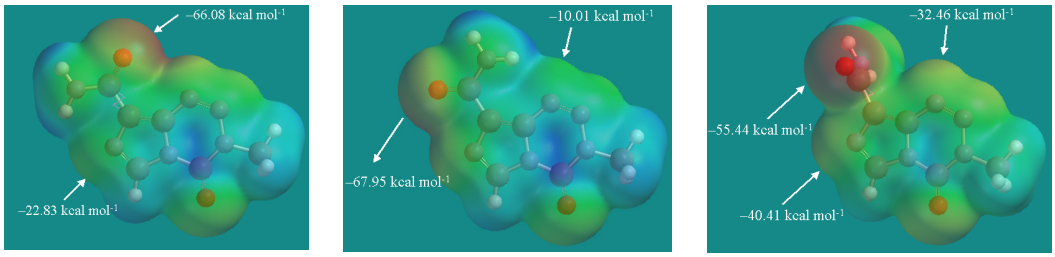

Figure 10. Electrostatic surface map of TMZ conformers *A*, *B* and *C*. The charges at amide O and heterocyclic N atoms are shown.

Energy relationships: It is difficult to measure the melting point of TMZ polymorphs 1 and 2 (as an indicator of solid form stability) because temozolomide decomposes upon heating. Therefore the stability of polymorphs 1, 2 and 3 is verified through energy computations, phase transitions, density as well as packing fraction. Crystal density (ρ_{calc}) and packing fraction follows the order polymorphs 1 > 2 > 3 (1.669, 1.626, 1.573 g cm^{-3}; 74.9 %, 72.7 %, 70.5% respectively). Lattice energy calculations (Cerius^2, COMPASS) are consistent with polymorph 1 as the stable polymorph (–33.19 kcal mol^{-1}) followed by polymorph 2 (–32.04 kcal mol^{-1}) as shown in table 2. TMZ polymorph 3 crystals of TMZ obtained in an early experiment could not be reproduced in the subsequent batches. The disappearing nature[19b] of polymorph 3 is due to destabilization from a strained conformer *B* which is 1.44 kcal mol^{-1} higher in energy than conformer *A*. Although crystal lattice energy of polymorph 3 is lower than that of 1 and 2 (Table 2), the strained conformer *B* destabilizes the total crystal energy of form 3. This situation, namely a strained conformer being stabilized in a lower crystal energy environment, is found to be quite general in conformational polymorph sets[12b] is discussed in detail in the subsequent sections.

Table 2. Crystal lattice energy U_{latt} of TMZ polymorphs computed in Cerius[2] (COMPASS force field).

Crystal structure (Data T)	Conformer	U_{latt} kcal mol^{-1}
Form 2 (100 K)	*A*	–32.04
Form 1 (100 K)	*A*	–33.19
Form 1 (298 K)	*A*	–33.84
Form 3[a] (298 K)	*A* + *B*	–34.17

[a]The crystal structure of metastable polymorph 3 could not be determined at 100K because it is disappearing polymorph.[19b]

4.3 Polymorphs of Furosemide

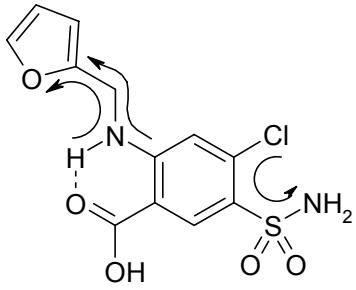

Furosemide or frusemide (5-(aminosulfonyl)-4-chloro-2-[(2-uranylmethyl) amino] benzoic acid, FMD) is an anthranilic acid derivative, which is a loop diuretic marketed under the brand name Lasix.[26a] The name lasix is derived from **la**sts **Six** (hours)-referring to the duration of action. The therapeutic effect is obtained after 30 to 60 min following an oral dose with a bioavailability of approximately 43–69%. It acts on the ascending loop of Henle in the kidney and causes the kidneys to get rid of unneeded water and salt from the body into the urine. It is also used to treat patients with high blood pressure. The molecular structure gives wealth of information especially for the conformationally flexible molecules in predicting whether it can exhibit polymorphism or not. The rigid portion of the molecule is the anthranillic acid moiety and the flexible portions are single bond rotation of sulfonamide group and the furan ring. An intramolecular N–H···O hydrogen bond renders rigidity to the anthranillic acid moiety; as a result C–C bond rotation of carboxylic moiety is not permitted. The sulfonamide and furan ring torsions may lead to different conformers in the solid sate, thereby increasing the chances of polymorphism.

The first crystal structure was reported by Fronckowiak[34a] in 1976 (refcode FURSEM) in the triclinic setting with one molecule in the asymmetric unit (Z' = 1). 3D coordinates were not reported but it was mentioned in the CSD that furfuryl group is disordered. Lamotte *et al.* in1978 (FURSEM01)[34b] reported another crystal structure with two molecules in the asymmetric unit (Z' = 2), also in triclinic setting. There is no disorder with furfuryl group. The *a*-axis is doubled when compared with the previous one (10.467 and 5.251 Å, Table 3). These are named as big unit cell (FURSEM01) with doubled *a*-axis and small unit cell (FURSEM). In 1983 another crystal structure was deposited in the CSD by Shin & Jeon (FURSEM02)[34c] with unit cell parameters matching the small unit cell. Even though the simulated powder patterns are found to be almost identical as shown in figure 11a, large differences in unit cell parameters between small and big unit cell structures created an ambiguity,[26,35,36] whether they relate to the same polymorph or two different polymorphs. A recent article by Hursthouse[36] entitled "Further errors in polymorph identification: furosemide and finasteride" in 2006 suggested that the reported crystal structures in the CSD are not different polymorphs, but relate to only one polymorph.

Table 3. Unit cell parameters reported for furosemide crystal structures in the CSD are compared with the crystal data of FMD form I discussed in this chapter.

	FURSEM	**FURSEM01**		**FURSEM02**	**AN867**[a]	**AN727**[a]	**AN734**[a]
		Not reduced	**Reduced**				
a [Å]	5.251	10.467(12)	9.584	5.234(3)	5.2336(8)	9.590(5)	9.5150(9)
b [Å]	8.771	15.801(15)	10.467	8.751(6)	8.7632(13)	10.454(5)	10.4476(10)
c [Å]	15.038	9.584(10)	15.725	15.948(15)	14.987(2)	15.701(8)	15.5826(10)
α [°]	101.77	71.87	93.47	103.68(12)	78.097(3)	93.505(9)	92.839(2)
β [°]	89.05	115.04	107.27	69.94(9)	89.130(3)	107.291(8)	107.088(2)
γ [°]	97.57	108.48	115.04	95.59(12)	82.330(3)	114.980(8)	116.088(2)
V [Å^3]	672.09	1332.843	1332.842	666.577	666.50(7)	1330.3(11)	1291.9(2)
Z'	1	2		1	1	2	2
3D	No	yes		yes	yes	yes	yes
Rf	8.0	6.8		11	9.35	7.16	6.68
Furan	disordered	ordered		disordered	disordered	ordered	ordered
cell	small	big		small	small	big	big
T [K]	298	298		298	298	298	100
Year	1976	1978		1983	2008	2008	2008

[a] AN867 (small unit cell at 298K), AN727(big unit cell at 298K) and AN734 (big unit cell at 100K) are recollected for form I crystal of furosemide.

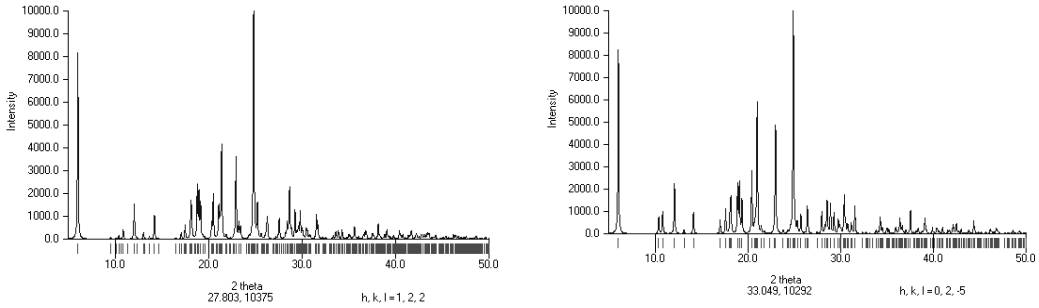

(a) (b)

Figure 11a. (a) Simulated PXRD patterns from the big unit cell (FURSEM01) (b) Simulated PXRD patterns from the small unit cell (FURSEM02). Powder patterns are identical.

Hursthouse in their paper reported that one of the crystallization experiments from methanol yielded plate like crystals on the walls and needle like crystals on the floor of the flask. Unit cell determination was carried out on both morphologies. Plate crystal matches small unit cell structure while the needle matches big unit cell structure (No data was collected; only routine unit cell checks were done). When the arrangement of molecules in the two crystal structures were analyzed from the data available from CSD, it is apparent that the symmetry independent molecules in the big unit cell structure lie alternately in analogous orientations along the *a*-axis except that they differ in the furan orientations only (Figure 11b). As a result the *h*-odd X-ray reflections receive contributions mainly from the atoms of the furan groups and are generally weak. Consequently in the cell determination of the small crystal, these were not picked up, so the halved cell was obtained.

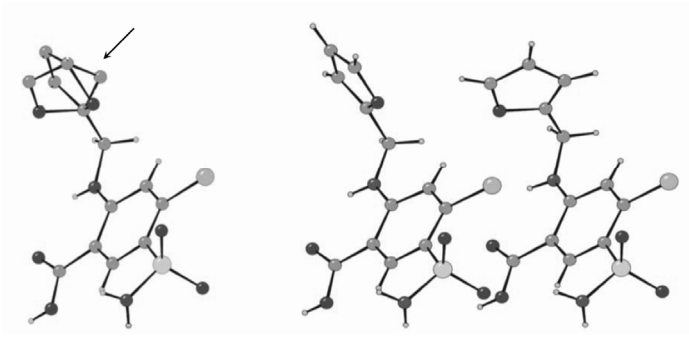

Figure 11b. A diagram showing relative orientation of the asymmetric units of small and big unit cell crystal structures of furosemide. The small unit cell has disorder in the furan ring.

We have also observed two types of crystals one plate like (very few) and needles to block in one of our crystallization experiment from *n*-propanol. Data were collected on both morphologies and *hkl* reflections were viewed in the RLATT program to confirm the points raised by Hursthouse. As suggested small unit cell crystal structure has few and very weak *h*-odd X-ray reflections shown as green spots in the RLATT (Figure 12a), are not considered in the cell determination, reduction and crystal structure solving. Therefore a single molecule is obtained in the asymmetric unit with furan ring disordered over two sites with equal occupancy. In comparison *h*-odd reflections in the big unit cell crystal structures are as many as *h*-even reflections and all the reflections are considered during cell determination (Figure 12b), resulting a big unit cell with two symmetry independent molecules with different furan ring orientations. As more number of reflections are considered for crystal structure solution, *R*-factor is lower for big unit cell structure. The choice of axes and angles for any particular crystal setting is based on the default settings that are encoded into most of the diffractometer software packages, which led to the gross differences between big and small unit cell crystal structures. Therefore both the crystal structures are not polymorphs but relate to same form I of furosemide.

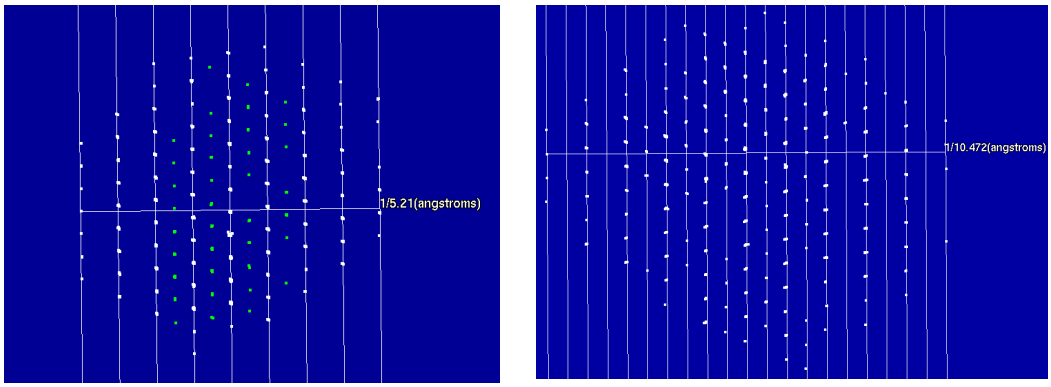

(a) (b)

Figure 12. (a) Reflections of small unit cell crystal structure viewed in RLATT program. The *h*-odd x-ray reflections are few in number (green color) and are not considered in unit cell determination therefore *a*-axis is 5.241Å. (b) Reflections of big unit cell crystal structure with equal number of *h*-odd and *h*-even reflections. Consequently *a*-axis is doubled. i.e. 10.472 Å.

Apart from FMD form I crystal structure in CSD, two papers[26b,c] have discussed about the polymorphism in furosemide. Totally six crystalline forms and one amorphous form have been discussed and characterized by PXRD, IR, DSC, SS-NMR, of which four are

true polymorphs (I, II, III and VI) and two are solvates, DMF (IV) and dioxane (V). A high temperature form VI is known to be obtained from phase transformations of form I, II and III. The PXRD pattern of form I matches the simulated powder pattern of the crystal structure reported in the CSD. In this chapter other polymorphs of furosemide are characterized by single crystal XRD and their stability relationships are established. The effect of conformational flexibility of furosemide on the hydrogen bonding and crystal packing is discussed.

4.3.1 Structural description and PXRD patterns of furosemide polymorphs

Crystallization from most of the solvents like methanol, ethanol, *n*-propanol, *i*-propanol, acetonitrile have always yielded form I. The formation of form II is solvent dependent as it was obtained exclusively from anhydrous methanol and some times from anhydrous ethanol. Form III is obtained only as few single crystals along with form I from acetic acid solvent. As the quantity of form III is less, its presence can not be detected by conventional PXRD and IR techniques. Single crystal XRD is the only method to identify and characterize this particular form. Experimental conditions mentioned for obtaining form III in the literature have always yielded form I only. Polymorphs of FMD are designated as form I, II, and III whereas TMZ polymorphs were designated as polymorph 1, 2 and 3.

FMD form I, 7a: This crystal structure is already reported in the CSD (FURSEM01, big unit cell structure) at RT. It is recollected at 100K for a better comparison with other polymorphs. It crystallized in the triclinic space group $P\bar{1}$ with two symmetry independent molecules of FMD in the asymmetric unit ($Z' = 2$). As mentioned earlier, two conformers are identical except in the orientation of furan ring. The secondary amine NH forms an intramolecular N–H···O with the carbonyl acceptor (N2–H2···O3: 1.91 Å, 2.744(5) Å, 137.6º; N5–H5···O8: 1.92 Å, 2.747(4) Å, 136.8º), which is common in all the polymorphs. Carboxylic acid dimer is formed between two symmetry independent molecules in the asymmetric unit (O4–H4 ···O8: 1.68 Å, 2.672(5) Å, 179.9º; O9–H9 ···O3: 1.65 Å, 2.635(5) Å, 173.1º). Such 1D growth units of acid dimer molecules extend into 2D corrugated sheet like structure parallel to (031) plane via weak C–H···O interactions (C8–H8B···O1: 2.54 Å, 3.155(6) Å, 114.7º; C11–H11···O6: 2.48 Å,

3.452(5)Å, 148.6º; C20–H20A···O6, 2.44 Å, 3.217(6) Å, 127.3º; Figure 13a). The NH donor and S=O acceptors of sulphonamide point up and down-wards from the 2D layer (Figure 13b) and form centro-symmetric dimers using one sulfonamide NH donor (N1–H1A···O2: 1.98 Å, 2.978(5) Å, 170.6º; N3–H3A···O7: 1.99 Å, 2.999(5) Å, 172.2º). The second NH donor connects centrosymmetric sulphonamide dimer by N–H···O hydrogen bonds (N1–H1B···O7: 2.28 Å, 3.099(6) Å, 137.2º; N3–H3B···O2: 1.99 Å, 2.926(6) Å, 151.9º; Figure 13c) and forms three dimensionally packed stair-case like structure. Sulfonamide dimer can be represented by a graph-set notation[37] $R_2^2(8)$ which is of similar origin to commonly observed 5.1 Å carboxamide packing. The crystal structure is dissected into 2D corrugated sheets and 3D packing to discuss all the hydrogen bonds in crystal structure.

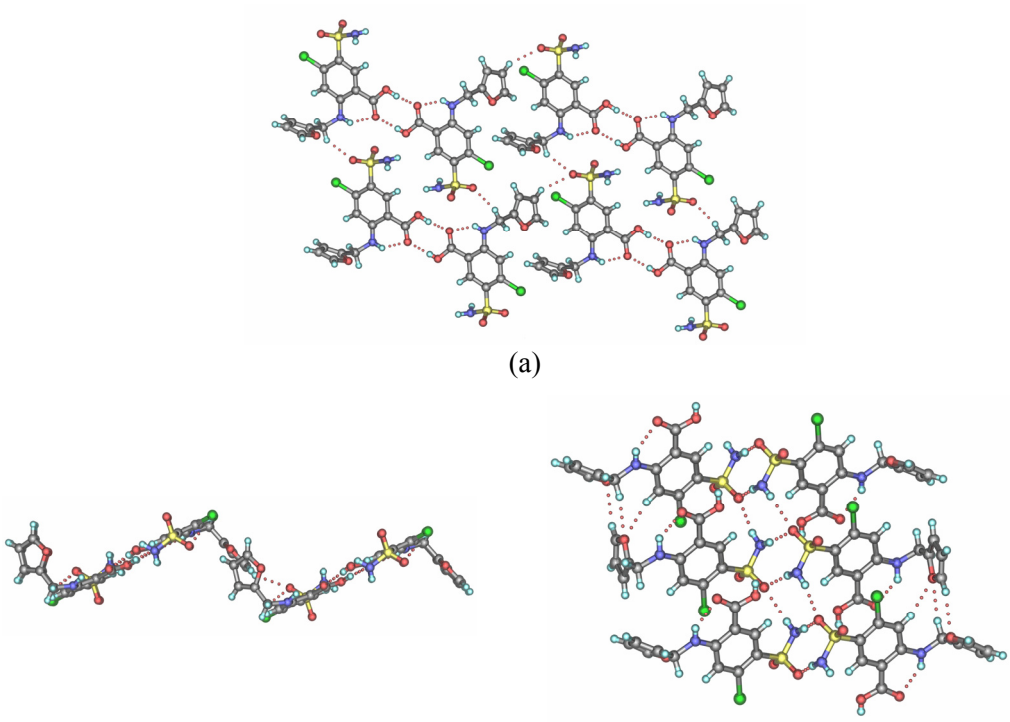

(a) (b) (c)

Figure 13. (a) Arrangement of molecules in a corrugated 2D sheet of FMD form I. (b) The sulfonamide O atoms and NH protons point up and downwards to form sulfonamide dimer in the third dimension. (c) 3D packing of the crystal structure.

FMD form II, 7b: It crystallized in the monoclinic space group $P2_1/c$ with one furosemide molecule in the asymmetric unit ($Z' = 1$). The furan ring is disordered over two sites with 75 % and 25 % site occupancy at the 298K as shown in figure 14a.

Disorder is settled at 100K (Figure 14b). This is a dynamic disorder arises due to the wagging of the flexible furan ring which is removed on lowering the temperature as the molecules are virtually frozen at 100K. Disorder in this form II should not be confused with furan ring disorder of the small unit cell structure of form I which arises due to the lack of *h*-odd reflections; hence disorder persists even at 100K.

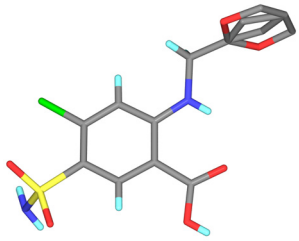

(a)

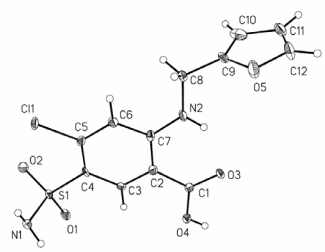

(b)

Figure 14. (a) The asymmetric unit of form II at 298K. Furan ring is disordered over two sites with 75 % and 25 % site occupancy. (b) The asymmetric unit of form II at 100K. ORTEP is drawn at 50 % probability of non-hydrogen atoms and there is no disorder.

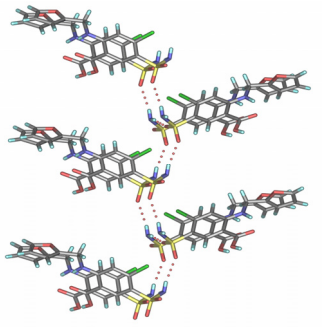

(a)

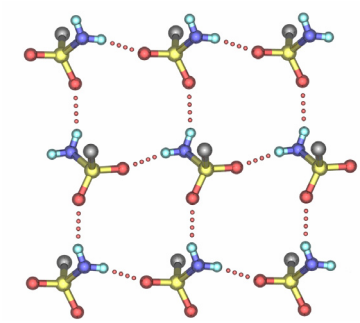

(b)

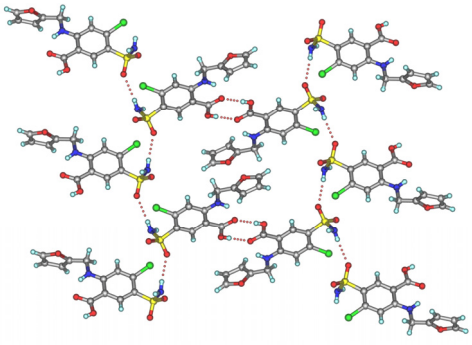

(c)

Figure 15. (a) Infinite chain of N–H···O hydrogen bonds between screw-related molecules, which further lead to square-network of sulfonamide synthons as shown in (b). The carboxylic acid dimer connects this square-net work of sulfonamide synthons as shown in (c).

Form II is a three dimensional architecture made of N–H···O hydrogen bonds. Unlike previous form I, sulphonamide dimer is not present; instead four molecules form a tetrameric sulphonamide synthon. Each furosemide molecule is connected to its two-fold screw related molecule via infinite chain of N–H···O bonds involving one of its sulfonamide NH donor and S=O acceptor (N1–H1A···O1: 2.17 Å, 3.113(4) Å, 154.4º; figure 15a). Such parallel infinite N–H···O chains are connected by other sulfonamide NH donor to form an infinite square-network of tetrameric sulfonamide synthons via N–H···O H bonds (N1–H1B···O2: 1.97 Å, 2.960(4) Å, 164.1º; figure 15b). The graph set notation of tetrameric sulfonamide synthon is $R_4^4(14)$. Carboxylic acid dimer synthon (O4–H4···O3: 1.65 Å, 2.640(3) Å, 178.0º) connects these parallel square-net work of molecules as shown figure 15c. Various other C–H···O interactions and close packing of furan ring complete the crystal packing.

FMD form III, 7c: It also crystallized in the triclinic space group $P\bar{1}$ like form I. Asymmetric unit contains one molecule of furosemide (Z' = 1). Apart from the common intramolecular hydrogen bond, another intramolecular hydrogen bond with adjacent chlorine atom is present (N1–H1B···Cl1: 2.66 Å, 3.252(4) Å, 117.0º). There is a centro-symmetric carboxylic acid dimer (O4–H4···O3: 1.67 Å, 2.644(3) Å, 168.5º) with inversion related molecule. These carboxylic acid dimer aggregates form zig-zag tapes via C–H···O dimer of sulfonamide (C3–H3···O2: 2.52 Å, 3.610(4) Å, 175.3º). Such tapes fill 2D corrugated sheet via close packing of the furan ring (Figure 16a). Sulfonamide NH and O atoms that point up and down-wards from the 2D layer form centro-symmetric dimers using one NH donor (N1–H1A···O2: 2.05 Å, 3.028(4) Å, 161.0º). Other NH donor and O acceptor join sulfonamide dimers by N–H···O H bonds (N1–H1A···O2: 2.35 Å, 2.911(4) Å, 113.9º; N1–H1B···O1: 2.37 Å, 3.178(4) Å, 136.2º; figure 16b). These two sulfonamide synthons are represented as $R_2^2(8)$ and $R_2^2(6)$ synthons. Even though sulfonamide synthons are different in these three polymorphs, the carboxylic acid group however forms similar acid dimer or $R_2^2(8)$ synthon (Figure 13, 15 and 16).

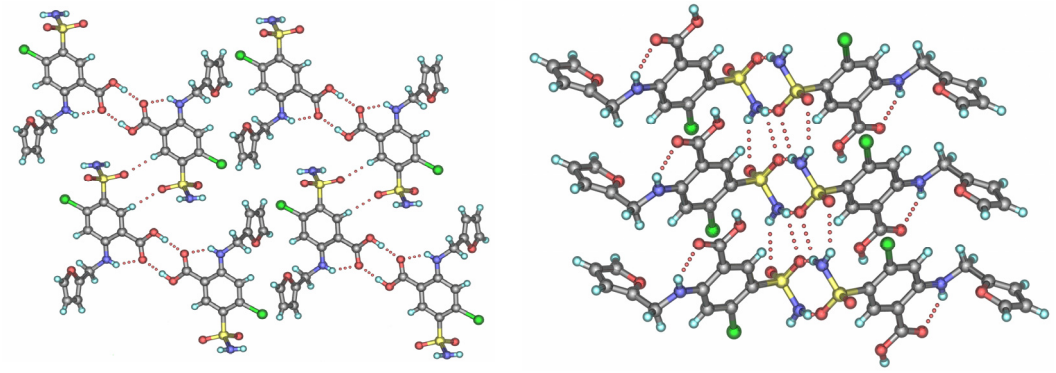

(a) (b)

Figure 16. (a) Arrangement of molecules in a corrugated 2D sheet of form III. (b) Sulfonamide forms a skewed dimer in its 3D packing.

Powder patterns: Simulated powder patterns of all the crystal structures of furosemide are compared with PXRD patterns reported in the literature.[26] All FMD forms I, II and III are found to be identical with earlier reported patterns as shown in figure 17.

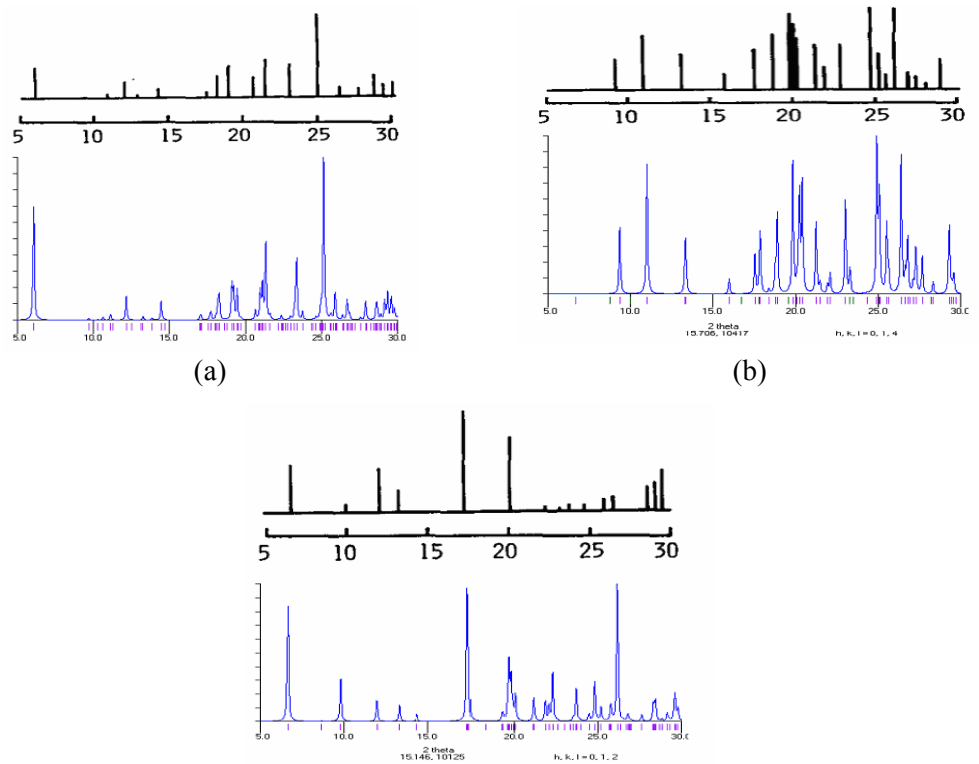

(a) (b)

(c)

Figure 17. Simulated powder patterns from crystal structures (blue), which are compared with PXRD patterns reported in the literature (black).[26] (a) Form I. (b) Form II. (c) Form III. All of them match nicely except for few minor differences after $2\theta > 20^{\circ}$ in form III crystal structure as shown in (c).

Table 4. Geometrical parameters of hydrogen bonds in furosemide polymorphs.

Polymorph	Interaction	H···A/ Å	D···A/ Å	∠D–H···A/ º
FMD form I	O4–H4 ···O8	1.68	2.672(5)	179.9
7a	O9–H9 ···O3	1.65	2.635(5)	173.1
	N1–H1A···O2	1.98	2.978(5)	170.6
	N1–H1B···O7	2.28	3.099(6)	137.2
	N2–H2···O3 Intra	1.91	2.744(5)	137.6
	N3–H3A···O7	1.99	2.999(5)	172.2
	N3–H3B···O2	1.99	2.926(6)	151.9
	N5–H5···O8 Intra	1.92	2.747(4)	136.8
	C3–H3···O7	2.55	3.137(6)	112.8
	C6–H6···O10	2.32	3.381(5)	163.4
	C11–H11···O6	2.48	3.452(5)	148.6
	C8–H8A···O10	2.60	3.611(6)	153.8
	C8–H8B···O1	2.54	3.155(6)	114.7
	C20–H20A···O6	2.44	3.217(6)	127.3
	C20–H20B···O1	2.50	3.312(6)	130.7
	C24–H24···O5	2.54	3.378(6)	132.7
FMD form II	O4–H4···O3	1.65	2.640(4)	178.0
7b	N2–H2···O3 intra	1.81	2.652(4)	138.2
	N1–H1A···O1	2.17	3.113(4)	154.4
	N1–H1B···O2	1.97	2.960(4)	164.1
	C8–H8A···O5	2.49	3.368(5)	136.4
	C8–H8B···O3	2.66	3.404(4)	125.0
	C11–H11···O2	2.77	3.594(5)	131.8
FMD form III	O4–H4···O3	1.67	2.644(3)	168.5
7c	N2–H2···O3 intra	1.86	2.670(4)	134.5
	N1–H1B···Cl1 intra	2.66	3.252(4)	117.0
	N1–H1A···O2	2.05	3.028(4)	161.0
	N1–H1A···O2	2.35	2.911(4)	113.9
	N1–H1B···O1	2.37	3.178(4)	136.2
	C3–H3···O2	2.52	3.610(4)	175.3
	C8–H8A···O1	2.24	3.310(4)	165.9

4.3.2 IR characterization of FMD polymorphs

Many peaks in the IR spectrum of furosemide form I exhibited marked differences in the respective positions of furosemide form II (Figure 18), indicating that hydrogen bonding of sulfonamide group is different in both the polymorphs in the solid-state. Form I has three characteristic peaks, 3400.0 cm^{-1} (asymmetric sulfonamide NH stretch), 3351.0 cm^{-1} (secondary amine NH vibration), 3285.6 cm^{-1} (symmetric sulfonamide NH stretch). In comparison form II has only two peaks in this region, 3347.4 cm^{-1} (secondary amine NH vibration) and 3253.9 cm^{-1} (symmetric sulfonamide NH stretch). Asymmetric stretch of sulfonamide of form II has disappeared perhaps due to the symmetrical environment of sulfonamide NH in the tetrameric sulfonamide synthon in the crystal structure of

form-II. The polymorphic mixture of form I and II obtained contains peaks of both forms i.e. 3399.9, 3350.2, 3285.4 and 3254.5 cm^{-1}.

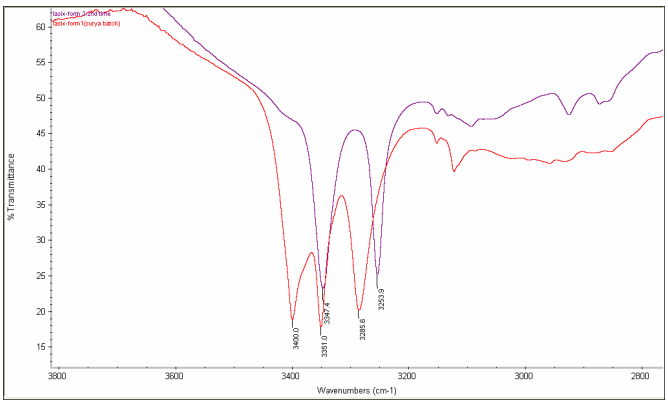

FMD form I

3400.0, 3351.0
3285.6 cm^{-1}

FMD form II

3347.4, 3285.9 cm^{-1}

Figure 18. IR spectrum (KBr, cm^{-1}) of furosemide polymorphs. Form I (red) with three sharp peaks while the form II (magenta) has only two peaks.

4.3.3 Grinding experiments and phase transitions of furosemide polymorphs

Forms I and II are obtained in sufficient quantities to carry out solid-state grinding experiments.[29] Phase changes have been characterized by PXRD and IR patterns. Form III is obtained only as few single crystals during the crystallization from acetic acid and the material is not sufficient for grinding and slurry conversion experiments.

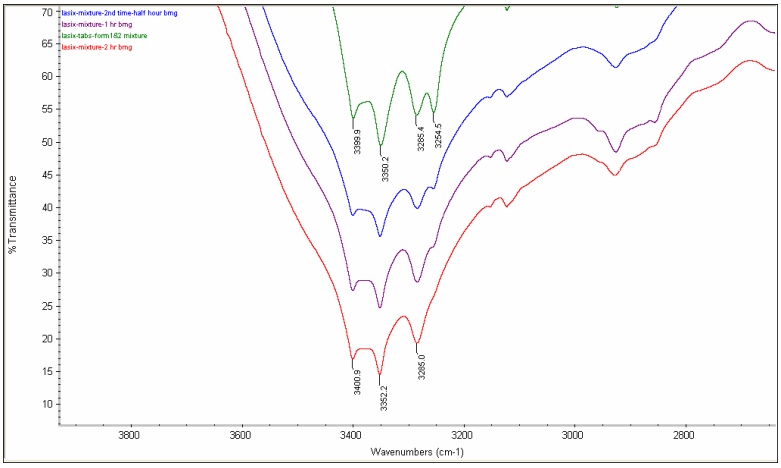

FMD mixture I + II, green
3399.9, 3350.2, 3285.4, 3254.5 cm^{-1}

After 30 min, blue
3400.6,3351.6, 3284.7, 3255.9 cm^{-1}

After 60 min, magenta
3401.0, 3351.9, 3284.7 cm^{-1}

After 120 min, red
3400, 3351, 3285.6 cm^{-1}, **FMD form I**

Figure 19. IR spectrum (KBr, cm^{-1}) recorded at regular intervals of grinding polymorph mixture (green colour spectra). After 30 min (blue), 60 min (magenta), 120 min (red). The polymorphic mixture converted to stable FMD form I after 60 min as shown by disappearance of one peak in the IR spectrum and the material showed no further change for further grinding for another 1h.

Mechanical grinding experiments on pure FMD form I and II in two different set of experiments showed no phase conversions. However when the polymorphic mixture (forms I + II) was subjected to grinding in mortar/pestle using of CH_3CN solvent, phase conversion occurred to form I in 1hr. Further grinding for another 1h showed no change in IR peaks (Figure 19) and in the relative positions of PXRD pattern (form I recovered), but increased the amorphous content in the material. The polymorphic mixture obtained was also subjected to slurry conversion which converted to form I completely in 2 days, indicating that form I is thermodynamically more stable form.

4.3.4 Thermal analysis of FMD polymorphs

The Differential Scanning Calorimetry (DSC) thermograms of form I showed two endotherms (Figure 20). The first endotherm occurs in the range 129-135 ˚C with peak temperature at 133˚C, indicating a phase transition. The Thermo Gravimetric Analysis (TGA) curve shows no weight loss over this temperature range suggesting that the first endotherm does not arise due to desolvation or decomposition of the compound. When the sample was allowed to cool after heating up to 150 ˚C, an exothermic peak observed at 133.5 ˚C suggesting that the phase transition is reversible and both the phases are enantiotropically related (black colour curve in figure 20). The second endotherm is a melting endotherm. It is a very small endotherm at 207 ˚C, immediately followed by the compound decomposition to 2-chlorosulfonyl anthranillic acid with sharp exothermic peak in the range 207-217 ˚C. The physical and morphological changes undergone by the samples during the process heating were monitored using Hot Stage Microscopy (HSM). Interestingly there are no morphological changes of crystals observed in the first endotherm temperature range as shown in figure 21. The compound did not melt however there was gradual degradation in the range 200-215 ˚C indicated by the blackening of the sample. The DSC curve of form II lacks the first endotherm. The decomposition of furosemide occurs at temperature lower than form I (T_{onset} is 201 ˚C for form II and 207 ˚C for form I). Similar observations were noted in the HSM snapshots of form II crystals (figure 22). Unlike form I, form II showed a clear melting of the compound followed by decomposition. Apart from the thermal decomposition of furosemide at high temperature,[38a,b] photolytic degradation is also observed in the literature[38c] as shown in scheme 3 which is evident from the change in colour from white

to yellow on long storage. Form I crystals are observed to be relatively more stable and resistant to degradation than form II crystals.

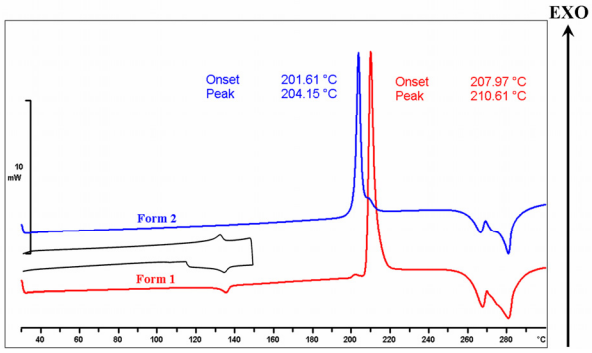

Figure 20. DSC curves of form I (red) and II (blue) of furosemide polymorphs. Heat-cool-heat cycle of form I is shown in black colour.

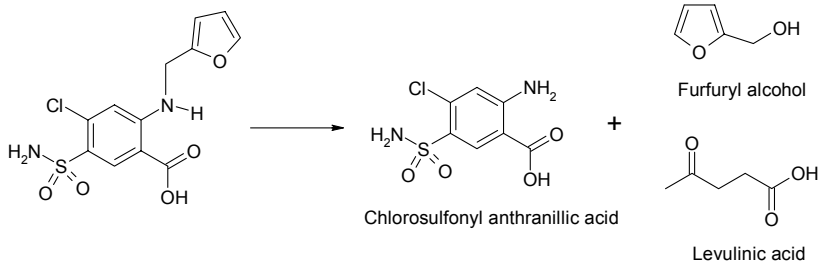

Scheme 3. Decomposition of Furosemide to CSA and other by-products.

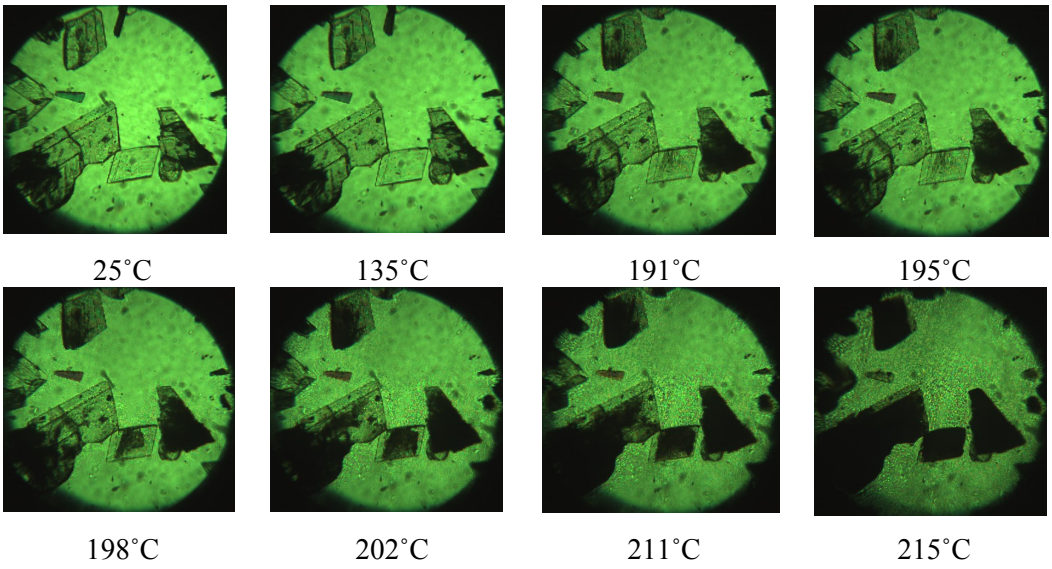

Figure 21. HSM snapshots recorded at different temperature for FMD form I crystals. There is no phase change observed at 135˚C. There is a gradual degradation of compound at higher temperature indicated by blackening of crystals.

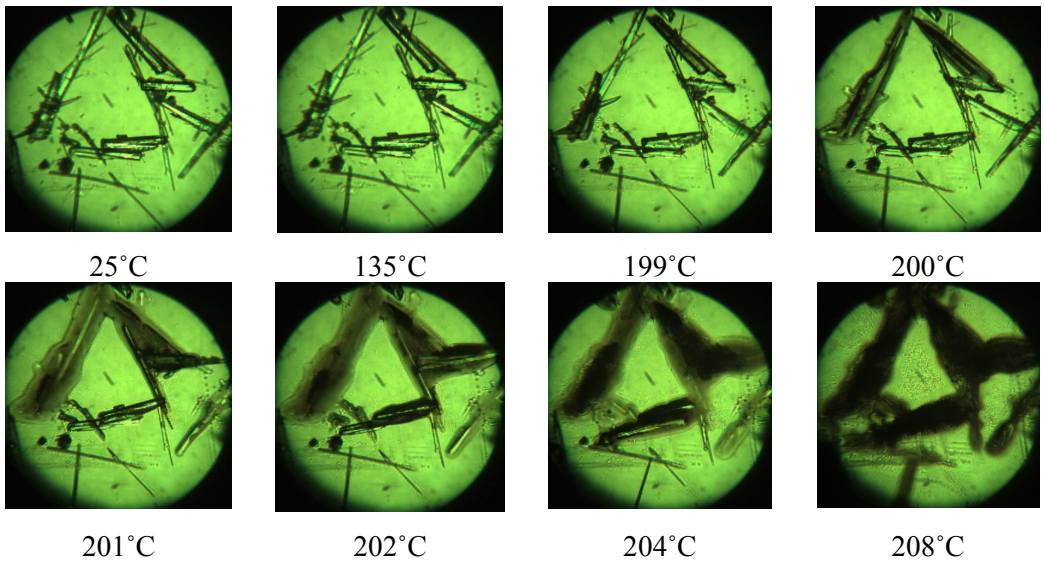

Figure 22. HSM snapshots recorded at different temperature for FMD form II crystals. Unlike form I, form II showed a clear melting of the compound at 200˚C followed by decomposition.

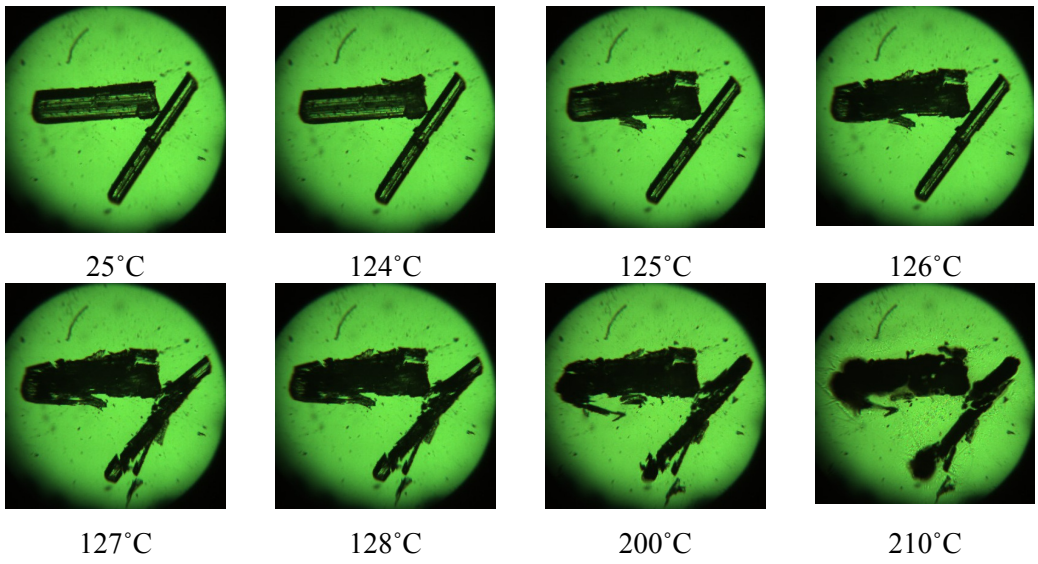

Figure 23. HSM snapshots recorded at different temperature for FMD form III. Crystals get cracked in the temperature range of 125-130 ˚C, followed by decomposition after 200˚C.

The advantage with HSM techniques is that wealth of information is known even with 1 or 2 crystals. This is illustrated using form III crystals for which DSC, TGA, PXRD, IR was not recorded due to the lack of sample in sufficient quantity. These crystals were seen to undergo an abrupt physical change resulting in the break up of the crystals in the

temperature range 125-130 ˚C, which may be due mechanical stress caused due to the arrangement of molecules in the crystal lattice or a phase transition (Figure 23).

4.3.5 Lattice and conformer energy calculations

Lattice energies for furosemide polymorphs are calculated in Cerius^2 using DREIDING 2.21 and COMPASS force fields. The energy values obtained from DREIDING do not appear to be reliable because of the large differences between them (form I, –87.83; form II, –65.549; form III, –71.873 kcal mol^{-1}) and the energy values obtained from COMPASS force filed are too close to infer any stability relationships amongst the polymorph sets (form I, –41.653; form II, –41.778; and form III, –41.533 kcal mol^{-1}). Generally the lattice energy values are less than 1 kcal mol^{-1} for concomitant polymorph systems due to which they appear in the same flask during the crystallization. Several crystallization experiments on furosemide yielded concomitant mixture of form I + II from methanol, form I + III from acetic acid, and form II + III from *n*-propanol solvent, suggesting that all the crystal structures in principle should have almost close lattice energy values. Crystal density and packing fraction follow the stability order: Form I > form II > form III (D_c = 1.700, 1.637 and 1.622 g/cm^3; Packing fraction = 74.0 %, 71.1% and 70.6 %) in accordance with the stability order from phase transitions and slurry conversion studies as discussed in the previous sections. Form I is the thermodynamically most stable polymorph at room temperature and form II and III are metastable forms.

There are four different conformers of furosemide molecule obtained from three polymorphs analyzed (two in form I and one each in form II and III). The overlay of all four conformers is shown in figure 24b. The conformational flexibility is due to torsions of sulfonamide and furfuryl ring (Figure 24a). Conformer energies were calculated in Gaussian 03 (DFT, B3LYP/6-31G (d,p), Table 5) by fixing the main torsion angles to the experimental values but bond distances were allowed to relax at the nearest local minima. The two symmetry independent molecules in form I are almost identical except in the furfuryl ring torsions attached to secondary amine moiety. The energy difference between these molecules is 0.1 kcal mol^{-1} (Table 5) which concludes that the furfuryl ring torsions have minimal effect on the conformer energy of the molecule. These two

conformers are 4.447 and 4.551 kcal mol^{-1} higher in energy than the global minima conformer or stable conformer present in the form III. The sulfonamide torsion (τ_1) in the stable conformer of form III is 55.7˚, whereas it is –166.0 and 163.2˚ for higher energy conformers of form I. In form II, the torsion (–79.9˚) is few degrees greater than the stable conformer (55.7˚), consequently its energy is marginally higher than form III stable conformer by 0.71 kcal mol^{-1}. In order to see how the conformer energy varies with different sulfonamide torsions with respect to adjacent chlorine, we have scanned a half a circle of the torsion with 10 deg increments at each step, starting from 0 to 180 deg, and their energy values are plotted against the torsion angle changes. Other half of the torsion map is generated symmetrically as the molecule is planar. Furosemide molecule is truncated to N-methyl instead of N-furfuryl for faster number crunching and moreover the furfuryl group is observed to have almost no effect on the conformer energy (Figure 25).

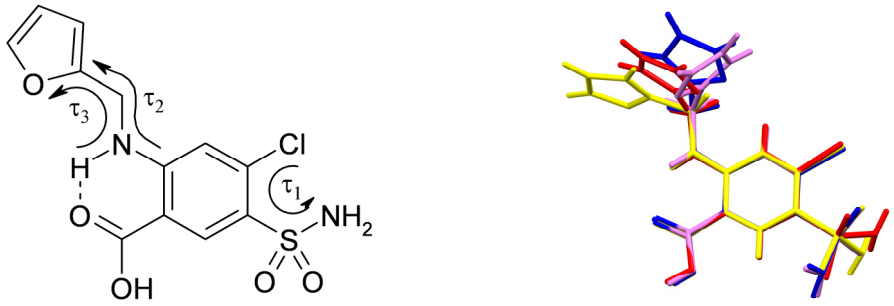

(a) (b)

Figure 24. (a) Molecular diagram of furosemide with three torsion angles. (b) Overlay of four conformers observed in three polymorphs of furosemide. Form I (pink and blue), form (yellow) and form (red).

Table 5. Conformer energy computed in Gaussian 03 (DFT, B3LYP/6-31G (d,p)).

Conformer	τ_1 / °	τ_2 / °	τ_3 / °	Energy kcal mol^{-1}
Form I_A	–166.0	83.9	–68.2	+4.447
Form I_B	163.2	–61.4	–57.6	+4.551
Form II	–79.9	–166.4	–78.2	+0.713
Form III	55.7	91.3	–59.9	0

The sulfonamide torsion renders the furosemide molecule with two energy minima as evident from the torsion map as shown in figure 25. The global minima occurs in the torsion range 50-80˚, and any conformer in this torsion range is likely to have energy difference of only 1 kcal mol^{-1} from the stable conformer at 60˚. The second minima which is higher than the first minima by ~4 kcal mol^{-1} occurs in the range 160-180˚. Energy of various conformers with different torsion angles observed experimentally in furosemide polymorphs are compared from the calculated energy-torsion map (Figure 25). Their energy values are in the expected ranges for all three forms and are shown on the torsion map. The CSD[7] was then searched for all structures that contain sulfonamide moiety adjacent to chlorine atom. There are 53 structures that match the required criteria and their sulfonamide torsion angles verified. Except for 3 entries (FURSEM01, RESRIR and REZXEZ), all of them have values in the range 50-80˚, suggesting that most of the crystal structures have conformers in the first energy minima. Hydrochlorothiazide[39] is a furosemide derivative used as diuretic is worthy to mention in this context. There are 10 crystal structures (two polymorphs and eight solvated forms) of this drug in the CSD and interestingly all of them have torsion angles between 50-80˚ i.e. in the first energy minima.

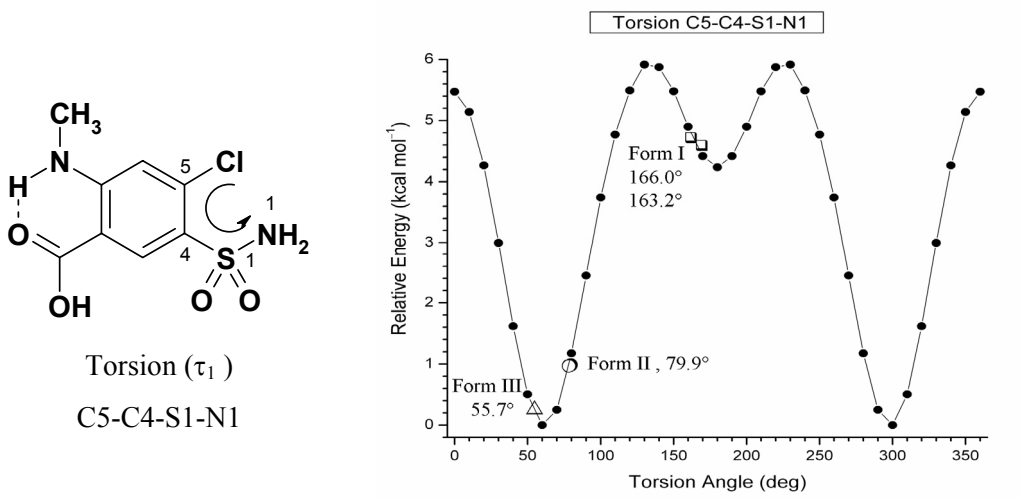

Figure 25. Furosemide molecule is truncated to its N-methyl derivative. Energy values are plotted against sulfonamide torsion angle. The energy values correlated from the torsion map are in the expected range: Form I (❑), form II (❍) and form III (△).

4.4 Systematic effects in conformational polymorphs

In general conformational flexibility introduces two potential complications to the crystallization process which are not encountered by rigid molecules. Firstly, a greater number of structural options are available for crystallization, giving rise to polymorphs that differ not only in the mode of packing but also in molecular conformation.[11] Secondly, the rate of crystallization may be significantly reduced by conformational flexibility as it has to select the right conformer from the wrong ones.[40] 5-methyl-2-[(2-nitrophenyl)amino]-3-thiophenecarbonitrile (ROY, because of its red, orange and yellow colored forms)[11a,b] is a conformationally flexible molecule known to exist in nine polymorphs, of which single crystal X-ray structures are reported for seven of these forms with different conformers in their crystal structures. Earlier studies of conformational polymorphism have shown that the bond lengths and angles do not differ significantly between polymorphs because of high energy penalty for bond stretching, compression or distortion. However rotation about C–C single bonds or single bond torsions have energy requirements of 0.5-3 kcal mol^{-1}, which is comparable to the lattice energy differences observed between polymorphs (< 4 kcal mol^{-1}).[12] This means that the energy penalty in molecular conformation can be compensated by the lattice energy gained through intermolecular interactions and close packing. In a classical example, the flat conformation of *ortho*-H biphenyl is favoured in the solid state although it lies ~1.5 kcal mol^{-1} above the lowest (gas-phase) energy conformation, which has an inter-ring twist angle of 44˚. The herringbone T-motif stabilizes the metastable planar conformation in biphenyl crystal structures. Brock and Minton[41] referred to the stabilization of strained conformers by crystal packing forces as a systematic effect. Thus, molecular conformation and hydrogen bonding can influence each other and in turn the overall crystal packing. An excellent review by Nangia[12b] showed that these systematic effects are common in conformationally flexible molecular crystals and found to occur in 16 out of 23 conformational polymorphic systems analyzed.

This intra and intermolecular energy compensation reduces total crystal energy differences, which increases the likelihood of polymorphism. Normally for rigid molecules, the total energy difference between the polymorphs is given by crystal lattice energy i.e. $\Delta E_{total} = \Delta U_{latt}$. But for conformationally flexible molecule, destabilization

energy from the higher energy conformer should be added to the lattice energy i.e. $\Delta E_{total} = \Delta U_{latt} + \Delta E_{conf}$, which decreases the total energy difference between the polymorphs and thereby increasing the polymorphs promiscuity. This observation is of significant relevance to pharmaceutical industry because typical drug molecules represent a confluence of conformational mobility and functional complexity. This is illustrated by furosemide and temozolomide molecules with sufficient conformational flexibility and functional diversity. The two high energy conformers of furosemide form I (4.447 and 4.551 kcal mol^{-1} higher in energy than the global minima conformer) are stabilized in the stable crystal lattice of form I due to better hydrogen bonding and other non-covalent forces. Similarly the metastable conformer *B* of temozolomide which is 1.44 kcal mol^{-1} higher in energy than conformer *A*, is stabilized in the lower crystal lattice of form 3. However there are few examples where the stable conformer is present in the stable crystal lattice. One such example is ROY molecule,[11a] where the stable perpendicular conformation is present in the thermodynamic yellow crystal form. The role of solvent in conformer stabilization and crystal nucleation are surely important during the crystallization of conformationally flexible molecules.[5b,19a]

4.5 Synthon Polymorphism in molecular crystals

Supramolecular synthon-based polymorphism or synthon polymorphism[42] arises due to different hydrogen bond synthons in different polymorphs. Polymorphic crystal structures of hydrogen bonding functional groups may be analyzed at two levels: the primary level of cyclic synthon or strong hydrogen bonds and the secondary level of single hydrogen bonds or weak interactions. When there is a substantial difference in the hydrogen bond synthons between polymorphs as in acid dimer and catemer or acid–acid and acid–pyridine synthons, they belong to the primary level synthon polymorph category. However in many crystal structures, the most important or principal hydrogen bond synthon remains same in all the polymorphs and the differences are only due to other hydrogen bonds. These are called as secondary level synthon polymorphs illustrated by tetramorphic pyrazinamide. All four forms have similar amide dimer motifs and they differ only in their *anti* N–H hydrogen bonding. A few common examples of primary synthon polymorphs are sulfathiazole,[5b] isonicotinamide,[27b] and tetrolic acid[43] as shown in figure 26.

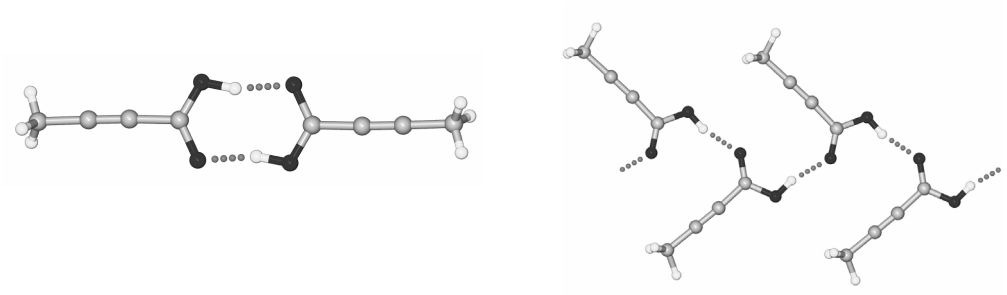

(a) (b)

Figure 26. Different hydrogen bond synthons in tetrolic acid polymorphs. (a) Carboxylic acid dimer. (b) Carboxylic acid catemer.

Polymorphs 1, 2 and 3 of TMZ exhibit secondary level synthon polymorphism. They have the same amide dimer, indicated by graph-set notation[37] $R_2^2(8)$, but the *anti* NHs make different intermolecular interactions: N–H···O and N–H···N in TMZ polymorph 1 (**6a**), the donor is intermolecularly not bonded in polymorph 2 (**6b**), and N–H···Ns are present in polymorph 3 (**6c**) as shown in figure 27. On the contrary, FMD polymorphs exhibit primary level synthon polymorphism. The interacting sulfonamide is differently hydrogen bonded in three forms: sulfonamide dimer, $R_2^2(8)$, in FMD form I (**7a**), sulfonamide tetramer, $R_4^4(14)$, in form II (**7b**) and a modified sulfonamide dimer, $R_2^2(8)$ and $R_2^2(6)$, in form III (**7c**) as shown in figure 28. The sulfonamide moiety is similar to carboxamide except that it has an extra S=O acceptor. It can either prefer to use a single acceptor or use both acceptors in hydrogen bond formation with donor N–H groups. FMD form I synthon is similar to the commonly observed carboxamide 5.1 Å motif which uses one of its one S=O acceptor and two sulfonamide N–H donors in synthon formation. On the other hand, form II and III utilizes both acceptors and donors in the sulfonamide synthons, and make different synthons. The carboxylic acid in all these forms is involved in the acid dimer which is at the secondary level of polymorphism.

The subtle differences in the conformations can have a drastic effect on the crystal packing. The anti-depressant drug Venlafaxine hydrochloride[11f] is one such example with flexible $–OCH_3$ group which can undergo rotation about C–O bond, is known to exist in three anhydrous forms. It is either present on the same side of the –OH group (*cis* conformer) or on the opposite side of –OH group (*trans* conformer) as shown in figure 29. Form 1 contains crystal packing via *trans* conformer, whereas form 2 contains *cis*

conformer only. Interestingly the newly discovered stable third polymorph contains both conformers present in the asymmetric unit.[11f]

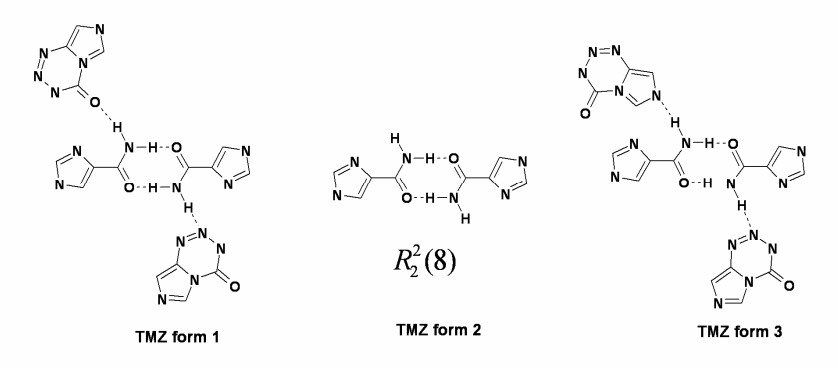

Figure 27. Polymorphs 1, 2 and 3 of TMZ exhibit secondary level synthon polymorphism. They have the same amide dimer, $R_2^2(8)$, but the *anti* NHs make different intermolecular interactions.

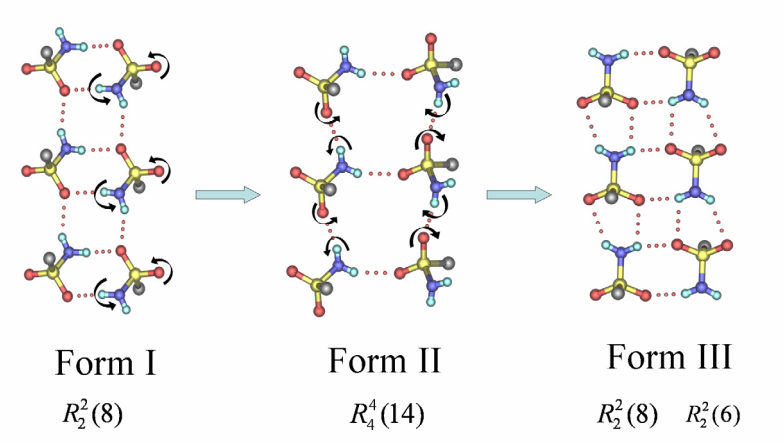

Figure 28. FMD polymorphs exhibit primary level synthon polymorphism. The sulfonamide is differently hydrogen bonded in three forms: sulfonamide dimer in form I, sulfonamide tetramer in form II and a modified or skewed sulfonamide dimer in form III. Curved arrow shows movement of SO_2NH group to give different synthons.

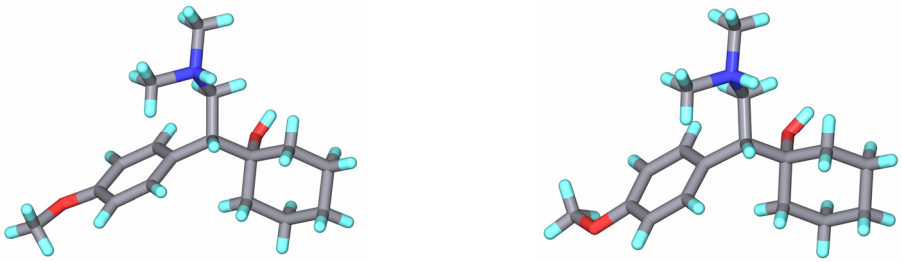

Trans conformer *Cis* conformer

Figure 29. Conformers of Venlafaxine drug via C–C bond rotation of $–OCH_3$ group.

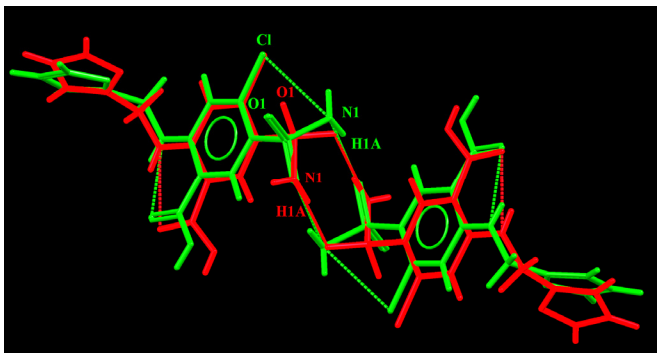

Figure 30. Form I shown in red colour has torsion angles τ_1 = 166˚ and 163.2˚. Form III is shown as green colour has τ_1 = 55.7˚. Hydrogen bond motifs in form I and III are almost identical because of similar orientation of sulfonamide NH donors and O acceptors for dimer H-bonding, even as there are large differences in their torsion angles.

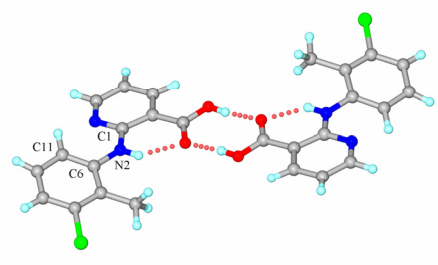

BIXGIY02 (–22.2˚)

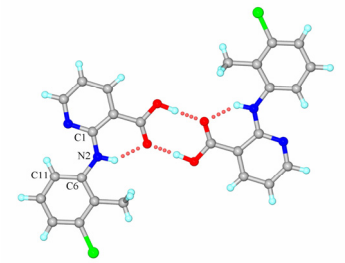

BIXGIY03 (–0.6˚)

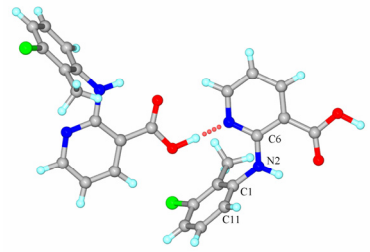

BIXGIY (–111.9˚)

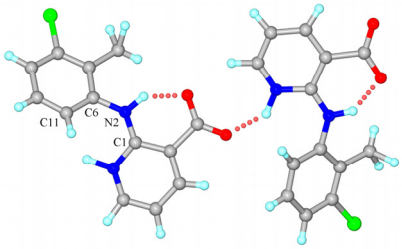

BIXGIY04 (42.6˚)

Figure 31. Different hydrogen bonded synthons of BIXGIY polymorphs arising from different conformers. Phenyl ring C11–C6–N2–C1 torsion angles are indicated along with refcodes.

The change of the sulfonamide moiety conformation in FMD form III (τ_1 = 55.7˚) to II (τ_1 = 79.9˚) has severely affected the hydrogen bond motifs which resulted in a distorted sulfonamide dimer in form III, whereas it is a sulfonamide tetramer in form II. Interestingly the hydrogen bond motifs in form I and III are almost identical, although there is a large difference in their torsion angle (τ_1 = ~165˚ in form I, 55.7˚ in form III). This is because conformers in form I and III have similar orientation of the sulfonamide

NH donor and S=O acceptor, except that they are in opposite direction, i.e. sulfonamide NH away from chlorine atom (red conformer) in form I and towards chlorine atom in form III (green conformer) as shown in figure 30. Hence both the conformers can still form sulfonamide dimer with minor differences. Different conformers leading to different hydrogen bonded synthon is noted in analgesic and anti inflammatory drug 2-(2-Methyl-3-chloroanilino)-nicotinic acid (refcode BIXGIY)[44] which contains four forms that differ in the phenyl ring torsion attached to secondary amine: carboxylic acid dimer in BIXGIY02 (–22.2˚) and BIXGIY03 (–0.6˚), carboxylic acid–pyridine synthon with proton located on carboxylic acid in BIXGIY (–111.9˚), and carboxylate–pyridinium synthon with proton migrated from carboxylic acid to pyridine moiety in BIXGIY04 (42.6˚) as shown in figure 31.

4.6 Conclusions

Polymorphs of antitumour drug Temozolomide and loop diuretic Furosemide are characterized by single crystal XRD to study the influence of conformer changes on hydrogen bonding and crystal packing. These are observed to be conformational polymorphs, having different conformations in different crystal structures. TMZ can undergo rotation about the C_{amide}–$C_{imidazole}$ bond to give two conformers, *A* and *B*. Conformer *B* is 1.44 kcal mol^{-1} higher in energy than conformer *A*. The stable conformer *A* is present in TMZ polymorphs 1 (**6a**) and 2 (**6b**) whereas both conformers crystallized in TMZ polymorph 3 (**6c**). Solid-state phase transitions, slurry conversions, lattice energy calculations, packing fraction and density values showed that the original polymorph 1 is the most stable polymorph followed by polymorphs 2 and 3. The metastable nature of TMZ polymorphs 2 and 3 is due to the presence of unused hydrogen bond donors/ acceptors and strained conformer *B* respectively. Polymorph 3 crystals of TMZ obtained in an early experiment could not be reproduced in subsequent batches perhaps due to destabilization by strained conformer *B*.

Three polymorphs of Furosemide were characterized. Conformational flexibility and variations were examined at two places: important one is the orientation of sulfonamide group towards adjacent chlorine atom and minor one is the orientation of N-methyl furan rings torsions. Totally there are four conformers present in three polymorphs: FMD form

I (**7a**) has two molecules in the asymmetric unit whereas form II (7b) and III (**7c**) contain one molecule each. Systematic effects[12] are analyzed, where in high energy metastable conformers (4.44 and 4.55 kcal mol^{-1}) are compensated in the stable crystal lattice of FMD form I (**7a**), while the stable conformer is present in the metastable crystal lattice of form III. Similarly metastable conformer *B* of Temozolomide is also compensated in the stable crystal lattice of form 3 (**6c**). We conclude that conformational flexibility in organic molecules increases the likelihood of polymorphism. (1) Several conformers are available in the crystallization milieu (solution or melt phase) to form different hydrogen bond synthons and close-packing motifs. (2) The intra- and intermolecular energy compensation reduces total crystal energy differences, which increases the likelihood of polymorphism.

Polymorphism in both these systems is based on differences in conformations and hydrogen bond synthons. Interestingly different conformations of furosemide lead to different hydrogen bonded sulfonamide synthons: sulfonamide dimer in form I, tilted or skewed dimer in form III, and a tetrameric sulfonamide synthon in form II referred to primary level synthon polymorphs. Although the conformers in form I and III are largely different, they can still form sulfonamide dimer with minor differences. In comparison, all TMZ polymorphs are secondary synthon polymorphs in that the primary amide dimer synthon is the same but the secondary N–H···N/ N–H···O hydrogen bonds are different.

4.7 Experimental Section

Preparation of Polymorphs: Temozolomide was supplied by Dabur Research Foundation, India. Crystallization of TMZ from common solvents such as EtOH, *i*-PrOH, acetone and CH_3CN by slow evaporation resulted in single crystals of the known monoclinic polymorph 1. Attempted co-crystallization with carbamazepine (CBZ) in a 1:1 molar ratio (TMZ, 25 mg, 0.127 mmol + CBZ, 30 mg, 0.127 mmol) by dissolving the components in 5 mL EtOH and slow evaporation of the solvent gave single crystals of TMZ. Needle shaped crystals had a monoclinic unit cell (Polymorph 2) and a few irregular shaped crystals had the triclinic setting (polymorph 3). Attempts to reproduce polymorph 3 (disappeared polymorph)[19b] gave a concomitant mixture of polymorph 1 (plate or block morphology, dominant) and polymorph 2 (needle shaped, minor) but no

polymorph 3. Polymorph 2 was also obtained by TMZ and 3-hydroxypyridine-*N*-oxide co-crystallization in MeOH. No cocrystals were obtained in these experiments. Furosemide was extracted from commercial Lasix tablets using methanol solvent. NMR, IR and PXRD confirmed purity of the compound. Crystallization from most of the solvents like methanol, ethanol, *n*-propanol, *i*-propanol, acetonitrile always yielded FMD form I. Very fine needles of form II for single crystal data were obtained on slow evaporation of 50 mg of compound dissolved in 5 mL of anhydrous MeOH. Form III crystals were obtained concomitantly with form I when 50 mg of compound in 2 mL acetic acid or 75 mg in 4-5 mL of *n*-propanol.

X-ray crystal structures: Reflections on single crystals of TMZ and FMD polymorphs were collected on Bruker SMART-APEX CCD X-ray diffractometer (Mo-Kα radiation, λ = 0.71073 Å). SMART was used for collecting frames, indexing reflections, and determining lattice parameters. The integration of reflections intensity and scaling was carried out in SAINT. Absorption correction was done in SADABS[45] and SHELX-TL[46] was used for space group determination, structure solution, and least-squares refinements on F^2 to give satisfactory *R*-factor. Structures were solved by the direct methods. RLATT was used to visualize *hkl*-reflections for small and big unit cell structures of form I of furosemide. X-Seed[47] was used to prepare figures and packing diagrams.

Solid-state grinding and slurry conversion: 75-100 mg of TMZ polymorph 2 was ground in a ball-mill for 60 min. There is no change in PXRD and IR patterns. However when the mixture of polymorph 1 and 2 (25 mg of each) are ground in mortar/pestle for 15 min using 1 mL of CH_3CN solvent, the resulting IR and PXRD matches polymorph 1. These seeds of stable polymorph 1 are not required for phase transition in slurry conversion experiments. 100 mg of polymorph 2 is stirred in 5-8 mL of CH_3CN. Some material was filtered after 2days. IR and PXRD patterns of the filtered material match with TMZ polymorph 1 indicating phase transition from polymorph 2 to 1. No further change observed when the stirring was continued for a week. Similar experiments are carried on furosemide. Mixture of FMD form I and II is obtained when 500 mg of the compound is dissolved in 50-75 mL of MeOH, and evaporated slowly in an open beaker. This mixture was used for grinding and slurry conversion experiments. 200 mg of this polymorph mixture was shaken in a Wig-L-Bug type mixer mill equipped with 5 mL stainless steel grinding jar and balls of 4 mm diameter. Grinding was performed at 20 Hz

oscillation rate. IR and PXRD patterns are recorded at regular intervals, 30 min, 60 min and 120 min. Phase conversion of mixture to form I was complete with in 1h and further grinding for 1h more showed no change. In a different experiment, 100 mg of the mixture was made slurry in 5-8 mL of CH3CN and stirred for 2 days. Mixture was completely converted to form I. Further stirring on the slurry for a week only recovered form I, suggesting that FMD form I is the stable form. Powder X-ray diffraction patterns was recorded on a PANalytical 1830 (Philips Analytical) diffractometer using Cu-Kα X-radiation (λ = 1.54056 Å) at 35 kV power and 25 mA current over the 2θ range 5-50° at scan rate of 1° min^{-1}. Fourier transform IR (FT-IR on Nicolet 6700) spectra are recorded in the mid IR region (4000-400 cm^{-1}).

Computations: Conformer energies were calculated in Gaussian 03 (DFT, B3LYP/6-31G (d,p)).[48] Since the observed conformation in the crystal structure is usually different from the gas phase minimized conformer and often higher in energy, constrained optimization of the crystal conformer was carried out by keeping the main torsion angles fixed but allowing bond distances and angles to relax at the nearest local minima (E_{conf}). Lattice energies were computed in Cerius^2 using the COMPASS and DREIDING 2.21 force field.[49] Crystal structures were minimized (U_{latt}) by allowing small variations in cell parameters but not gross differences between the calculated and experimental crystal lattice. The electrostatic potential map of the three conformers *A*, *B* and the perpendicular amide conformation *C* are computed in Spartan 04,[50] HF/6-31G**.

4.8 References

1) S. R. Byrn, R. R. Pfeiffer and J. G. Stowell, *Solid-State Chemistry of Drugs*; SSCI: West Lafayette, IN, **1999**.
2) W. C. McCrone, in *Physics and Chemistry of the Organic Solid State*, Vol. *2*, eds. D. Fox, M. M. Labes and A. Weissberger, Wiley Interscience, New York, **1965**, pp. 725-767.
3) W. F. Ostwald, *Z. Phys. Chem.* **1897**, *22*, 289.
4) http://www.bristol.ac.uk/Depts/Chemistry/MOTM/diamond/diamond.htm
5) (a) R. J. Davey, K. Allen, N. Blagden, W. I. Cross, H. F. Lieberman, M. J. Quayle, S. Righini, L. Seton, G. J. T. Tiddy, *CrystEngComm* **2002**, *4*, 257. (b) N. Blagden, R. J. Davey, H. F. Lieberman, L. Williams, R. Payne, R. Roberts, R.

Rowe, R. Docherty, *J. Chem. Soc. Faraday Trans.* **1998**, *94*, 1035. (c) D. Das, R. Banerjee, R. Mondal, J. A. K. Howard, R. Boese, G. R. Desiraju, *Chem. Commun.* **2006**, 555. (d) G. R. Desiraju, *Nat. Mater.* **2002**, *1*, 77.

6) J. Bernstein, *Polymorphism in Molecular Crystals*, Clarendon, Oxford, **2002**.
7) Cambridge Structural Database, CSD, version 5.29, ConQuest 1.10, November 2007 release, January update.
8) E. W. Pienaar, M. R. Caira, A. P. Lotter, *J. Cryst. Spectro. Res.* **1993**, *23*, 785.
9) P. Corradini, Chem. Ind. (Milan), **1973**, *55*, 122.
10) (a) J. Bauer, S. Spanton, R. Henry, J. Quick, W. Dziki, W. Porter, J. Morris, *Pharma. Res.* **2001**, *18*, 856. (b) S. R. Chemburkar, J. Bauer, K. Deming, H. Spiwek, K. Patel, J. Morris, R. Henry, S. Spanton, W. Dziki, W. Porter, J. Quick, P. Bauer, J. Donaubauer, B. A. Narayanan, M. Soldani, D. Riley, K. McFarland, *Org. Process Res. Dev.* **2000**, *4*, 413.
11) (a) L. Yu, G. A. Stephenson, C. A. Mitchell, C. A. Bunnell, S. V. Snorek, J. J. Bowyer, T. B. Borchardt, J. G. Stowell, S. R. Byrn, *J. Am. Chem. Soc.* **2000**, *122*, 585. (b) S. Chen, I. A. Guzei, L. Yu, *J. Am. Chem. Soc.* **2005**, *127*, 9881. (c) V. S. S. Kumar, A. Addlagatta, A. Nangia, W. T. Robinson, C. K. Broder, R. Mondal, I. R. Evans, J. A. K. Howard, F. H. Allen, *Angew. Chem. Int. Ed.* **2002**, *41*, 3848. (d) S. K. Chandran, N. K. Nath, A. Nangia, *Cryst. Growth Des.* **2008**, *8*, 140. (e) M. Rafilovich, J. Bernstein, *J. Am. Chem. Soc.* **2006**, *128*, 12185. (f) S. Roy, P. M. Bhatt, A. Nangia, G. J. Kruger, *Cryst. Growth Des.* **2007**, *7*, 476. (g) S. Roy, A. Nangia, *Cryst. Growth Des.* **2007**, *7*, 2047. (h) C. Platteau, J. Lefebvre, S. Hemon, C. Baehtz, F. Danede, D. Prevost, *Acta. Crystallogr.* **2006**, *B61*, 80.
12) (a) A. Nangia, *J. Ind. Inst. Science* **2007**, *87*, 133. (b) A. Nangia, *Acc. Chem. Res.* **2008**, *41*, 595.
13) D. Giron, *Thermo. Chimi. Acta.* **1995**, *248*, 1.
14) R. Hilfiker, *Polymorphism in the Pharmaceutical Industry*, Wiley–VCH, Weinheim, **2006**.
15) H. G. Brittan, *Polymorphism in Pharmaceutical Solids*, Marcel Dekker, New York, **1999**.

16) (a) *Cryst. Growth Des.* **2008**, *8*, 1-362. (b) *Cryst. Growth Des.* **2003**, *3*, 867-1040. (c) *Cryst. Growth Des.* **2004**, *4*, 1087-1441. (c) *Adv. Drug. Del. Rev.* **2001**, *48*, 1-136. (d) *Adv. Drug. Del. Rev.* **2004**, *56*, 241-414.

17) (a) T. L. Threlfall, *Analyst* **1995**, *120*, 2435. (b) J. Bernstein, R. J. Davey, J. -O. Henck, *Angew. Chem. Int. Ed.* **1999**, *38*, 3440. (c) H. G. Brittan, *J. Pharm. Sci*, **2007**, *96*, 705. (d) J. Bernstein, *Chem. Commun.* **2005**, 5007. (e) B. Rodríguez-Spong, C. P. Price, A. Jayashankar, A. J. Matzger , N. Rodríguez-Hornedo, *Adv. Drug. Del. Rev.* **2004**, *56*, 241. (f) G. P. Stahly, *Cryst. Growth Des.* **2007**, *7*, 1007.

18) (a) G. M. Day, A. V. Trask, W. D. S. Motherwell, W. Jones, *Chem. Commun.* **2006**, 54. (b) P. Vishweshwar, J. A. McMahon, M. Oliveira, M. L. Peterson, M. J. Zaworotko, *J. Am. Chem. Soc.* **2005**, *127*, 16802. (c) A. D. Bond, R. Boese, G. R. Desiraju, *Angew. Chem. Int. Ed.* **2007**, *46*, 618.

19) (a) S. Khoshkoo, J. Anwar, *J. Phys. D. Appl. Phys.* **1993**, *26*, B90. (b) J. D. Dunitz, J. E. Bernstein, *Acc. Chem. Res.* **1995**, *28*, 193. (c) I. Weissbuch, M. Lahav, L. Leiserowitz, *Cryst. Growth Des.* **2003**, 3, 125. (d) P. K. Thallapally, R. K. R. Jetti, A. K. Katz, H. L. Carrell, K. Singh, K. Lahiri, S. Kotha, R. Boese, G. R. Desiraju, *Angew. Chem. Int. Ed.* **2004**, *4*, 1149. (e) J. M. Kelleher, S. E. Lawrence, H. A. Moyniham, *CrystEngComm* **2006**, *8*, 327. (f) M. Long, A. L. Grzesiak, A. J. Matzger, *J. Am. Chem. Soc.* **2002**, *124*, 14834.

20) J. Bernstein, in *Polymorphism in the Pharmaceutical Industry*, ed. R. Hilfiker, Wiley–VCH, Weinheim, **2006**, pp. 365.403.

21) R. Hilfiker, S. M. De Paul, M. Szelagiewicz, in *Polymorphism in the Pharmaceutical Industry*, eds. R. Hilfiker, Wiley–VCH, Weinheim, **2006**.

22) J. M. Miller, B. M. Collman, L. R. Greene, D. J. W. Grant, A. C. Blackburn, *Pharma. Dev. Tech.* **2005**, *10*, 291.

23) S. L. Morissette, Ö. Almarsson, M. L. Peterson, J. F. Remenar, M. J. Read, A. V. Lemmo, S. Ellis, M. J. Cima, C. R. Gardner, *Adv. Drug. Del. Rev.* **2004**, *56*, 275.

24) J. Van de Streek, S. Motherwell, *Acta Crystallogr.* **2005**, *B61*, 504.

25) (a) http://en.wikipedia.org/wiki/Temozolomide. (b) P. R. Lowe, C. E. Sansom, C. H. Schwalbe, M. F. G. Stevens, A. S. Clark, *J. Med. Chem.* **1992**, *35*, 3377.

(c) I. Adin, C. Iustain, *US Pat.* 2005/0187206 A1, Aug. 25, **2005**. The nine forms are numbered I–IX.

26) (a) http://en.wikipedia.org/wiki/Furosemide. (b) C. Doherty, P. York, *lnt. J. Pharma,* **1988**, *47*, 141. (c) Y. Matsuda, E. Tatsumi, *Int. J. Pharma*, **1990**, *60*, 11.

27) (a) A. Nangia, G. R. Desiraju, *Top. Curr. Chem*. **1998**, *198*, 57. (b) C. B. Aakeröy, A. M. Beatty, B. A. Helfrich, M. Nieuwenhuyzen, *Cryst. Growth Des*. **2003**, *3*, 159.

28) (a) C. Bilton, J. A. K. Howard, N. N. L. Madhavi, A. Nangia, G. R. Desiraju, F. Allen, C. C. Wilson, *Chem. Commun.* **1999**, 1675. (b) Z.-Q. Zhang, J. N. Njus, D. J. Sandman, C. Guo, B. H. Foxman, P. Erk, R. van Gelder, *Chem. Commun.* **2004**, 886.

29) (a) L. S. Reddy, P. M. Bhatt, R. Banerjee, A. Nangia, G. J. Kruger, *Chem. Asian J.* **2007**, *2*, 505. (b) A.V. Trask, W. Jones, *Top. Curr. Chem.* **2005**, *254*, 41. (c) A. V. Trask, N. Shan, W. D. S. Motherwell, W. Jones, S. Feng, R. B. H. Tan, K. J. Carpenter, *Chem. Commun.* **2005**, 880. (d) T. Friščić, L. Fábián, J. C. Burley, W. Jones, W. D. S. Motherwell, *Chem. Commun.* **2006**, 5009.

30) C. Gu, V. Young, D. J. W. Grant, *J. Pharma. Sci.* **2001**, *90*, 1878.

31) (a) M. C. Etter, *Acc. Chem. Res.* **1990**, *23*, 120. (b) M. C. Etter, *J. Phys. Chem.* **1991**, *95*, 4601.

32) (a) T. Senju, T. Hoki, J. Mizuguchi, *Acta Crystallogr.* **2005**, E*61*, o1061. (b) T. Senju, N. Nishimura, T. Hoki, J. Mizuguchi, *Acta Crystallogr.* **2005**, E*61*, o2596. (c) N. Panina, R. van de Ven, P. Verwer, H. Meekes, E. Vlieg, G. Deroover, *Dyes and Pigments* **2008**, *79*, 183.

33) (a) G. R. Desiraju, *CrystEngComm* **2002**, *4*, 499. (b) T. C. Lewis, D. A. Tocher, S. L. Price, *Cryst. Growth Des.* **2005**, *5*, 983. (c) J. D. Dunitz, W. B. Schweizer, *CrystEngComm* **2007**, *9*, 266. (d) R. M. Ibberson, W. G. Marshall, L. E. Budd, S. Parsons, C. R. Pulham, C. K. Spanswick, *CrystEngComm* **2008**, *10*, 465. (e) A. L. Grzesiak, M. Lang, K. Kim, A. J. Matzer, *J. Pharma. Sci*. **2003**, *92*, 2260.

34) (a) M. Fronckowiak, H. Hauptman, *ACA Abstr. Papers*, **1976**, 9. (b) J. Lamotte, H. Campsteyn, L. Dupont, M. Vermeire, *Acta Cryst.* **1978**, *B34*, 689. (c) W. Shin, G. S. Jeon, *Seoul U. J. Pharm. Sci*, **1983**, *8*, 45.

35) J. N. Latosińska, M. Latosińska, W. Medycki, J. Osuchowicz, *Chem. Phy. Lett.* **2006**, *430*, 127.

36) S. Karami, Y. Li, D. S. Hughes, M. B. Hursthouse, A. E. Russell, T. L. Threlfall, M. Claybourn, R. Roberts, *Acta Crystallogr.* **2006**, *B62*, 689.

37) (a) M. C. Etter, J. C. MacDonald, J. Bernstein, *Acta. Crystallogr.* **1990**, *B46*, 256. (b) J. Bernstein, R. E. Davis, L. Shimoni, N. –L. Chang, *Angew. Chem. Int. Ed.* **1995**, *34*, 1555.

38) (a) M. M. De Villiers, J. G. van der Watt, A. P. Lotter, *Int. J. Pharma.* **1992**, *88*, 275. (b) H. Beyers, S. F. Malan, J. G. Van der Watt, M. M. de Villiers, *Drug. Dev. Ind. Pharma.* **2000**, *26*, 1077. (b) S. Carda-Broch, J. Esteve-Romero, M. C. García-Alvarez-Coque, *J. Pharma. Biomed. Anal.* **2000**, *23*, 803.

39) A. Johnston, A. J. Florence, N. Shakland, A. R. Kennedy, K. Shakland, S. L. Price, *Cryst. Growth Des.* **2007**, *7*, 705.

40) L. Yu, S. M. Reutzel-Edens, C. A. Mitchell, *Org. Proc. Res. Dev.* **2000**, *4*, 396.

41) C. P. Brock, R. P. Minton, *J. Am. Chem. Soc.* **1989**, *111*, 4586.

42) (a) R. K. R. Jetti, R. Boese, J. A. R. P. Sarma, L. S. Reddy, P. Vishweshwar, G. R. Desiraju, *Angew. Chem., Int. Ed.* **2003**, *42*, 1963. (b) B. R. Sreekanth, P. Vishweshwar, K. Vyas, *Chem. Commun.* **2007**, 2375.

43) (a) V. Benghiat, A. Gavezzotti, *J. Chem. Soc., Perkin Trans. 2,* **1972**, 1763. (b) S. Parveen, R. J. Davey, G. Dent, R. G. Pritchard, *Chem. Commun.* **2005**, 1531.

44) M. Takasuka, H. Nakai, M. Shiro, *J. Chem. Soc. Perkin Trans. 2*, **1982**, 1061.

45) G. M. Sheldrick, *SADABS*, Program for Empirical Absorption Correction of Area Detector Data, University of Göttingen, Germany, **1997**.

46) G. M. Sheldrick, *SHELXS-97 and SHELXL-97*, Programs for the Solution and Refinement of Crystal Structures, University of Göttingen, Germany, **1997**.

47) Barbour, L. J. *X-Seed*, Graphical Interface to *SHELX-97* and *POV-Ray*, University of Missouri-Columbia, USA, **1999**.

48) Gaussian 03, Revision B.05, www.gaussian.com.

49) Crystal lattice energy program, www.accelrys.com.

50) Electrostatic Surface Potential maps were generated in Spartan 04 at the RHF/ 6-31G** level, www.wavefun.com.

CHAPTER 5

CARBOXMIDE–PYRIDINE-*N*-OXIDE SYNTHON IN COCRYSTAL DESIGN

5.1 Introduction

Chemical crystallographers have studied molecular complexes and molecular compounds for over a century.[1] There is a resurgence of interest in multi-component solid-state assemblies[2] under the banner of a new name, cocrystal, in which two or more compounds coexist through hydrogen bonds or non-covalent interactions. An advantage of cocrystals is that existing properties of solids can be manipulated by altering hydrogen bonding motifs and introducing hydrophilic/hydrophobic groups in the second component. These are more attractive in pharmaceutical industry[3] as several problems encountered with Active Pharmaceutical Ingredients (APIs), in terms of their solubility, dissolution rates, and stability which can be surmounted without the need to make or break covalent bonds of the drug molecule.

The synthon approach[4] provides rational strategies for the construction of binary/ ternary cocrystals in supramolecular synthesis, crystal engineering,[2] and pharmaceutical solids.[3] This approach mainly relies on the strong hydrogen bonds between the molecules as a principle means to control molecular self assembly during crystallization. Identification of such robust synthons is now possible from a statistical analysis of the Cambridge Structural Database.[5] A hierarchy of supramolecular synthons was established by Allen et. al.[6] by calculating the probability of occurrence of 75 common non-covalent ring motifs constructed from O–H···O, O–H···N, N–H···O and N–H···N hydrogen bonds. In general, recognition between unlike functional groups or heterosynthon (acid–pyridine, acid–amide) has greater probability[7] of formation than between identical groups or homosynthon (acid–acid and amide–amide) because of greater enthalpic advantage of hydrogen bonds between unlike functional groups. Acid–pyridine heterosynthon is the most popular and frequently occurring hydrogen bond motif in the CSD, and has an occurrence probability of over 90%[8a] compared to <50% frequency for other strong hydrogen bond synthons, such as acid–acid, amide–amide, and acid–amide (Scheme 1).[8b] Nangia,[2b,2c,2f,7a] Aakeröy,[2a,2h,2i,7b] Jones,[2d,13a,16b,22] and Zaworotko[2g,3b,3c,3d,8b] have

extensively utilized acid–pyridine and acid–amide synthons to construct various binary/ternary/quaternary cocrystals.

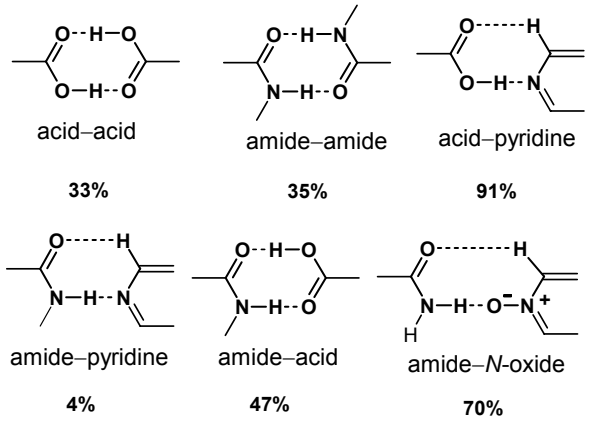

Scheme 1. Strong hydrogen bond homosynthons and heterosynthons with their occurrence probability indicated. Amide–*N*-oxide frequency is estimated from this chapter results.

5.2 Design of novel amide–pyridine-*N*-oxide heterosynthon

Unlike acid–pyridine heterosynthon, carboxamide and pyridine groups do not generally aggregate via amide–pyridine heterosynthon because the amide N–H donor is not as strong compared to acid O–H, accordingly N–H···N interaction is weaker than N–H···O hydrogen bond of the amide dimer. This is reflected in the low incidence of amide–pyridine synthon (only 4 %)[9a] in CSD structures containing primary amide and pyridine functionalities. Our research group addressed this problem in finding a complementary functional group as pyridine-*N*-oxide for the amide and designed a novel amide–pyridine-*N*-oxide heterosynthon[9] by exploiting the better acceptor strength of anionic oxygen. Pyridine-*N*-oxide (N^+–O^-) is a stronger acceptor than pyridyl N because of its anionic character. For example, pK_{HB} values of pyridine N, amide O and *N*-oxide O^- are 1.86, 1.96 and 2.70 (increasing basicity) and, moreover, electrostatic surface potential (ESP) charges at the electronegative atoms (e.g. isonicotinamide: N –43.7, O –47.4 kcal mol^{-1}; isonicotinamide *N*-oxide: O^- –53.3, O –43.1 kcal mol^{-1}) parallel the same trend. In terms of energy, the amide–pyridine-*N*-oxide two-point heterosynthon of N–H···O^- and C–H···O hydrogen bonds has an enthalpic advantage, ΔE_{HB}, of ~3.0 kcal mol^{-1} is more stable than the constituent amide–amide and pyridine-*N*-oxide homosynthons of N–H···O and C–H···O^- H bonds (Scheme 2). The "amide–pyridine-*N*-oxide" heterosynthon is

sustained by *syn*(amide)N–H···O$^-$(oxide) hydrogen bond and auxiliary (*N*-oxide)C–H···O(amide) interaction, is also referred as "amide–*N*-oxide" synthon in this chapter.

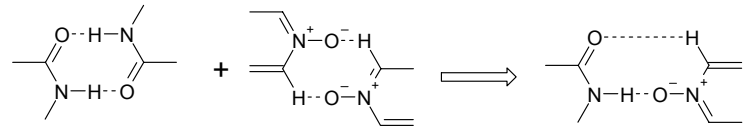

1.	–13.11	–9.63	ΔE_{synNH} = –0.50	–11.62
2.	–12.29	–9.88	ΔE_{synNH} = 0.39	–10.94
3.	–11.77	–9.00	E_{synNH} = –0.15	–10.46

1 = acetamide and pyridine *N*-oxide
2 = isonicotinamide *N*-oxide
3 = N-methylacetamide and pyridine N-oxide

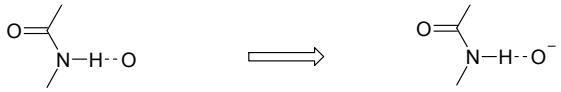

Scheme 2. Hydrogen bond synthon energy of amide–*N*-oxide heterosynthon calculated in Spartan 04 (HF/6-31G**) for **1** and **2**, Gaussian 03 (HF/6-31G+g(d,p) for **3**. The net stabilization in heterosynthon compared to homosynthons, ΔE_{HB}, is ~3 kcal mol^{-1}.

5.3 Evaluating the robustness of amide–pyridine-*N*-oxide heterosynthon

Previous results from our group[9a,9b] deal with four crystal structures containing the amide and *N*-oxide moiety in the same molecule: isonicotinamide-*N*-oxide, nicotinamide-*N*-oxide, pyrazinamide-*N*-oxide, picolinamide-*N*-oxide. Also three multi- component cocrystals bipyridine-*N,N′*-dioxide–phenobarbital, bipyridine-*N,N′*-dioxide–barbituric acid, and picoline-*N*-oxide–saccharin were studied. The amide–*N*-oxide synthon is present in all these crystal structures except picolinamide-*N*-oxide which contains amide dimer synthon in the crystal structure. From these preliminary results we concluded that there is a competition between amide–*N*-oxide heterosynthon and amide–amide homosynthon. It is difficult to assess the robustness of amide–*N*-oxide synthon because the synthon is novel and there are very few crystal structures in the CSD with amide and *N*-oxide functional moieties. In this present chapter, 13 additional cocrystals of carboxamide APIs and pyridine-*N*-oxide partners (Table 1) are discussed to find out amide–*N*-oxide synthon probability occurrence, and reasons for its absence in crystal structures. Finally the scope of amide–*N*-oxide heterosynthon in pharmaceutical solids[3]

is discussed. The amide–*N*-oxide heterosynthon is represented as a single and two point motifs as shown in scheme 3.

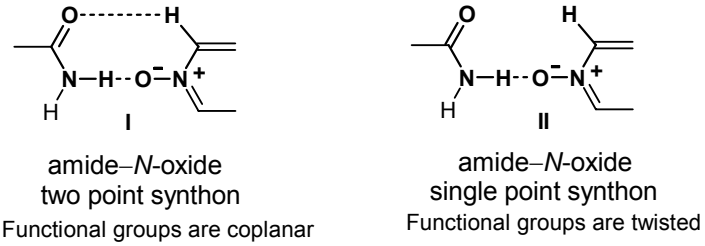

Scheme 3. Amide–*N*-oxide heterosynthon as a two point and single point synthons.

Table 1. Carboxamide APIs and pyridine-*N*-oxide partners used in cocrystals preparation.

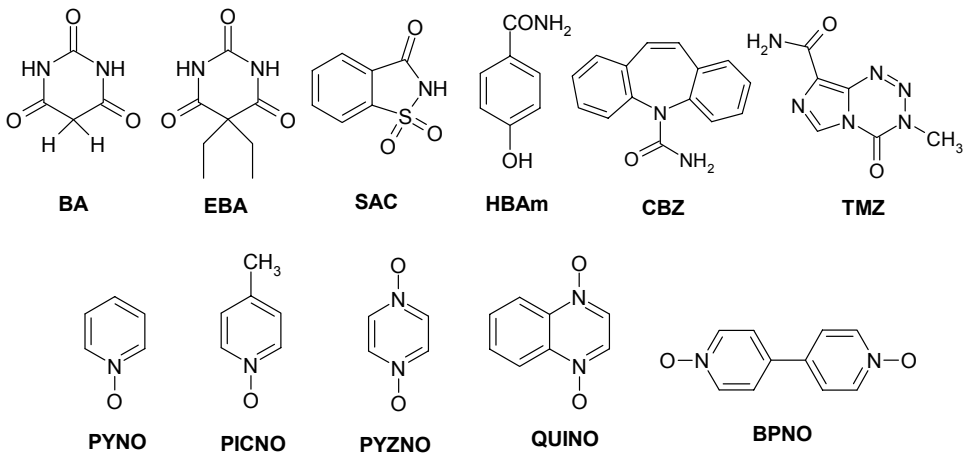

No	Cocrystal	No	Cocrystal
8	BA•QUINO (1:1)	**14**	HBAm•BPNO (1:0.5)
9	BA•PICNO (1:2)	**15**	HBAm•PYZNO•H_2O (1:0.5:1)
10	BA•PYZNO (1:0.5)	**16**	CBZ•QUINO (1:1)
11	SAC•BPNO (1:0.5)	**17**	CBZ•PYZNO (1:0.5)
12	EBA•PYNO (1:1)	**18T**	TMZ•BPNO (1:0.5)
13	EBA•PICNO (1:2)	**18M**	TMZ•BPNO (2:1)
		19	TMZ•BPNO (1:1)

5.3.1 Structural description of 13 cocrystals

Barbituric acid / quinoxaline-*N,N*'-dioxide (8): This 1:1 cocrystal crystallized in monoclinic space group $P2_1/n$. Barbituric acid, BA, molecules are connected by a centro-

symmetric amide dimer (N3–H3···O3: 1.93 Å, 2.935(1) Å, 176º). Quinoxaline-*N,N'*-dioxide, QUINO, molecules form a helix along the *b*-axis via C5–H5···O1 interaction (2.28 Å, 3.091(2) Å,130º). There is a single point amide–*N*-oxide synthon, N4–H4···O2 hydrogen bond (1.93 Å, 2.757(1) Å, 174º) in this crystal structure which connects QUINO C–H···O helices and amide dimers of BA molecules as shown in figure 1.

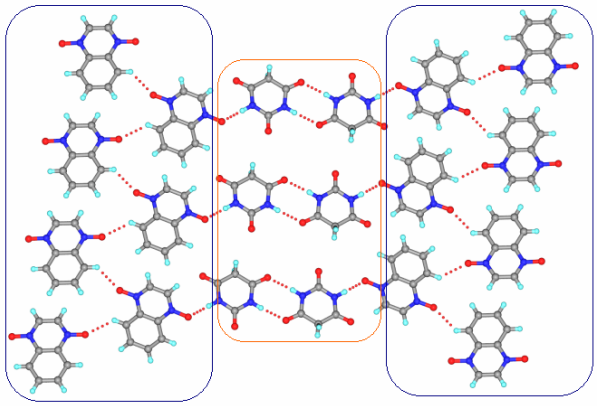

Figure 1. Amide dimer homosynthon between barbituric acid molecules and the single point amide–*N*-oxide (N–H···O^{-} hydrogen bond) with quinoxaline-*N,N'*-dioxide in cocrystal **8**.

Barbituric acid / 4-methylpyridine-*N*-oxide (9): This 1:2 cocrystal crystallized in triclinic space group $P\bar{1}$. 4-methylpyridine-*N*-oxide, PICNO, molecules flank on either side of each BA molecule sustained by amide–*N*-oxide synthons (N1–H1···O4: 1.75 Å, 2.746(2) Å, 171º; N2–H2···O5: 1.80 Å, 2.797(2) Å, 171º). A second symmetry-independent PICNO molecule forms dimers via C5–H5···O5 (2.14 Å, 3.222(2) Å, 174º) and C11–H11···O4 (2.24 Å, 3.312(2) Å, 170º) interactions. These motifs repeat in the crystal structure to generate 2D sheet structure as shown in figure 2.

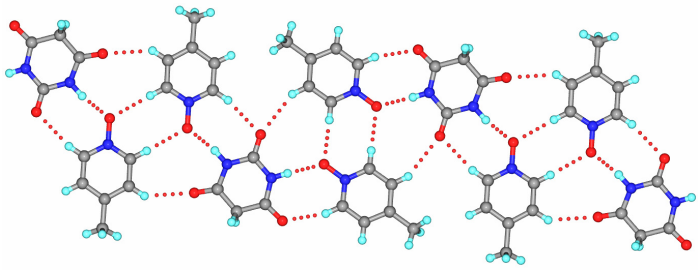

Figure 2. The amide–*N*-oxide heterosynthon connects BA and PICNO molecules in cocrystal **9** and the assembly of molecules in a 2D sheet like structure.

Barbituric acid / pyrazine-*N,N*'-dioxide (10): This 1:0.5 cocrystal crystallized in monoclinic space group $P2_1/n$. PYZNO molecule resides at the inversion center. The BA molecules extend into 1D zigzag tape through a centro-symmetric amide dimer N1–H1···O1 hydrogen bond (1.80 Å, 2.798(2) Å, 172º). PYZNO participates in amide–*N*-oxide synthon with amide group on the other side of BA molecule (N2–H2···O4: 1.78 Å, 2.785(2) Å, 172º; C6–H6···O2: 2.45 Å, 3.437(3) Å, 151º) as shown in figure 3a.

Saccharin / 4,4'-bipyridine-*N,N'*-dioxide (11): This 1:0.5 cocrystal crystallized in monoclinic space group $P2_1/n$. A strong N2–H1···O1 hydrogen bond (1.68 Å, 2.663(2) Å, 163º) connects constituent molecules in the cocrystal. The *N*-oxide acceptor is involved in bifurcated C4–H4···O1 interaction (2.06 Å, 3.136(2) Å, 170º) with an aromatic C–H donor to generate helices along the *b*-axis as shown in figure 3b.

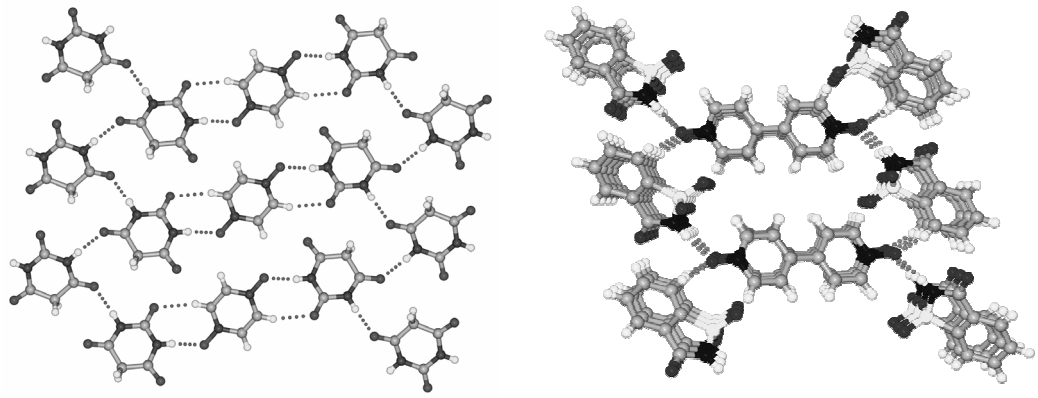

(a) (b)

Figure 3. Pyrazine-*N,N'*-dioxide molecules connect tapes of barbituric acid on either side via amide–*N*-oxide heterosynthon in cocrystal **10**. (b) A helix via amide–*N*-oxide N–H···O^- and C–H···O hydrogen bonds between saccharin and 4,4'-bipyridine-*N,N*'-dioxide molecules in cocrystal **11 (**viewed down the *b*-axis).

Diethyl barbituric acid (Barbital) / Pyridine-*N*-oxide (12): It crystallized in monoclinic space group $P2_1/c$ with one molecule each of ethyl barbital, EBA, and pyridine-N-oxide, PYNO, in the asymmetric unit. Amide–*N*-oxide heterosynthon (N2–H2···O1, 2.821(1) Å, 173º; C1–H1···O2, 3.356(1) Å, 148º, figure 4a) and hydrogen bonding of PYNO with the second amide N–H donor of EBA (N3–H3···O1, 2.867(1) Å, 172º) produce a helical assembly along the *b*-axis.

Barbital / 4-Methylpyridine-*N*-oxide (13): The cocrystal crystallized in monoclinic space group $P2_1/c$ with 1:2 stoichiometries of EBA and PICNO. Four PICNO molecules accept N–H···O$^-$ bonds from two EBA molecules (N1–H1···O8: 1.75 Å, 2.742(3) Å, 167º; N2–H2···O7: 1.74 Å, 2.735(3) Å, 170º; N3–H3···O6: 1.74 Å, 2.733(3) Å, 166º; N4–H4···O5: 1.74 Å, 2.743(3) Å, 172º, figure 4b). Picoline-*N*-oxide molecules extend into a tape through C–H···O interactions along the *a*-axis and extend into sheets in the *ab*-plane which intercalate barbital molecules through N–H···O$^-$ hydrogen bonds.

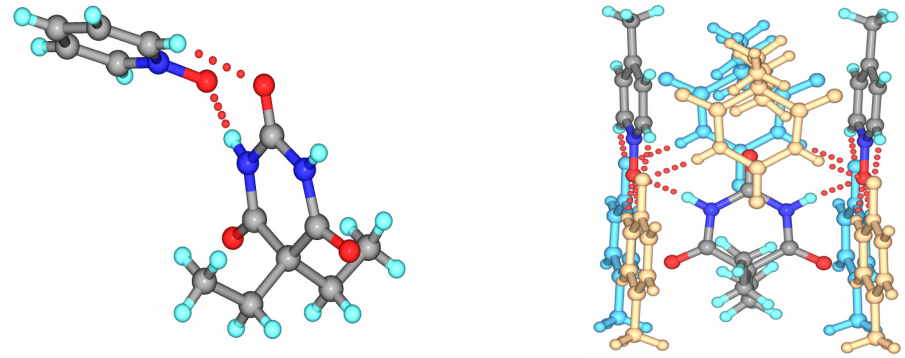

(a) (b)

Figure 4. (a) Amide–*N*-oxide heterosynthon between barbital and pyridine-*N*-oxide molecules in cocrystal **12**. (b) N–H···O$^-$ hydrogen bond between barbital and *N*-oxide molecules. There are two such symmetry-independent clusters in cocrystal **13** shown in different colors (yellow and blue).

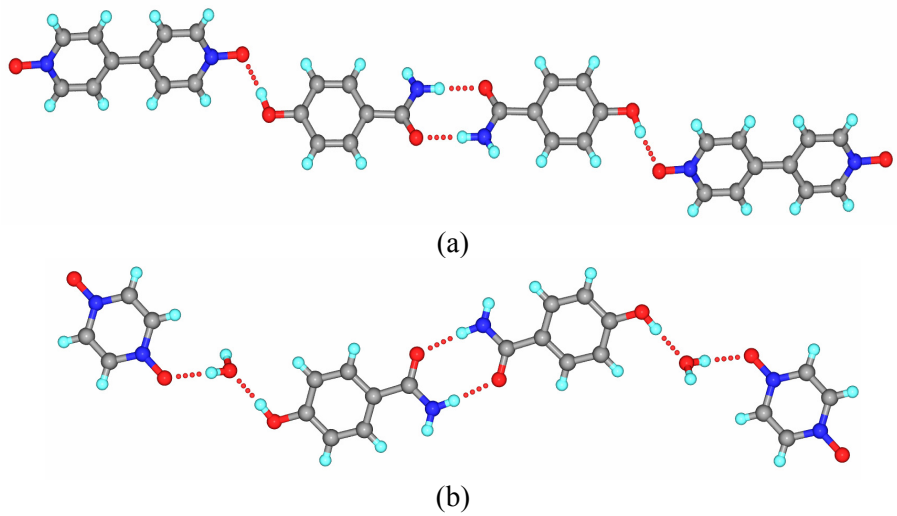

(a) (b)

Figure 5. (a) 1D tape of amide dimer homosynthon and O–H···O$^-$ hydrogen bond in cocrystal **14**. (b) 1D tape of amide dimer homosynthon and water interrupted hydroxyl to *N*-oxide hydrogen bonds in cocrystal **15**.

4-Hydroxybenzamide / 4,4'-bipyridine-*N*,*N*'-dioxide (14): This cocrystal was synthesized to study the influence of a competing hydroxyl group on the amide group during self-assembly. The cocrystal structure is in triclinic space group $P\bar{1}$ and contains one 4-hydroxybenzamide and half bipyridine-dioxide molecules in the asymmetric unit. Now the amide group assembles via dimer homosynthon (N1–H1A···O1: 1.88 Å, 2.892(3) Å, 179º) whereas *N*-oxide forms hydrogen bonds with the hydroxyl group (O2–H2···O3: 1.65 Å, 2.627(3) Å, 173º) as shown in figure 5a. The *N*-oxide also accepts bifurcated hydrogen bond from amide *anti* N–H donor (N1–H1B···O3: 2.07 Å, 3.024(3) Å, 158º).

4-Hydroxybenzamide / pyrazine-*N*,*N*'-dioxide hydrate (15): It crystallized in triclinic space group $P\bar{1}$ with one HBAm, half PYZNO and one water molecule in the asymmetric unit. The O3 of water interrupts the hydroxyl to *N*-oxide hydrogen bond (O4–H4A···O3: 1.85 Å, 2.822(3) Å, 169 º; O2–H2···O4: 1.69 Å, 2.666 Å, 174º, figure 5b). Amide dimer homosynthon (N1–H1A···O1: 1.91 Å, 2.911(3) Å, 171º) and *anti* N–H donating to *N*-oxide (N1–H1B···O3: 2.01 Å, 2.988(3) Å, 162º) complete the strong hydrogen bond network in the ternary cocrystal.

Carbamazepine / quinoxaline-*N*,*N*′-dioxide (16): This 1:1 cocrystal crystallized in the triclinic space group $P\bar{1}$. A centrosymmetric amide dimer is formed between inversion related CBZ molecules using *syn* N–H donor (N1–H1A···O1: 1.90 Å, 2.910(3) Å, 174º). CBZ *anti* N–H donates to an *N*-oxide of QUINO (N1–H1B···O3: 2.02 Å, 2.899(3) Å, 145º). Adjacent CBZ dimers are connected by QUINO molecules (Figure 6a). There is a C–H···O dimer (C16–H16···O3: 2.45 Å, 3.235(3) Å, 129º) between inversion-related *N*-oxide molecules which fill the voids between amide dimers in the structure. The second *N*-oxide moiety is also involved in C–H···O dimer (C19–H19···O4: 2.46 Å, 3.309(3) Å, 135º) to connect layers of CBZ dimers.

Carbamazepine and pyrazine-*N*,*N*'-dioxide, 17: It crystallized in monoclinic space group $P2_1/c$ with one CBZ and half PYZNO molecule in the asymmetric unit. Similar to cocrystal **16**, there is amide dimer homosynthon between CBZ molecules (N1–H1A···O1: 1.97 Å, 2.940(7) Å, 160º) and *anti* amide N–H bonds to *N*-oxide of PYZNO

in cocrystal (Figure 6b; N1–H1B···O3: 2.10 Å, 3.034(7) Å, 152º). There is a helix along the *c*-axis via N1–H1A···O1, N1–H1B···O3 and C–H···O hydrogen bonds. This cocrystal is isostructural to CBZ–benzoquinone cocrystal in the CSD. Both benzoquinone and pyrazine-*N*,*N*'-dioxide have similar molecular size and position of hydrogen bonding acceptor groups, therefore these crystal structures could be referred to as supramolecular equivalents, or functional group exchange leading to similar crystal packing.

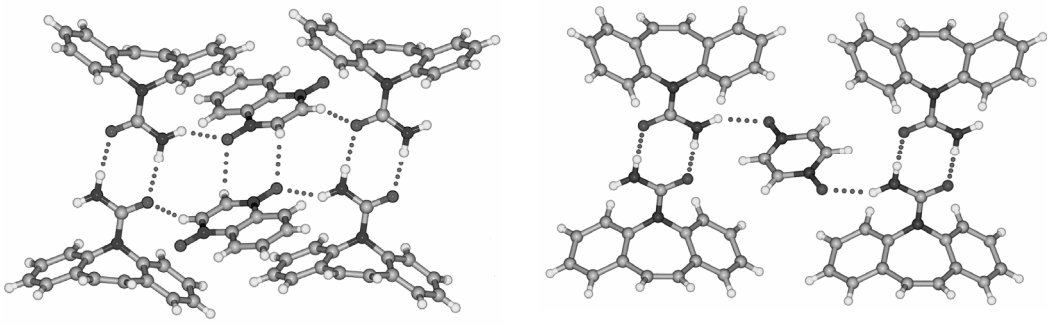

(a) (b)

Figure 6. (a) Amide dimers of CBZ are connected by *anti* N–H···O$^-$ hydrogen bonds of quinoxaline-dioxide and C–H···O dimers in cocrystal **16**. (b) Hydrogen bonded dimers of CBZ are connected by *anti* N–H···O$^-$ hydrogen bond of pyrazine-dioxide in cocrystal **17**.

Temozolomide and Bipyridine *N*,*N*'-dioxide (18T) : Co-crystallization of a 2:1 molar ratio of temozolomide (TMZ) and BPNO from CH_3CN/EtOH afforded a 1:0.5 TMZ•BPNO crystalline adduct (cocrystal **18T** in the triclinic space group $P\bar{1}$). The amide *syn* N–H interacts with the carbonyl of tetrazine via N1–H1A···O2 (2.10 Å, 3.085(2) Å, 164.4º) and the *anti* N–H is bonded to imidazole N acceptor (N1–H1B···N2: 2.10 Å, 2.996(2) Å, 145.8º). With assistance from C4–H4···O2 interaction (2.33 Å, 3.398(2) Å, 166.4º) a 1D tape of TMZ dimers runs along [001]. Such TMZ tapes are sandwiched between ribbons of BPNO molecules to make a 2D sheet in the (210) plane as shown in figure 7. Surprisingly, neither the amide N–H···O dimer synthon nor the amide–pyridine-*N*-oxide heterosynthon is present in this crystal structures. The absence of these commonly observed synthons suggested that there could be another polymorph.

Temozolomide and Bipyridine *N*,*N*'-dioxide (18M): This 2:1 cocrystal crystallized from DMSO with two molecules of TMZ and one molecule of BPNO in monoclinic space group $P2_1/c$ (**18M**). The amide *syn* NH donors of crystallographically different TMZ molecules (shown as capped-stick and ball-and-stick models in figure 8) form

hydrogen bond with *N*-oxide of BPNO via N–H···O$^-$ hydrogen bonds (N1–H1A···O6: 1.81 Å, 2.826(1) Å, 177º; N7–H7A···O5: 1.84 Å, 2.851(2) Å, 172º). However, the *anti* N–H of one TMZ molecule makes no intermolecular contact whereas it is long for the second molecule (N1–H1B···O6: 2.47 Å, 3.375(1) Å, 147.7º). Other weak interactions (C14–H14···O1: 2.06 Å, 3.129(1) Å, 168.5º; C19–H19···O1: 2.31 Å, 3.396(1) Å, 173.8º) complete crystal packing.

Temozolomide and Bipyridine *N*,*N*'-dioxide (19): This 1:1 cocrystal of TMZ and BPNO cocrystal was obtained from DMF in the chiral space group $P2_12_12_1$. BPNO forms a linear 1D ribbon of C–H···O dimers (C12–H12···O3: 2.17 Å, 3.240(7) Å, 167.8 º; C7–H7···O4: 2.11 Å, 3.195(7) Å, 173.5 º). A TMZ molecule is bonded to one of the *N*-oxides from amide *syn* NH bond (N1–H1A···O3: 1.86 Å, 2.857(6) Å, 167.2 º). The crystal structure has alternating tapes of TMZ and BPNO molecules in a 2D sheet (Figure 9). Here too the amide *anti* N–H has no intermolecular contact. A likely reason for co-crystallization in multiple compositions of 1:0.5, 2:1 and 1:1 is the presence of different N/O acceptor groups in temozolomide.

5.3.2 Synthon trends

Zaworotko[3d] classified hydrogen bonding changes in going from single component to cocrystal structure into two categories. The first type is when the cocrystal former acts only as a spacer but the original homosynthon is retained. Cocrystals **14** to **17** having amide–amide dimer homosynthon fall into this category 1 structures. On the other hand, when there is substantial change in hydrogen bonding because of cocrystal former functional groups, e.g. acid or amide dimer homosynthon changing to acid–pyridine, amide–acid or amide–*N*-oxide heterosynthon, then the structure belongs to category 2. All other cocrystals with amide–*N*-oxide motif belong to this category 2. Cocrystal **18T** without amide dimer or amide–*N*-oxide also placed in this category as there is a substantial change in hydrogen bonding because of BPNO cocrystal former. The second category structures are more likely to result in significant differences in the solid state property for API cocrystals since there are significant structural differences in going from homo- to heterosynthon.

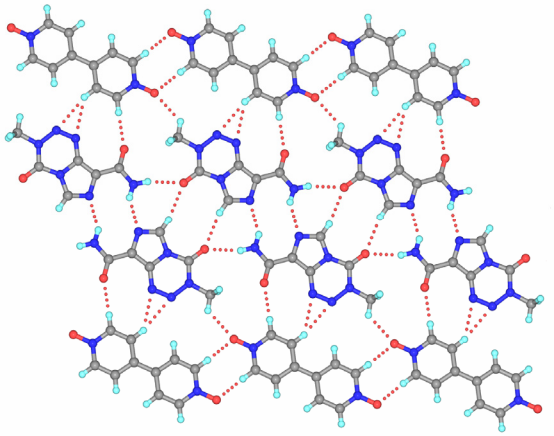

Figure 7. N–H···O and N–H···N hydrogen bonds between TMZ molecules and C–H···O interaction with BPNO in cocrystal **18T** (1:0.5). Usually formed amide dimer homosynthon or amide–*N*-oxide heterosynthon are absent in this crystal structure.

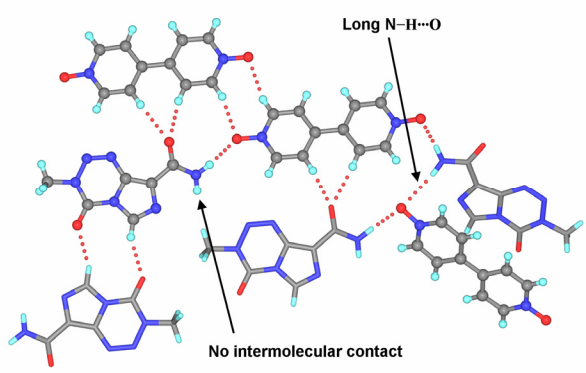

Figure 8. Amide–*N*-oxide hydrogen bonds in TMZ•BPNO cocrystal **18M** (2:1). Symmetry-independent TMZ molecules are shown as capped-stick and ball-and-stick models. One *anti* N–H···O bond is long (2.47 Å) and the other *anti* NH donor has no intermolecular contact.

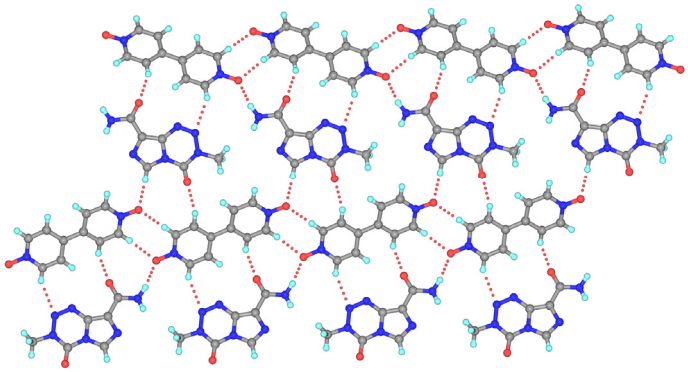

Figure 9. Amide–*N*-oxide hydrogen bonds in TMZ•BPNO cocrystal **19** (1:1). There are alternate tapes of TMZ and BPNO molecules in the 2D sheet structure. The *anti* NH donor makes intramolecular N–H···N interaction with imidazole N atom.

There are 35 crystal structures that contain amide and *N*-oxide moiety (13 crystal structures discussed in this chapter + 7 structures from our previous work + 15 structures from CSD[5a] and recent papers[11]). The amide–*N*-oxide heterosynthon is present in 24 structures (70%) whereas amide dimer homosynthon occurs in 6 structures. 1 cocrystal (18T) has neither amide–*N*-oxide nor amide dimer in its crystal structure. In other 4 crystal structures, either water or solvent interrupts the formation of stronger amide–*N*-oxide heterosynthon. There are mainly three reasons for the absence of amide–*N*-oxide synthon: firstly the presence of intramolecular N–H···O hydrogen bond as in picolinamide-*N*-oxide. Secondly when there is a competition from a hydroxyl/water in 4-hydroxybenzamide cocrystals **14** and **15**, amide dimer is favoured. Similar observation is noted in the dipolymorphic nitronyl nitroxide uracil derivative.[11] Both alpha and beta forms have strong amide–*N*-oxide synthon in their crystal structures. However, in its monohydrate crystal structure, water molecule interrupts the formation of amide–*N*-oxide synthon (Figure 10). Lastly steric factors also favour the homo-dimer as noted above in carbamazepine cocrystals **16** and **17**. The steric factors promoting the amide dimer homosynthon in cocrystal **16** is verified by crystal structure prediction.

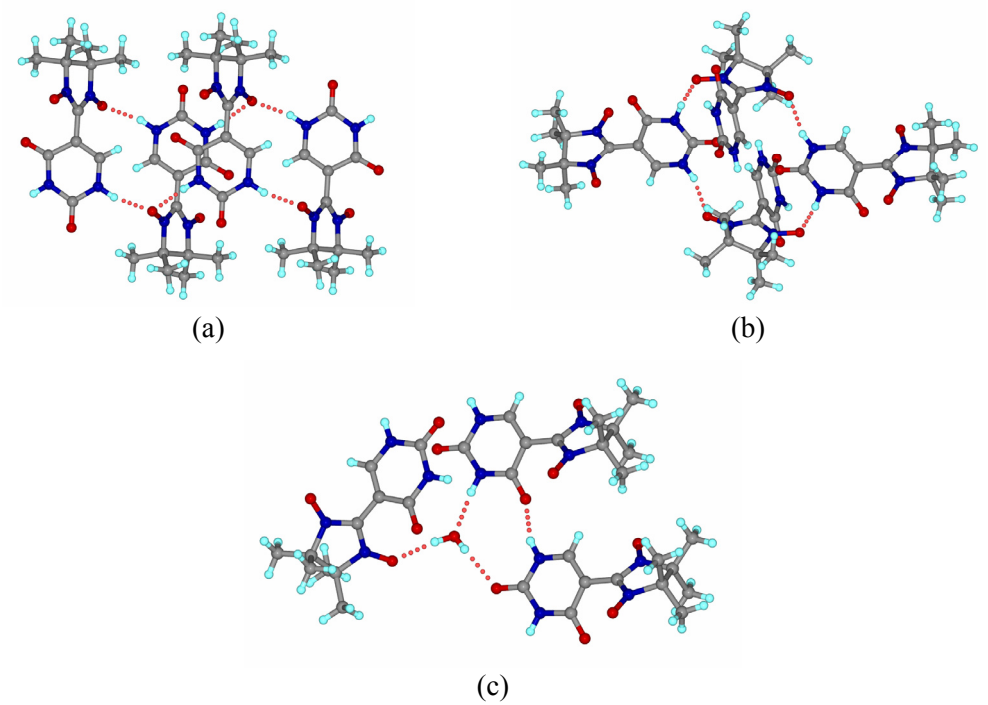

Figure 10. Three forms of nitronyl nitroxide uracil derivative. (a) α form. (b) β form. (c) Monohydrate. Both alpha and beta forms have amide–*N*-oxide synthon, whereas water interrupts the formation of this amide–*N*-oxide in monohydrate crystal structure.

5.3.3 Crystal Structure Reproduction

As the stronger amide–*N*-oxide synthon is absent in cocrystals **16** and **17,** a thorough screening was undertaken by varying the solvent and crystallization conditions to find out if any other strongly hydrogen bonded amide–*N*-oxide cocrystal exists. Experiments were unsuccessful to produce new polymorphic or different stoichiometry cocrystal. We then turned our attention to crystal structure reproduction to know reasons for amide–*N*-oxide synthon absence. The *ab initio* crystal structure prediction[12] of an organic molecule is a difficult challenge but this subject generates immense interest in pharmaceutical polymorphism. The advantage of this method is that several putative structures can be generated computationally which further allow comparison of homo- and hetero-synthons, hydrogen bonding and the associated molecular packing for each predicted structure frames. The 1:1 carbamazepine–quinoxaline-*N,N′*-dioxide cocrystal (**16**) was selected for structure prediction (reproduction) test case in the observed $P\bar{1}$ space group alone because simulation of multi-component systems[13a] or single-molecule crystal structures of $Z' > 1$[13b] is more difficult than the single component structures ($Z' = 1$) at the present time. Moreover, this simulation is only to identify whether the experimentally observed structure falls in the lowest energy ten frames of predicted structures and to see if any structures with amide–*N*-oxide synthon.

Crystal structures were calculated in Cerius^2 program package[14a] using Polymorph Predictor module and COMPASS force field. The energy range for 10 lowest frames is ~3 kcal mol^{-1}, a value that is comparable to hydrogen bond energy difference, ΔE_{HB}, between amide dimer homosynthon and amide–*N*-oxide heterosynthon. We therefore expected the 10 lowest energy structures to show homo- and/or hetero-synthon hydrogen bonding. As expected, among the 10 lowest energy frames in $P\bar{1}$ space group, seven structures contain amide homo dimer and one structure with amide–*N*-oxide heterosynthon, and two structures without amide dimer and amide–*N*-oxide synthon. Structure prediction frames are listed in Table 2. Unit cell of the 3rd lowest energy frame or frame 3 matches remarkably well (within 3%) with the observed crystal structure in $P\bar{1}$ space group and their energies are identical. Match of the observed crystal structure with any one of the low energy frames (typically between frames 1 to 5, <1 kcal mol^{-1} above the global minimum) is considered to be a good result in the current day.

Table 2. Ten lowest energy crystal structure frames computed in Polymorph Predictor. The energy difference between predicted frames 1-10 is 3.02 kcal mol^{-1}.

S. No	U_{latt} / kcal mol^{-1}	Density / g cm^{-3}	*a* / Å	*b* / Å	*c* / Å	*α* / °	*B* / °	*γ* / °	*V* / Å^3
				Experimental crystal structure (**16**)					
Exp (obs)	**----**	**1.35**	**7.284**	**10.688**	**14.13**	**100.25**	**102.46**	**109.08**	**977.7**
Exp (min)	**–57.573**	**1.45**	**7.041**	**10.613**	**13.825**	**101.80**	**103.65**	**107.91**	**911.4**
				Predicted frames of cocrystal (**16**)					
1	–57.803	1.45	10.582	13.100	6.920	83.21	72.24	89.50	906.9
2	–57.703	1.46	10.545	13.744	6.854	72.95	72.56	83.85	905.9
3	**–57.573**	**1.45**	**10.782**	**13.955**	**7.041**	**105.70**	**110.50**	**100.10**	**911.4**
4	–55.736	1.46	8.898	7.1522	15.458	68.57	85.45	79.95	901.7
5	–55.248	1.40	7.918	12.092	12.045	64.17	69.06	68.54	938.9
6	**–55.087**	**1.46**	**8.3682**	**7.715**	**14.452**	**79.52**	**82.01**	**83.87**	**905.4**
7	–55.079	1.42	9.448	13.321	8.2156	90.20	105.10	110.70	928.6
8	–55.001	1.42	9.721	12.441	8.328	100.4	105.99	99.48	927.4
9	–54.819	1.46	10.565	7.283	12.481	84.14	70.86	84.82	901.0
10	–54.809	1.41	8.809	10.008	11.382	89.45	81.22	70.63	934.7

Establishing isostructurality is important when one has a large list of predicted structures and the aim is to identify predicted structure(s) that match with the experimentally observed structure. Once similar structures are identified, the matching molecular clusters are superimposed to visualize the extent of similarity between the two structures. The default size molecule cluster is 15, a central molecule plus its 14 nearest neighbours. Structures are deemed to be the same when all 15 molecules in the coordination shell match nicely. The rms deviation gives a numerical measure of similarity or identity. COSET program (COmpare, SEarch and Topology)[14b] allows comparison of structures to identify similar crystal structures within a specified tolerance. The overlay of 15 nearest-neighbour molecules shows excellent superposition, rms deviation of 0.335, and good overlay in 2θ and intensity of powder X-ray diffraction peaks (Figure 11). N–H···O and C–H···O hydrogen bonds between carbamazepine and quinoxaline-dioxide molecules are identical in the experimental and simulated frame 3 (Figure 5a and 12a). The 6th lowest energy predicted structure i.e. frame 6, contains amide–*N*-oxide *syn* N–H···O$^-$ hydrogen bond (Figure 12b). Visualization of this structure suggests that a reason for the non-occurrence of amide–*N*-oxide heterosynthon in CBZ cocrystals is steric. The *anti* NH donor surprisingly is not hydrogen bonded to the available *N*-oxide acceptor in

computed 6th frame because the dibenzazepine ring of this rigid, butterfly-shaped molecule, which overhangs just above the *anti* NH donor, blocks close approach of potential hydrogen bond acceptors (Figure 12b). There is however a long, bent (CBZamide)N–H···π(QUINO phenyl) interaction (3.08 Å, 124°).

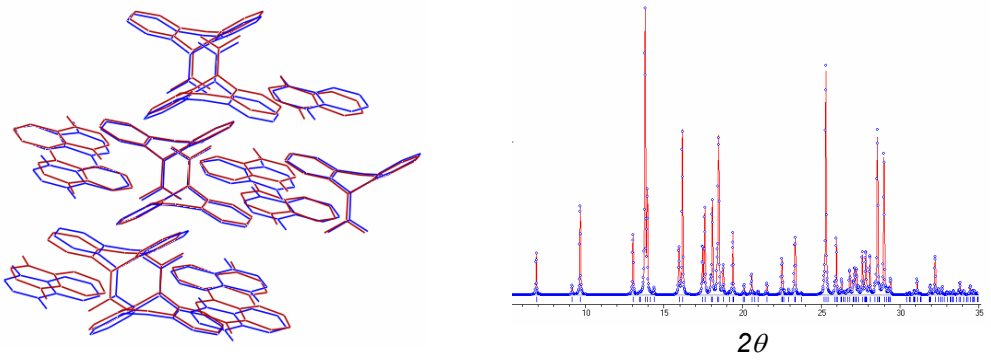

(a) (b)

Figure 11. Overlay of 15 molecules of experimental carbamazepine–quinoxaline-*N*,*N*'-dioxide cocrystal (red) and simulated frame 3 (blue). (b) Overlay of PXRD pattern of experimental minimized (red) and predicted frame 3 (blue) shows excellent match.

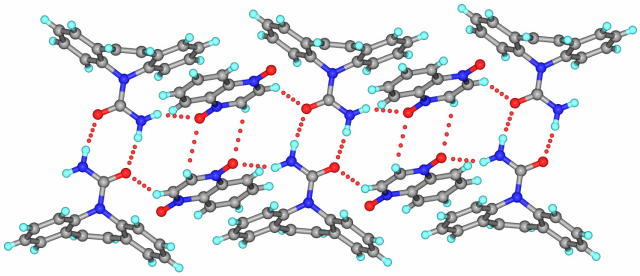

(a)

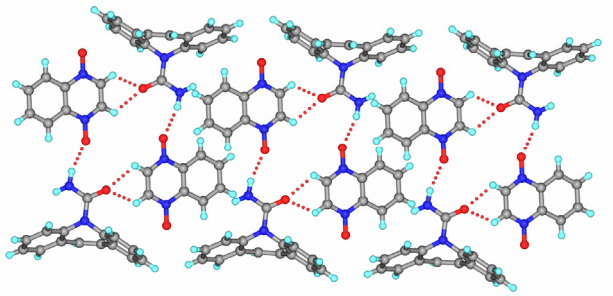

(b)

Figure 12. (a) Polymorph Predictor frame 3 of CBZ•QUNIO cocrystal to show amide dimer homosynthon of *syn* NH groups and *anti* N–H···O$^-$(oxide) hydrogen bond, matches with the observed hydrogen bonding and molecular packing as shown in figure 5a. (b) Predicted frame 6 has *syn* amide–*N*-oxide hydrogen bond but the *anti* NH is free, offering a possible reason for the non-occurrence of amide–*N*-oxide heterosynthon in carbamazepine cocrystals.

5.4 Polymorphism in cocrystals

The absence of commonly observed amide dimer homosynthon and amide–*N*-oxide heterosynthon synthon in TMZ•BPNO cocrystal **18T** (1:0.5) suggested that there could be another polymorph or a strongly hydrogen bonded cocrystal. Further experiments by changing the solvent and crystallization conditions yielded two additional TMZ•BPNO cocrystals **18M** (2:1) and **19** (1:1), both of them contain amide–*N*-oxide synthon as anticipated. The chemical composition of **18M** is same as cocrystal **18T** except that previous one contains two molecules of TMZ and one molecule of BPNO and the later has one molecule of TMZ and half molecule of BPNO residing on the inversion center. These are called as polymorphs of cocrystals with different crystal packing arrangements. Polymorphism in cocrystals or multi-component crystals[15] is very recent and there are only 33 cocrystal polymorph sets up to the January 2008 release of the CSD (24 structure sets have strong hydrogen bonding functional groups + 9 sets are sustained by weak C–H···O interactions or π–π stacking) when compared to 1600 polymorphic systems of single component crystals.[5a]

It is difficult to infer pyridine-N-oxide cocrystal stability from melting point because of compound decomposition. The density of cocrystal **18T** is higher than **18M** (1.592, 1.576 g cm^{-3}). Lattice energy calculations place cocrystal **18T** (–33.27 kcal mol^{-1}) substantially more stable than **18M** (–30.32 kcal mol^{-1}) given that energy differences between polymorphs are generally small suggesting that the cocrystal **18T** is more stable than **18M**. Grinding[16] of cocrystal **18M** in a ball-mill for 1 h showed complete conversion to cocrystal **18T** based on PXRD comparison (Figure 13). Further grinding of cocrystal **18T** did not indicate any phase change, indicating that the stability order is consistent with density and lattice energy values. The metastable nature of cocrystal **18M** may be traced to the unused amide *anti* N–H donor and imidazole N acceptor in intermolecular hydrogen bonding (Figure 8) reasons similar to temozolomide polymorph 2 (**6b**) in chapter 4. The facile phase transition of TMZ•BPNO cocrystal **18M** to **18T** by grinding may therefore be understood as stabilization from more number of hydrogen bonds in the product. Although the amide–pyridine-*N*-oxide N–H···O^{-} hydrogen bond in structure **18T** (1.81, 1.84 Å) is quite strong (more stable than amide N–H···O by ~3 kcal mol^{-1}), the unutilized *anti* NH donor and imidazole N acceptor make the crystal structure

kinetically metastable. After grinding for 1h, hydrogen bond reorganization takes place and a single strong N–H···O$^-$ hydrogen bond in **18M** is replaced by two H bonds in structure **18T**, N–H···O with tetrazine C=O and N–H···N with imidazole N (Figure 14).

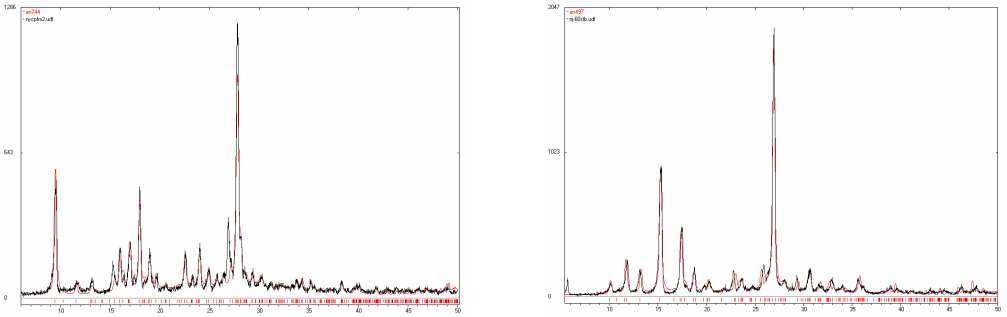

(a) (b)

Figure 13. Powder X-ray diffraction patterns – Intensity vs. *2θ*. (a) Freshly prepared cocrystal **18M** (100% purity). (b) Pure cocrystal **18M** ground in a mechanical ball mill for 1 h showed quantitative transformation to cocrystal **18T**. (c) Further grinding for 1 h showed no change (cocrystal **18T** recovered). These phase transitions indicate that cocrystal **18T** is the thermodynamic phase and cocrystal **18M** is a metastable polymorph. The black trace is the experimental PXRD and red lines are simulated from the X-ray crystal structure. There is a good match of observed and calculated peaks.

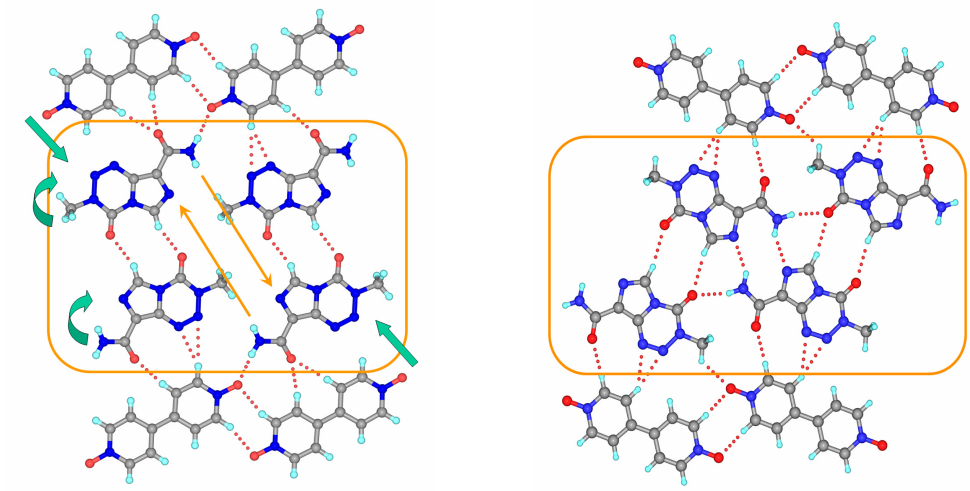

(a) (b)

Figure 14. Hydrogen bond reorganization in TMZ•BPNO 2:1 cocrystal **18M** (a) to 1:0.5 cocrystal **18T** (b). Cocrystal **18M** has strong amide–pyridine-*N*-oxide N–H···O$^-$ hydrogen bond. The unused amide *anti* N–H donors in cocrystal **18M** (a, indicated by thin double arrows) move close to the imidazole N acceptors in cocrystal **18T** (b) by 45º rotation and about half a molecular length translation. One strong N–H···O$^-$ hydrogen bond is broken and replaced by N–H···O and N–H···N bonds. Molecular rotation and translation in (a) are indicated by thick arrows.

Cocrystals **18T** and **18M** are also analyzed as synthon polymorphs,[17] with different hydrogen boned synthons between two components in their crystal structures. Recently Vishweshwar et. al. reported polymorphic cocrystals of 4-hydroxy benzoic acid / 2,3,5,6-tetramethyl pyrazine[15a] with different synthons. The more stable form 2 has hierarchic synthons,[10] i.e. acid–pyrazine and hydroxyl–carbonyl, whereas metastable form 1 has non-hierarchic acid–acid and hydroxyl–pyrazine synthons (Figure 15). In contrary to these results, the stable TMZ•BPNO cocrystal **18T** has non-hierarchic tapes of amide N–H···O hydrogen bonds and N–H···N dimer while the metastable cocrystal **18M** has hierarchic amide–pyridine-*N*-oxide synthon (Figure 16).

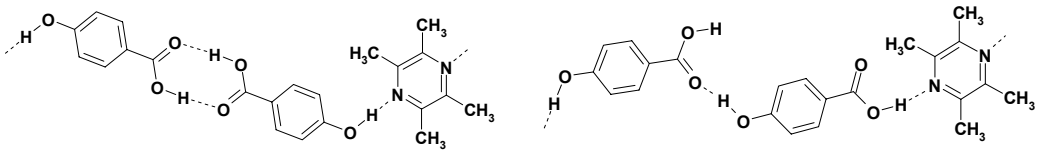

(a) (b)

Figure 15. (a) Form 1 of hydroxybenzoic acid–tetramethyl pyrazine with acid–acid and hydroxyl–pyrazine synthons. (b) Form 2 with acid–pyrazine and hydroxyl–carbonyl synthons.

(a) (b)

Figure 16. (a) Cocrystal **18T** without amide dimer and amide–*N*-oxide synthons. (b) Polymorphic cocrystal **18M** with strong amide–*N*-oxide heterosynthon.

The common structural feature in TMZ polymorphs (single component) of chapter 4 and TMZ•BPNO cocrystal polymorphs (multi-component) discussed in this chapter 5 is that the metastable modification has unused hydrogen bond donors/ acceptors[18] whereas all good donors and acceptors are used in hydrogen bonding in the stable form. The *anti* NH does not make intermolecular hydrogen bond in metastable TMZ polymorph 2 (**6b**) and TMZ•BPNO cocrystal **18M**. The reorganization of functional groups upon grinding results in the unused atoms making new hydrogen bonds in the stable form, i.e. N–H···O in TMZ polymorph 1 (**6a**) and N–H···O and N–H···N bonds in cocrystal **18T**. Conformational polymorphism arising out of different conformers *A* and *B* in TMZ single component polymorphs discussed in chapter 4 is not observed in cocrystal

polymorphs **18T** and **18M**. Both cocrystals have stable conformer *A* and occurrence of polymorphism may be ascribed to different hydrogen bond synthons and presence of unused hydrogen bond donor/acceptors. Apart from the TMZ·BPNO polymorphic cocrystal system, two more example are chosen from 33 cocrystal polymorph sets deposited in CSD to illustrate the reasons for occurrence of polymorphism in cocrystals. N,N'-bis(4-bromophenyl) melamine and 5,5-diethylbarbituric acid (refcodes JICTUK01/10) is a dimorphic substance. Polymorphism in this cocrystal is due to changes in conformation of bromo-phenyl ring attached to melamine. One of the phenyl rings is planar and other is perpendicular to melamine (–8.73˚, –87.9˚) in $P2_1/n$ cocrystal as shown in figure 17a. Whereas both the phenyl rings are planar (–9.04˚, –8.21˚) in $P\bar{1}$ cocrystal as shown in figure 17b. Polymorphism in 1:1 cocrystal of benzoquinone/1,4-dihydroxy benzene (refcodes QUIDON/01) arise due to differences in packing. Both cocrystal polymorphs have similar linear tapes of O–H···O hydrogen bonds, however the arrangements of these tapes are different in polymorphs. Triclinic cocrystal has a parallel linear tapes connected by C–H···O H-bonds in a layered structure (Figure 18a), whereas these tapes are arranged perpendicularly to each other and extend into third dimension in the monoclinic cocrystal (Figure 18b).

(a) (b)

Figure 17. Conformational polymorphism in JICTUK01/10. (a) One of the phenyl rings is planar and other is perpendicular to melamine (–8.73˚, –87.9˚) in $P2_1/n$ cocrystal (b) Both the phenyl rings are planar (–9.04˚, –8.21˚) in $P\bar{1}$ cocrystal.

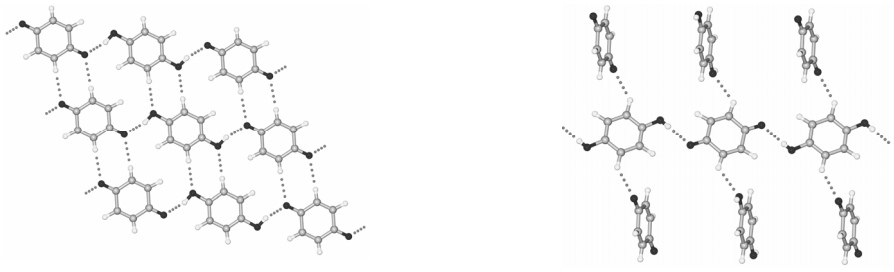

(a) (b)

Figure 18. Packing polymorphism in JICTUK01/10. (a) 1D tapes of molecules are arranged in a sheet in triclinic cocrystal. (b) 1D tapes of molecules are arranged perpendicularly to each other in the monoclinic cocrystal.

It appears that the differences in cocrystal polymorphs arise due to reasons similar to those for single component polymorphic structures, i.e. differences in conformation, hydrogen bonding, and/ or molecular packing. This could mean that the not so frequent occurrence of polymorphism in cocrystals (33 sets) compared to classical polymorphism in single component crystals (1600 sets), is not due to a fundamental structural difference but for the simple reason that studies on cocrystals are very recent and the time dedicated for multi-component crystals is less when compared to single component molecules. An early notion that cocrystals are less prone to polymorphism should be reviewed in due course.

5.5 Hydration stability in cocrystals

The molecular complexes or cocrystals containing therapeutic molecules represent an emerging class of pharmaceutical materials offering the potential to optimize physical/chemical properties. These are called as pharmaceutical cocrystals[3] formed between an Active Pharmaceutical Ingredients (API) with another pharmaceutically acceptable molecule in the solid-state. The resulting multi-component solid with a distinct physicochemical profile is designed such that it will improve properties in terms of solubility, melting point, physical stability and/or hygroscopic stability of the substance. The proof of concept with 4-methylpyridine-*N*-oxide in relation to controlling hydration is discussed now. Picoline-*N*-oxide, PICNO, is a hygroscopic compound and readily absorbs moisture from the atmosphere during storage and handling. Vacuum drying of wet PICNO at 110-120 °C showed water absorption bands in its IR spectrum after 3 h. A cocrystal of barbital and picoline-*N*-oxide in 1:2 ratio (**13**) was prepared by grinding in mortar-pestle for 15 min and the resulting crystalline solid was exposed to different relative humidity conditions (ca. 50% and then 100%). IR spectra were recorded at regular intervals (Figure 19), from a few days up to a month, to monitor the increase in intensity of H_2O absorption peaks. These qualitative results show that there is substantial improvement in the hydration stability of a pyridine-*N*-oxide by cocrystal formation. An advantage with the amide–*N*-oxide heterosynthon is that hydrogen bonding in the EBA•PICNO cocrystal **13** is sufficiently different from that of amide dimer of EBA and C–H···O dimer of PICNO (Figure 20), which resulted in hygroscopic stability of cocrystal **13** over simple picoline-*N*-oxide molecule.

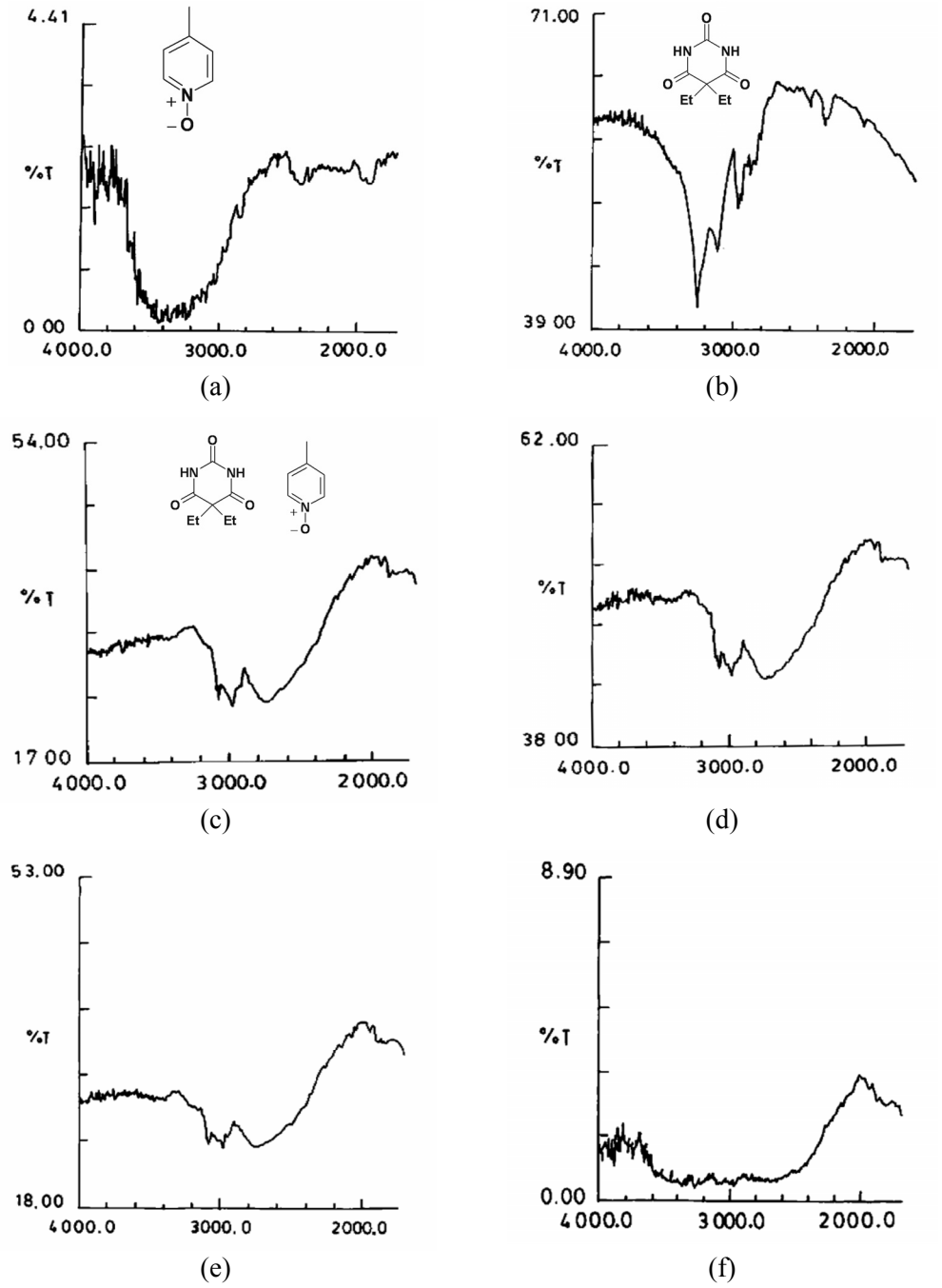

Figure 19. Infrared spectra. (a) 4-Methylpyridine-*N*-oxide, the starting material has significant amount of moisture based on the broad OH band centered at 3500 cm^{-1}. (b) Barbital has peaks at 3242, 3109, 2961, 2879 cm^{-1}. (c) Cocrystal as prepared, peaks at 3076, 2980 and 2754 cm^{-1}. (d) Cocrystal in open air after 3 days, peaks at 3076, 2980 and 2739 cm^{-1}. (e) Cocrystal in open air after 4 weeks, peaks at 3076, 2976 and 2725 cm^{-1}. (f) Cocrystal in RH 100% after 1 day, the broad band indicates moisture. There is insignificant moisture uptake at 50% RH even after 1 month but the crystal hydrates in saturated water vapour environment 100% RH).

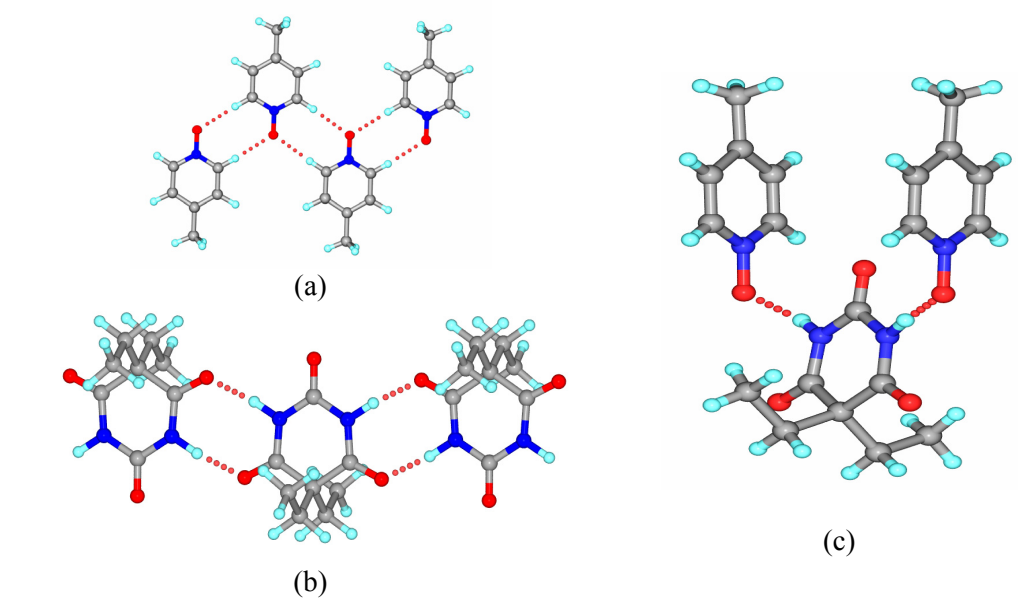

Figure 20. (a) C–H···O dimer of 4-methylpyridine-*N*-oxide. (b) Amide dimer homosynthon which is present in all four polymorphs of barbital drug. (b) Strong amide–*N*-oxide hydrogen bonds in EBA•PICNO cocrystal **13** (2:1).

In pharmaceutical formulations certain classes of drugs pose particular problems. One such problem arises in the case of hygroscopic drugs, which tend to absorb water from the air. This is disadvantageous because moisture uptake enhances molecular mobility and can affect flow, compaction, dissolution, stability, storage, and final product during drug processing and formulation. Many examples are reported wherein the role of water was found to be very crucial in promoting the solid-state phase transitions to hydrate/ metastable anhydrate or an amorphous form and sometimes disintegrating the salts to individual components or inducing drug–excipient interactions. Delavirdine methanesulfonate[19] is one such example which has adversely affected in their dissolution profile when its tablets were exposed to high relative humidity conditions. It was observed that the change in moisture content in the stressed tablets was shown to cause the salt to dissociate, resulting in the free base and methanesulfonic acid, which further lead to a subsequent acid–base reaction between the methanesulfonic acid and excipient in the tablets. Norfloxacin is another unusual example, where tablet dissolution behaviour was adversely affected in lower humidities. The water molecules induce proton transfer between norfloxacin molecules in the solid state, as the anhydrate (neutral COOH) converts into norfloxacin dihydrate (ionic COO^- form) at higher relative humidity conditions.[19,20] The change from a neutral crystal to an ionic crystal after

exposure to 75% RH at room temperature resulted in a higher dissolution rate, because of ionic form (Figure 21). While proton transfer may not be considered a major change in the molecular structure, water effect on the solid-state properties is definitely significant.

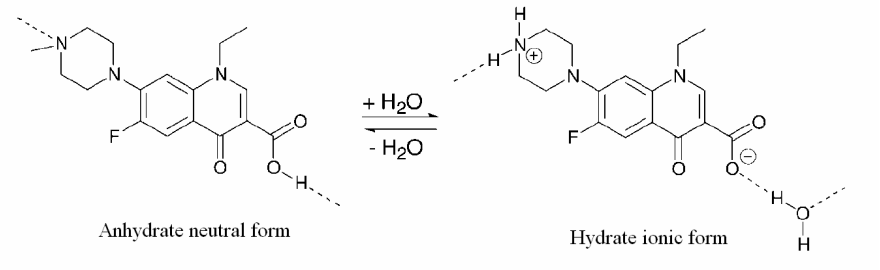

Figure 21. Hydration induced proton transfer in norfloxacin forms. Norfloxacin anhydrous neutral form was converted to ionic dihydrate form at 75% RH conditions.

Hygroscopicity is therefore a challenging problem for certain drugs. Such compounds must be handled in controlled humidity environments during manufacture and the final product must be packaged in individual moisture resistant blisters in order to prevent changes or degradation of the product. An alternative to deal with hygroscopic solids is by choosing a non-hygroscopic crystalline form of an API. It could be a different polymorph, solvate, salt or cocrystal which is resistant to hydration at ambient RH conditions. Recent patent highlights that a pharmaceutical composition comprising of propylene glycol solvate of an API (celecoxib sodium propylene glycol solvate)[21] has a decreased hygroscoipicity and increased aqueous solubility when compared to pure API (celecoxib sodium salt). Caffeine and theophylline drugs[22] are other examples that get converted to hydrates at 98% RH, while their cocrystals with oxalic acid are stable at 98% RH for 7 weeks. Co-crystallization or non-covalent modification of API is therefore an emerging alternative method to modify physical and chemical properties, especially for neutral drug molecules, has a potential utility in pharmaceutical formulation. Several amorphous, crystalline, hygroscopic, or poorly soluble drugs can be made more soluble, more stable, and less hygroscopic by co-crystallization with a suitable cocrystal former which satisfy otherwise free hydrogen bond donors/ acceptors sites in the drug molecule.

The cocrystals of APIs discussed in this chapter do not classify as pharmaceutical cocrystals because of the *N*-oxides are not under GRAS (generally regarded as safe) list of chemicals.[23] However, it is known in the literature that the oxidation of pyridine

nitrogen to *N*-oxide often enhances drug-like behaviour to give molecules with good oral bioavailability, pharmacokinetic properties, solubility, and metabolic stability. Affinity at the target receptor or binding site may also increase because of stronger hydrogen bonding with the drug molecule. Further, *N*-oxide is a common route for phase 1 metabolism of drugs containing pyridine moiety and these metabolites often contribute to drug action. Many new *N*-oxide drug molecules (anti HIV, anti-viral and anti-bacterial drugs)[24] are popular targets for medicinal chemists. A phosphodiestarse-IV-inhibitor of *N*-oxide active pharmaceutical ingredient[25] is a highly hygroscopic molecule known to exhibit eight forms of anhydrate/hydrates and undergo variety of phase transformations on changing relative humidity conditions. The stronger hydrogen bond acceptor strength of *N*-oxide in these molecules could be exploited to make predictable cocrystals with amide type cocrystal formers to optimize their physical properties. Cocrystals of antitumour drug temozolomide with GRAS carboxylic acid or carboxamide molecules are synthesized to improve hydrolytic stability of TMZ is discussed in the next chapter 6.

5.6 Conclusions

A novel carboxamide–pyridine-*N*-oxide heterosynthon sustained by *syn*(amide)N–H···O^-(oxide) hydrogen bond and auxiliary (*N*-oxide)C–H···O(amide) interaction was designed by exploiting the better acceptor strength of the anionic oxygen. Synthon robustness was evaluated in 35 crystal structures that contain amide and pyridine-*N*-oxide functional groups. Amide–pyridine-*N*-oxide heterosynthon competes with amide dimer homosynthon. 24 structures have amide–pyridine-*N*-oxide, 6 structures with amide–amide dimer, and remaining structures are devoid of both amide dimer and amide–*N*-oxide synthons. Amide dimer synthon is present in three situations: presence of an intramolecular N–H···O hydrogen bond as in picolinamide-*N*-oxide, competition from another strong hydroxyl (–OH) group in cocrystal **14** and **15,** and lastly steric factors imposed by dibenzazepine group of CBZ in cocrystals **16** and **17** as confirmed from crystal structure prediction on CBZ•QUINO (1:1) cocrystal **16** in Cerius^2.

Temozolomide forms three different stoichiometry cocrystals **18T**, **18M** and **19** (1:0.5, 2:1 and 1:1) with 4,4'-bipyridine-*N,N′*-dioxide. Structures **18T** and **18M** exhibit synthon polymorphism in cocrystals. The stable cocrystal **18T** has neither amide–*N*-oxide nor

amide dimer synthon whereas metastable cocrystal **18M** contains strong amide–*N*-oxide heterosynthon. More interestingly, this strongly hydrogen bonded cocrystal **18M** converts to cocrystal **18T** with moderate hydrogen bonds upon grinding for one hour. The metastable nature of cocrystal **18M** is ascribed to unused hydrogen bond donors/ acceptors in the crystal structure which are completely utilized in the stable polymorphic cocrystal **18T**. Apart from generating diverse supramolecular structures, cocrystals offer the potential to modify physical and chemical properties of substances. 4-picoline-*N*-oxide deliquesces within a day; while its 2:1 picoline-*N*-oxide and ethyl barbituric acid cocrystal (**13)** assembled by amide–*N*-oxide heterosynthon does not absorb moisture at 50% relative humidity (RH) levels up to four weeks. Cocrystal **13** has better resistance to hydration as the hydrogen bonding in crystal structure is completely different from that of individual components.

5.7 Experimental Section

Crystal Structure Prediction (CSP): Lattice energy minimization of experimental structures was carried out using version 4.8 of Cerius^2 molecular modeling environment running on Silicon Graphics workstations. COMPASS force field was applied. The minimized structure was used as a model for running a rigid polymorph prediction using polymorph predictor (PP) module. Structures were generated keeping the molecular conformation rigid. Conformational variations were expected to be minimal for these rigid molecules except torsions in the azepine-amide portion of CBZ. Structure clustering, energy computations and ranking in increasing lattice energy were performed next. COSET program was used for PP analysis and RMSD calculations on experimental and predicted structures.

Hydration stability: The Lancaster catalogue indicates that picoline-*N*-oxide is hygroscopic and should be tightly sealed. When 0.5-1.0 gm of the compound was left in an open petri dish for one day the solid deliquesces completely. The relative humidity was ca. 50% (in the range 45-55%) under ambient conditions of Hyderabad climate during the experiment period of December 2006 (temperature range 25-35 ºC). We performed a qualitative experiment to assess the gross differences in hydration nature of 4-picoline-*N*-oxide compared to its cocrystal with barbital wherein the *N*-oxide moiety is

engaged in strong bonding with an amide partner. The solid was placed in a petri dish exposed to ambient humidity conditions (ca. 50% RH) for the specified time and IR spectra were recorded to monitor water absorption peaks. In the second experiment, the solid was placed in 100 mL beaker, which was kept in a closed jar containing distilled water to expose the sample to 100 % relative humidity conditions for a specified time and IR spectra were recorded.

Cambridge Structural Database (CSD): There are 35 crystal structures that contain amide and *N*-oxide moiety (13 crystal structures discussed in this chapter + 7 structures from our previous work + 15 structures from CSD and recent papers). The amide–*N*-oxide heterosynthon is present in 24 structures (cocrystals **8-13**, **18M**, **19**, ADECIW, BAFTEH, BAQZOI, GEYWOW, JEDKUZ, MEGCUX, MEGDAE, MEGDAE, MEGDEI, MEGDIM, MEGDUY, RBBHMU, YEQHUX, ZIVQEA, HALLUC, alpha and beta forms of nitronyl nitroxide uracil derivative) and 11 structures with out amide–*N*-oxide heterosynthon (cocrystals **14-17**, **19**, CETQUO, FAQRIY, JOCPUM, UGISUY, MEGDOS and monohydrate of nitronyl nitroxide uracil derivative). A second search was carried out in CSD for cocrystal polymorphs. All polymorphs with 3D coordinates reported, No errors, Not Polymeric, No ions were searched in Version 5.29, ConQuest 1.10, January 2008 update to give 5167 hits. Crystal structures with high disorder were excluded. There are totally 33 polymorphic sets of which 24 cocrystal sets (AJAJEA, ENAZOI, EXUQUJ, HADKUT, IJETOG, JICTUK, MACCID, MUROXA, QUIDON, SAYMUB, TECCAF01, TEHNAW, WOTZAG, XETZIG, ZIGPAG, WATERP, ODOBIT, GIDLUB, PTZTCQ, UNEZAO, UNEZES, KIHYOQ, ULAWAF and 4,4-dihydroxybenzophenone•1,2-bis (4-Pyridyl) ethylene) have strong hydrogen bonding groups whereas 9 sets (ABUNIU, DURZAR, IJETEW, NAPYMA, NARSOP, RIFQAY, SEOTCR, TAMBUE, FAHLEF) do not have strong H-bonding groups. They contain other non-covalent intermolecular interactions and/ or π-stacking.

Synthesis of cocrystals

BA·QUINO (8): 40 mg (0.312 mmol) of barbituric acid and 50.6 mg (0.312 mmol) of quinoxaline-*N,N'*-dioxide [1:1] were ground in mortar/pestle for 5 minutes with 5 drops of acetonitrile and dissolved in10 mL of acetonitrile. Slow evaporation of solvent resulted in yellow colored block like 1: 1 cocrystals over a period of 2–3 days.

BA·PICNO (9): 50 mg (0.390 mmol) of barbituric acid and 85 mg (0.780 mmol) of 4-methylpyridine-*N*-oxide [1:2] were dissolved in 6-8 mL of THF and allowed to evaporate slowly over a period of 3-4 days to get needle shaped 1:2 cocrystals.

BA·PYZNO (10): 50 mg (0.390 mmol) of barbituric acid and 43.7 mg (0.390 mmol) of pyrazine-*N,N′*-dioxide [1:1] were dissolved in 3 mL of water and allowed to evaporate slowly over a period of 3-4 days to get irregular block shaped 1: 0.5 cocrystals.

SAC·BPNO (11): 50 mg (0.272 mmol) of saccharin and 25.6 mg (0.136 mmol) of bipyridine- *N,N′*-dioxide [1:0.5] were ground in mortar/pestle for 5 minutes adding 5 drops of acetonitrile and later dissolved in 10-15 mL of acetonitrile. Slow evaporation of the solvent over a period of 2-3 days resulted in needle shaped 1:0.5 cocrystals.

EBA·PYNO (12): Cocrystal was obtained when 50 mg (0.271 mmol) of barbital and 50.3 mg (0.543 mmol) of pyridine-*N*-oxide [1:2] were dissolved in 5-8 mL of EtOAc and allowed to evaporate slowly over a period of 3-4 days to yield 1:1 cocrystals.

EBA·PYNO (13): Cocrystal was obtained when 50 mg (0.271 mmol) of barbital and 59 mg (0.543 mmol) of 4-methylpyridine-*N*-oxide [1:2] were dissolved in 5-8 mL of EtOAc and allowed to evaporate slowly over a period of 3-4 days to yield 1:0.5 cocrystals.

HBAm·BPNO (14): Cocrystal was obtained when 36.4 mg (0.265 mmol) of 4-hydroxy benzamide and 50 mg (0.265 mmol) of bipyridine-*N,N′*-oxide [1:1] were dissolved in 5 mL of acetone, 5 mL of methanol, and 2 mL of water and allowed to evaporate slowly in a beaker to yield colorless plate shaped 1:0.5 cocrystals after 3 to 4 days.

HBAm·PYZNO (15): Cocrystal was obtained when 53.7 mg (0.392 mmol) of 4-hydroxy benzamide and 40 mg (0.392 mmol) of pyrazine-*N,N'*-oxide [1:1] were dissolved in 5 mL water and allowed to evaporate slowly in a beaker to get 1:0.5:H_2O cocrystals.

CBZ·QUINO (16): Cocrystal was obtained when 50 mg (0.211 mmol) of carbamazepine and 22.4 mg (0.106 mmol) of quinoxaline-*N,N'*-oxide [1:0.5] were ground in mortar/pestle using acetonitrile as solvent for liquid assisted grinding. After the new binary phase material was confirmed by IR, it was dissolved in 8 mL acetonitrile and allowed to evaporate slowly to get pale yellow coloured 1:1 cocrystal after 3-4 days.

CBZ·PYZNO (17): Cocrystal was obtained when 80 mg (0.339 mmol) of carbamazepine and 19 mg (0.169 mmol) of pyrazine-*N,N'*-oxide [1:0.5] were ground in mortar/pestle using acetonitrile as solvent for liquid assisted grinding. After the new binary phase material was confirmed by IR, it was dissolved in 5 mL DMF and allowed to evaporate slowly to get pale colourless 1:0.5 cocrystal after 3-4 days.

TMZ·BPNO (18T): 46.5 mg of TMZ (0.24 mmol) and 27.1 mg of BPNO (0.12 mmol) were dissolved in a mixture of 6 mL CH_3CN and 2 mL EtOH (3:1) and the solvents were allowed to evaporate slowly. Both 1:0.5 cocrystal and hydrate of TMZ appeared concomitantly after a few days.

TMZ·BPNO (18M): 46.5 mg of TMZ (0.24 mmol) and 27.1 mg of BPNO dihydrate (0.12 mmol) were dissolved in 2 mL of DMSO and allowed to evaporate in a beaker over a period of 2 weeks to get 2:1 of TMZ and BPNO stoichiometry cocrystal.

TMZ·BPNO (19): 50 mg of TMZ (0.24 mmol) and 54.2 mg of BPNO dihydrate (0.24 mmol) were dissolved in 5 mL of DMF and allowed to evaporate in a beaker over a period of 2 weeks to get 1:1 of TMZ and BPNO stoichiometry cocrystal.

5.8 References

1) (a) A. I. Kitaigorodskii, *Mixed Crystals*. Springer, Berlin, **1984**, pp 275-318. (b) F. H. Herbstein, *Crystalline Molecular Complexes and Compounds*, IUCr Monographs, Vol. 1-2, Oxford University Press, Oxford, **2005**.
2) (a) C. B. Aakeröy, D. J. Salmon, *CrystEngComm* **2005**, *7*, 439. (b) B. R. Bhogala, S. Basavoju, A. Nangia, *CrystEngComm* **2005**, *7*, 551. (c) B. R. Bhogala, S. Basavoju, A. Nangia, *Cryst. Growth Des*. **2005**, *5*, 1683. (d) A. V. Trask, W. D. S. Motherwell, W. Jones, *Cryst. Growth Des.* **2005**, *5*, 1013. (e) X. Gao, T. T. Friščić, L. R. MacGillivray, *Angew. Chem., Int. Ed.* **2004**, *43*, 232. (f) B. R. Bhogala, A. Nangia, *Cryst. Growth Des.* **2003**, *3*, 547. (g) R. D. B. Walsh, M. W. Bradner, S. Fleishman, L. A. Morales, B. Moulton, N. Rodríguez-Hornedo, M. J. Zaworotko, *Chem. Commun.* **2003**, 186. (h) C. B. Aakeröy, A. M. Beatty, B. A. Helfrich, *J. Am. Chem. Soc.* **2002**, *124*, 14425. (i) C. B. Aakeröy, A. M. Beatty, B. A. Helfrich, *Angew. Chem., Int. Ed.* **2001**, *40*, 3240.
3) (a) N. Rodríguez-Hornedo, Guest Editor, Special Section on Pharmaceutical Cocrystals, *Mol. Pharma.* **2007**, *4*, 299–434. (b) P. Vishweshwar, J. A. McMahon, M. J. Zaworotko, in *Frontiers in Crystal Engineering*, E. R. T. Tiekink and J. J. Vittal, Eds., Wiley, Chichester, **2006**, pp. 25-49. (c) Ö. Almarsson, M. J. Zaworotko, *Chem. Commun.* **2004**, 1889. (d) S. G. Fleischman, S. S. Kuduva, J. A. McMahon, B. Moulton, R. D. B. Walsh, N. Rodríguez-Hornendo, M. J. Zaworotko, *Cryst. Growth Des.* **2003**, *3*, 909.

4) (a) G. R. Desiraju, *Angew. Chem., Int. Ed. Engl.* **1995**, *34*, 2311. (b) A. Nangia, G. R. Desiraju, *Top. Curr. Chem*. **1998**, *198*, 57.

5) (a) Cambridge Structural Database, CSD, version 5.29, ConQuest 1.10, November **2007** release, January update. (b) A. Nangia, *CrystEngComm* **2002**, *4*, 93. (c) J. Chisholm, E. Pidcock, J. V. De streek, L. Infantes, S. Motherwell, F. H. Allen, *CrystEngComm* **2006**, *8*, 11.

6) F. H. Allen, W. D. S. Motherwell, P. R. Raithby, G. P. Shields, R. Taylor, *New. J. Chem*. **1999**, 25.

7) (a) P. Vishweshwar, A. Nangia, V. M. Lynch, *Cryst. Growth Des.* **2003**, *3*, 783. (b) C. B. Aakeröy, J. D. Salmon, *CrystEngComm* **2004**, *6*, 19.

8) (a) T. Steiner, *Acta Crystallogr.* **2001**, B*57*, 103. (b) J. A. McMahon, J. A Bis, P. Vishweshwar, T. R. Shattock, O. L. McLaughlin, M. J. Zaworotko, *Z. Kristallogr.* **2005**, *220*, 340.

9) (a) L. S. Reddy, N. J. Babu, A. Nangia, *Chem. Commun.* **2006**, 1369. (b) B. K. Saha, R. Banerjee, A. Nangia, G. R. Desiraju, *Acta Crystallogr*. **2006**, E*62*, o2283. (c) N. J. Babu, L. S. Reddy, A. Nangia, *Mol. Pharma.* **2007**, *4*, 417.

10) (a) M. C. Etter, *Acc. Chem. Res.* **1990**, *23*, 120. (b) M. C. Etter, *J. Phys. Chem.* **1991**, *95*, 4601.

11) (a) R. Feher, K. Wurst, D. B. Amabilino, J. Veciana, *Inorg. Chimi. Acta.* **2008**, DOI: 10.1016/j.ica.2008.03.066. (b) R. Feher, K. Wurst, D. B. Amabilino, J. Veciana, *Mol. Cryst. Liq. Cryst.* **1999**, *334*, 333.

12) S. L. Price, *Encyclopedia of Supramolecular Chemistry*, Eds J. L Atwood, J. Steed, Marcel Dekker, New York, **2004**, pp 371-379.

13) (a) A. J. C Cabeza, G. M. Day, W. D. S. Motherwell, W. Jones, *J. Am. Chem. Soc.* **2006,** *128*, 14466. (b) G. M. Day, W. D. S. Motherwell, H. Ammon, S. X. M. Boerrigter, R. G. Della Valle, E. Venuta, A. Dzyabchenko, J. D. Dunitz, B. Schweizer, B. P. van Eijck, P. Erk, J. C. Facelli, V. E. Bazterra, M. B. Ferraro, D. W. M. Hofmann, F. J. J. Leusen, C. Liang, C. C. Pantelides, P. G. Karamertzanis, S. L. Price, T. C. Lewis, H. Nowell, A. Torrisi, H. A. Scheraga, Y. A. Arnautova, M. U. Schmidt, P. A. Verwer, *Acta Crystallogr.* **2005**, B*61*, 511.

14) (a) Polymorph Predictor and Cerius^2 suite of programs are software products of Accelrys Inc., http://www.accelrys.com. (b) COSET is developed and

distributed by Cambridge Crystallographic Data Center, http://www.ccdc.cam.ac.uk, chisholm@ccdc.cam.ac.uk.

15) (a) B. R. Sreekanth, P. Vishweshwar, K. Vyas, *Chem. Commun.* **2007**, 2375. (b) J. A. Bis, P. Vishweshwar, R. A. Middleton, M. J. Zaworotko, *Cryst. Growth Des.* **2006**, *6*, 1048. (c) S. L. Childs, K. I. Hardcastle, *Cryst. Growth Des.* **2007**, *7*, 1291. (d) J. A. Bis, P. Vishweshwar, D. Weyna, M. J. Zaworotko, *Mol. Pharma.* **2007**, *4*, 401. (e) W. W. Porter III, S. C. Elie, A. J. Matzger, *Cryst. Growth Des.* **2008**, *1*, 14.

16) (a) L. S. Reddy, P. M. Bhatt, R. Banerjee, A. Nangia, G. J. Kruger, *Chem. Asian J.* **2007**, *2*, 505. (b) A.V. Trask, W. Jones, *Top. Curr. Chem.* **2005**, *254*, 41.

17) R. K. R. Jetti, R. Boese, J. A. R. P. Sarma, L. S. Reddy, P. Vishweshwar, G. R. Desiraju, *Angew. Chem. Int. Ed.* **2003**, *42*, 1963.

18) (a) G. R. Desiraju, *CrystEngComm* **2002**, *4*, 499. (b) J. D. Dunitz, W. B. Schweizer, *CrystEngComm* **2007**, *9*, 266. (c) S. Roy, P. M. Bhatt, A. Nangia, G. J. Kruger, *Cryst. Growth Des.* **2007**, *7*, 476.

19) R. Hilfiker, F. Blatter, M. von Raumer, in *Polymorphism in the Pharmaceutical Industry*, ed R. Hilfiker, Wiley-VCH, Weinhein, **2006**.

20) W. Chongchoroen, S. R. Byrn, N. Sutanthavibul, *J. Pharm. Sci.* **2008**, *97*, 473.

21) M. Tawa, Ö. Almarsson, J. Remenar, *US Pat.* 2005/0015841 A1, Jan. 18, **2007**.

22) (a) A. Trask, W. D. S. Motherwell, W. Jones, *Int. J. Pharm*. 2006, 320, 114. (b) A. Trask, W. D. S. Motherwell, W. Jones, *Cryst. Growth Des.* **2005**, *5*, 1013.

23) GRAS chemicals list is available at http://www.cfsan.fda.gov/~dms/eafus.html.

24) (a) J. Balzarini, M. Stevens, E. D. Clercq, D. Schols, C. Pannecouque, *J. Antimicrob. Chemother.* **2005**, *55*, 135-138 (b) R. F. Anderson, S. Shinde, M. P. Hay, S. A. Gamage, W. A. Denny, *Org. Biomol. Chem*. **2005**, *3*, 2167. (c) K. M. Amin, M. M. F. Ismail, E. Noaman, D. H. Solimanb, Y. A. Ammard, *Bioorg. Med. Chem.* **2006**, *14*, 6917.

25) N. Varainkal, C. Lee, J. Xu, R. Calabria, N. Tsou, R. Ball, *Org. Proc. Res. Dev.* **2007**, *11*, 229.

CHAPTER 6

PHARMACEUTICAL COCRYSTALS OF TEMOZOLOMIDE

6.1 Introduction

The physical and chemical properties of any particular crystalline form of a drug depend on the internal arrangement of molecules in the crystals. Since different inter- and intramolecular interactions such hydrogen bonds, halogen interactions, π-stacking and van der Waals interactions are present in different crystalline forms, they will have different free energies and therefore exhibit different properties. As discussed in chapter 4, single-component crystals exhibit polymorphism and multi-component crystals exist as salt, hydrate, solvate and cocrystal. While selecting a crystalline form in pharmaceutical industry for drug development, one has to take two important factors i.e. solubility/bioavailability and stability into consideration. Accordingly the standard screening[1] in pharmaceutical industry involves searching for all possible crystalline forms initially and then selecting the best crystalline state of Active Pharmaceutical Ingredient (API), with optimal solubility and greater stability for further development. It could be a polymorph (Ritonavir), hydrate (Paroxetine HCl hemihydrtae), solvate (Indinavir sulphate ethanolate), or a salt (Atorvastatin calcium trihydrate) as shown in figure 1. In addition to these established crystalline API modifications, pharmaceutical cocrystals[2] or crystalline molecular complexes of an API with another pharmaceutically acceptable molecule have recently attracted the attention of pharmaceutical chemists as the resulting multi-component crystal possesses a distinct physicochemical profile, potentially enabling improvements in the properties of existing API.

Generally hydrates and solvates are formed unintentionally during crystallization. The stability of these crystalline forms needs special attention during processing and storage, as they are known to undergo phase transitions easily.[3] Sulfathiazole[4] is extremely promiscuous in terms of solvate formation with over one hundred solvates. The formation of salts,[5] or crystalline ionic complexes, is a more rational approach unlike solvate formation to alter the physicochemical properties of an API, but possesses several inherent drawbacks. It is normally targeted to one acidic or basic moiety on the molecule and therefore requires minimum of one ionizable center on the API of interest.

As a result non-ionizable pharmaceutical molecules are incapable of salt formation. On the other hand, pharmaceutical cocrystals which are emerging as a new class of pharmaceuticals, can address multiple functional groups and form complexes with neutral APIs that do not have ionizable groups, APIs that are not sufficiently acidic/ basic enough to form salts, and including those of salts. In addition, the space is not limited for binary[6a,b] combinations since ternary[6c,6d] and quaternary[6e] cocrystals are realistic possibilities. There is a large number of potential 'counter-molecules' which may be considered to be non-toxic, i.e. Generally Regarded As Safe (GRAS) chemicals[7] approved by Food and Drug Administration, may be selected as the second component. Such substances include food additives, preservatives, pharmaceutical excipients, vitamins, minerals, amino acids and other bio-molecules, as well as other APIs.

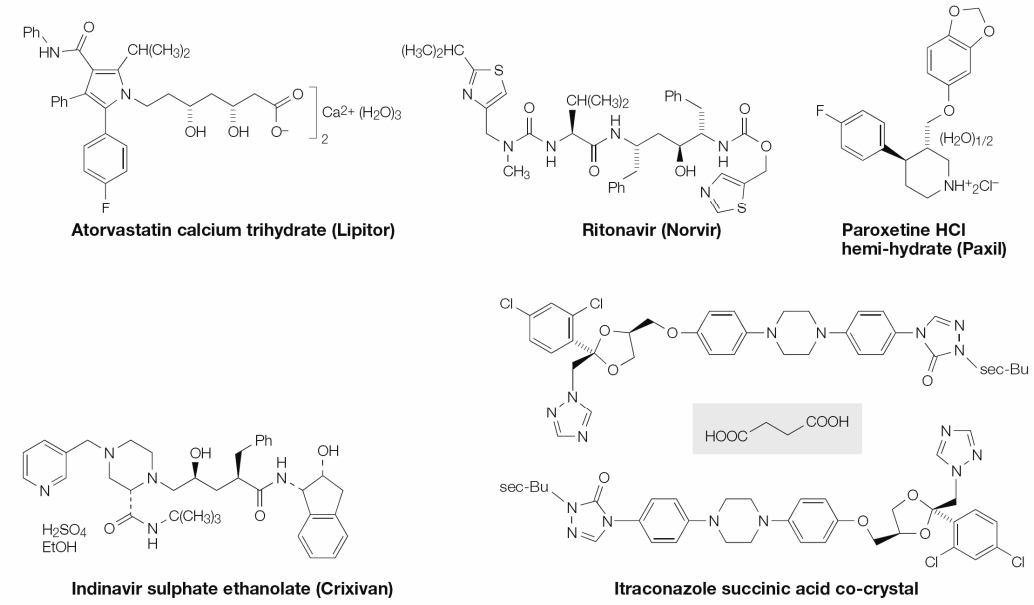

Figure 1. Different crystalline forms of few Active Pharmaceutical Ingredients.

The recent and rapid emergence of pharmaceutical cocrystals can be attributed to the following factors: design, diversity, discovery and development.[8] The most interesting aspect of cocrystals, undoubtedly, is the design of cocrystals taking the advantage of several strong hydrogen bonding groups present in the molecule. Due to large number of counter ions available for possible co-crystallization along with several hydrogen bond moieties predisposed on API, the diversity in crystalline forms is greatly enhanced for a pharmaceutical chemist. One can prepare several hundreds of cocrystals of which some

of them might exhibit enhanced solubility or stability. As discussed in chapter 5, the synthon[9] approach provides rational strategies for the construction of cocrystals and assessing the likelihood of formation of specific hydrogen bond synthons is possible from the statistical analysis of Cambridge Structural Database.[10] Normally all good hydrogen bond donors and acceptors are used in hydrogen bonding, and the best hydrogen bond donor tends to interact with the best hydrogen bond acceptor and so on, in a given crystal structure. Based on the functional groups in molecules and the hydrogen bond rules,[11] crystal engineering has recently gained control over the preparation of various stoichiometries of cocrystals. Further they can be easily prepared through solvent free or solvent reduced methods. Neat grinding, solvent-drop or liquid assisted grinding, slurry grinding and solvent mediated cocrystal formation are few general methods used for cocrystal preparation.[12] While cocrystals can be designed by synthon strategies, this does not mean that details of crystal structures or physical properties can be predicted before they are measured. Therefore all pharmaceutical cocrystals of an API are patentable inventions[13,8] like any other crystalline forms of APIs, and if they exhibit any clinical advantages, they may be used for further development.

Itraconazole, an antifungal agent, is extremely water insoluble and administered both orally and intravenously. In order to achieve the required oral bioavailability, the oral formulation of itraconazole is the amorphous form (as Sporanox beeds). Several cocrystals with a number of pharmaceutically acceptable 1,4-dicarboxylic acids, such as fumaric acid, succinic acid, malic acid and tartaric acid are prepared. Each cocrystal contains two API molecules and one acid cocrystal former, hydrogen bonded through carboxylic acid–triazole supramolecular synthons, to form a trimeric assembly (Figure 2a). It was observed that itraconazole cocrystals, especially itraconazole–L-malic acid or Succinic acid cocrystals,[14] exhibit a similar dissolution profile to that of the Sporanox beeds amorphous formulation. Therefore cocrystal of itraconazole is an alternate form for amorphous formulation. Carbamazepine and Saccharin (CBZ–SAC) cocrystal[15] appears to be superior to existing crystal forms of CBZ in the following respects: stability relative to the anhydrous polymorph of CBZ, favourable dissolution, suspension stability and favourable oral absorption profile in dogs. Fluoxetine HCl is an anti-depressant drug. It has been demonstrated that co-crystallization can also be employed

with already formed salt of API to modify its physical properties of fluoxetine HCl. The fluoxetine HCl–Succinic acid cocrystal,[16] as shown in figure 2b, exhibited twofold increase in aqueous solubility, however fluoxetine HCl–Benzoic acid cocrystal was found to decrease in aqueous solubility by ca. 50%. This study clearly demonstrates that only few cocrystals out of many cocrystals prepared exhibit desirable properties. A flurry of papers have been published in recent times on pharmaceutical cocrystals[17,18] taking the advantage of strong hydrogen bonds[17] and improving the existing properties of drug molecules in terms of solubility,[18a,b,c,d] bioavailability,[18e] stability and hydration control.[18f,g]

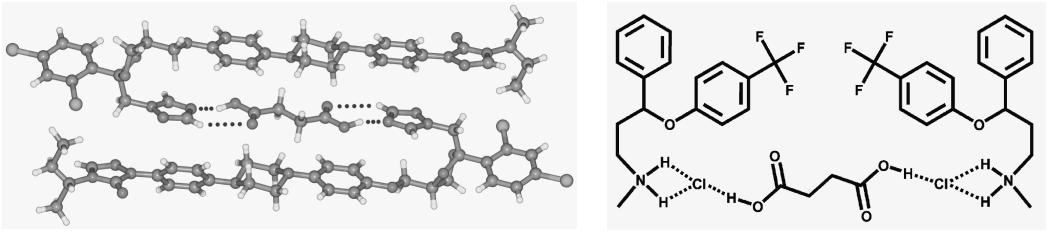

(a) (b)

Figure 2. (a) Itraconazole–Succinic acid cocrystal contains two API molecules and one acid cocrystal former. They are hydrogen bonded via carboxylic acid–triazole supramolecular synthons. (b) Succinic acid cocrystal of fluoxetine hydrochloride. Carboxylic acid to chloride ion synthon is present.

6.2 Need for a cocrystal of Temozolomide

Temozolomide (TMZ) acts as a prodrug by transporting a methylating agent (the methyldiazonium ion) to guanine bases within the major groove of DNA. The mechanism of activation of TMZ[19] involves hydrolytic cleavage of the tetrazinone ring at physiological *p*H to give an unstable monomethyl triazene [5-(3-methyltriazen-1-yl) imidazole-4-carboxamide (MTIC)], which then undergoes further cleavage to liberate the stable 5-aminoimidazole-4-carboxamide, and the highly reactive methyldiazonium ion (Scheme 1). This reactive species methylates guanine O6 and N7 positions in DNA and inhibits replication. The generation of small stable molecules, 5-aminoimidazole-4-carboxamide, CO_2 and N_2, provide the driving force for the mechanism of action of temozolomide.

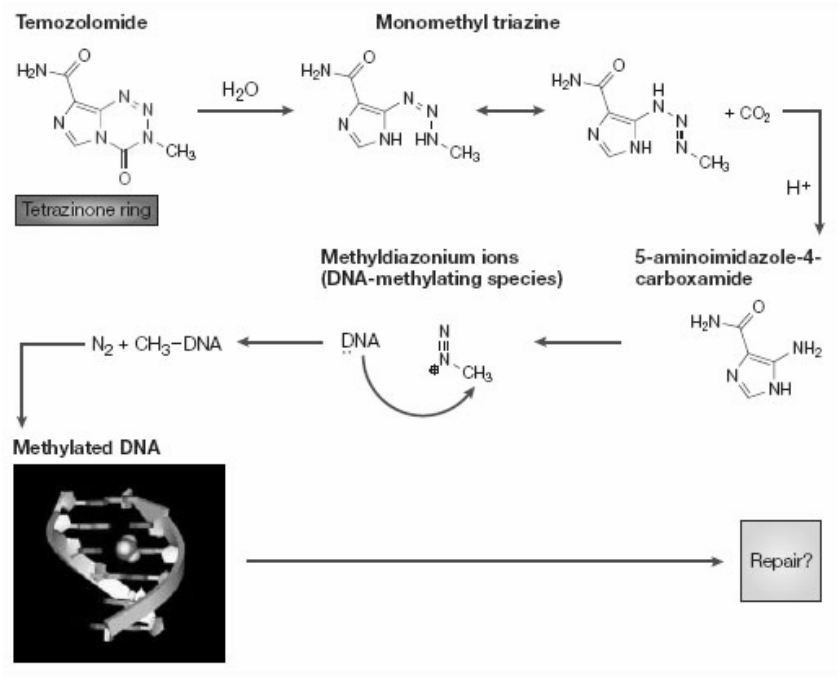

Scheme 1. Proposed mechanism of action for anti-tumour drug TMZ and its chemical reaction with DNA.

It is rapidly and almost completely absorbed after oral administration and a peak plasma concentration occurs in 1h. The material is non hygroscopic. However, there is a stability problem associated with TMZ.[19c] Temozolomide is generally obtained as a white precipitate but the material is sold as white to light tan/light pink powder.[19c] The light tan/pink powder is indicative of degradation. Special storage conditions like reduced humidity levels, suitable desiccants, low atmospheric oxygen levels and low light levels are specified for this compound in the drug leaflet. A recent patent[20a] showed that the sample containing 1.8% of water decomposes at a faster rate than the samples with >0.1 % water over a period of 6 months storage. Purity levels are tested by HPLC. Further, the white sample which was stored at 45% RH, started turning to pink color after 24h and the sample is distinctly pink after 4 days indicating decomposition. In view of the apparent tendency of temozolomide to decompose, there exists a need for products and methods to improve stability or shelf life of temozolomide. Apart from solid-state decomposition, it is known that, in solution, temozolomide is stable at acidic pH (<5) but labile at pH (>7).[19,21]

Two major problems that are encountered during crystallization are hydrolytic cleavage of TMZ tetrazinone ring via nucleophilic attack by water, methanol or ethanol (**20, 21** & **22,** Scheme 2) and the undesired formation of solvates (**23**, **24** & **25)** which get converted to anhydrous metastable TMZ polymorph 2 (**6b**) or sometimes mixture of TMZ polymorphs 1 (**6a**) and 2 (**6b**) in the later stages. The solubility of TMZ is limited to polar solvents only. The active component diazomethane required for bringing the antitumour activity is actually knocked off during this hydrolytic cleavage of tetrazinone ring. Recent patents[20b,c] also indicate the undesired solvate formation in CH_2Cl_2 and partial degradation in acetone-water combination. Therefore improving the stability of TMZ is crucial to prevent decomposition and improve its shelf life.

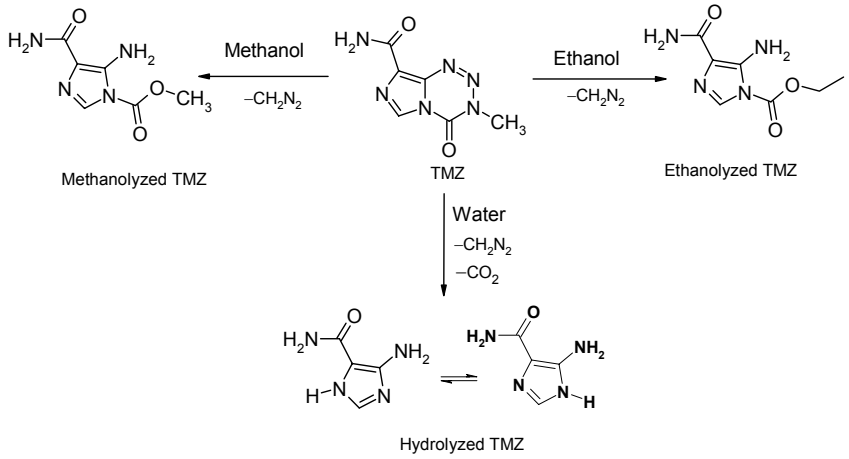

Scheme 2. Chemical reactions or hydrolytic cleavage of tetrazinone ring of TMZ upon dissolution in polar solvents like water, methanol and ethanol.

Hydrolyzed TMZ, 20: When temozolomide was crystallized from water, colourless aqueous solution turns yellowish immediately indicating TMZ hydrolysis. A brownish solid was obtained whose IR and ^{1}H-NMR values correspond to hydrolyzed product of TMZ i.e. 5-amino-3H-imiadazole-4-carboxamide. Several attempts to crystallize this material were unsuccessful. However, the monohydrate of hydrolyzed TMZ is reported in the CSD (refcode AIMZCX10, figure 3b).[22] It crystallized in the monoclinic $P2_1/a$ space group with one TMZ hydrolyzed molecule and a water molecule in the asymmetric unit. The carboxamide *anti* NH and imidazole NH forms a urea tape like structure along the *b*-axis (N2–H2···O1: 1.87, 2.847Å, 160.6º; N3–H4···O1: 1.96, 2.945Å, 162.9º). The water molecule acts as bridge between two such tapes and extends into a stair-case like structure via N–H···O hydrogen bonds as shown in figure 4. Water acts as donor to

imidazole N acceptor (O2–H7···N1: 1.93, 2.911Å, 179.5º) and accepts H-bond from amide *syn* NH (N3–H3···O2: 1.90, 2.856Å, 156.8º). These parallel stair-case units are connected by hydrogen bonds from water, amino and imidazole groups (O2–H8···N4: 2.04, 2.966Å, 155.8º; N4–H5···N1: 2.29, 3.296Å, 175.0º). Miscellaneous non-covalent interactions complete the crystal packing. The UV-VIS spectrum recorded at regular intervals of aqueous solution of temozolomide showed the gradual hydrolysis (Figure 3a). Initially there are three peaks in the electronic spectrum at 330 nm, 256 nm and 210 nm corresponding to the aromatic ring and carbonyl group of TMZ, $\pi - \pi^*$, $n - \pi^*$ and $n - \sigma^*$. The peak at 330 nm and 210 nm decreases in intensity as TMZ undergoes hydrolytic cleavage of tetrazinone ring carbonyl. While the 256 nm peak shifts towards higher wavelength at 266 nm with increase in intensity, indicating the increase in the concentration of TMZ hydrolyzed product. The *p*H of TMZ in aqueous solution is 6.0 on the 1st day and 6.3 on the 16th day. Similar UV-measurements on TMZ were reported in the literature.[21a,b]

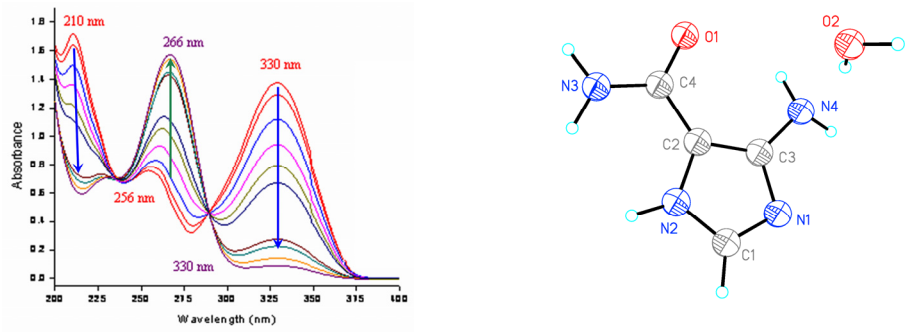

(a) (b)

Figure 3. (a) The UV spectrum recorded at regular intervals on the aqueous solution of TMZ. Its concentration gradually decreases as shown by blue arrows, while the concentration of degraded TMZ increases as shown by green arrow. (b) ORTEP diagram of monohydrate of TMZ hydrolyzed product.

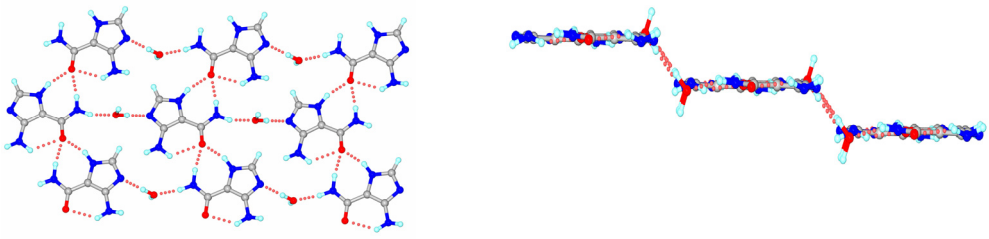

(a) (b)

Figure 4. Hydrogen bonds mediate stair-case like structure in the monohydrate of hydrolyzed TMZ crystal.

Methanolyzed TMZ, 21: Crystallization of TMZ from MeOH yielded dark red color crystals over a period of 2-3 days. Single crystal data on these crystals showed that the TMZ molecules have undergone partial decomposition as evident from 1:1 cocrystal of TMZ and methanolyzed TMZ in the asymmetric unit (Figure 5a). It crystallized in the monoclinic $P2_1/c$ space group. There is no amide dimer between TMZ and methanolyzed TMZ molecules. Instead a weak amide–imidazole synthon is present using *anti* NH of amide (N1–H1B···N8: 2.14, 3.035Å, 145.6º; N7–H7B···N2: 2.14, 3.046 (3) Å, 148.3º). The *syn* NH of TMZ forms a catemer (N1–H1A···O1: 1.93, 2.887 (3) Å, 156.5º) with a screw related TMZ along the [010] direction. A C4–H4···O2 dimer (2.24, 3.319 (3) Å, 170.0º) and a hydrogen bond between *syn* NH of methanolyzed TMZ molecule with a tetrazinone of TMZ (N7–H7A···O2: 2.13, 3.088(3) Å, 157.8º) connect parallel catemer network of molecules (Figure 5b). The amino group of methanolyzed TMZ forms two intramolecular hydrogen bonds with adjacent carbonyl acceptors.

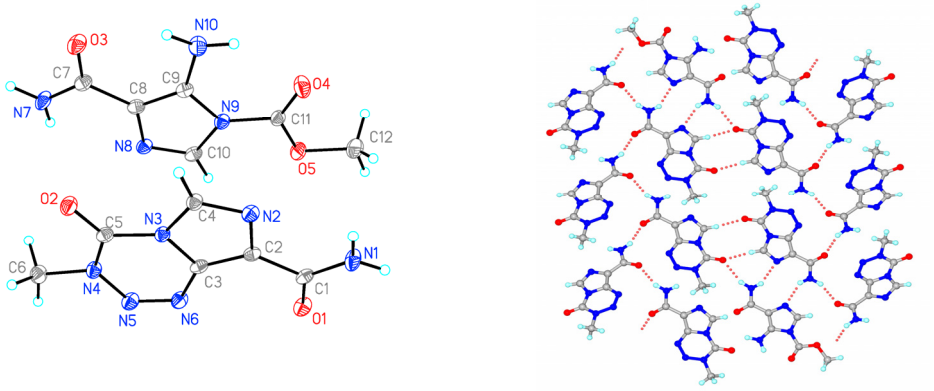

(a) (b)

Figure 5. ORTEP diagram of partially methanolyzed TMZ and TMZ (1:1). (b) Hydrogen bonding in **21** crystal structure.

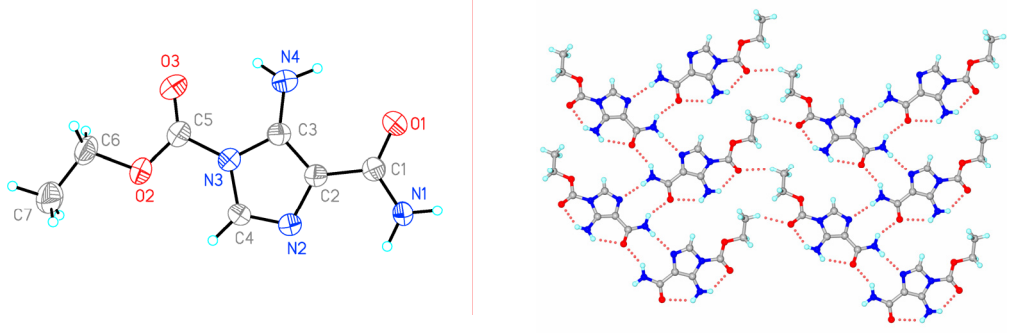

(a) (b)

Figure 6. ORTEP diagram of ethanolyzed TMZ. (b) Layered crystal structure of ethanolyzed TMZ.

Ethanolyzed TMZ, 22: Crystallization of TMZ from ethanol yielded ethanolyzed temozolomide crystals after 4-5 days. The rate of degradation is generally higher in water than MeOH, which in turn is faster than EtOH. The ethanolyzed product crystallized in the monoclinic $P2_1/c$ space group with one molecule in the asymmetric unit (Figure 6a). The amino group forms two intramolecular hydrogen bonds with carbonyl of amide and ethyl ester. Amide dimer is not present in this crystal structures, instead a weaker amide–imidazole synthon is present. This synthon has two distinct N–H···O hydrogen bonds, one with carbonyl of amide (N1–H1B···O1: 2.16, 3.049(2) Å, 144.9º) and another with imidazole N acceptor (N1–H1A···N2: 2.03, 3.036(3) Å, 169.9º). These interactions repeat in the crystal structures to form a zig-zag tape along [010] direction. These tapes are connected by a weak C7–H7B···O3 (2.57, 3.529(4) Å, 146.7º) interactions in the 2D layer (Figure 6b). An intermolecular N4–H4A···O1 dimer (2.22, 2.974(3) Å, 130.2º) between ethanolyzed TMZ molecules connects parallel 2D layers and extend into third dimension.

Monohydrate of Temozolomide, 23: Single crystals of TMZ monohydrate suitable for mounting were obtained during attempted co-crystallization with BPNO in CH_3CN and EtOH solvent mixture (3:1). TMZ–BPNO cocrystal (**18T**) discussed in chapter 5 and monohydrate of TMZ appeared concomitantly. Bulk material of monohydrate crystals of TMZ can be prepared from supersaturated solution of CH_3CN. It crystallized in the monoclinic space group $P2_1/m$ with one molecule of TMZ (50% atom occupancy) and a water molecule (50% atom occupancy) in the asymmetric unit, which resides on the mirror plane. There is no amide dimer present in the hydrate structure. TMZ molecules form one dimensional tapes along the [100] direction *via* O3–H3A···O1 (1.68, 2.650(2) Å, 167.7º), N1–H1B···O3 (1.83, 2.842(2) Å, 175.9º), and O3–H3B···N2 (2.04, 2.868(2) Å, 140.2º) interactions. Two such parallel tapes are connected by N1–H1A···O2 (2.01, 2.995(2) Å, 163.7º) H-bonds and it is also assisted by a weak C6–H6B···O1 (2.49, 3.517(2) Å, 157.3º) interaction to form a 2D sheet in the (030) plane as shown in figure 7a. Two dimensional sheets are held by π-stacking.

Nitromethane solvate of temozolomide, 24: It crystallized in triclinic space group $P\bar{1}$ with 1:1 of TMZ and CH_3NO_2 in the asymmetric unit. The amide moiety of TMZ connects to tetrazinone ring using *syn* NH (N1–H1A···O1 (1.87, 2.870(1) Å, 170.2º), and

a C4–H4···O2 dimer (2.08, 3.156(1) Å, 168.4º) extends TMZ molecules as a tape along the [100] direction. Nitromethane solvent connects two parallel tapes of TMZ molecules (N1–H1B···O3, 2.26, 3.253(2) Å, 167.6º; C6–H6A···O3, 2.59, 3.186(2) Å, 113.8º; C7–H7A···N5, 2.57, 3.502(2) Å, 143.5º and C7–H7C···O1, 2.34, 3.290(2) Å, 144.7º) and expand the molecular recognition into third dimension (Figure 7b).

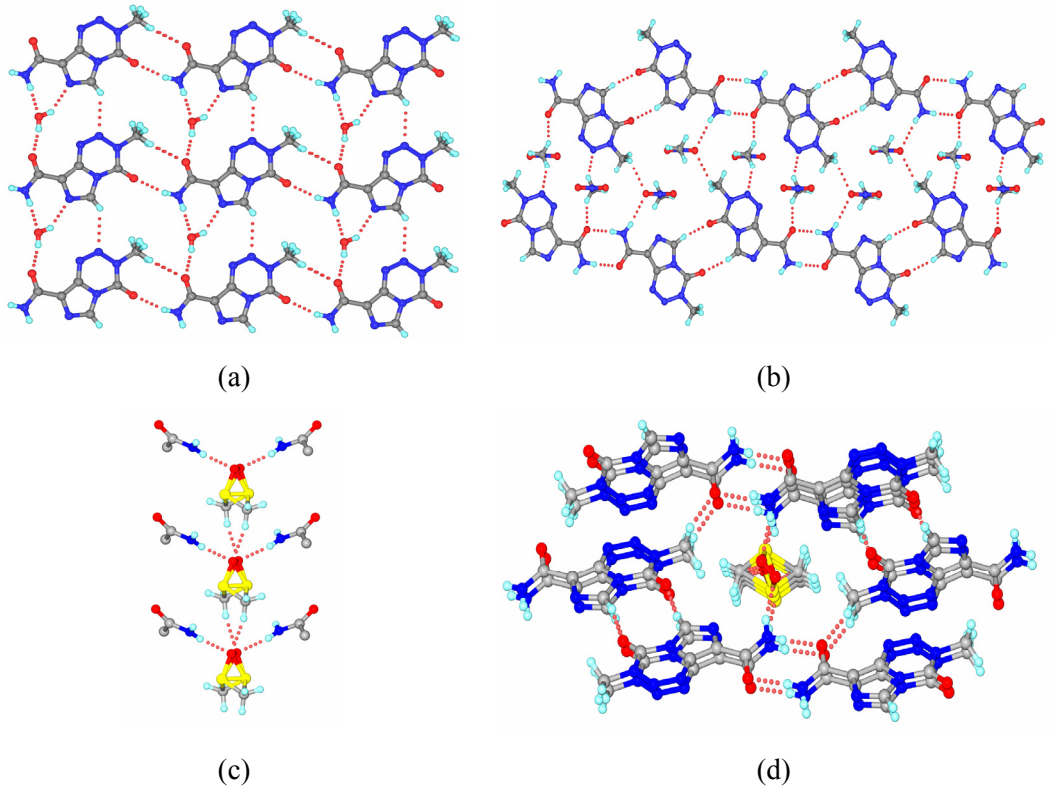

Figure 7. (a) Hydrogen bonding in the layered structure of TMZ monohydrate. (b) Nitromethane solvate of TMZ crystal structure. Solvent molecules are trapped in between the tapes of TMZ molecules. (c) DMSO solvate of TMZ. Solvent molecule is disordered over two sites with 50 % occupancy and forms H-bonds with TMZ (only amide portion is shown). (d) Six TMZ molecules are helically arranged around the DMSO solvent.

DMSO solvate of temozolomide, 25: It crystallized in the monoclinic space group *C*2/*c* and the asymmetric unit contains one molecule of TMZ and half molecule of DMSO. The solvent molecule is disordered over two sites with equal occupancy (Figure 7c). TMZ molecules form one dimensional tapes via amide *syn* NH dimer N1–H1A···O1 (1.93, 2.930(6) Å, 171.6º) and C4–H3···O2 dimer (2.16, 3.232(4) Å, 168.0º). *Anti* NH is connected to the oxygen of the disordered DMSO molecule. There is a helix of six molecules along the [010] direction via N1–H1A···O1 dimer, C4–H3···O2 dimer and C6–

H6C···O1 (2.30, 3.347 Å, 163.0º, figure 7d) leaving cavities along the *b*-axis. These cavities are occupied by the disordered DMSO molecules and form N1–H1B···O3 hydrogen bond (1.78, 2.744(6) Å, 159.6º) between sulfoxide acceptor and *anti* NH donor of TMZ. DMSO molecules are also held by C7–H7A···O3 interactions (2.15, 3.199(6) Å, 163.2º; 2.48, 3.456(6) Å, 149.6º) along the axis of the cavity as shown in figure 7c.

Pharmaceutical hydrates/solvates[3] are very important crystalline forms of some drugs molecules. Norfloxacin[23] is a typical example where its dihydrate is thermodynamically more stable form although three anhydrous norfloxacin forms[23b,c] and several other hydrates are characterized. In few cases it is difficult to obtain an anhydrous form of the drug, as obvious from the hundred solvates of sulfathiazole drug.[4] The tendency to form solvates or hydrates depends on the nature of molecule. There are mainly two reasons for their occurrence:[24] Firstly the host/drug forms a rigid molecular network in the crystal structure leaving some cavities behind. Such cavities are filled by small solvent molecules for a better close packing. Secondly there is a donor/acceptor imbalance in the drug molecule which is reconciled by including water or solvent molecule in the crystal lattice. Although solvates/ hydrates diversify the number of crystalline forms, they are in general not preferred unless they have advantageous properties over the anhydrous form, because most of the solvents are volatile and they are prone to undergo various phase changes (dehydration/desolvation) during processing and formulation. During these phase transitions, the crystalline nature may be retained or completely destroyed leading to an amorphous form or stable/metastable anhydrous form and often mixture of forms, affecting the content uniformity in solid processing. Cephradine dihydrate dehydrates to amorphous form which undergoes subsequent oxidation, as the amorphous form is less stable than the crystalline form.[3a] Norfloxacin,[23] Nitrofurantoin[26] are some examples, where the bioavailability of the drug is affected due to undesired phase transitions. The solvent molecule in all the solvated crystal structures of TMZ discussed above has strong hydrogen bonds with the host molecule. Upon their desolvation at RT over a period of few days, all of them underwent phase transformation to anhydrous metastable polymorph 2 (**6b**) of TMZ /or some times mixture form 1 (**6a**) and 2 (**6b**). These crystal structures are discussed in chapter 4. Such phase transitions can affect the physicochemical profile of a particular drug at various stages.

In summary, the decomposition of temozolomide at prolonged storage, hydrolytic cleavage of TMZ tetrazinone ring by nucleophilic attack by water, methanol or ethanol (**20, 21** & **22**) and the undesired formation of solvates (**23, 24, & 25**) and their phase transitions at subsequent stages are the main reasons to look for another crystalline product with improved properties. During the hydrolysis, the active species diazomethane required for bringing the antitumour effect is knocked off. Therefore improving the stability of TMZ is crucial. With the knowledge that TMZ is stable at acidic *p*H <5 but labile at *p*H >7,[21] it was co-crystallized with some GRAS organic acid *p*H adjusters[21e] to adjust *p*H of solution and thereby improving drug stability during crystallization. Several cocrystals of TMZ with organic acids are prepared so that the *p*H of the solution is controlled and there will be lesser extent of hydrolysis in water compared to pure TMZ, and hence expected to be used as controlled release of the drug in its cocrystal form. The possibility that the cocrystals are chemically less susceptible to hydration is another factor as discussed in chapter 5.

6.3 Cocrystals of Temozolomide with acid partner

Several mono and di-carboxylic acids which are safe chemicals are co-crystallized with temozolomide. Crystals of formic acid and acetic acid are referred as cocrystals in this chapter although there is an ongoing debate on the usage of term cocrystal when the second component is in the liquid phase.[2c,12a,17b] All cocrystals were easily formed by grinding the individual components in mortar-pestle for 10-15 min prior to dissolving them in aqueous or other polar solvents for crystallization over a period of 4-5 days. Temozolomide did not show any hydrolytic cleavage by water molecule during the co-crystallization, because the *p*H of the solution is altered by the organic acid.

Cocrystal of TMZ and Formic acid monohydrate (2:1:1), 26: It crystallized in the triclinic space group $P\bar{1}$ with two molecules of TMZ, one molecule of formic acid and a water molecule in the asymmetric unit. Both conformers *A* (stable) and *B* (metastable) of TMZ are present. There is a centrosymmetric amide dimer between the TMZ conformer *B* using its *syn* NH (N1–H1A···O1:1.88, 2.891(6) Å, 177.0º). There is also another centrosymmetric dimer of conformer *A,* interrupted by water and formic acid molecules. The proton of formic acid is migrated to water and forms hydrogen bond between

hydronium cation and a formate anion. The hydrogen bonds between amide *syn* NH to formate ion (N7–H7A···O6: 1.96, 2.970(7) Å, 174.2º), formate ion to water (O5–H7···O7: 1.68, 2.655(6) Å, 171.3º), and water to carbonyl of TMZ (O5–H5B···O3: 1.84, 2.717(6) Å, 146.7º) complete the second centrosymmetric dimer interrupted by water and formate ion. These two dimers are positioned adjacent to each other and held by N1–H1B···O6, C13–H13···O1, O5–H5A···N2, C6–H6B···N8, N7–H7B···N5, C4–H4···N11 and C12–H12B···O2 hydrogen bonds. These hydrogen bonds and a C10–H14···O4 dimer (2.28, 3.337(7) Å, 164.6º) repeat in the crystal to produce a sheet like structure in the (-332) plane (Figure 8a). The two dimensional sheets are stacked in the third dimension. Interestingly 2D layer section of this crystal structure is similar to the layered arrangement of molecules of disappeared polymorph 3 (**6c**) of chapter 4 as shown in figure 8a and 8b. Both structures **26** and **6c** have conformers *A* and *B* of TMZ. The similarity in the crystal packing of **26** and **6c** is reflected in unit cell dimensions: *a* = 8.173(12) /8.500(2); *b* = 11.626(17) /10.004(3); *c* = 11.735(17) /11.309(3) Å, for cocrystal **26** /polymorph **6c**). The variations in the axes and angles are due to second component formic acid and an extra water molecule.

Cocrystal of TMZ and Acetic acid (1:1), 27: It crystallized in the triclinic space group $P\bar{1}$ with one molecule of TMZ (conformer *A*) and one molecule of acetic acid in the asymmetric unit. The expected amide–acid heterosynthon is present (N1–H1A···O4: 1.94, 2.923(4) Å, 163.1º; O3–H3···O1: 1.64, 2.621(4) Å, 174.5º) using *syn* NH of the amide. These hetero-dimer units are connected side-by-side via two hydrogen bonds: *anti* NH to oxygen of COOH (N1–H1B···O3: 2.13, 3.075(5) Å, 155.1º) and imiadazole CH to tetrazine N (C4–H4···N6: 2.34, 3.412(5) Å, 169.2º) and extend along the [100] direction. These molecules expand into sheet like layered structure via close packing of methyl groups and a weak C–H···O interaction (Figure 9a). Layers are held by stacking and carbonyl···carbonyl dipolar attractions.

Cocrystal of TMZ and Oxalic acid (1:0.5), 28: It crystallized in the monoclinic space group *C*2/*c* and the asymmetric unit contains one molecule of TMZ (conformer *A*) and a half molecule of oxalic acid residing on the inversion centre. TMZ is involved in the formation of robust amide–acid heterosynthon (N1–H1A···O4: 1.93, 2.916(3) Å, 164.4º; O3–H3···O1: 1.59, 2.557(2) Å, 166.1º) using the *syn* NH. The *anti* NH is involved in the

formation of intramolecular N1–H1B···N2 using the imidazole nitrogen and it also helps in connecting such parallel tapes of acid–amide dimer *via* N1–H1B···O3 interaction (2.13, 3.103(2) Å, 160.3º). All the potential hydrogen bond acceptors/donors are involved in hydrogen bonding. These columnar tapes of molecules extend into layered structure (Figure 9b) via close packing of the methyl groups similar to that of acetic acid cocrystal.

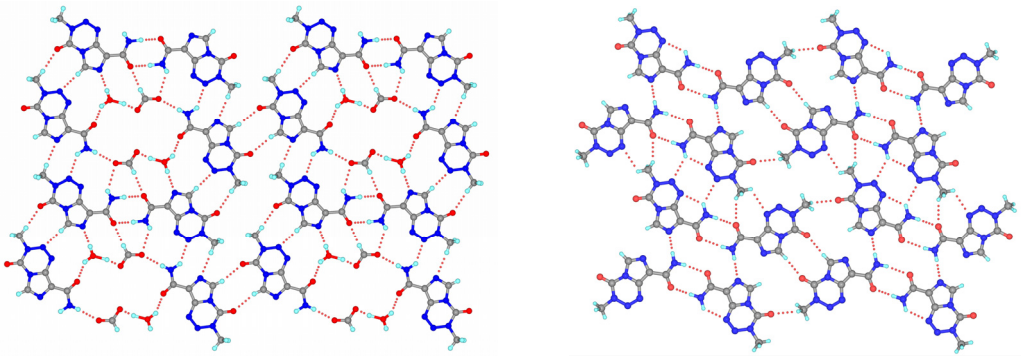

(a) (b)

Figure 8. (a) Hydrogen bonding in the layered structure of cocrystal **26**. (b) Layer of TMZ polymorph 3 (**6c**). Crystal packing in both crystal structures and same except that cocrystal **26** has more number of H-bonds due to formate and hydronium ion.

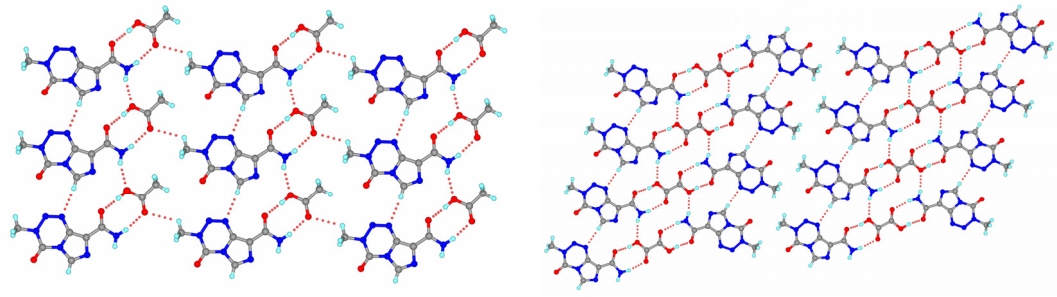

(a) (b)

Figure 9. Hydrogen bonds in (a) Acetic acid cocrystal. (b) Oxalic acid cocrystal. Acid–amide heterosynthon is present in both the layered crystal structures.

Cocrystal of TMZ and Succinic acid (1:0.5), 29: It crystallized in the monoclinic space group $P2_1/n$ with one molecule of TMZ (conformer *A*) and a half molecule of succinic acid residing on the inversion centre in the asymmetric unit. TMZ forms the amide–acid heterosynthon using the *syn* NH (N1–H1A···O3: 1.93, 2.903(3) Å, 161.2º; O4–H4A···O1: 1.63, 2.609(2) Å, 171.0º, figure 10a). The *anti* NH forms a helix along the *b*-axis via N1–H1B···O2 hydrogen bond (2.21, 3.022(3) Å, 136.6º, figure 10b). The packing of the molecules are similar to that of anhydrous TMZ polymorph 1 (**6a**) discussed in chapter 4.

The amide dimer synthon which is present in TMZ polymorph 1(Figure 10c) is broken by the succinic acid in cocrystal **29**, i.e. it acts as a bridge between the two TMZ molecule and forms acid–amide synthon (Figure 10a and 10c). Helix mediated by *anti* NH of amide persists in both the crystal structures (Figure 10b).

Cocrystal of TMZ and DL-malic acid (1:0.5), 30: It crystallized in the monoclinic *C*2/c space group and the asymmetric unit contains one molecule of TMZ (conformer *A*) and a half molecule of disordered malic acid. Although malic acid contains one OH moiety, it is disordered over two sites as shown in figure 10e, such that molecule now becomes symmetric and resides on the inversion center, to give a half molecule of malic acid in the asymmetric unit. Hydroxyl group only participates in intramolecular hydrogen bonds and has no affect on the over all crystal packing. The crystal packing is almost identical to succinic acid cocrystal as shown in the figure 10a and 10d. The homo dimer present in TMZ polymorph 1 (**6a**) is interrupted by malic acid molecule making a robust amide–acid heterosynthon (N1–H1A···O3: 1.91, 2.913(5) Å, 167.4º; O4–H4A···O1: 1.62, 2.589(5) Å, 167.8º). The *anti* NH, as usual forms a helix with tetrazinone ring (N1–H1B···O2: 2.17, 3.018(5) Å, 140.3º) along the [010] direction. The arrangement of molecules is observed to be similar in TMZ polymorph 1 (**6a**), succinic acid (**29**) and malic acid (**30**) cocrystals.

Cocrystal of TMZ, *p*-Aminobenzoic acid monohydrate (3:1:1), 31: It crystallized in the monoclinic space group $P2_1/c$ with three molecules of TMZ (all conformer *A*), one molecule of PABA, and a water molecule in the asymmetric unit. It contains both amide dimer homosynthon and amide–acid heterosynthon interrupted by a water molecule in its crystal structure. Crystal packing to some extent is identical to TMZ polymorph 1 (**6a**). The amide dimer is present between two symmetry independent molecules using *syn* NH (N1–H1A···O5: 1.87, 2.879(6) Å, 173.0º; N13–H13A···O1: 2.08, 3.056(6) Å, 161.4º). The *anti* NH of the TMZ forms a helix with carbonyl of tetrazinone ring (N1–H1B···O2: 2.11, 3.043(6) Å, 152.4º) along the *b*-axis similar to TMZ polymorph 1(Figure 10c and 11). PABA connects these two TMZ molecules using its amine NH donors (N19–H19B···O5: 2.12, 3.049(8) Å, 151.1º; N19–H19A···O2: 2.13, 3.119(8) Å, 165.8º) as shown in figure 11, and it connects the third TMZ molecule via acid–amide heterosynthon interrupted by water molecule (O8–H8···O9: 1.60, 2.579(8) Å, 171.3º;

O9–H9A···O3: 1.79, 2.776(8) Å, 173.0º; and N7–H7A···O7: 1.96, 2.959(6) Å, 170.2º). Several other hydrogen bonds connect the inversion related helices and complete the crystal packing.

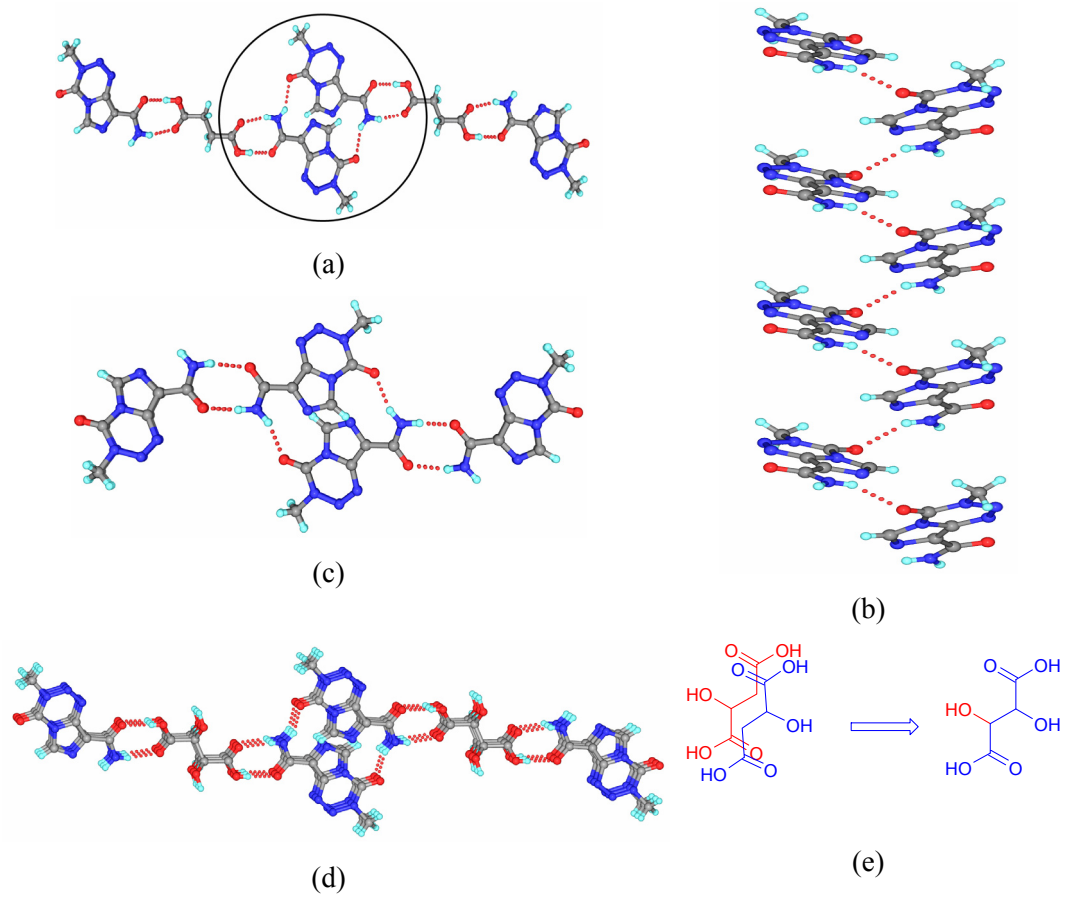

Figure 10. (a) Acid–amide heterosynthon in succinic acid cocrystal. The anti NH forms a helix along the b-axis with O=C of tetrazinone ring is encircled. (b) The encircled helix is viewed along the axis. (c) Crystal packing of TMZ polymorph 1 (**6a**). (d) Crystal packing of TMZ−DL–malic acid cocrystal. The amide dimer synthon in polymorph 1 is interrupted by acid–amide heterosynthon in cocrystals **29** and **30**. However helix mediated by the anti NH (encircled portion) remains same in all these crystal structures. (e) Disorder in malic acid.

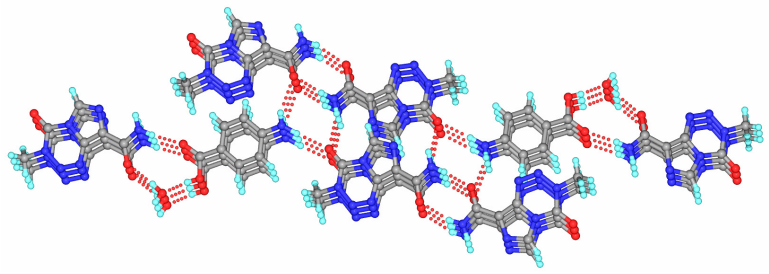

Figure 11. Amide dimer homosynthon and acid–amide interrupted by water molecule are present in the helical architecture of TMZ-PABA cocrystal.

Cocrystal of TMZ and Fumaric acid monohydrate (1:0.5:1), 32: It crystallized in the triclinic space group $P\bar{1}$ with one molecule of TMZ (conformer *A*), half molecule of fumaric acid residing on inversion center, and a water molecule in the asymmetric unit. The carboxylic acid forms a centrosymmetric acid dimer interrupted by a water molecule (O3–H3···O5: 1.58, 2.563(1) Å, 171.1º; O5–H5A···O4: 1.80, 2.788(1) Å, 175.0º). These interrupted acid dimers extend as a tape along [010] direction. There is another tape of TMZ molecules via N1–H1B···N2 dimer (2.27, 3.199(2) Å, 151.3º) and a C4–H4···O2 dimer (2.23, 3.255(2) Å, 156.0º). The *syn* NH of TMZ makes hydrogen bond with O=C of tetrazinone ring (N1–H1A···O2: 2.37, 3.0656(3) Å, 124.6º). These linear tapes of TMZ dimers are sandwiched between the ribbons of water interrupted fumaric acid molecules, and are connected by O5–H5B···O1 (1.89, 2.768(1) Å, 145.9º) hydrogen bond with water in the crystal structure (Figure 12a). A weak N1–H1A···O1 (2.31, 3.212(1) Å, 148.0º) *syn* NH amide dimer and other C–H···O interactions between the corrugated layers complete the overall crystal packing.

Cocrystal of TMZ and Salicylic acid (1:1), 33: This cocrystal was obtained during an attempted co-crystallization with aspirin in CH_3CN solvent. Aspirin undergoes hydrolysis to salicylic acid during crystallization. This crystal structure is in the triclinic space group $P\bar{1}$ contains one molecule of TMZ (conformer *B*) and one molecule of salicylic acid in the asymmetric unit. TMZ is involved in the formation of acid–amide heterosynthon with salicylic acid (N1–H1A···O4: 2.04, 3.053(4) Å, 162.5º; O5–H5···O1: 1.50, 2.544(3) Å, 169.3º). The *anti* NH is involved in intramolecular N1–H1B···N2 with tetrazine nitrogen. It also participates in the intermolecular hydrogen bond with inversion related TMZ molecule *via* N1–H1B···N5 interaction (2.55, 3.269(4) Å, 128º), and extend into a ribbon of TMZ–Salicylic acid molecules via C6–H6C···O2 dimer (2.35, 3.435(3) Å, 177.8º), C4–H4···O3 (2.32, 3.315(3) Å, 152.0º) and other C6–H6B···O4 hydrogen bonds (2.48, 3.433(4) Å, 145.8º). A C10–H10···O1 (2.39, 3.384(4) Å, 150.8º) connects parallel ribbons of TMZ–Salicylic acid heterosynthon molecules and forms a layered structure as shown in figure 12b. Layers are held by weak C–H···O interactions.

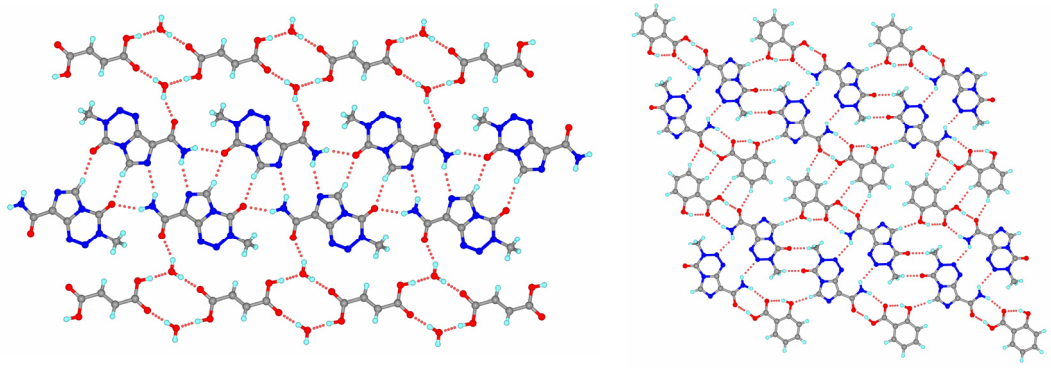

(a) (b)

Figure 12. (a) The layered structure of TMZ and fumaric acid. Linear tapes of TMZ molecules are sandwiched between the ribbons of water interrupted acid dimer. (b) Layered structure of TMZ and salicylic acid which contains acid–amide heterosynthon and other intermolecular hydrogen bonds in the crystal structure.

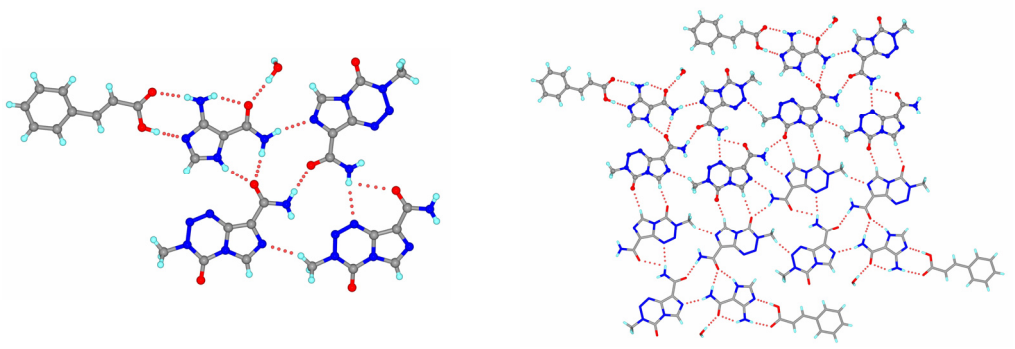

(a) (b)

Figure 13. Hydrogen bonding in the cluster of 5 molecules present in the asymmetric unit. Water OH points above the plane to connect to the next layer of molecules. (b) Hydrogen bonds in the layered structure of TMZ−Cinnamic acid cocrystal.

Cocrystal of TMZ, hydrolyzed TMZ and Cinnamic acid monohydrate (3:1:1:1), 34:

Crystals appeared when cinnamic acid and TMZ are dissolved in 1:1 molar ratio in water. We observed that cinnamic acid has precipitated after few hours after the crystallization is set up. The solution was undisturbed and left it for crystallization to take place. Few brown crystals appeared after 4-5 days on complete evaporation of water. Single crystal diffraction data showed that the TMZ molecules have undergone partial decomposition. It crystallized in the triclinic space group $P\bar{1}$ with three molecules of TMZ (two conformer *A*, and one conformer *B*), one hydrolyzed TMZ and a water molecule in the asymmetric unit. It is a monohydrate of a ternary cocrystal.

Surprisingly the ternary cocrystal does not contain usual amide dimer or amide–acid heterosynthon. Cinnamic acid forms acid–imidazole synthon with hydrolyzed TMZ molecule (O9–H9···N21: 1.70, 2.681(3) Å, 172.3º; N22–H22B···O8: 1.94, 2.910(4) Å, 160.2º). The hydrolyzed TMZ molecule uses its amide NH and forms hydrogen bonds with two TMZ molecules (conformer *A* and *B*, N20–H20···O1: 1.81, 2.763(4) Å, 155.0º; N19–H19B···O1: 1.88, 2.888(4) Å, 176.0º; N19–H19A···N8: 2.13, 3.131(4) Å, 166.8º). The third TMZ molecule is connected to other TMZ molecules via N7–H7A···N18 (2.36, 3.355(4) Å, 167.1º) and C18–H18B···N2 (2.29, 3.278(4) Å, 150.3º) hydrogen bonds. The water makes H-bond with degraded TMZ molecule (O10–H10B···07: 1.83, 2.812(4) Å, 177.3º). All these five molecules or cluster of 5 molecules present in the asymmetric unit forms hydrogen bonds in the same plane (Figure 13a), except one of the water OH donors which points one of its above the plane and connects to the next layer of molecules via O10–H10A···O5 bond (2.04, 3.007(4) Å, 165.8º). These cluster of 5 molecules are connected to their inversion related cluster of 5 molecules by a centrosymmetric N13–H13B···N14 dimer (2.34, 3.236(4) Å, 146.4º) and extend into a layered structure in the (223) plane as shown in figure 13b.

6.4 Cocrystals of Temozolomide with amide partner

Encouraged by the structural diversity of acid partners and conformational flexibility of TMZ molecule, we further extended our study to amide cocrystal formers from the GRAS list.

Cocrystal of TMZ and Isonicotinamide (2:1), 35: It crystallized in the triclinic space group $P\bar{1}$ and the asymmetric unit contains two molecules of TMZ (conformer *A* and conformer *B*) and one molecule of isonicotinamide. The crystal structure contains two distinct amide dimer synthons: a centrosymmetric homo amide dimer formed between two inversion related TMZ conformer *A* molecules (N7–H7A···O3: 1.86, 2.870(3) Å, 174.3º), and a hetero amide dimer formed between conformer *B* and isonicotinamide molecule (N1–H1A···O5: 1.88, 2.886(3) Å, 171.2º; N13–H13A···O1: 2.20, 3.199(3) Å, 167.3º). These hetero amide dimer units are connected to their inversion related molecules by N13–H13B···O1 hydrogen bonds (2.08, 2.861(3) Å, 132.3º) and C15–H15···N2 (2.34, 3.289(3) Å, 145.0º). The distance between two such hetero amide dimer

molecules is 5.1 Å as shown in figure 14a, which is the characteristic repeat distance in primary amides. Several N7–H7B···N6 (2.47, 3.338(3) Å, 143.1º), C9–H9···O5 (2.15, 3.220(3) Å, 171.3º), C6–H6B···O3 (2.29, 3.368(3) Å, 172.0º), C18–H18···O4 (2.14, 3.079(3) Å, 142.7º), and C12–H12B···N11 dimer (2.40, 3.463(4) Å, 164.8º) hydrogen bonds connect these hetero and homo dimer molecules and extend them into a layered crystal structures (Figure 14b). The layered cocrystal structure resembles the layered structure of TMZ polymorph 3 (**6c**) as shown figure 8b. The isonicotinamide molecule is able to replace one of the TMZ molecules in the 2D layer without disturbing the over all hydrogen bonding network. The unit cell dimensions are: a = 9.645(3) /8.500(2); b = 10.609(3) /10.004(3); c = 11.735(17) /10.925(3) Å, for cocrystal **35** and TMZ form 3 (**6c**). The important hydrogen bonds present in crystal structures are same for both structures, since both TMZ and isonicotinamide are rigid and contains $CONH_2$ moiety.

Cocrystal of TMZ and Nicotinamide (2:1), 36: TMZ and nicotinamide are co-crystallized with the intent of obtaining an isostructural cocrystal to the **35**, as the difference is only in the position of amide group with respect to pyridyl N atom between nicotinamide and isonicotinamide. It crystallized in the monoclinic space group $P2_1/c$ with two molecules of TMZ (conformer *A* and conformer *B*) and one molecule of nicotinamide in the asymmetric unit. Although the cocrystal stoichiometry is same in both cocrystals **35** and **36**, crystal packing is entirely different. Isonicotinamide cocrystal is layered whereas the nicotinamide cocrystal is helical. There are two types of amide dimers in the crystal structure. A centrosymmetric homo amide dimer is formed between two TMZ conformer *A* molecules (N7–H7A···O3: 1.91, 2.915(3) Å, 172.3º) and a hetero amide dimer is between conformer *B* and nicotinamide molecule (N1–H1A···O5: 1.83, 2.833(3) Å, 172.3º; N13–H13A···O1: 1.99, 2.989(3) Å, 167.7º). Comparison of these two cocrystal structures shows that the hetero-dimer connected to its inversion related hetero-dimer of molecules or cluster of 4 molecules is planar in isonicotinamide cocrystal **35** (Figure 14a and 14b), while it is helical in nicotinamide cocrystal **36** (figures 14c and 14d) which is mediated by N13–H13A···O1, (1.99, 2.989(3) Å, 167.7º) and N13–H13B···O1 (2.05, 3.003(3) Å, 156.6º). Despite several co-crystallization attempts, we have not been able to crystallize cocrystals of benzamide and picolinamide with TMZ to compare their structural motifs.

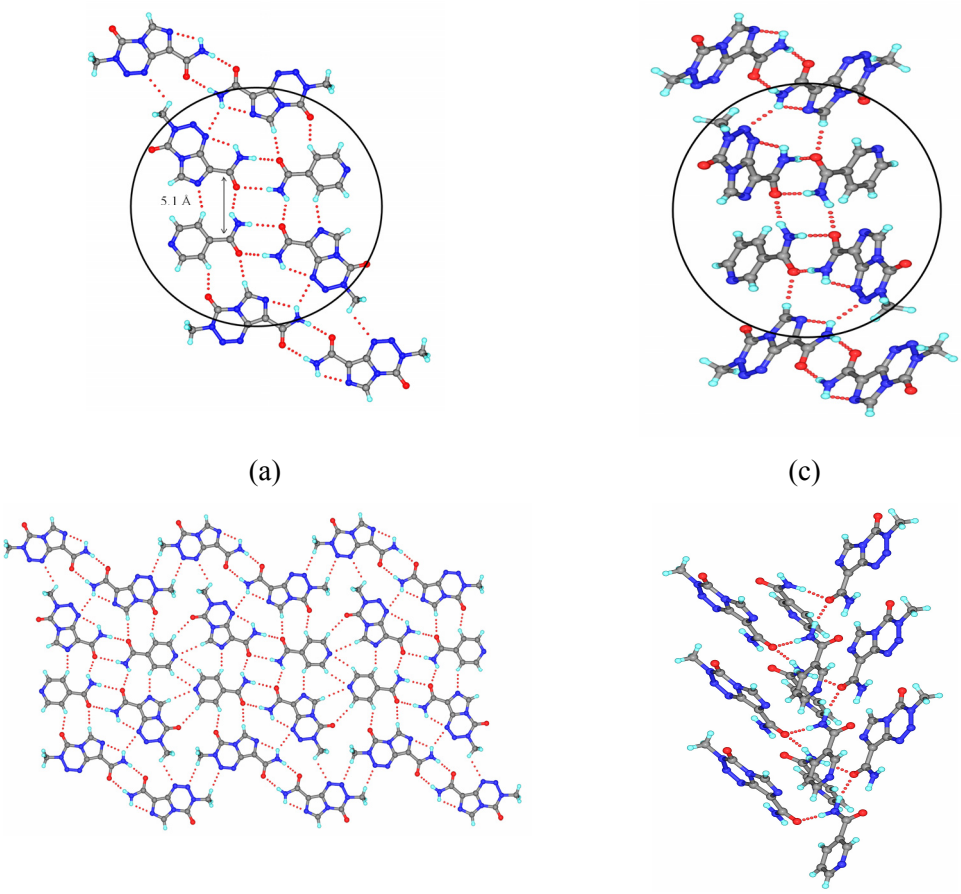

Figure 14. The cluster of four molecules as encircled is planar in isonicotinamide cocrystal (a), whereas they are helically arranged in nicotinamide cocrystal (c). (b) Layered isonicotinamide cocrystal. (d) Helical arrangement in nicotinamide cocrystal.

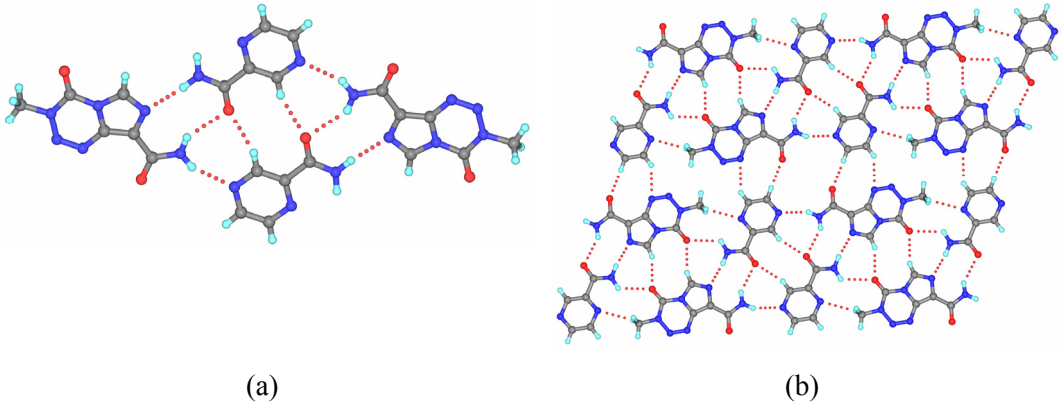

Figure 15. (a) The amide–pyrazine and amide–imidazole hydrogen bonds between TMZ and PYZMD. (b) Layered structure of TMZ-PYZMD cocrystal.

Cocrystal of TMZ and Pyrazinamide (1:1), 37: It crystallized in the triclinic space group $P\bar{1}$ with one molecule each of TMZ (conformer *A*) and pyrazinamide in the asymmetric unit. Surprisingly the stronger amide dimer synthon is not present in this crystal structure. Instead a weaker amide–pyrazine synthon is formed between *syn* NH of TMZ and pyrazine N atom (N1–H1A···N9: 2.08, 3.020(4) Å, 154.0º). Similarly the pyrazinamide donates its *syn* NH to imidazole N and accepts a hydrogen bond from *anti* NH of TMZ, and forms another weaker amide–imidazole synthon (N7–H7A···N2: 2.00, 3.006(3) Å, 169.0º; N1–H1B···O3: 2.26, 3.127(3) Å, 142.7º). Inversion related molecules are connected by weak C9–H9···O3 (2.26, 3.292(3) Å, 157.7º), C10–H10···O1 (2.18, 3.269(4) Å, 177.8º) interactions as shown in figure 15. These hydrogen bonds repeat in the crystal and forms a layered structure along the (434) plane as shown in figure 15b. There are no hydrogen bonds present in between the layers and π-stacking and carbonyl···carbonyl dipolar interactions build the third dimension in the crystal structure.

Cocrystal of TMZ and 4-hydroxy benzamide (2:1), 38: It crystallized in the triclinic space group $P\bar{1}$ and the asymmetric unit contains two molecules of TMZ (both are conformer *A*) and a 4-hydroxy benzamide. One of the symmetry independent TMZ molecule forms a centrosymmetric hydroxyl interrupted amide dimer (N1–H1A···O5: 2.06, 3.068(2) Å, 170.9º; O5–H5A···O1: 1.72, 2.705(2) Å, 172.7º) and extends as tape via C4–H4···O2 dimer (2.28, 3.300(3) Å, 155.5º, figure 16a). The amide group of 4-hydroxy benzamide forms centrosymmetric dimer (N13–H13A···O6: 1.84, 2.849(3) Å, 176.3º) between inversion-related molecule and connects to the next layer of tapes leading to the formation of square network of molecules as shown in figure 16b. Cavities in the square network are occupied by the second symmetry independent TMZ molecules. The second symmetry independent TMZ is connected to first TMZ via amide–imidazole synthon (N1–H1B···O3: 2.36, 3.249(3) Å, 146.0º; N7–H7A···N2: 2.05, 3.057(3) Å, 172.8º). A C10–H10···O4 dimer (2.17, 3.244(3) Å, 168.7º) and N13–H13B···N11 (2.21, 2.998(3) Å, 133.4º) are other hydrogen bonds with square network of molecules.

Cocrystal of TMZ and Saccharin (1:0.5), 39: Slow evaporation of TMZ and SAC in methanol gave two types of crystals. The needle to block like crystals matched with TMZ polymorph 2 (**6b**) and the diamondoid morphology is the cocrystal of TMZ and

saccharin. It crystallized in the triclinic space group $P\bar{1}$ and the asymmetric unit contains one molecule of TMZ (conformer *B*) and half molecule of saccharin. The saccharin molecule resides on the inversion centre in disordered orientation with 50% occupancy (Figure 17a). TMZ molecules form one dimensional tape via centrosymmetric amide dimer (N1–H1A···O1: 1.88, 2.890(3) Å, 176.1º) and a C4–H4···O2 dimer (2.23, 3.300(3) Å, 165.6º). Such parallel 1D tapes are connected by the disordered saccharin via N7–H7A···O1 hydrogen bond (1.79, 2.678(7) Å, 143.7º, figure 17b). The layered packing is similar to the nitromethane solvate of TMZ. Saccharin plays the role of two nitromethane molecules and connects the parallel tapes. Layers are stacked in the third dimension.

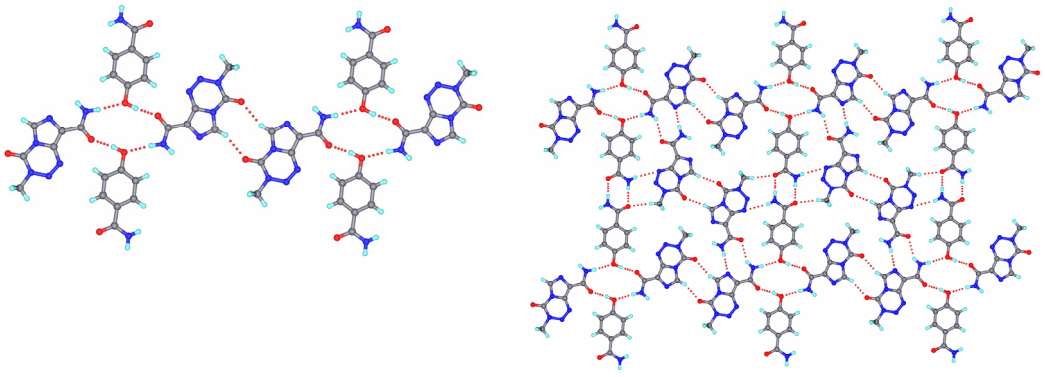

(a) (b)

Figure 16. (a) A centrosymmetric amide dimer interrupted by hydroxyl group. (b) Layered structure of cocrystal of TMZ–4-hydroxyl benzamide containing a square net work of molecules.

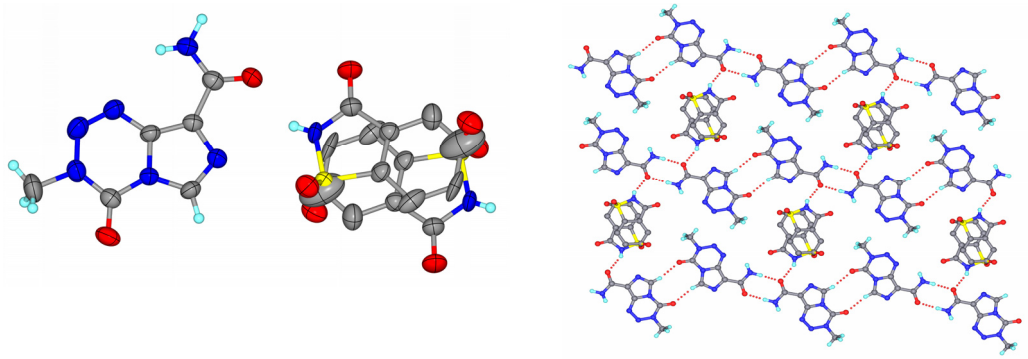

(a) (b)

Figure 17. ORTEP drawn at 50% probability of non-hydrogen atoms. Saccharin is disordered over two sites with 50% occupancy of atoms. (b) Disordered saccharin connects TMZ tapes and forms a layered crystal structure.

Table 1. Hydrogen bond geometrical parameters of crystal structures discussed in this chapter. O–H, N–H and C–H distances are neutron normalized.

Compound	Interaction	H···A/ Å	D···A/ Å	∠D–H···A/ º
20	N2–H2···O1	1.87	2.8469	160.6
AIMZCX10	N3–H3···O2	1.90	2.8563	156.8
	N3–H4···O1	1.96	2.9454	162.9
	N4–H5···N1	2.29	3.2969	175.0
	N4–H6···O1 Intra	2.36	3.0079	120.3
	O2–H7···N1	1.93	2.9115	179.5
	O2–H8···N4	2.04	2.966	155.8
	C1–H1···O2	2.31	3.2620	145.6
21	N1–H1A···O1	1.93	2.887(3)	156.5
	N1–H1B···N8	2.14	3.035(3)	145.6
	N1–H1B···N2 Intra	2.38	2.796(3)	103.4
	N7–H7A···O2	2.13	3.088(3)	157.8
	N7–H7B···N2	2.14	3.046(3)	148.3
	N7–H7B···N8 Intra	2.46	2.865(3)	102.8
	N10–H10A···O4 Intra	2.06	2.768(3)	124.4
	N10–H10B···O3 Intra	2.20	2.855(3)	120.6
	C4–H4···O2	2.24	3.319(2)	170.0
	C6–H6B···O4	2.33	3.258(3)	141.7
22	N1–H1A···N2	2.03	3.036(3)	169.9
	N1–H1B···N2 Intra	2.48	2.844(3)	100.3
	N1–H1B···O1	2.16	3.049(3)	144.9
	N4–H4A···O1 Intra	2.31	2.946(3)	118.5
	N4–H4A···O1	2.22	2.974(3)	130.2
	N4–H4B···O3	2.09	2.778(3)	123.0
	C7–H7B···O3	2.57	3.529(4)	146.7
	C7–H7C···N4	2.71	3.634(4)	142.8
23	N1–H1A···O2	2.01	2.995(2)	163.7
	N1–H1B···O3	1.83	2.842(2)	175.9
	N1–H1B···N2 intra	2.46	2.837(2)	101.8
	O3–H3A···O1	1.68	2.650(2)	167.7
	O3–H3B···N2	2.04	2.868(2)	140.2
	C4–H4···N5	2.69	3.565(3)	137.9
	C6–H6B···O1	2.49	3.517(2)	157.3
24	N1–H1A···O1	1.87	2.870(1)	170.2
	N1–H1B···O3	2.26	3.253(2)	167.6
	N1–H1B···N2 intra	2.36	2.769(1)	103.0
	C4–H4···O2	2.08	3.156(1)	168.4
	C6–H6A···O3	2.59	3.186(2)	113.8
	C6–H6B···N5	2.69	3.659(2)	148.9
	C6–H6C···N6	2.69	3.773(2)	179.0
	C7–H7A···N5	2.57	3.502(2)	143.5
	C7–H7C···O1	2.34	3.290(2)	144.7
	C7–H7C···N4	2.67	3.487(2)	131.6
25	N1–H1A···O1	1.93	2.930(6)	171.6
	N1–H1B···O3	2.34	3.336(6)	167.7
	N1–H1B···O3	1.78	2.744(6)	159.6
	N1–H1B···S1	2.44	3.315(5)	145.0
	C4–H3···O2	2.16	3.232(4)	168.0
	C6–H6A···N2	2.81	3.802(4)	151.9
	C6–H6C···O1	2.30	3.347(4)	163.0
	C7–H7A···O3	2.15	3.199(6)	163.2
	C7–H7A···O3	2.48	3.456(6)	149.6
	C7–H7B···N2	2.54	3.495(5)	146.5

26	N1–H1A···O1	1.88	2.891(6)	177.0
	N1–H1B···O6	2.43	3.164(7)	128.5
	N1–H1B···N2 Intra	2.31	3.010(6)	124.8
	O5–H5A···N2	1.94	2.919(7)	169.6
	O5–H5B···O3	1.84	2.717(6)	146.7
	O5–H7···O7	1.68	2.655(6)	171.3
	N7–H7A···O6	1.96	2.970(7)	174.2
	N7–H7B···N8 Intra	2.24	2.772(7)	110.9
	N7–H7B···N5	2.30	3.164(7)	141.3
	C4–H4···N11	2.18	3.240(7)	164.5
	C6–H6B···N8	2.35	3.435(7)	175.9
	C12–H12B···O2	2.37	3.429(7)	163.1
	C13–H13···O1	2.13	3.208(8)	171.4
	C10–H14···O4	2.28	3.337(7)	164.6
27	N1–H1A···O4	1.94	2.923(4)	163.2
	N1–H1B···O3	2.13	3.074(5)	155.1
	N1–H1B···N2 Intra	2.21	2.740(4)	110.7
	O3–H3···O1	1.64	2.621(4)	174.5
	C4–H4···N6	2.34	3.412(5)	169.2
28	N1–H1A···O4	1.93	2.916(3)	164.4
	N1–H1B···N2 intra	2.28	2.735(3)	105.6
	N1–H1B···O3	2.13	3.103(2)	160.3
	O3–H3···O1	1.59	2.557(2)	166.1
	C4–H4···N6	2.26	3.335(3)	172.5
	C6–H6A···O3	2.43	3.492(4)	167.7
29	N1–H1A···O3	1.93	2.903(3)	161.2
	N1–H1B···N2 intra	2.36	2.771(3)	103.6
	N1–H1B···O2	2.21	3.022(3)	136.6
	O4–H4A···O1	1.63	2.609(2)	171.0
30	N1–H1A···O3	1.91	2.913(5)	167.4
	N1–H1B···N2 Intra	2.32	2.759(6)	104.9
	N1–H1B···O2	2.17	3.018(5)	140.3
	O4–H4A···O1	1.62	2.589(5)	167.8
	C4–H4···N6	2.44	3.515(6)	170.9
	C6–H6B···O6	2.42	3.471(1)	162.4
31	N1–H1A···O5	1.87	2.879(6)	173.0
	N1–H1B···N2 Intra	2.31	2.740(6)	103.7
	N1–H1B···O2	2.11	3.043(6)	152.3
	N7–H7A···O7	1.96	2.959(6)	170.2
	N7–H7B···N8 Intra	2.36	2.773(6)	104.0
	N7–H7B···O4	2.16	3.142(7)	162.5
	O8–H8···O9	1.60	2.579(8)	171.3
	O9–H9A···O3	1.79	2.776(8)	173.0
	N13–H13A···O1	2.08	3.056(6)	161.4
	N13–H13B···N14 Intra	2.40	2.792(6)	101.8
	N13–H13B···N5	2.36	3.234(7)	144.3
	N19–H19A···O2	2.13	3.119(8)	165.8
	N19–H19B···O5	2.12	3.049(8)	151.1
	C10–H10···N12	2.29	3.350(7)	165.6
	C16–H16···N17	2.29	3.346(8)	163.7
	C16–H16···N18	2.35	3.283(8)	142.8
32	N1–H1A···O2	2.37	3.0656(1)	124.6
	N1–H1A···O1	2.31	3.212(2)	148.0
	N1–H1B···N2 Intra	2.43	2.817(2)	101.4
	N1–H1B···N2	2.27	3.199(2)	151.3
	O3–H3···O5	1.58	2.563(1)	171.7
	O5–H5A···O4	1.80	2.788(1)	175.0
	O5–H5B···O1	1.89	2.768(1)	145.9
	C4–H4···O2	2.23	3.255(2)	156.0
	C6–H6A···O3	2.39	3.432(2)	159.6

33	N1–H1A···O4	2.07	3.053(4)	162.5
	N1–H1B···N6 intra	2.31	3.031(4)	127.6
	N1–H1B···N5	2.55	3.269(4)	127.8
	O3–H3···O4 intra	1.67	2.603(3)	156.3
	O5–H5··O1	1.57	2.544(3)	169.3
	C4–H4···O3	2.32	3.315(3)	152.0
	C6–H6A···N2	2.53	3.462(4)	143.9
	C6–H6B···O4	2.48	3.433(4)	145.8
	C6–H6C···O2	2.35	3.435(4)	177.8
	C10–H10···O1	2.40	3.384(4)	150.8
34	N1–H1A···O3	1.78	2.784(4)	173.6
	N1–H1B···N2 Intra	2.30	2.774(4)	107.0
	N7–H7A···N18	2.36	3.355(4)	167.1
	N7–H7B···N12 Intra	2.26	3.013(4)	130.0
	N13–H13A···O2	2.19	3.099(3)	147.5
	N13–H13B···N14 Intra	2.34	2.766(4)	104.0
	N13–H13B···N14	2.34	3.236(4)	146.4
	N19–H19A···N8	2.13	3.131(4)	166.8
	N19–H19B···O1	1.88	2.888(4)	176.0
	N20–H20···O1	1.81	2.763(4)	155.0
	N22–H22A···O7	2.08	2.834(4)	129.1
	N22–H22B···O8	1.94	2.910(4)	160.2
	O9–H9···N21	1.70	2.681(3)	172.3
	O10–H10A···O5	2.04	3.007(4)	165.8
	O10–H10B···O7	1.83	2.812(3)	177.4
	C4–H4···O6	2.08	3.117(4)	158.6
	C6–H6B···N11	2.09	3.147(4)	162.8
	C10–H10···O10	2.19	3.153(4)	146.6
	C30–H30···O4	2.20	3.204(4)	151.8
	C18–H18B···N2	2.29	3.278(4)	150.3
35	N1–H1A···O5	1.88	2.886(3)	171.2
	N1–H1B···N6 intra	2.29	3.018(3)	127.7
	N7–H7A···O3	1.86	2.870(3)	174.3
	N7–H7B···N8 intra	2.29	2.764(3)	107.3
	N7–H7B···N6	2.47	3.338(3)	143.1
	N13–H13A···O1	2.20	3.199(3)	167.3
	N13–H13B···O1	2.08	2.861(3)	132.3
	C6–H6B···O3	2.29	3.368(3)	172.0
	C9–H9···O5	2.15	3.220(3)	171.3
	C12–H12B···N11	2.40	3.463(4)	164.8
	C15–H15···N2	2.34	3.289(3)	145.0
	C18–H18···O4	2.14	3.079(3)	142.7
36	N1–H1A···O5	1.83	2.833(3)	172.2
	N1–H1B···N6 intra	2.28	3.028(3)	129.8
	N1–H1B···N8	2.69	3.335(3)	122.1
	N7–H7A···O3	1.91	2.915(3)	172.3
	N7–H7B···N8 intra	2.38	2.799(3)	103.6
	N7–H7B···N5	2.46	2.970(3)	110.3
	N7–H7B···N6	2.35	3.193(3)	140.6
	N13–H13A···O1	1.99	2.989(3)	167.7
	N13–H13B···O1	2.05	3.003(3)	156.6
	C4–H4···N11	2.40	3.399(3)	152.5
	C6–H6A···O3	2.36	3.403(3)	160.8
	C10–H10···O5	2.15	3.194(3)	160.8
	C17–H17···N2	2.42	3.407(3)	150.2
	C18–H18···O4	2.50	3.438(3)	144.1
37	N1–H1A···N9	2.08	3.020(4)	154.0
	N1–H1B···N2 intra	2.38	2.785(4)	103.0
	N1–H1B···O3	2.26	3.127(3)	142.7
	N7–H7A···N2	2.01	3.006(4)	169.0

	N7–H7B···O2	2.52	3.179(3)	122.4
	N7–H7B···N8 intra	2.23	2.674(4)	104.7
	C4–H4···O2	2.28	3.290(3)	154.0
	C9–H9···O3	2.26	3.292(3)	157.7
	C10–H10···O1	2.18	3.269(4)	177.8
	C11–H11···N6	2.46	3.377(4)	141.0
38	N1–H1A···O5	2.06	3.068(2)	170.9
	N1–H1B···N2 intra	2.41	2.828(3)	103.8
	N1–H1B···O3	2.36	3.249(3)	146.0
	N7–H7A···N2	2.05	3.057(3)	172.8
	N7–H7B···N8 intra	2.25	2.749(3)	108.7
	N13–H13A···O6	1.84	2.849(3)	176.3
	N13–H13B···N11	2.22	2.998(3)	133.4
	O5–H5A···O1	1.73	2.705(2)	172.7
	C4–H4···O2	2.28	3.300(3)	155.5
	C10–H10···O4	2.17	3.244(3)	168.7
	C18–H18···O1	2.27	3.074(3)	129.3
39	N1–H1A···O1	1.88	2.890(3)	176.1
	N1–H1B···N6 intra	2.27	3.029(3)	130.9
	N1–H1B···O10	2.46	3.288(4)	138.7
	N7–H7A···O1	1.79	2.678(7)	143.7
	N7–H7A···N2	2.39	3.171(7)	133.4
	C4–H4···O2	2.23	3.300(3)	165.6

6.5 Results and discussion

Cocrystals of TMZ with COOH partners are expected to be more useful than $CONH_2$ partners as they bring down solution *p*H levels <5 during the crystallization, circumventing degradation of TMZ molecules, and thereby improving the hydrolytic stability. The donor/acceptor imbalance of TMZ molecule is matched by the cocrystal former. As anticipated, most of the cocrystals with COOH partners, even though crystallized from polar solvents like water and methanol did not show any considerable hydrolysis of TMZ even after a week long period of crystallization (Table 3). In comparison, TMZ when dissolved in water without acidic cocrystal former underwent decomposition within 1 day. The succinic acid cocrystal of TMZ is a representative of all these acidic cocrystals which did not undergo degradation. The cinnamic acid cocrystal **34** however showed partial degradation of TMZ, although pK_a of succinic acid (~4.1) and cinnamic acid are comparable (~4.4). Its crystal structure contains one molecule of hydrolyzed TMZ for every three molecules of TMZ along with cinnamic acid and water (Figure 13a). Therefore cinnamic acid may not be a suitable candidate for cocrystal formation for improving the TMZ stability. This partial degradation is perhaps due to differences in the solubility of individual components in water, which resulted in the early precipitation of cinnamic acid from the aqueous solution which leads to a rise in *p*H

of the aqueous solution. Secondly, as the hydrolysis is in process, both TMZ and hydrolyzed TMZ which co-exist in solution crystallize out with $Z' = 3$, a similar explanation was invoked for explaining conformational polymorphs and presence of multiple molecules in the asymmetric unit i.e. $Z' > 1$.[25] Similarly cocrystal **21** has undergone partial decomposition which contains TMZ and methanolyzed TMZ in 1:1 stoichiometry. These two cocrystals **34** and **21** represent an intermediate stage during the course of degradation reaction, whereas hydrolyzed TMZ (**20**) and ethanolyzed TMZ (**22**) crystals are final degraded products.

Table 2. Crystal structures of TMZ prepared and discussed in this chapter 6.

S.No	Crystal structure	Stoichiometry	Predominant Synthon	Conformer
		Hydrolyzed TMZ		
20	Hydrolyzed TMZ · H_2O	1:1	Amide–water (X)	*A*
21	TMZ · Methanolyzed TMZ	1:1	Amide–tetrazinone VI Amide catemer (II)	*A*
22	Ethanolyzed TMZ		Amide–imidazole (V)	-
		TMZ solvates		
23	TMZ · H_2O	1:1	Amide–tetrazinone (VI)	*A*
24	TMZ · $MeNO_2$	1:1	Amide–amide (I)	*A*
25	TMZ · DMSO	1:0.5	Amide–amide (I)	*A*
		TMZ cocrystals with COOH partners		
26	TMZ · Formic acid · H_2O	2:1:1	Amide–acid (XI) Amide–amide (I)	*A* + *B*
27	TMZ · Acetic acid	1:1	Amide–acid (XI)	*A*
28	TMZ · Oxalic acid	1:0.5	Amide–acid (XI)	*A*
29	TMZ · Succinic acid	1:0.5	Amide–acid (XI)	*A*
30	TMZ · DL Malic acid	1:0.5	Amide–acid (XI)	*A*
31	TMZ · *p*-Aminobenzoic acid · H_2O	3:1:1	Amide–acid (XI) Amide–amide (I)	*A*
32	TMZ · Fumaric acid · H_2O	1:0.5:1	Amide–amide (I) Amide–tetrazinone (VI)	*A*
33	TMZ · Salicylic acid	1:1	Amide–acid (XI)	*B*
34	TMZ · Hydrolyzed TMZ · Cinnamic acid · H_2O	3:1:1:1	Amide–amide (XI) Acid–imidazole (XIII)	*A* + *B*
		TMZ cocrystals with $CONH_2$ partners		
35	TMZ · Isonicotinamide	2:1	Amide–amide (I)	*A* + *B*
36	TMZ · Nicotinamide	2:1	Amide–amide (I)	*A* + *B*
37	TMZ · Pyrazinamide	1:1	Amide–pyrazine (III) Amide–imadazole (IV)	*A*
38	TMZ · 4-hydroxybenzamide	2:1	Amide–amide (I)	*A*
39	TMZ · Saccharin	1:0.5	Amide–amide (I)	*B*

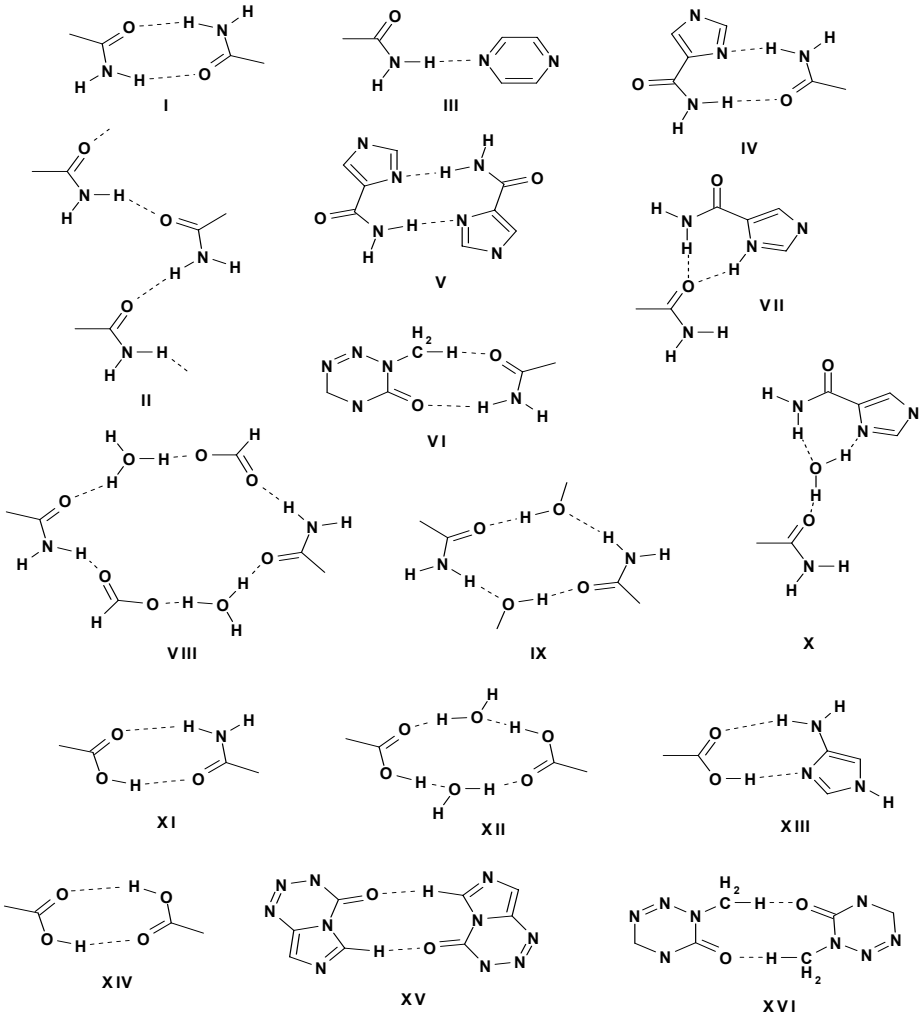

Scheme 3. Various hydrogen bond synthons observed in crystal structures of TMZ.

Apart from improving the stability of temozolomide as cocrystal solids, TMZ molecule exhibits variety of structural synthons in 20 crystal structures discussed in this chapter. Structure directing synthons are summarized in the table 2 and their motifs are shown in scheme 3. The predominant synthon for amide functional moiety in the absence of any other interfering functional moieties is undoubtedly dimer synthon (84%) followed by catemer or infinite chain of N–H···O hydrogen bonds (14%).[17c] However in the presence of several hydrogen bond acceptors, possibility of amide moiety interacting with other groups is more. In this context, the competition between stronger and weaker synthons is evaluated systematically when multiple functional groups like amide, acid, imidazole, tetrazine, pyridine and pyrazine are present during co-crystallization experiments. The

amide dimer synthon (**I**) is present 8 of the 11 crystal structures (3 hydrolyzed TMZ structures + 3 TMZ solvates + 5 cocrystals of TMZ with amide partner) that contain amide and heterocyclic N acceptor atoms. Although amide dimer is the most recurring motif, several hydrogen bonding motifs are possible in these crystal structures: amide catemer (**II**) and imidazole amide dimer (**V**) in cocrystal **21**, urea tape like synthon (**VII**) in **20,** amide–pyrazine (**III**) and amide–imidazole synthons (I**V**) in pyrazinamide cocrystal **37**, amide–tetrazinone (**VI**) in **23,** water or hydroxyl interrupted amide synthons **IX** and **X** in **38** and **34** respectively. When the acid group is introduced along with heterocyclic N acceptors, carboxylic acid–amide heterosynthon (**XI**) dominates the amide dimer homosynthon (**I**). It is present in **7** out of **9** cocrystals with COOH partner indicating the better strength of acid–amide synthon. Water interrupted acid dimer (**XII**) in cocrystal **32,** water and acid interrupted amide dimer in cocrystal 26 (**VIII**), acid–imidazole synthon (**XIII**) in **34,** and amide dimer (**I**) in **31** and **32** are the other motifs observed other than acid–amide (**XI**) synthon. There are only 5 accessible hydrogen bond motifs when acid, amide and heterocyclic N groups are present. In comparison, there are **10** accessible hydrogen bonding possibilities (**I-VII**, **IX, and X**) when the acid moiety is not present, signifying more likelihood for polymorphism. Perhaps this could be one reason why TMZ is known to exist in 9 polymorphic forms,[27] although so far only three of them were characterized by single crystal diffraction as discussed in chapter 4.[28]

The chances of polymorphism are likely to be more especially for crystal structures with unexpected weaker synthons. Cocrystal of pyrazinamide with TMZ (**37**) is one such example with weaker amide–pyrazine (**III**) and amide–imidazole synthons (I**V**). Since the expected amide dimer synthon is absent in pyrazinamide cocrystal **37**, a thorough polymorphic screening is underway to screen for a strongly hydrogen bonded cocrystal. Indeed such a polymorph screening resulted in two strongly hydrogen bonded cocrystals (2:1 and 1:1) of TMZ and BPNO, which was earlier known to exist in 1:0.5 stoichiometry cocrystal without expected amide dimer or amide–*N*-oxide synthons (discussed in chapter 5).[28] Dimorphs of isonicotinamide typify a similar situation wherein one form has stronger amide dimer synthon while the second one has weaker amide–pyridine synthon.[10a]

The conformer flexibility of temozolomide is noted in cocrystals. TMZ can undergo rotation about the C_{amide}–$C_{imidazole}$ bond to give two conformers, *A* and *B*, both of which are stabilized by intramolecular N–H···N interaction with different N acceptor atom. Conformer *B* is 1.44 kcal mol^{-1} higher in energy than *A*. In this chapter, four cocrystals have metastable conformer *B* of TMZ along with conformer *A* in the crystal lattice, while salicylic acid and saccharin cocrystals have exclusively conformer *B*. The prevailing notion for conformational flexible molecules is that, several conformers are in dynamic equilibrium with one another in solution and some of them crystallize out depending on crystal packing interactions and energies, i.e. intra and intermolecular compensation as discussed in chapter 4.[25,30] Interestingly, we have observed transitions from conformer *A* to *B* in the solid-state. Mere grinding of TMZ material (polymorph 1 and conformer *A*) and salicylic acid or saccharin for 15 min resulted in the respective cocrystals (**33** and **39,** figure 18) that have conformer *B* along with the respective cocrystal former in the asymmetric unit. However grinding TMZ polymorph 1 (conformer *A*) for more than one hour showed no phase transition (conformer *A* recovered), but the transition from *A* to *B* was apparent in cocrystals. The energy required for conformer *A* to *B* transition is ~8 kcal mol^{-1}as it has to cross-over the high-energy perpendicular conformation *C* (chapter 4). Present results indicate that high energy conformer transitions are not restricted to solution, but they can also be induced by mechanical grinding in the solid-state, provided the resulting cocrystal or a polymorph should be able to stabilize the metastable conformer through better hydrogen bonds and close packing.

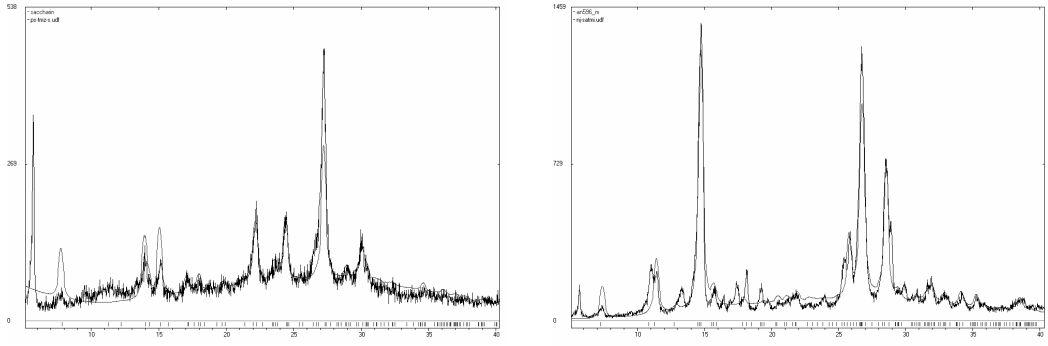

(a) (b)

Figure 18. (a) PXRD pattern of the grounded material of TMZ and saccharin for 15 min matches with simulated PXRD pattern of cocrystal **39**. (b) PXRD pattern of grounded material of TMZ and Salicylic acid matches with simulated pattern of cocrystal **33**.

Isostructural pairs of molecules with functional group replacements are reported in single component crystals. Chapter 2 discusses the isostructural replacement of phenyl CH donor by a pyrazine N acceptor in single component crystals. However isostructural relationship between single and multi-component crystals is rarely discussed in the literature. These are strictly not defined as isostructural, but have been referred by another descriptor called as local similarity or synthonmorphism in crystals.[31] Establishing such isostructural relationships is important to understand similarities and dissimilarities between single and multi-component crystals. The 2D layer arrangement in formic acid cocrystal (**26**) and isonicotinamide cocrystal (**35**) is similar to the layered arrangement of molecules in TMZ polymorph 3 (**6c**) in terms of hydrogen bonding. Isonicotinamide is able to replace one of the TMZ molecules in polymorph **3** with similar hydrogen bonding network (Figure 19). Small molecules hydronium and formate ions in cocrystal **26** interrupt the amide dimer homosynthon in polymorph 3. Two dimensional similarity in these crystal structures is attributed to the recurrent amide dimer hydrogen bonds.[32] Incidentally all these crystal structures have both conformers *A* and *B*. Therefore, it appears that both the conformers are needed to stabilize the layered arrangement.

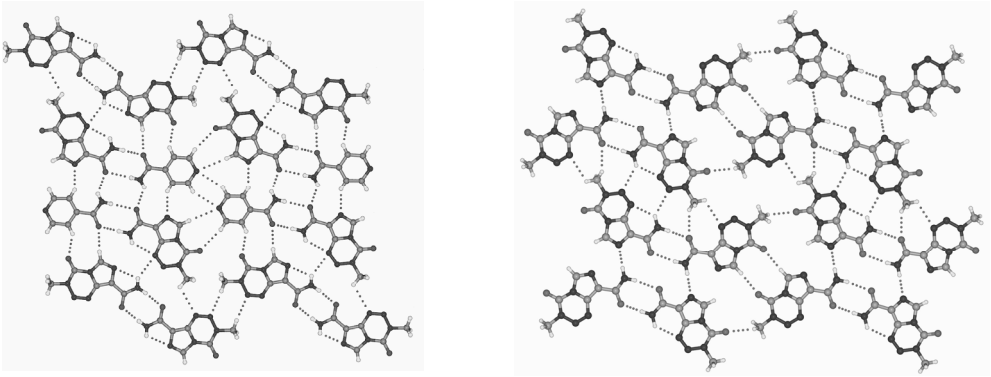

(a) (b)

Figure 19. (a) 2D section of 2:1 cocrystal of TMZ and Isonicotinamide. (b) 2D section of TMZ polymorph 3. Note that both crystal structures have identical layered arrangement of molecules. Both conformers *A* and *B* of TMZ are present in two crystal structures.

Nicotinamide cocrystal (**36**) although contains same stoichiometry as isonicotinamide cocrystal (2:1), and contains both conformers *A* and *B*, its crystal packing is totally different. Cocrystal **26** is layered while **35** is helical structure. Hence it is difficult to

predict which crystals are likely to be isostructural especially in cases of strongly hydrogen bond crystals. Crystal packing in cocrystals of succinic acid (**29**) and DL-Malic acid (**30**) are some what similar to TMZ polymorph 1 (**6a**), except that acid molecule now bridges between two amide molecules as shown in figures 10.

6.6 Conclusions

The chemical stability is special concern for anti-tumour drug temozolomide. It undergoes degradation on storage. Special storage conditions like reduced humidity levels, suitable desiccants low atmospheric oxygen levels and low light levels are specified for this compound. Two major problems that are encountered during crystallization are hydrolytic cleavage of TMZ tetrazinone ring by nucleophilic attack by water, methanol or ethanol (**20, 21** & **22**) and undesired formation of solvates (**23**, **24** & **25)**. The active species diazomethane required for bringing the antitumour activity is actually knocked off during this hydrolytic cleavage of tetrazinone ring. Therefore improving the stability of TMZ is crucial.

With the knowledge that TMZ is stable at acidic *p*H <5 but labile at *p*H >7, it was co-crystallized with some of the GRAS organic acid *p*H adjusters to improve its stability during crystallization. The presence of carboxamide and several N-heterocycle functional groups of TMZ were exploited for facile cocrystal preparation with different acid and amide partners. As anticipated, most of the cocrystals with COOH partners, even though crystallized from polar solvents like water and methanol did not show any considerable hydrolysis of TMZ even after a week long period of crystallization. In comparison, TMZ when dissolved in water without acidic cocrystal former underwent hydrolytic cleavage within 1 day. The cinnamic acid cocrystal **34** showed partial hydrolysis of TMZ. This partial decomposition is due to differences in the solubility of individual components in water.

The recurrence of stronger synthons and their competition with weaker synthons is evaluated systematically when multiple functional groups are present during co-crystallization experiments. The amide dimer synthon is present 8 of the 11 crystal structures. Even though amide dimer is the most recurring motif, several other hydrogen

bonding motifs (10 synthons) are realized in the solid-state. When acid group is introduced along with amide and N heterocyclic groups, stronger acid–amide synthon dominates over amide dimer (7 out of 9 cocrystals) and there are 5 other accessible hydrogen bond motifs. The reduced number of accessible hydrogen bond motifs from 10 to 6 is due to greater enthalpic advantage of amide–acid synthon during the crystallization and thus reduced scope for polymorphism.

The conformer flexibility of temozolomide is noted in cocrystals and the cocrystals containing metastable conformer *B* of TMZ can be easily prepared by mere grinding of TMZ (conformer *A* of polymorph 1) and the respective cocrystal former. The present results indicate that high energy conformer transitions are not restricted in solution, but they can also be induced by grinding in the solid-state. Isostructural relationship between single and multi-component cocrystals is discussed. The 2D layer arrangement in formic acid cocrystal (**26**) and isonicotinamide cocrystal (**35**) is found to be identical to the layered arrangement of molecules in TMZ polymorph 3.

6.7 Experimental section

Preparation of hydrolyzed TMZ, 20: 100 mg of the TMZ was dissolved in 5-7 mL of water. The colourless aqueous solution of TMZ turned yellowish over a period of 3 to 4 d. A brownish non-crystalline solid was obtained whose IR and ^{1}H-NMR spectra are different from temozolomide spectra. The hydrolysis of TMZ was studied by UV-spectroscopy. UV scans were recorded at regular intervals on the aqueous solution of temozolomide (2mg of TMZ dissolved in 75 mL water).

Temozolomide: IR (KBr pellet): 3425, 3389, 3287, 3198, 3113, 1761, 1732, 1682, 1601, 1452, 1402, 1354, 1265, 1215, 111, 1041, 1003, 947, 848, 802, 731, 709, 632,611, 561 and 511 cm^{-1}. ^{1}H-NMR (DMSO-d_6): 3.87 (methyl 3H), 7.67 (amide 1NH), 7.79 (amide 1NH) and 8.81 (imidazole CH).

Hydrolyzed temozolomide: IR (KBr pellet): 3476, 3364, 3211, 2926, 1672, 1614, 1556, 1460, 1354, 1277, 1161, 1028, 939, 781 and 543 cm^{-1}. ^{1}H-NMR (DMSO-d_6): 5.52 (amino NH_2), 6.70 (amide NH_2) and 7.01 (imidazole CH) and 11.37 (acid COOH). Cocrystals 28-39 were ground in mortar/pestle for 15 min adding few drops of CH_3CN, prior to dissolving in the respective solvent for crystallization. Co-crystallization with

amide partners resulted in partial decomposition of TMZ which is evident from the black material along with some single crystals.

Table 3. Crystallization conditions.

Cocrystal No	Temozolomide	Cocrystal former CCF	Solvent/ Conditions	Time (Days)
20	100 mg (0.52 mmol)	----------	5-7 mL water	3 to 4
21	50 mg (0.26 mmol)	----------	5-8 mL Methanol	1 to 3
22	50 mg (0.26 mmol)	----------	8 mL Ethanol	5 to 6
23	50 mg (0.26 mmol)	27 mg BPNO (0.128 mol)	In 25 mL conical flask CH_3CN + EtOH (3:1) Attempted cocrystallization	2 to 3
	200 mg (1.04 mmol)	----------	15-20 mL CH_3CN Bulk material obtained	1 to 2
24	50 mg (0.26 mmol)	----------	6-8 mL of CH_3NO_2	2 to 3
25	200 mg (1.04 mmol)	----------	1.5-2 mL DMSO	1
26	50 mg (0.26 mmol)	----------	2-4 mL Formic acid	4 to 5
27	50 mg (0.26 mmol)	----------	2-4 mL of Acetic acid	4 to 5
28	40 mg (0.21 mmol)	37 mg (0.42 mmol) Oxalic acid	9 mL of CH_3CN or 5 mL water	2 to 3
29	50 mg (0.26 mmol)	31 mg (0.26 mmol) Succinic acid	8 mL of MeOH or 5 mL water	4 to 5
30	50 mg (0.26 mmol)	17 mg (0.13 mmol) DL–Malic acid	5 mL water	2 to 3
31	40 mg (0.21 mmol)	28 mg (0.21 mmol) PABA	5 mL CH_3CN	2 to 3
32	50 mg (0.26 mmol)	29 mg (0.26 mmol) Fumaric acid	11 mL of CH_3CN Pink colored crystals	2 to 3
33	50 mg (0.26 mmol)	46 mg (0.26 mmol) Aspirin	7 mL of CH_3CN Aspirin hydrolyzed to SA	1 to 2
34	50 mg (0.26 mmol)	41 mg (0.26 mmol) Cinnamic acid	10-15 mL of water CH_3CN/water	2 to 4
35	50 mg (0.26 mmol)	32 mg (0.26 mmol) Isonicotinamide	10 mL CH_3CN or Acetone	2 to 3
36	50 mg (0.26 mmol)	64 mg (0.52 mmol) Nicotinamide	15 mL Acetone	2 to 3
37	50 mg (0.26 mmol)	32 mg (0.26 mmol) Pyrazinamide	8 mL of CH_3CN	2 to 3
38	50 mg (0.26 mmol)	36 mg (0.26 mmol) 4-hydroxy benzamide	8-10 mL Acetone	2 to 3
39	40 mg (0.20 mmol)	38 mg (0.20 mmol) Saccharin	5-6 mL Methanol	2 to 3

6.8 References

1) (a) S. R. Byrn, R. R. Pfeiffer and J. G. Stowell, *Solid-State Chemistry of Drugs*; SSCI: West Lafayette, IN, **1999**. (b) R. Hilfiker, *Polymorphism in the Pharmaceutical Industry*, Wiley–VCH, Weinheim, **2006**. (c) S. L. Morissette, Ö. Almarsson, M. L. Peterson, J. F. Remenar, M. J. Read, A. V. Lemmo, S. Ellis, M. J. Cima, C. R. Gardner, *Adv. Drug. Del. Rev.* **2004**, *56*, 275.
2) (a) N. Rodríguez-Hornedo, Guest Editor, Special Section on Pharmaceutical Cocrystals, *Mol. Pharma.* **2007**, *4*, 299–434. (b) P. Vishweshwar, J. A. McMahon, M. J. Zaworotko, in *Frontiers in Crystal Engineering*, E. R. T. Tiekink and J. J. Vittal, Eds., Wiley, Chichester, **2006**, pp. 25-49. (c) Ö. Almarsson, M. J. Zaworotko, *Chem. Commun.* **2004**, 1889. (d) P. Vishweshwar, J. A. McMahon, J. A. Bis, M. J. Zaworotko, *J. Pharma. Sci*. **2006**, *95*, 499. (e) W. Jones, W. D. S. Motherwell, A. V. Trask, *Mat. Res. Soc.* **2006**, *31*, 875. (f) C. R. Gardner, C. T. Walsh, Ö. Almarsson, *Nat. Rev.* **2004**, *3*, 926. (g) M. L. Peterson, M. B. Hickey, M. J. Zaworotko, Ö. Almarsson, *J. Pharm. Pharmaceut. Sci.* **2006**, *9*, 317.
3) (a) K. R. Morris, in *Polymorphism in Pharmaceutical Solids*, ed. H. G. Brittan Marcel Dekker, New York, **1999,** pp 125-182. (b) R. K. Khankari, D. J. W. Grant, *Thermo. Chimica. Acta.* **1995**, *248*, 61.
4) A. L. Bingham, D. S. Hughes, M. B. Hursthouse, R. W. Lancaster, S. Tavener, T. L. Threlfall, *Chem. Commun.* **2001**, 603.
5) P. H. Stahl, M. Nakano, in *Hand Book of Phamaceutical salts: Properties, selection, and use.* Eds. P. H. Stahl, C. G. Wermuth, New York, Wiley-VCH, **2002**, pp 83-116.
6) (a) B. R. Bhogala, S. Basavoju, A. Nangia, *CrystEngComm* **2005**, *7*, 551. (b) C. B. Aakeröy, D. J. Salmon, *CrystEngComm* **2005**, *7*, 439. (c) B. R. Bhogala, S. Basavoju, A. Nangia, *Cryst. Growth Des*. **2005**, *5*, 1683. (d) C. B. Aakeröy, A. M. Beatty, B. A. Helfrich, *Angew. Chem., Int. Ed.* **2001**, *40*, 3240. (e) B. R. Bhogala, A. Nangia, *New. J. Chem.* **2008**, *32*, 800.
7) GRAS chemicals list is available at http://www.cfsan.fda.gov/~dms/eafus.html.
8) N. Shan, M. J. Zaworotko, *Drug. Disc. Today* **2008**, *13*, 440.

9) (a) G. R. Desiraju, *Angew. Chem. Int. Ed. Engl.* **1995**, *34*, 2311. (b) A. Nangia, G. R. Desiraju, *Top. Curr. Chem*. **1998**, *198*, 57.

10) (a) Cambridge Structural Database, CSD, version 5.29, ConQuest 1.10, November 2007 release, January update. (b) F. H. Allen, W. D. S. Motherwell, P. R. Raithby, G. P. Shields, R. Taylor, *New. J. Chem*. **1999**, 25.

11) (a) M. C. Etter, *Acc. Chem. Res.* **1990**, *23*, 120. (b) M. C. Etter, *J. Phys. Chem.* **1991**, *95*, 4601.

12) (a) L. S. Reddy, P. M. Bhatt, R. Banerjee, A. Nangia, G. J. Kruger, *Chem. Asian J.* **2007**, *2*, 505. (b) A.V. Trask, W. Jones, *Top. Curr. Chem.* **2005**, *254*, 41. (c) A. Jayasankar, A. Somwangthanaroj, Z. J. Shao, N. Rodríguez-Hornedo, *Pharma. Res.* **2006**, *23*, 2381. (d) S. L. Childs, N. Rodríguez-Hornedo, L. S. Reddy, A. Jayasankar, C. Maheshwari, L. McCausland, R. Shipplett, B. C. Stahly, *CrystEngComm* **2008**, *10*, 856. (e) N. Rodríguez-Hornedo, S. J. Nehm, K. F. Seefeldt, Y. Pagán-Torres, C. J. Falkiewicz, *Mol. Pharma.* **2006**, *3*, 362.

13) A. V. Trask, *Mol. Pharma.* **2008**, *4*, 301.

14) J. F. Remenar, S. L. Morissette, M. L. Peterson, B. Moulton, J. M. MacPhee, H. R. Guzmán, Ö. Almarsson, *J. Am. Chem. Soc.* **2003**, *125*, 8456.

15) (a) M. B. Hickey, M. L. Peterson, L. A. Scoppettuolo, S. L. Morrisette, A. Vetter, H. Guzmán, J. F. Remenar, Z. Zhang, M. D. Tawa, S. Haley, M. J. Zaworotko, Ö. Almarsson, *Eur. J. Pharm. Biopharm.* **2007**, *67*, 112. (b) S. G. Fleischman, S. S. Kuduva, J. A. McMahon, B. Moulton, R. D. B. Walsh, N. Rodríguez-Hornendo, M. J. Zaworotko, *Cryst. Growth Des.* **2003**, *3*, 909.

16) S. L. Childs, L. J. Chyall, J. T. Dunlap, V. N. Smolenskaya, B. C. Stahly, G. P. Stahly, *J. Am. Chem. Soc.* **2004**, *126*, 13335.

17) (a) L. S. Reddy, N. J. Babu, A. Nangia, *Chem. Commun.* **2006**, 1369. (b) N. J. Babu, L. S. Reddy, A. Nangia, *Mol. Pharma.* **2007**, *4*, 417. (c) J. A. McMahon, J. A Bis, P. Vishweshwar, T. R. Shattock, O. L. McLaughlin, M. J. Zaworotko, *Z. Kristallogr.* **2005**, *220*, 340. (d) I. A. D. H. Oswald, W. D. S. Motherwell, S. Parsons, E. Pidcock, C. R. Pulham, *Crystallogr. Rev.* **2004**, *10*, 57. (e) P. Vishweshwar, J. McMahon, M. L. Peterson, M. B. Hickey, T. R. Shattock, M. J. Zaworotko, *Chem. Commun.* **2005**, 4601. (f) A. V. Trask, J. van de Streek, W. D. S. Motherwell, W. Jones, *Cryst. Growth Des.* **2005**, *5*, 2233.

18) (a) A. M. Chen, M. E. Ellison, A. Peresypkin, R. M. Wenslow, N. Variankaval, C. G. Savarin, T. K. Natishan, D. J. Mathre, P. G. Dormer, D. H. Euler, R. G. Ball, Z. Ye, Y. Wang, I. Santos, *Chem. Commun.* **2007,** 419. (b) S. Basavoju, D. Bostrom, S. P. Velaga, *Cryst. Growth Des.* **2006**, *6*, 2699. (c) S. Basavoju, D. Bostrom, S. P. Velaga, *Pharma. Res.* **2008**, *25,* 530. (d) B. Srivijiya, P. Vishweshwar, B. R. Sreekanth, K. Vyas, *CrystEngComm* **2008**, *10*, 283. (e) D. P. McNamara, S. L. Childs, J. Giordano, A. Iarriccio, J. Cassidy, M. S. Shet, R. Mannion, E. O'Donnell, A. Park, *Pharma. Res.* **2006**, *23*, 1888. (f) A. V. Trask, W. D. S. Motherwell, W. Jones, *Cryst. Growth Des.* **2005**, *5*, 1013. (g) A. Trask, W. D. S. Motherwell, W. Jones, *Int. J. Pharm*. **2006**, *320*, 114.

19) (a) J. Arrowsmith, S. A. Jennings, A. S. Clark, M. F. G. Stevens, *J. Med. Chem.* **2002**, *45*, 5458. (b) M. J. M. Darkes, G. L. Plosker, B. Jarvis, *Am J Cancer* **2002**, *1*, 55. (c) http://www.spfiles.com/pitemodar.pdf

20) (a) O. Braverman, R. Feishtein, A. Weisman, J. Kaspi, *US Pat.* 2006/0222792 A1, Oct. 5, **2006**. (b) L. S. Pathi, R. D. Rao, K. R. Narayanrao, *WO* 2008/038031 A1. **2008**. (c) O. Etlin, M. Alnabari, Y. Sery, E. Danon, O. Arad, J. Kaspi, *US Pat.* 2006/0183898 A1. Aug 17, **2006**.

21) (a) B. J. Denny, R. T. Wheelhouse, M. F. G. Stevens, L. L. H. Tsang, J. A. Slack, *Biochemistry* **1994**, *33*, 9045. (b) J. Arrowsmith, S. A. Jennings, D. A. F. Langnel, R. T. Wheelhouse, M. F. G. Stevens, *J. Chem. Soc. Perkin Trans. 1* **2000**, 4432. (c) G. Saravanan, M. Ravikumar, M. J. Jadhav, M. V. Suryanarayana, N. Someswararao, P. V. R. Acharyulu, *Chromatographica* **2007**, *66*, 291. (d) H. Kim, P. Likhari, D. Parker, P. Statkevich, A. Marco, C. Lin, A. A. Nomeir, *J. Pharma. Biomed. Anal.* **2001**, *24*, 461. (e) E. Fenyvesi, M. Vikmon, J. Szeman, E. Redenti, M. Delcanale, P. Ventura, J. Szejtli, *J. Inclusion Phenomena and Macrocylic Chemistry* **1999**, *33*, 339.

22) K. Simon, J. Scahawartz, A. Kálmán, *Acta. Crystallogr.* **1980**, *B36*, 2323.

23) (a) T. Hu, S. Wang, T. Chen, S. Lin, *J. Pharma. Sci.* **2002**, *91*, 1351. (b) R. Barbas, F. martí, R. Prohens, C. Puigjaner, *Cryst. Growth Des.* **2006**, *6*, 1463. (c) R. Barbas, F. martí, R. Prohens, C. Puigjaner, *J. Therm. Anal. Cal.* **2007**, *89*, 687.

24) (a) A. Nangia, G. R. Desiraju, *Chem. Commun.* **1998**, 605. (b) A. Nangia, in Nanoporous Materials: Science and Engineering, eds. G. Q. Lu, X. S. Zaho,

Imperial college press, **2004**, pp 165-187. (c) L. Infantes, J. Chisholm, S. Motherwell, *CrystEngCommun.* **2003**, *5*, 480. (d) A. Gillon, N. Feeder, R. J. Davey, R. Storey, *Cryst. Growth Des.* **2003**, *3*, 663.

25) S. Roy, R. Banerjee, A. Nangia, G. J. Kruger, *Chem. Eur. J.* 2006, *12*, 3777.

26) (a) E. W. Pienaar, M. R. Caira, A. P. Lotter, *J. Cryst. Spectro. Res.* **1993**, *23*, 785. (b) M. Ostuka, Y. Matsuda, *J. Pharma. Pharmacology* **1993**, *45*, 406. (c) M. Otsuka, R. Teraoka, Y. Matsuda, *Pharma. Res.* **1992**, *9*, 307.

27) I. Adin, C. Iustain, *US Pat. 2005/0187206 A1*, Aug. 25, **2005**. The nine forms are numbered I–IX.

28) Y. Li, J. Han, G. G. Z. Zhang, D. J. W. Grant, R. Suryanarayan, *Pharma. Dev. Tech.* **2000**, *5*, 257.

29) N. J. Babu, L. S. Reddy, S. Aitipamula, A. Nangia, *Chem. Asian. J.* **2008**, *3*, 1122.

30) (a) A. Nangia, *J. Ind. Inst. Science* **2007**, *87*, 133. (b) A. Nangia, *Acc. Chem. Res.* **2008**, *41*, 595. (c) L. Yu, S. M. Reutzel-Edens, C. A. Mitchell, *Org. Proc. Res. Dev.* **2000**, *4*, 396.

31) H. Karfunkel, H. Wilts, Z. Hao, A. Iqbal, J. Mizuguchi, Z. Wu, *Acta. Crystallogr.* **1999**, *B55*, 1075.

32) L. Fábián, A. Kálaman, *Acta. Crystallogr.* **2004**, *B60*, 547.

CHAPTER 7

CONCLUSIONS

7.1 Structural origins of polymorphism in single and multi-component crystals

Crystal engineering,[1] or non-covalent synthesis in the solid state, requires an understanding of intermolecular forces. The hydrogen bond is a reliable non-covalent tool in the construction of supramolecular architectures due to its strength and directionality compared to other intermolecular interactions. Since different inter- and intramolecular interactions such hydrogen bonds, halogen interactions, π-stacking and van der Waals interactions are present in different crystal structures, different crystalline materials will have different free energies of their crystal structures. Different physical properties such as solubility, dissolution rate, crystal habit, melting point, thermal and particle morphology are exhibited by polymorphs. As single molecular entities, molecular solids can show polymorphism. Multi-component crystals include salts, hydrates, solvates and cocrystals. The structural differences between polymorphs originate through two mechanisms, namely, packing polymorphism and conformational polymorphism.[2] In this context four polymorphic systems were discussed in the thesis at an increasing level of complexity (scheme 1).

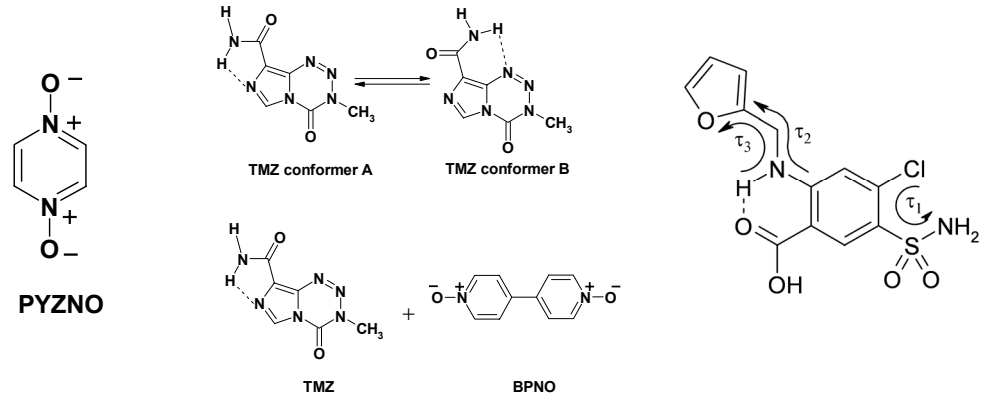

Rigid Planar Pyrazine-*N,N′*-dioxide	Semi-rigid planar Temozolomide with one torsion	Conformationally flexible Furosemide with three torsions

Scheme 1. Polymorphic systems discussed in the thesis

Pyrzine-*N,N′*-dioxide is rigid planar molecule and polymorphism is due to different packing arrangements of molecules connected by infinite chain of C–H···O hydrogen bonds. The smallest structural building unit or a trimer molecule is planar in form 1 (**5a**) but helical in form 2 (**5b**). Next level of complexity is illustrated by the amide torsion polymorphs of Temozolomide (TMZ) and its cocrystal polymorphs with bipyridine-*N,N′*-dioxide (BPNO). Temozolomide is a hetero aromatic molecule with one accessible torsion along the C_{amide}–$C_{imidazole}$ bond to give two conformers, *A* and *B*. TMZ polymorphs 1 (**6a**) and 2 (**6b**) have stable conformer *A*, while polymorph 3 (**6c**) has both conformers *A* and *B*. The structural origins of polymorphism in 1 and 2 are due to the presence of unused hydrogen bonds which are utilized in the stable form, whereas polymorph 3 is of mixed origin, i.e. conformational and packing polymorphism. Polymorphic cocrystals of TMZ and BPNO exemplify synthon polymorphism,[3] i.e. different hydrogen bond synthons present in crystal structures. Both cocrystals (**18T** and **18M,** figure 1) have stable conformer *A*. The presence of unused hydrogen bonds in cocrystals are similar to single component TMZ polymorphs 1 and 2, is the main reason for polymorphism. It appears that the differences in cocrystal polymorphs arise due to reasons similar to those for single component polymorphic structures, i.e. differences in conformation, hydrogen bonding, and/ or molecular packing.

(a) (b)

Figure 1. (a) Cocrystal **18T** without amide dimer and amide–*N*-oxide synthons. (b) Polymorphic cocrystal **18M** with strong amide–*N*-oxide heterosynthon.

Polymorphism in furosemide is due to an even higher level of complexity at the molecular level. Interestingly different conformations of furosemide lead to different hydrogen bonded sulfonamide synthons: sulfonamide dimer in form I (**7a**), tilted or skewed dimer in form III (**7c**), and a tetrameric sulfonamide synthon in form II (**7b**) referred to primary level synthon polymorphs (Figure 2). Systematic effects are analyzed wherein high energy metastable conformers (4.44 and 4.55 kcal/mol) are stabilized in the stable crystal lattice of FMD form I, while the stable conformer is present in a metastable

FMD form III crystal lattice. Similarly metastable conformer *B* of TMZ is stabilized in the stable crystal lattice of polymorph 3. We conclude that conformational flexibility in organic molecules increases the likelihood of polymorphism. (1) Several conformers are available in the crystallization milieu (solution or melt phase) to form different hydrogen bond synthons and close-packing motifs.[4] (2) The intra- and intermolecular energy compensation reduces total crystal energy differences, which increases the likelihood of polymorphism.[5] Since most of the drug molecules are conformationally flexible, the chances of polymorphism are more when compared to rigid molecules.

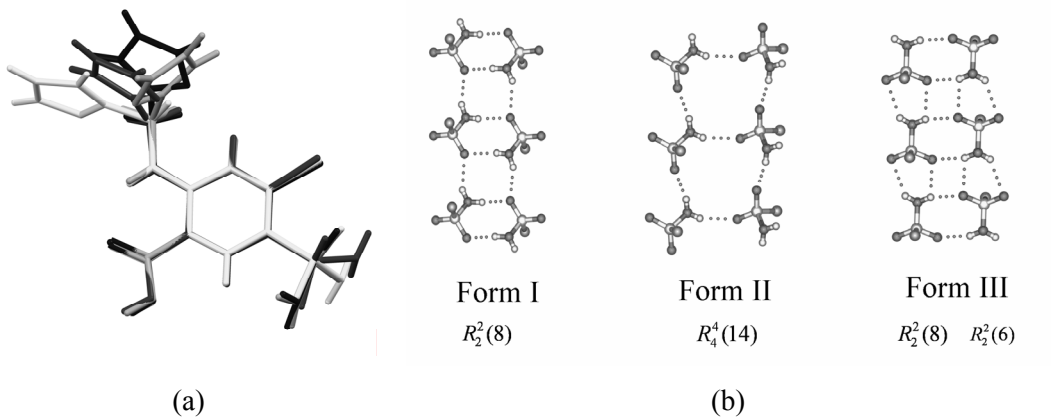

Figure 2. (a) Overlay of four conformers observed in three polymorphs of furosemide. (b) The sulfonamide is differently hydrogen bonded in three forms: sulfonamide dimer in form I, sulfonamide tetramer in form II and a skewed sulfonamide dimer in form III. Graph-set notation of various synthons is indicated.

The phenomenon of polymorphism finds applications in pharmaceutical industry.[6] Consequently polymorph screening, characterizing all the possible crystalline forms of drug, identification of stable polymorph in the early stages of drug development are regarded an indispensable step in drug development. Because energy differences between polymorphs are usually relatively small, form inter-conversion is common. In the absence of solvents and humidity, the thermodynamically stable polymorph is the only one that is guaranteed not to convert into another polymorphic form and it is most often chosen for drug development. Four examples discussed in this thesis are thoroughly screened and characterized by single crystal XRD, PXRD, IR and DSC. Their stability relationships between polymorphs is established by multiple methods, Lattice energy calculations, density and packing fraction, solid-state grinding, solvent assisted grinding, slurry conversions or solvent mediated transformations, seeding experiments and thermal analysis, which in general can be applied to any polymorphic system.

7.2 Synthon robustness as a design element for cocrystal synthesis

Unlike the robust acid–pyridine heterosynthon, carboxamide and pyridine groups generally do not aggregate via amide–pyridine heterosynthon because N–H···N interaction is considerably weaker than N–H···O hydrogen bond of the amide dimer. The pyridine-*N*-oxide was selected as a complementary group for carboxamide to exploit the better acceptor strength of the anionic oxygen to form carboxamide–pyridine-*N*-oxide heterosynthon. Amide–pyridine-*N*-oxide heterosynthon competes with amide dimer homosynthon (Figure 3). In order to establish synthon robustness, 20 crystal structures are analyzed (13 cocrystals from this chapter and 7 structures from a previous thesis in our group[7]) that contain amide and pyridine-*N*-oxide functional groups. 14 structures have amide–pyridine-*N*-oxide, 5 structures with amide–amide dimer and one structure contains neither of the expected synthons. Amide–pyridine-*N*-oxide (70%) probability is considered to be a reliable heterosynthon for the construction of binary/ ternary cocrystals[8] in supramolecular synthesis, crystal engineering, and pharmaceutical solids. Apart from structural diversity, cocrystals offer the potential to modify physical and chemical properties of substances, e.g. hydration. 4-picoline-*N*-oxide deliquesces within a day; while its 2:1 picoline-*N*-oxide and barbital cocrystal **13** held by amide–*N*-oxide heterosynthon does not absorb moisture at 50% relative humidity (RH) levels up to four weeks.

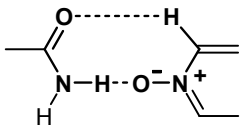

(a)

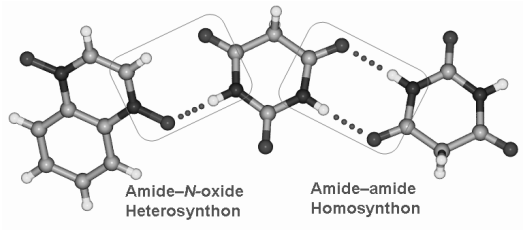

(b)

Figure 3. (a) Amide–pyridine-*N*-oxide heterosynthon. (b) Barbituric acid and quinoxaline-*N*,*N*′-dioxide (1:1) cocrystal has both amide–*N*-oxide and amide homo-dimer in the same structure.

Pharmaceutical cocrystals[9] are a subclass of cocrystals that are formed between an API and a Generally Regarded As Safe (GRAS) chemicals designed to improve the properties of drug molecules like solubility, stability and hydration control, etc. The recent and rapid emergence of pharmaceutical cocrystals can be attributed to the following factors: design, diversity, discovery and development. The diversity in crystalline forms is

greatly enhanced for a pharmaceutical chemist due to the large number of counter-molecules available for possible co-crystallization along with several hydrogen bond moieties predisposed on API.

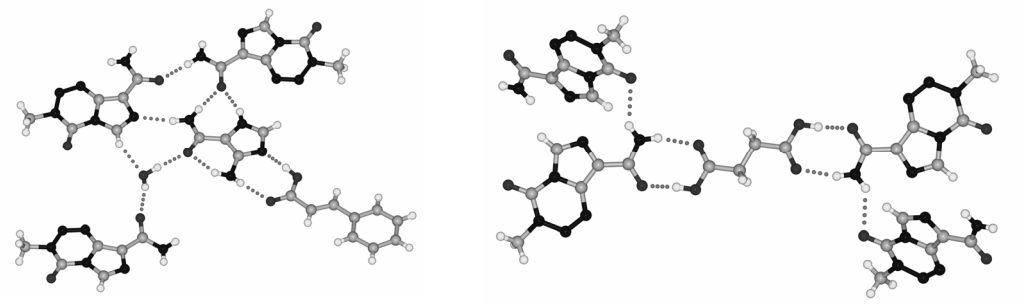

(a) (b)

Figure 4. (a) Hydrogen bonding in partially hydrolyzed TMZ–Cinnamic acid cocrystal hydrate. (b) Amide–acid synthon in TMZ–Succinic acid cocrystal. It is stable to hydrolysis when crystallized from water.

Chemical stability is a special concern for anti-tumour drug temozolomide. The white color of Temozolomide turns to light tan/pink powder is indicative of degradation. Two major problems that are encountered during crystallization are the hydrolytic cleavage of TMZ tetrazinone ring by nucleophilic attack by water, methanol or ethanol (**20, 21** & **22**). The active species diazomethane required for bringing the antitumour activity is actually knocked off during this hydrolytic cleavage of tetrazinone ring. Therefore improving the stability of TMZ is crucial. With the knowledge that TMZ is stable at acidic *p*H <5 but labile at *p*H >7, it was co-crystallized with some GRAS organic acid *p*H adjusters to improve its stability. The presence of carboxamide group in TMZ was exploited for facile cocrystal preparation with different acid and amide partners. Cocrystals of TMZ with COOH partners are more useful than $CONH_2$ partners as they bring down solution *p*H levels below <5 during crystallization thus circumventing degradation of TMZ molecules, and thereby improving the hydrolytic stability. The cinnamic acid cocrystal **34** is the only cocrystal that showed partial hydrolysis of TMZ. The asymmetric unit of contains one molecule of hydrolyzed product for every three molecules of TMZ as shown in figure 4a. This partial hydrolysis may be due to differences in the solubility of individual components in water. Therefore cinnamic acid may not be a suitable candidate for cocrystal formation for improving the TMZ stability.

Succinic acid cocrystal with TMZ (**29,** figure 4b) is a representative of all the other cocrystals with COOH partners that did not undergo hydrolysis.

7.3 Isostructurality in molecular crystals

Isostructurality[10] refers to identical packing arrangement of chemically distinct compounds in a crystal and is inversely related to the phenomenon of polymorphism, which, instead refers to the ability of a single compound to crystallize in different packing arrays. Both polymorphism and isostructurality are important in crystal engineering, materials science and pharmaceutical chemistry in order to know all possible crystal forms of a drug or replace one molecule with another without disturbing the crystalline order.[6,11] Isostructural pairs of molecules with functional group replacements are reported for O–H ⇔ C–H, N–H ⇔ C–H, halogen exchange, P=O ⇔ P(l.p.), H ⇔ *t*-Bu, etc (⇔ indicates functional group exchange). However, when the role of the modifying atom is changed (from donor to acceptor, N ⇔ C–H replacement), consequences are severe on hydrogen bonding and overall crystal packing because a strong acceptor is replaced by a weak phenyl C–H donor.

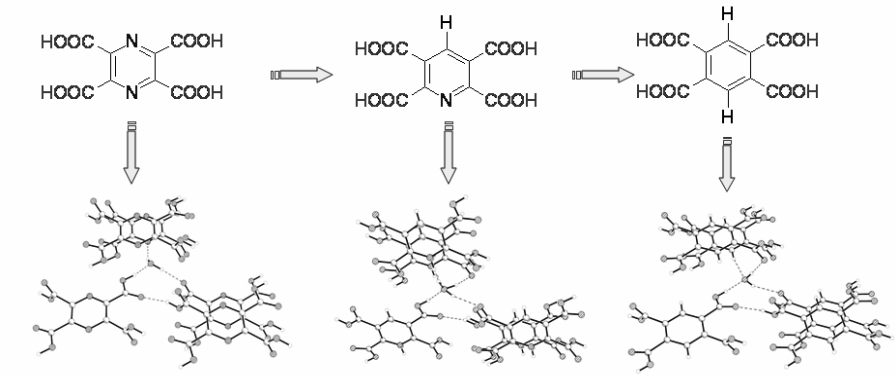

Figure 5. Pyrazinyl → pyridyl → phenyl isostructural C–H ⇔ N replacement due to multi-center synthon of hydrogen bonds around the flexible water molecule.

Interestingly pyrazine, pyridine and benzene tetracarboxylic acid are three dimensionally isomorphous. The multi-center synthon sustained by strong O–H···O H-bonds and flexibility of H_2O in orienting their hydrogen bond donor/ acceptor groups is central to isostructurality (O_{water}–H···N ⇔ C–H···O_{water}). Water is able to serve as a H-bond donor to N acceptor in pyrazine and pyridine tetra acids and C–H···O acceptor in pyridine and

benzene tetra acids by a slight reorganization of its donor hydrogen atoms so that the four acid molecules bonded to it occupy similar positions in the respective crystal structures (Figure 5). A similar C–H···O to O–H···N reorganization as in tetra acids takes place in the 2D layer motif of benzene and pyridine tri acids.

The governing factors to permit or hinder the formation of similar molecular arrays in the solid state are mainly the size of the molecules and substituents, chemical character of the substituent and site of the substitution. The similar size and chemical nature of pyrazine-*N,N′*-dioxide and benzoquinone gave identical cocrystals with carbamazepine as discussed in chapter 5. The isostructural relationship between single and multi-component crystals is rarely discussed in the literature.[12] Establishing such isostructural relationships is important to understand similarities and dissimilarities between single and multi-component crystals. The 2D layer arrangement in isonicotinamide cocrystal (**35**) is same as that of layered TMZ polymorph 3 (**6c**) in terms of recurrent amide dimer hydrogen bonds (Figure 6). Interestingly both crystal structures have conformers *A* and *B*. It appears that both the conformers are needed to stabilize the layered arrangement. In general, isostructural crystals are not obtained with conformationally flexible molecules, as each conformation can often lead to different crystal packing. Nevertheless furosemide polymorphs I (**7a**) and III (**7c**) have sulfonamide dimer, although the sulfonamide torsions in conformers of form I and III are largely different (~165˚ in form I, 55.7˚ in form III).

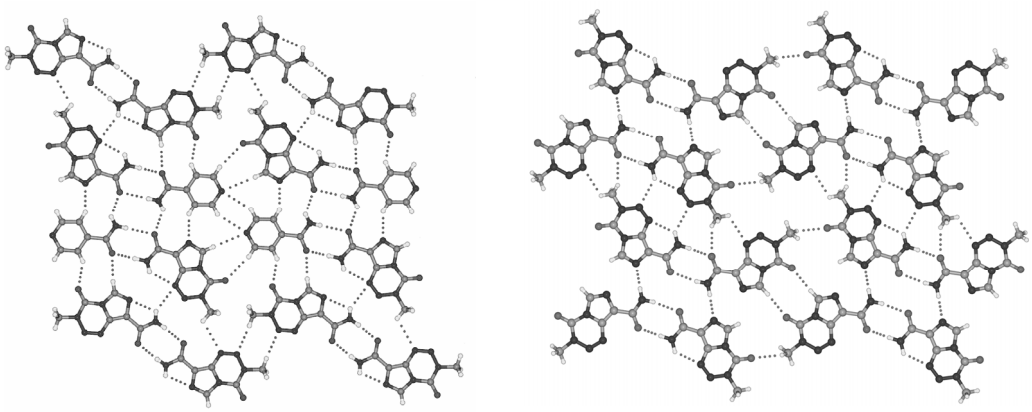

(a) (b)

Figure 6. (a) 2D section of 2:1 cocrystal of TMZ and Isonicotinamide. (b) 2D section of TMZ polymorph 3. Note that both crystal structures have identical layered arrangement of molecules. Both conformers *A* and *B* of TMZ are present in two crystal structures.

7.4 Reasons for multiple molecules in the asymmetric unit

There is a significant fraction (8.3%) of molecules containing more than one molecule in the asymmetric unit ($Z' > 1$) in the CSD.[13] Even though there is a large volume of scattered literature on the statistics of Z', a comprehensive understanding of why and when these high Z' structures occur is still not clear to this date. Moreover with the rising interest in organic crystal structure prediction,[14] it is necessary to understand this phenomenon in terms of the principles of packing or even to ascertain if there is any relationship between its occurrence and attributes such as chemical functionality, molecular weight or crystal system. Based on Steed's seminal review[15] and Brock's studies on alcohols[16a,b] and other literature reports,[16c] Nangia[5] has summarized some of the reasons for multiple molecules. (1) The molecule has a packing problem because of its awkward shape, which is reconciled by having two or more molecules in the asymmetric unit. (2) A conflict or frustration between the demands of directional hydrogen bonding and isotropic filling is reconciled through $Z' > 1$. (3) There are several low-lying molecular conformations inter-converting in solution and more than one molecule may crystallize out separately because of kinetic factors.

Secrets about the reasons of high Z' are best revealed in a polymorphic system, where the high Z' form can easily be compared with its low Z' (typically 1 or 0.5) polymorph.[17] Upon noting that C–H···O interactions are shorter (stronger) in high Z' in PYZNO form 1 and in a different polymorphic system 4,4-diphenyl-2,5-cylcohexadienone from our group,[4] we examined the generality of our observation in polymorph clusters in the CSD. Out of 38 polymorphic systems that can only form C–H···O interactions, the higher Z' crystal structure has shorter C–H···O interaction in 26 cases (68% probability), and the lower Z' form has shorter interaction in 12 cases. Number of significant short and linear interactions (<2.3 Å and >150°) are more frequent in high Z' polymorphs. Similar study was extended to O–H···O bonded polymorph clusters and found that higher Z' structure has shorter O–H···O bond distances in 22/32 sets. Analysis of the interaction geometry in C–H···O /and O–H···O H-bonded polymorph sets indicate that there is a connection between hydrogen bond strength and multiple molecules in the asymmetric unit. We believe that shorter (stronger) hydrogen bonds in high Z' crystal structures have enthalpic advantage in bringing together multiple molecules during the crystal nucleation. Clusters

of molecules formed may directly carry over from solution to the solid state without final stages of reorganization and symmetry evolution to the lower Z' form thus providing a chemical and thermodynamic basis for multiple Z' crystal structures sustained by C–H···O / O–H···O interactions.

Steed commented that high Z' structures are "fossil relic" of the fastest growing crystal nucleus or "early snapshot or kinetic form".[15] Desiraju[18] commented that the higher Z' structure is a "crystal on the way". In a pair of polymorphs with variable Z', the higher Z' structure represents to a less stable, high energy minima in the crystallization pathway towards the final thermodynamic crystal with lower Z'. However there are many $Z' > 1$ structures that that do not exhibit polymorphism,[19] or exhibit polymorphism in that all have high $Z' > 1$. Benzidine[20] is a tetramorphic with variable Z' (1.5, 3, 4, 4) crystal structures. 5-Methyl pyrazine-2,3-dicarboxylic acid always crystallizes with $Z' = 3$ in space group $P6_5$ even after repeated crystallizations, contains rare acid–pyridine trimer synthon. The requisite criteria for making this acid–pyridine trimer synthon is the presence of minimum two molecules in the asymmetric unit as concluded in chapter 2. Many polymorphic systems are reported in the literature where the high Z' crystal structure is more stable than the lower Z' form. Three out of four polymorphic systems (PYZNO, TMZ, and FMD) discussed in the present thesis have $Z' > 1$ in the stable crystal lattice. The high Z' polymorph of Venlafaxine hydrochloride is thermodynamically stable, while its lower Z' forms are metastable.[21] Therefore it is too early to draw any conclusions at this stage whether all $Z' > 1$ structures are kinetic or not. As more crystal structures and polymorph clusters of variable Z' are deposited in the database, current hypotheses such as crystals on the way, H-bond strength promoting high Z', and thermodynamic stability of lower Z' structures should get refined with time.

7.5 References

1. (a) G. R. Desiraju, *Crystal Engineering: The Design of Organic Solids*, Elsevier, Amsterdam, **1989**. (b) D. Braga, L. Brammer, N. R. Champness, *CrystEngComm* **2005**, *7*, 1.
2. J. Bernstein, *Polymorphism in Molecular Crystals*, Clarendon, Oxford, **2002**.
3. B. R. Sreekanth, P. Vishweshwar, K. Vyas, *Chem. Commun.* **2007**, 2375.

4. (a) V. S. S. Kumar, A. Anthony, A. Nangia, W. T. Robinson, C. K. Broder, R. Mondal, I. R. Evans, J. A. K. Howard and F. H. Allen, *Angew. Chem. Int. Ed.*, **2002**, *41*, 3848. (b) S. Roy, R. Banerjee, A. Nangia, G. J. Kruger, *Chem. Eur. J.* **2006**, *12*, 3777.
5. (a) A. Nangia, *J. Ind. Inst. Science* **2007**, *87*, 133. (b) A. Nangia, *Acc. Chem. Res.* **2008**, *41*, 595.
6. (a) R. Hilfiker, *Polymorphism in the Pharmaceutical Industry*, Wiley–VCH, Weinheim, Weinheim, **2006**. (b) H. G. Brittan, *Polymorphism in Pharmaceutical Solids*, Marcel Dekker, New York, **1999**.
7. L. S. Reddy, N. J. Babu, A. Nangia, *Chem. Commun.* **2006**, 1369.
8. (a) C. B. Aakeröy, J. D. Salmon, *CrystEngComm* **2004**, *6*, 19. (b) B. R. Bhogala, S. Basavoju, A. Nangia, *CrystEngComm* **2005**, *7*, 551.
9. N. Shan, M. J. Zaworotko, *Drug. Disc. Today* **2008**, *13*, 440.
10. (a) A. I. Kitaigorodskii, *Organic Chemical Crystallography*, Consultants Bureau, **1961**, pp 222-240. (b) A. Kálmán, L. Párkáanyi, L. Fábián, *Acta Crystallogr.* **1993**, *B49*, 1039.
11. Z. Hao, A. Iqbal, *Chem. Soc. Rev.* **1997**, *26*, 203.
12. H. Karfunkel, H. Wilts, Z. Hao, A. Iqbal, J. Mizuguchi, Z. Wu, *Acta Crystallogr.* **1999**, *B55*, 1075.
13. T. Steiner, *Acta Crystallogr.* **2000**, *B56*, 673.
14. S. L. Price, *Encyclopedia of Supramolecular Chemistry*, Eds J. L Atwood, J. Steed, Marcel Dekker, New York, **2004**, pp 371-379.
15. J. W. Steed, *CrystEngComm* **2003**, *5*, 169.
16. (a) C. P. Brock, L. L. Duncan, *Chem. Mater.* **1994**, *6*, 1307. (b) C. P. Brock, J. D. Dunitz, *Chem. Mater.* **1994**, *6*, 118. (c) A. Gavezzotti, G. Fillippini, *J. Phys. Chem*. **1994**, *98*, 4831.
17. D. Das, R. Banerjee, R. Mondal, J. A. K. Howard, R. Boese, G. R. Desiraju, *Chem. Commun.* **2006**, 555.
18. G. R. Desiraju, *CrystEngComm* **2007**, *9*, 91.
19. K. M. Anderson, J. W. Steed, *CrystEngComm* **2007**, *9*, 328.
20. M. Rafilovich, J. Bernstein, *J. Am. Chem. Soc.* **2006**, 128, 12185.
21. S. Roy, P. M. Bhatt, A. Nangia, G. J. Kruger, *Cryst. Growth Des.* **2007**, *7*, 476.

APPENDIX

Table 1. Crystallographic data for structures discussed in this thesis.

Crystal Data	235PYZTA	PYR256TA	PYR246TA
Emp. Formula	$(C_7H_4N_2O_6).2(H_2O)$	$(C_9H_5N_1O_8).\ 2(H_2O)$	$(C_8H_5N_1O_6).2(H_2O)$
Formula wt.	248.15	291.17	247.16
Crystal system	Triclinic	Triclinic	Orthorhombic
Space group	$P\bar{1}$	$P\bar{1}$	$P2_12_12_1$
T [K]	120(K)	100(2)	298(2)
a [Å]	5.2830(3)	5.5311(6)	5.9452(12)
b [Å]	6.6497(3)	6.2566(7)	9.4204(19)
c [Å]	13.8423(7)	9.0041(10)	18.370(4)
α [deg]	93.064(2)	70.187(2)	90
β [deg]	90.513(2)	76.251(2)	90
γ [deg]	103.009(2)	72.714(2)	90
Z	2	1	4
Volume [Å^3]	473.02	276.64(5)	1028.8(4)
D_{calc} [g/cm^3]	1.742	1.748	1.596
N-total	7415	2884	5714
N-independent	2172	1089	1213
N-observed	1887	1062	1097
R_1 [I>2σ(I)]	0.0331	0.0336	0.0407
wR_2	0.0937	0.0845	0.0962
GOF	1.043	1.120	1.080

5M23PYZDA	PYZNO 5a	PYZNO 5b	TMZ −1 6a
$C_7H_6N_2O_4$	$C_4H_4N_2O_2$	$C_4H_4N_2O_2$	$C_6H_6N_6O_2$
182.14	112.09	112.09	194.17
Hexagonal	Orthorhombic	Monoclinic	Monoclinic
$P6_5$	*Pnma*	$P2_1/c$	$P2_1/c$
100(2)	293(2)	293(2)	100(2)
13.6937(7)	11.8672(18)	3.7239(13)	17.2127(11)
13.6937(7)	12.2217(19)	11.010(4)	7.2061(5)
21.345(2)	6.4287(10)	5.683(2)	13.1651(8)
90	90	90	90
90	90	96.237(5)	108.868(1)
90	90	90	90
18	8	2	8
3466.3(4)	932.4(2)	231.62(14)	1545.21(17)
1.571	1.597	1.607	1.669
15628	4790	2286	15132
2305	956	455	2977
1985	643	401	2451
0.0513	0.0605	0.0564	0.0407
0.0992	0.1584	0.1220	0.0916
1.022	1.151	1.240	1.020

TMZ −2 **6b**	**TMZ −3** **6c**	**FMD −I** **7a**	**FMD −II, 298K** **7b**
$C_6H_6N_6O_2$	$C_6H_6N_6O_2$	$C_{12}H_{11}ClN_2O_5S$	$C_{12}H_{11}ClN_2O_5S$
194.17	194.17	330.74	330.74
Monoclinic	Triclinic	Triclinic	Monoclinic
$P2_1/n$	$P\bar{1}$	$P\bar{1}$	$P2_1/c$
100(2)	293(2)	100(2)	298(2)
6.8218(5)	8.500(2)	9.5150(9)	5.0309(10)
7.4881(6)	10.004(3)	10.4476(10)	10.254(2)
15.6303(12)	11.309(3)	15.5826(16)	26.803(5)
90	99.270(4)	92.839(2)	90
96.5340(10)	108.857(5)	107.088(2)	94.70(3)
90	109.192(5)	116.7470(10)	90
4	4	4	4
793.25(11)	820.1(4)	1291.9(2)	1378.1(5)
1.626	1.573	1.700	1.580
4173	8304	13411	14001
1560	3129	5061	2725
1428	1530	3466	2053
0.0366	0.0617	0.0668	0.0817
0.0903	0.0948	0.1258	0.1603
1.050	0.948	1.050	1.150

FMD −II, 100K **7b**	**FMD −III** **7c**	**BA•QUINO** **8**	**BA•PICNO** **9**
$C_{12}H_{11}ClN_2O_5S$	$C_{12}H_{11}ClN_2O_5S$	$(C_4H_4N_2O_3)$• $(C_8H_6N_2O_2)$	$(C_4H_4N_2O_3)$• $2(C_6H_7NO)$
330.74	330.74	290.24	346.34
Monoclinic	Triclinic	Monoclinic	Triclinic
$P2_1/c$	$P\bar{1}$	$P2_1/n$	$P\bar{1}$
100(2)	100(2)	293(2)	293(2)
5.0097(5)	4.8764(7)	10.3850(9)	8.4083(7)
10.1086(11)	10.4999(14)	7.2222(6)	9.8893(9)
26.620(3)	13.6407(18)	16.3763(14)	10.6761(9)
90	78.065(2)	90	73.2010(10)
95.396(2)	86.721(2)	93.6860(10)	79.022(2)
90	82.589(2)	90	74.182(2)
4	2	4	2
1342.1(2)	677.29	1225.72(18)	811.64(12)
1.637	1.622	1.573	1.417
13596	7005	12226	6726
2655	2631	2410	3187
2101	2063	1898	2369
0.0596	0.0562	0.0381	0.0516
0.1249	0.1139	0.1018	0.1316
1.116	1.052	1.03	1.04

BA•PYZNO 10	**SAC•BPNO 11**	**EBA•PYNO 12**	**EBA•PICNO 13**
$(C_4H_4N_2O_2)$•	$(C_7H_5NO_3S)$•	$(C_8H_{12}N_2O_3)$•	$(C_8H_{12}N_2O_3)$•
$0.5(C_4H_4N_2O_3)$	$0.5(C_{10}H_8N_2O_2)$	(C_5H_5NO)	$2(C_6H_7NO)$
184.14	554.54	279.30	402.45
Monoclinic	Monoclinic	Monoclinic	Monoclinic
$P2_1/n$	$P2_1/n$	$P2_1/c$	$P2_1/c$
293(2)	100(2)	293(2)	100(2)
5.258(3)	6.5207(4)	7.2276(5)	8.2106(5)
6.478(3)	14.0377(9)	19.5811(12)	23.9166(15)
22.118(11)	13.1232(9)	9.9928(6)	20.6318(13)
90	90	90	90
95.795(8)	104.2800(10)	98.1360(10)	96.6700(10)
90	90	90	90
4	4	4	8
749.5(7)	1164.12(13)	1399.99(15)	4024.0(4)
1.632	1.582	1.325	1.329
7435	6302	10123	25727
1511	2288	2750	7922
1390	2024	2413	4351
0.0434	0.0362	0.0398	0.0537
0.1079	0.0954	0.1116	0.1696
1.06	1.08	1.04	1.01

HBAm•BPNO 14	**HBAm•PYZNO 15**	**CBZ•QUINO 16**	**CBZ•PYZNO 17**
$(C_7H_7NO_2)$•	$(C_7H_7NO_2)$• 0.5	$(C_{15}H_{12}N_2O)$•	$(C_{15}H_{12}N_2O)$•
$0.5(C_{10}H_8N_2O_2)$	$(C_4H_4N_2O_2)$ •H_2O	$(C_8H_6N_2O_2)$	$0.5(C_4H_4N_2O_2)$
462.46	211.20	398.41	292.31
Triclinic	Triclinic	Triclinic	Monoclinic
$P\bar{1}$	$P\bar{1}$	$P\bar{1}$	$P2_1/c$
293(2)	293(2)	293(2)	293(2)
5.692(4)	6.409(4)	7.284(2)	10.237(4)
9.482(6)	7.372(4)	10.688(4)	27.247(12)
10.751(7)	11.064(6)	14.132(5)	5.135(2)
69.893(10)	96.127(14)	100.250(5)	90
84.232(10)	97.22(3)	102.463(5)	102.708(7)
84.969(10)	105.350(9)	109.079(5)	90
2	2	2	4
541.2(6)	497.7(5)	977.8(6)	1397.2(10)
1.419	1.418	1.353	1.390
5499	3642	9904	14153
2133	1948	3808	2789
1518	1210	2757	2339
0.0455	0.0473	0.0548	0.1380
0.1323	0.1309	0.1295	0.2868
1.03	0.97	1.06	1.29

TMZ•BPNO 18T	TMZ•BPNO 18M	TMZ•BPNO 19	Hydrolyzed TMZ 20 (AIMZCX10)
$2(C_6H_6N_6O_6)$• $1(C_{10}H_8N_2O_2)$	$2(C_6H_6N_6O_6)$• $1(C_{10}H_8N_2O_2)$	$(C_6H_6N_6O_6)$• $(C_{10}H_8N_2O_2)$	$(C_4H_6N_4O).(H_2O)$
576.52	576.52	382.35	144.14
Monoclinic	Monoclinic	Orthorhombic	Monoclinic
$P2_1/c$	$P2_1/c$	$P2_12_12_1$	$P2_1/a$
100(2)	100(2)	100(2)	298(2)
6.6957(5)	6.6957(5)	6.6838(15)	6.586(5)
9.6801(7)	9.6801(7)	10.035(2)	9.972(6)
37.654(3)	37.654(3)	24.051(6)	9.499(5)
90	90	90	90
95.510(2)	95.510(2)	90	91.30(10)
90	90	90	90
4	4	4	4
2429.3(3)	2429.3(3)	1613.1(6)	623.7(7)
1.576	1.576	1.574	1.535
24686	24686	16058	
4799	4799	1816	
4172	4172	1542	
0.0399	0.0399	0.0719	
0.1012	0.1012	0.1329	
1.043	1.043	1.126	

Methanolyzed TMZ 21	Ethanolyzed TMZ 22	TMZ•H_2O 23	TMZ•$MeNO_2$ 24
$(C_6H_8N_4O_3)$. $(C_6H_6N_6O_2)$	$C_7H_{10}N_4O_3$	$(C_6H_6N_6O_2).H_2O$	$(C_6H_6N_6O_2)$. $(C_1H_3NO_2)$
378.33	198.19	212.18	255.21
Monoclinic	Monoclinic	Monoclinic	Triclinic
$P2_1/c$	$P2_1/c$	$P2_1/m$	$P\bar{1}$
100(2)	293(2)	293(2)	293(2)
7.7535(6)	8.472(3)	7.5134(9)	6.4279(12)
7.5254(6)	7.610(3)	6.3187(7)	8.1654(15)
27.035(2)	14.213(5)	9.5330(11)	10.443(2)
90	90	90	96.834(3)
97.0370(10)	97.363(6)	92.868(2)	93.827(3)
90	90	90	97.772(3)
4	4	2	2
1565.6(2)	908.8(6)	452.01(9)	537.31(17)
1.605	1.449	1.559	1.577
9628	8881	2710	4997
3091	1800	974	1830
2422	1709	858	1718
0.0597	0.0630	0.0385	0.0346
0.1378	0.1435	0.1071	0.0875
1.16	1.30	1.03	1.10

TMZ•DMSO **25**	**TMZ•Formic acid** **26**	**TMZ•Acetic acid** **27**	**TMZ•Oxalic acid** **28**
$2(C_6H_6N_6O_2).$ (C_2H_6OS)	$2.(C_6H_6N_6O_2).$ $(H_3O).(CHO_2)$	$(C_6H_6N_6O_2).$ (C2H4O2)	$2(C_6H_6N_6O_2).$ (C2H2O4)
466.47	452.38	254.22	478.37
Monoclinic	Triclinic	Triclinic	Monoclinic
C2/c	$P\bar{1}$	$P\bar{1}$	*C*2/*c*
100(2)	293(2)	293(2)	293(2)
27.4264(16)	8.173(12)	6.648(3)	14.882(2)
5.2420(3)	11.626(17)	8.960(4)	6.6222(9)
15.5513(9)	11.735(17)	9.499(4)	19.655(3)
90	64.73(2)	88.420(7)	90
119.5440(10)	74.09(3)	78.748(7)	101.156(2)
90	89.31(3)	80.931(7)	90
4	2	2	4
1945.1(2)	963(2)	548.0(4)	1900.4(5)
1.593	1.560	1.541	1.672
8785	8751	5723	6714
1718	3278	2165	1873
1645	1769	1339	1383
0.0593	0.0587	0.0665	0.0532
0.1267	0.1472	0.1623	0.1453
1.22	0.95	1.01	1.07

TMZ•Succinic acid **29**	**TMZ•Malic acid** **30**	**TMZ•PABA** **31**	**TMZ•Fumaric acid** **32**
$2(C_6H_6N_6O_2).$ $(C_4H_6O_4)$	$2(C_6H_6N_6O_2).$ $(C_4H_5O_5)$	$3(C_6H_6N_6O_2).$ $(C_7H_7NO_2).(H_2O)$	$2(C_6H_6N_6O_2).$ $(C_4H_4O_4).2(H_2O)$
506.42	521.42	737.66	540.44
Monoclinic	Monoclinic	Monoclinic	Triclinic
P21/n	*C*2/*c*	$P2_1/c$	$P\bar{1}$
100(2)	293(2)	293(2)	100(2)
12.7511(13)	22.597(16)	32.785(16)	7.1198(5)
7.0092(7)	7.275(6)	7.309(4)	8.9202(6)
12.9685(14)	13.144(10)	13.056(7)	9.5007(6)
90	90	90	63.5460(10)
118.3580(10)	91.819(13)	90.897(10)	87.3900(10)
90	90	90	87.2050(10)
2	4	4	1
1019.97(18)	2160(3)	3128(3)	539.38(6)
1.649	1.603	1.566	1.664
10137	5601	12150	5602
2016	2080	5999	2100
1735	1348	3133	1983
0.0512	0.0907	0.1051	0.0384
0.1161	0.1677	0.2316	0.1032
1.09	1.14	1.09	1.07

TMZ•Salicylic acid 33	**TMZ•Cinnamic acid 34**	**TMZ•Isonicotinamide 35**	**TMZ•Nicotinamide 36**
$(C_6H_6N_6O_2).(C_7H_6O_3)$	$3(C_6H_6N_6O_2).(C_9H_8O_2).(C_4H_6N_4O).(H2O)$	$2(C_6H_6N_6O_2).(C_6H_6N_2O)$	$2(C_6H_6N_6O_2).(C_6H_6N_2O)$
332.29	874.80	510.46	510.46
Triclinic	Triclinic	Triclinic	Monoclinic
$P\bar{1}$	$P\bar{1}$	$P\bar{1}$	$P2_1/c$
293(2)	100(2)	293(2)	293(2)
6.9915(14)	7.6729(9)	9.645(3)	12.4071(11)
8.5449(17)	15.6743(17)	10.609(3)	6.6310(6)
12.682(3)	15.8325(18)	10.925(3)	26.504(2)
74.003(3)	84.551(2)	87.125(5)	90
87.822(4)	78.781(2)	75.546(4)	92.190(2)
82.328(4)	85.675(2)	87.003(4)	90
2	2	2	4
721.8(3)	1856.1(4)	1080.2(5)	2177.7(3)
1.529	1.565	1.569	1.557
4408	14191	10890	15373
2838	7337	4197	4298
1697	5827	2875	2689
0.0592	0.0728	0.0511	0.0507
0.1480	0.1618	0.1412	0.1324
0.98	1.13	1.04	1.03

TMZ•Pyrazinamide, 37	**TMZ•4-hydroxy benzamide, 38**	**TMZ•Saccharin 39**
$(C_6H_6N_6O_2).(C_5H_5N_3O)$	$2(C_6H_6N_6O_2).(C_7H_7NO_2)$	$2(C_6H_6N_6O_2).(C_7HNO_3S)$
317.29	525.47	567.49
Triclinic	Triclinic	Triclinic
$P\bar{1}$	$P\bar{1}$	$P\bar{1}$
293(2)	293(2)	293(2)
8.5570(11)	9.834(3)	6.521(3)
9.2537(12)	10.797(3)	8.064(4)
10.3924(14)	11.809(3)	11.952(5)
68.398(2)	107.047(4)	76.591(7)
89.951(2)	101.419(4)	75.856(7)
63.129(2)	101.835(4)	87.095(7)
2	2	1
668.77(15)	1127.8(5)	592.8(5)
1.576	1.547	1.590
7002	11757	6039
2632	4393	2294
1655	3259	1528
0.0532	0.0457	0.0470
0.1378	0.1276	0.1240
1.03	1.02	1.03

ABOUT THE AUTHOR

N. Jagadeesh Babu, son of Devakinandana Rao and Pushpa, was born in Tekkali, Srikakulam District of Andhra Pradesh, India, in 1981. He received his primary education in Tekkali and completed his secondary school education in Jawahar Navodaya Vidyalaya of Seethampeta. He then completed his intermediate education from Sarada Jr.College, SKLM. After the completion of his B.Sc. and M.Sc. (Chemistry) from Sri Sathya Sai Institute of Higher Learning (Sri Sathya Sai University), he joined the School of Chemistry, University of Hyderabad to pursue the Ph.D. degree in 2003. He qualified for GATE examination in February 2003. He was awarded research fellowship by University Grants Commission (JRF and SRF) during 2003-2008. He is the recipient of Dr. K. V. Rao Scientific Society Annual Research Awards 2008 under the category of Chemistry and Allied Sciences.

List of Publications

1) Variable temperature neutron diffraction analysis of a very short O–H···O hydrogen bond in 2,3,5,6-pyrazinetetracarboxylic acid dihydrate: Synthon assisted short O_{acid}–H···O_{water} hydrogen bonds in a multi-center array.

   Peddy Vishweshwar, **N. Jagadeesh Babu**, Ashwini Nangia, Sax A. Mason, Horst Puschmann, Raju Mondal and Judith A. K. Howard.

   J. Phys. Chem. A **2004**, *108*, 9406–9416.

2) Carboxamide–pyridine-*N*-oxide heterosynthon for crystal engineering and pharmaceutical cocrystals.

   L. Sreenivas Reddy, **N. Jagadeesh Babu** and Ashwini Nangia.

   Chem. Commun. **2006**, 1369–1371. (Cover picture, April 7th issue, 2006)

3) Multiple *Z′* in carboxylic acid-pyridine trimer synthon and Kagomé lattice in the structure of 5-methylpyrazine-2,3-dicarboxylic acid.

   N. Jagadeesh Babu and Ashwini Nangia.

   Cryst. Growth Des. **2006**, *6*, 1995–1999. (Cover picture, September 2006 issue)

4) Water-mediated multicenter synthon and aromatic C–H → N isostructurality.

   N. Jagadeesh Babu and Ashwini Nangia.

   Cryst. Growth Des. **2006**, *6*, 1753–1756.

5) Amide−*N*-Oxide heterosynthon and amide dimer homosynthon in cocrystals of carboxamide drugs and pyridine *N*-Oxides.

   N. Jagadeesh Babu, L. Sreenivas Reddy and Ashwini Nangia.

   Mol. Pharma. **2007**, *4*, 417–434.

6) High *Z′* polymorphs have shorter C−H···O interactions and O−H···O hydrogen bonds.

   N. Jagadeesh Babu and Ashwini Nangia.

   CrystEngComm **2007**, *9*, 980–983.

7) Water mediated tube in tetrapeptide cyclo(Phe-Pro-Leu-Aha) trihydrate and crystal structure of cyclo(D-Phe-Pro-Leu-Aha) anhydrate.

   B. M. Rajesh, J. Iqbal, **N. Jagadeesh Babu** and Ashwini Nangia.

   CrystEngComm **2007**, *9*, 860–864.

8) Crystal structures of *N*-Aryl-*N′*-4-Nitrophenyl ureas: Molecular conformation and weak interactions direct the strong hydrogen bond synthon

L. Sreenivas Reddy, Sreekanth K. Chandran, Sumod George, **N. Jagadeesh Babu** and Ashwini Nangia

Cryst. Growth Des. **2006**, *7*, 2675–2690.

9) Lewis-Acid Catalyzed One-Pot, Three Component Route to Chiral 3,3'-Bipyrroles

Sumit Dey, Churala Pal, Debkumar Nandi, Venkatachalam Sesha Giri, Marek Zaidlewicz, Marek Krzeminski, Lidia Smentek, B. Andes Hess, Jr., Jacek Gawronski, Marcin Kwit, **N. Jagadeesh Babu**, Ashwini Nangia and Parasuraman Jaisankar

Org. Lett. **2008**, *10*, 1373–1376.

10) Polymorphs and polymorphic cocrystals of Temozolomide

N. Jagadeesh Babu, L. Sreenivas Reddy, S. Aitipamula and Ashwini Nangia

Chem. Asian. J. **2008**, *3*, 1122–1133. (Cover picture, 3rd July 2008 issue)

11) Polymorphism in Furosemide.

N. Jagadeesh Babu, C. N. Surya and Ashwini Nangia
(Manuscript under preparation)

12) Pharmaceutical cocrystals of Temozolomide.

N. Jagadeesh Babu, Palash Sanphui and Ashwini Nangia
(Manuscript under preparation)

Polymorphic cocrystals of Temozolomide and 4,4'-bipyridine-N,N'-dioxide (shown as yellow and red butterfly arrays) have different hydrogen-bonding and molecular-packing arrangements. Published as cover art in Chem. Asian. J. 2008, July issue.